PALACKÝ UNIVERSITY OLOMOUC

Faculty of Science

Department of Biochemistry

Metabolism and function of cytokinins in fungi from order *Hypocreales* and identification of auxin transporter in *Claviceps purpurea*

Ph.D. Thesis

Autor:	**Josef Vrabka**
Study program:	P1416 Biochemistry
Study branch:	Biochemistry
Form of study:	full-time
Supervisor:	doc. RNDr. Jitka Frébortová, Ph.D.
Submitted:	2019

I hereby declare that this thesis has been written solely by myself and that all the sources used in this thesis are cited and included in the References part.

In Olomouc 15th April 2019 ……..

Josef Vrabka

Acknowledgments

I want to thank

- to Dr. Petr Galuszka, my supervisor and friend, for his support and enthusiasm for Claviceps project, which allowed formation of this thesis
- to Dr. Jitka Frébortová for her help with interpretation and discussion of results, patience and supervision during last year of Ph.D.
- to Dr. Véronique Bergougnoux-Fojtík for critical reading and help with Fusarium manuscript
- to Dr. Ondřej Novák for cytokinin analysis
- to Dr. Aleš Pěnčík for auxin analysis
- to Dr. David Zalabák for help with cloning and valuable advices through my Ph.D. study
- to Dr. Paul Tudzynski and Dr. Janine Hinsch from Münster University for help during my internship
- to Michaela Hradilová for all her help in *Claviceps* laboratory and maintenance of WT strains
- to Kristýna Hromadová and Cintia Florencia Marchetti for their optimistic and cheerful attitude even in bad times
- to all the members of the Department of Molecular Biology
- to my wife Hana, my family and friends for their support

Bibliografická identifikace:

Jméno a příjmení autora	Josef Vrabka
Název práce	Metabolismus a funkce cytokininů v houbách z řádu *Hypocreales* a identifikace transportéru auxinu v *Claviceps purpurea*
Typ práce	disertační
Pracoviště	Oddělení molekulární biologie, Centrum regionu Haná pro biotechnologický a zemědělský výzkum
Vedoucí práce	doc. RNDr. Jitka Frébortová, Ph.D.
Rok obhajoby práce	2019

Abstrakt

Předkládaná disertační práce je zaměřena na rostlinné hormony cytokiny a auxiny u vláknitých hub z řádu *Hypocreales* a sestává ze čtyř částí. První část práce slouží k seznámení se zkoumanými houbovými organismy a shrnuje současné informace o metabolismu, transportu a signalizaci cytokininů a auxinů, zároveň je popsána jejich role v interakci s mikroorganismy.

Cílem druhé části práce je studium role cytokininů u houby *Claviceps purpurea*. Byla sledována odezva v expresi vybraných genů zapojených do metabolismu cytokininů u hostitelského rostliny žita (*Secale cereale*) pomocí kvantitativní real-time PCR (qPCR), zároveň byly změřeny hladiny cytokininů v různých fázích infekce u napadených a kontrolních rostlin. V genomu *C. purpurea* byly odhaleny geny s předpokládaným zapojením do biosyntézy cytokininů. Jejich funkce byla potvrzena heterologní expresí v *Escherichia coli*, purifikací pomocí afinitní chromatografie a biochemickou charakterizací. Byla stanovena rychlost enzymatické reakce a substrátová preference. Pro další ověření byly geny transformovány do rostlin *Arabidopsis thaliana* s expresí řízenou konstitutivním promotorem a sledována změna fenotypu.

Třetí část je zaměřena na sledování exprese genů *de novo* biosyntézy cytokininů u vybraných druhů rodu *Fusarium* během infekce semenáčků kukuřice (*Zea mays*).

Zároveň byla hodnocena i změna exprese genů biosyntézy a degradace cytokininů u napadených rostlin.

Poslední část je věnována identifikaci předpokládaného auxinového transportéru u *C. purpurea*. Homologní rekombinací byli připraveni deleční mutanti, u kterých byly stanoveny hladiny auxinů. Pro určení subcelulární lokalizace bylo využito pozorování fúzního proteinu s GFP pomocí fluorescenční mikroskopie. Pravděpodobná funkce byla ověřena transformací *A. thaliana* a následnou fenotypizací homozygotních linií.

Klíčová slova	Cytokininy, auxiny, Claviceps, Fusarium, metabolismus, transport
Počet stran	100
Počet příloh	2
Jazyk	Anglický

Bibliographical identification:

Author's first name and surname	Josef Vrabka
Title	Metabolism and function of cytokinins in fungi from order *Hypocreales* and identification of auxin transporter in *Claviceps purpurea*
Type of thesis	Ph.D. thesis
Department	Department of Molecular Biology, Centre of the Region Haná for Biotechnological and Agricultural Research
Supervisor	Dr. Jitka Frébortová
The year of presentation	2019

Abstract

Presented thesis is focused on plant hormones cytokinins and auxins in filamentous fungi from order *Hypocreales* and consists of four parts. The first part of the work is introduces studied fungal organisms and summarizes current information about the metabolism, transport and signaling of cytokinins and auxins, concurrently describing their role in interaction with microorganisms.

The aim of the second part is to study the role of cytokinins in *Claviceps purpurea*. Response in expression of selected genes involved in cytokinin metabolism in rye host plant (*Secale cereale*) was followed using quantitative real-time PCR (qPCR), and cytokinin levels were measured at various stages of infection in infected and control plants. Genes with putative function in cytokinin biosynthesis were detected in the *C. purpurea* genome. Their function was confirmed using heterologous expression in *Escherichia coli* and subsequent purification by affinity chromatography followed by biochemical characterization. The rate of enzymatic reaction and substrate preference was determined. For further verification, the genes were transformed into *Arabidopsis thaliana* under the control of constitutive promotor and the change in phenotype was observed.

The third part is focused on the expression of *de novo* cytokinin biosynthesis genes in selected *Fusarium* species during infection of maize seedlings (*Zea mays*). At the same time, the change in cytokinin biosynthesis and degradation genes in infected plants was also followed.

The last part is devoted to identification of putative auxin transporter in *C. purpurea*. Deletion mutants were prepared by homologous recombination and auxin levels were determined. Subcellular localization was observed with the GFP fusion protein by fluorescence microscopy. The predicted function was verified by transformation of *A. thaliana* and subsequent phenotyping of homozygous lines.

Keywords	Cytokinins, auxins, Claviceps, Fusarium, metabolism, transport
Number of pages	100
Number of appendices	2
Language	English

CONTENTS

Part I: Objectives

1. Review on biology of *Claviceps purpurea* and *Fusarium* spp.
2. Review on cytokinins and auxins, their metabolism, transport, and role in host-pathogen interaction
3. Study of cytokinin metabolism in *Claviceps purpurea*
4. Clarify origin of cytokinin accumulation in maize infected by *Fusarium* spp.
5. Identification of putative auxin efflux carrier in *Claviceps purpurea*

Part II: Introduction

Order *Hypocreales* (division *Ascomycota*) contains 237 fungal genera with very different lifestyles – from insect pathogens (*Cordyceps*), over mycoparasites (*Trichoderma*) to soil saprobes, plant associated pathogens (*Fusarium*) and exclusive cereal biotrophs (*Claviceps*). Genus *Fusarium* belongs to one of the most studied filamentous fungi, widely distributed on all continents. Some fusaria can produce mycotoxins in crops that can affect human and animal health if they enter the food chain and thus are considered as economically important plant pathogenic species. Related biotrophic pathogen from the same order, *Claviceps purpurea,* is widely used in the pharmaceutical industry for its ability to produce ergot alkaloids. Approximately half of the world production of ergot-based therapeutics comes from field produced ergot, which originates as a product of rye field infection by the industrial fungus strains (Hulvová *et al.*, 2013).

The theoretical introduction of this work is aimed at acquainting readers with studied organisms and bringing them closer to the issue of plant hormones cytokinins and auxins in fungi and bacteria.

Ergot fungus *Claviceps purpurea*

The genus *Claviceps* (order *Hypocreales*), also called ergot, contains approximately 60 species of biotrophic fungi living on monocots plants, primarily cereals. Molecular phylogeny study placed ancestor of *Claviceps* to South America in the Paleocene (Píchová *et al.*, 2018). *Claviceps purpurea* has strict organ specificity, infecting unfertilized ovaries (Hinsch and Tudzynski, 2015). The basis of this strict organ specificity is unclear, but probably involves specific recognition of the stigmatic surface. As genuine biotroph, infection is not accompanied by visible plant defense response (Oeser *et al.*, 2017). Impact on agriculture is not in decreased yield, but rather in contamination of grains with alkaloids toxic to mammals, present in late stage of fungal infection – sclerotia. Most abundant group of alkaloids is ergot alkaloids (EAs) such as clavines or ergopeptines causing ergotism (in humans also called St. Anthony's fire). Medieval poisonings were caused by ingestion of bread made from infected rye, currently is human ergotism eliminated by appropriate agricultural procedures. However, the impact is still noticeable for livestock (Coufal-

Majewski *et al.*, 2016). EAs are important substance in pharmacology, obtained either from parasitic or axenic production (Hulvová *et al.*, 2013).

Despite *Claviceps purpurea* being true biotroph, it can be cultivated in axenic culture and effective transformation techniques are available. Gene knock-outs obtained by homologous recombination revealed necessary aspects for successful infection process (Oeser *et al.*, 2002; Mey *et al.*, 2002; Giesbert *et al.*, 2008).

Infection cycle

In spring, sexual life cycle starts in overwintering sclerotia, creating stroma heads with perithecia (Figure 1). Mature ascospores are released from perithecia, distributed by wind or insect on host plants. Ascospore lands on stigma, preferentially at the stigmatic hairs and fungal hyphae starts oriented grow through stigmal cell wall toward base of ovary, mainly intercellularly. Penetration of fungus into plant tissue is without formation of specialized structure (e. g. appresoria) and relies on enzymatic digestion (Haarmann *et al.*, 2009). Plant cells in contact with fungal hyphae remain healthy and alive. Avoidance to plant immune system lies in *Claviceps* camouflage imitating pollen tube growth with help of small effector proteins (Oeser *et al.*, 2017). When hyphae reach vascular tissue on the base of ovary (rachilla), rapid colonization of whole ovary with branched hyphae occurs (sphacelial stage). This stage of infection is accompanied with honeydew production, fluid derived from phloem and filled with conidia. *Claviceps* has developed specific techniques to maintain the phloem exudate flow, implying cytokinins (as plant hormones controlling source-sink nutrient mobilization) might have important role in early stage of infection (Hinsch *et al.*, 2015). Honeydew helps to spread infection on uninfected spikes via direct touch of spikes or by attracting insect. Two weeks post–infection honeydew production stops and dark hard sclerotia are being formed, securing infection for next season. Sclerotium is natural source of ergot alkaloids, with levels of EA up to 2% of dry weight (Hulvová *et al.*, 2013).

Claviceps infection competes with pollen, as only unfertilized ovary can serve as host. This attribute is exploited in field EAs production, where male sterile lines of rye are used. Rye, as a cross-pollinated cereal, is the major and most susceptible host; cross-pollinated cereals have fully opened florets exposed to inoculum.

Figure 1 | Life cycle of *Claviceps purpurea*. (1) open rye floret; (2) fungal grow through ovary; (3) honeydew production; (4) insect transmit infection to new spikes; (5) sclerotia ripening; (6) overwintering of sclerotia in soil; (7) sporangial formation; (8) release of ascospores from perithecia (Hulvová *et al.*, 2013).

Genus *Fusarium*

The genus *Fusarium* (order *Hypocreales*) covers many species of filamentous fungi found readily in soil around the world and associated with multiple crop species. At least 80% of all cultivated plants are associated with at least one disease caused by a *Fusarium* species (Leslie and Summerell, 2008). Moreover, *Fusarium* species have recently emerged

as human pathogens associated with invasive infections of immune compromised patients (Guarro and Gene 1995; Dignani and Anaissie 2004). Although it can interact with plants as an endophyte, its growth as a biotroph, hemibiotroph or necrotroph cause significant agronomic losses worldwide. Currently, the genus *Fusarium* is divided into 20 species complexes and nine monotypic lineages (O'Donnell *et al.*, 2013). Species from the *Fusarium fujikuroi* complex (FFC) are best known for their ability to induce diseases such as "bakanae" in rice (Matic *et al.*, 2017), ear and stalk rot in maize (Presello *et al.*, 2008), pitch canker in pine (Gordon, 2006) and mango malformation disease (MMD) in mango (Freeman *et al.*, 2014). Some disease symptoms can be clearly linked to hormone production by the fungi. In fact, culture filtrate of *Fusarium fujikuroi* (*Gibberella fujikuroi*) was the first source from which gibberellins (GAs) were isolated and identified several decades ago (Hedden and Sponsel, 2015). It was only later discovered that GAs are ubiquitous plant hormones that promote normal stem elongation. The contribution of additional GAs to infected rice plants by *F. fujikuroi* leads to abnormally long stems which is the typical "bakanae" symptom observed. The gene cluster responsible for GA synthesis in *F. fujikuroi* has been extensively characterized (Tudzynski and Hölter, 1998).

To obtain nutrients, plant pathogenic fungi have to avoid plant immune system. Evolution has endowed fungal pathogens with array of peptide effectors and metabolites, which help them control host plant and secure favorable environment (Lo Presti *et al.*, 2015). Among the metabolites contributing to the successful infection are the plant hormones, whether directly produced by the fungal pathogen or produced by plant under pathogen control.

Phytohormones

Phytohormones are key players in plant growth, differentiation and development and are defined as naturally occurring mobile compounds that influence physiological processes already at very low concentrations. The classical groups are auxins, gibberellins, ethylene, cytokinins, brassinosteroids, jasmonates and abscisic acid. Two major phytohormones, cytokinins and auxins, have been originally defined as cell division promoting compounds (Skoog and Armstrong, 1970). Today it is known that they are not only important for cytokinesis but act as crucial factors in various plant developmental and

physiological processes including interaction with pathogenic or beneficial microorganisms.

Interestingly, phytohormones are not exclusively synthesized by plants, but their production was confirmed in a number of plant-interacting microorganisms. Known biosynthetic pathways of phytohormones may differ in microorganisms and plants. Nevertheless, the ability of fungi to produce phytohormones has been proved mostly by their presence in mycelia or culture media, but information about genes or respective enzyme activities has been missing.

Cytokinins

Cytokinins are hormones that play major role in plant growth and development, concurrently affecting nutritional signaling and responses to biotic and abiotic stimuli (Galuszka *et al*., 2008). Natural cytokinins are derived from adenine, substituted on N6 with isoprenoid or aromatic side chain. Various sugar conjugates of cytokinins (nucleosides, nucleotides, glucosides) exist, however free bases have superior biological activity and sugar conjugates serve as translocation or storage forms (Sakakibara, 2006).

An overview of cytokinin biosynthesis, metabolism and degradation

De novo cytokinin biosynthesis (Figure 2) begins with modification of adenine (in nucleotide form) on N6 position with isoprenoid moiety from dimethylallyl diphosphate (DMAPP). This step is catalyzed by AMP or ADP/ATP dependent adenylate isopentenyltransferase (IPT, EC 2.5.1.27 or 2.5.1.112) and leads to isopentenyl (iP) nucleotide (Kakimoto, 2001; Takei *et al*., 2001). The first cytokinin biosynthetic activity and biosynthetic gene were detected in the slime mold *Dictyostelium discoideum* (Taya *et al.,* 1978) and *Agrobacterium tumefaciens* (Akiyoshi *et al.,* 1984), respectively. Both microorganisms preferred AMP as substrate for IPT, which led to conclusion that AMP is favored substrate for IPTs. However, all plant IPTs have lower K_m for either ATP or ADP (Kakimoto *et al.*, 2001; Abe *et al.*, 2007). Currently, consensus is that AMP is main IPT substrate in microorganisms, whereas plants strictly prefer ATP/ADP.

Hydroxylation of iP nucleotide by cytokinin-specific cytochrome P450 monooxygenase gives rise to *trans*-zeatin (tZ) nucleotide. Free bases of respective

cytokinin nucleotides are released by cytokinin-specific phosphoribohydrolase known as *lonely guy* (LOG, EC 3.2.2.n) (Kurakawa *et al*., 2007).

Cytokinin pool is also supplied by second biosynthetic pathway, present in bacteria and all eukaryotic organisms. Adenine bound in tRNA is prenylated by tRNA isopentenyltransferase (tRNA-IPT, EC 2.5.1.75); this reaction increases fidelity of translation by stabilization of codon–anticodon binding (Konevega *et al*., 2006). Decomposition of tRNA contributes to cytokinin pool in plants: degradation of modified tRNA is source of majority of *cis*-zeatin (cZ) in *Arabidopsis thaliana* (Miyawaki *et al.,* 2006). Surprisingly, moss *Physcomitrella patens,* model for plant development and evolution, has tRNA-IPT pathway as the only source of cytokinins (Lindner *et al.*, 2014).

De novo biosynthesis of cytokinins in fungi employing unique bifunctional enzyme IPT-LOG was for the first time identified in *Claviceps purpurea* (Hinsch *et al.*, 2015) as described in this thesis (Part IV). The presence of IPT-LOG was later confirmed also in *Fusarium* species (Niehaus *et al.*, 2016; Sørensen *et al.*, 2018). In both, Claviceps and Fusarium species, the *IPT-LOG* gene is a part of small gene cluster together with the gene encoding cytochrome P450 monooxygenase (Hinsch *et al.*, 2015). Two or even three cytokinin biosynthesis clusters were identified in genomes of *F. fujikuroi* species complex (Niehaus *et al.*, 2016). Total pool of cytokinins in *C. purpurea* is supplied also by tRNA decay, which is essential source of cZ (Hinsch *et al.*, 2016).

Level of biologically active cytokinins in plant tissue is controlled by several ways of deactivation – glycosylation, ribosylation and irreversible degradation by cytokinin oxidase/dehydrogenase (CKX). Glycosylation takes place either at nitrogen on the adenine ring (N-glycosylation) or at hydroxyl of side chain (O-glycosylation). O-glycosylation of cytokinins causes loss of biological activity, however the reaction is reversible and modified cytokinins thus serve as storage form (Sakakibara, 2006). N7 or N9-glycosylated cytokinins are irreversibly deactivated and can be further processed by CKX degradation (Galuszka *et al.*, 2007). Catabolism via CKX (EC 1.5.99.12) is responsible for most of cytokinin degradation. In a single enzymatic step, side chain is removed. The enzymatic activity was first observed already in the 1970s (Pačes *et al.*, 1971), but genes and enzymatic principle were described at the turn of millennium (Houba-Hérin *et al.*, 1999; Morris *et al.*, 1999, Galuszka et al., 2001). CKX is a flavoenzyme with covalently bound FAD using artificial electron acceptors for its reoxidation *in vitro*; putative natural electron

acceptors benzoxazinones were identified in maize (Frébortová *et al.*, 2010). Most plants have several *CKX* genes, whose protein products differ in substrate specificity, subcellular localization and expression in specific tissue. Entire set of *CKX* genes was described for Arabidopsis and maize so far (Galuszka *et al.*, 2007; Zalabák *et al.*, 2014).

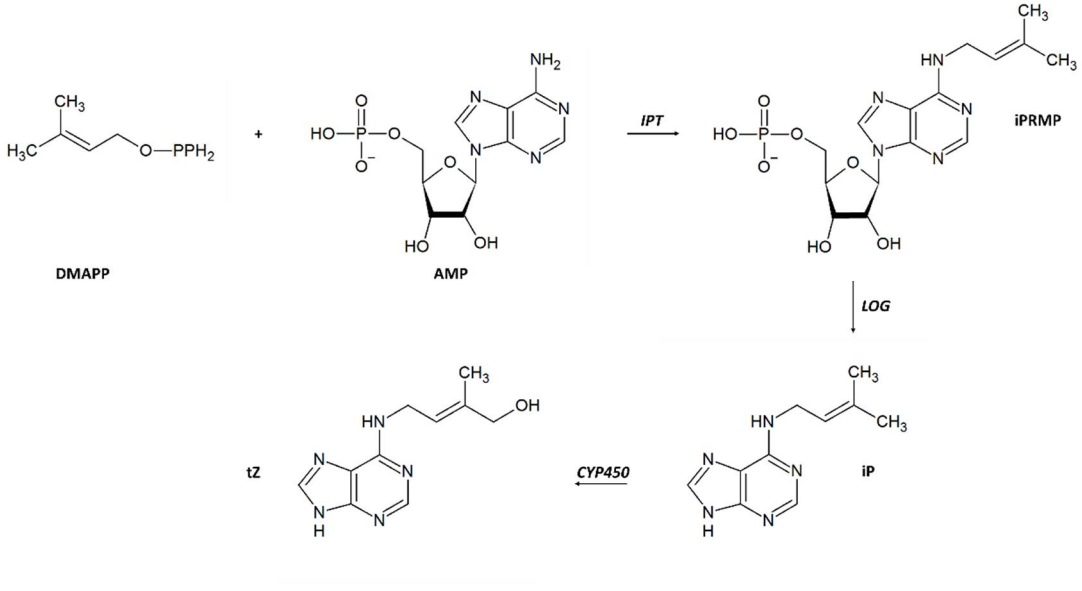

Figure 2 | *De novo* biosynthesis of cytokinins iP and tZ. Adenine nucleotide (AMP or ADP/ATP) is prenylated using DMAPP in reaction catalyzed by IPT. Free base is released by hydrolysis of phosphoribose moiety by LOG. Side chain of iP can be hydroxylated to tZ by CYP450.

Cytokinin signaling

Perception and transduction of cytokinin signal in plants is mediated by three components – histidine protein kinase receptor (HK), histidine-containing phosphotransfer protein (HP) and response regulators (RR). The cytokinins are synthesized as nucleotides, but for signaling the only active forms are free bases and ribosides.

Briefly, upon cytokinin binding to HK receptor (a transmembrane protein), receptor is dimerized and autophosphorylated on conserved histidine residues, followed by phosphate transfer to an aspartate in receiver domain at the C-end of receptor (Kakimoto, 2003). Its hormone-sensing domain is located on the outer side of the membrane, whereas the histidine kinase and receiver domains are located on the cytosolic side (Steklov *et al.*, 2013). Localization of HK receptors is constantly discussed and oscillates from endoplasmic reticulum (Caesar *et al.*, 2011; Wulfetange *et al.*, 2011) to plasma membrane

(Zürcher *et al.*, 2016). All arguments for exact receptor localization are summarized in recent comprehensive review (Romanov *et al.*, 2018). There are three cytokinin HK receptors in Arabidopsis – AHK2, 3 and 4. Receptors differ in sensitivity and selectivity for various cytokinins, which allows response to environmental cues and controllable development (Zürcher and Müller, 2016). For example, both AHK3 and AHK4 recognize iP and tZ, but only AHK3 recognize also the *cis*-zeatin and dihydrozeatin (DHZ). AHK4 was not activated by cytokinin ribosides and ribotides, while AHK3 was (Spíchal *et al.*, 2004).

Signal in the form of phosphate is then transferred from receptor to HPs, which are known to travel between the cytosol and the nucleus. Earlier studies in Arabidopsis protoplasts reported that this translocation was cytokinin dependent, but more recent work disproved this theory and showed, that the translocation occurs continuously in a cytokinin-independent manner (Punwani *et al.*, 2010). The phosphate is in nucleus transmitted to response regulators, transcription factors regulating expression of cytokinin responsive genes (El-Showk *et al.*, 2013). Type-B RRs are positive regulators of cytokinin response and serve as transcription factors directly influencing expression of response genes (Argyros *et al.*, 2008). Type-A RRs are negative regulators that compete with type-B RR for the same signal from cytokinin intracellular signaling cascade and therefore mediate a negative feedback loop (Kiba *et al.*, 2003; Hirose *et al.*, 2007).

Cytokinin signaling pathway was believed to be unique for green plants; however, cytokinin receptor was characterized in phytopathogenic bacteria *Xanthomonas campestris* recently (Wang *et al.*, 2017). Receptor binds only iP and does not react to other cytokinins. Signal from receptor is transmitted to analog of RR with phosphodiesterase activity, which serves for degradation of secondary messenger cyclic di-guanylic acid. Final response of bacteria to cytokinin is an improved tolerance to oxidative stress. It has been hypothesized, that bacteria evolved detection of plant cytokinin to cope with innate immune response during infection process.

Putative cytokinin HK receptors were also identified in early diverging fungi using bioinformatics approach (Kabbara *et al.*, 2018). Homologues of receptors were found not only in plant root symbionts and endophytes, but also in fungi colonizing decaying plant material. These *in silico* results must be yet confirmed.

Cytokinin transport

Extensive experiments in Arabidopsis demonstrated that tZ-type cytokinins are transported shootward in xylem, whereas iP-type cytokinins move preferentially from the shoot to the root via symplastic connections in the phloem (reviewed in Kudo *et al.*, 2010; Zürcher and Müller, 2016).

First putative candidates for cytokinin transporter from family of purine permeases (PUP) were reported, however direct transport of tZ was confirmed just for AtPUP1 and AtPUP14 (Gillissen *et al.*, 2000; Bürkle *et al.*, 2003; Zürcher *et al.*, 2016). AtPUP14 is negative regulator of cytokinin signaling, loss of function mutation allowed ectopic cytokinin signaling accompanied by aberrant morphogenesis in embryos, roots, and the shoot apical meristem. It is localized in plasma membrane and imports into cytoplasm, depleting apoplastic pool of cytokinins out of the reach of plasma membrane receptors (Zürcher *et al.*, 2016).

Translocation of cytokinin nucleosides is possible via an equilibrative nucleoside transporter (ENT); adenosine import by AtENT6 was shown to be inhibited by isopentenyladenosine (iPR) and *trans*-zeatin riboside (tZR) in yeast heterologous assays (Hirose *et al.*, 2005, 2008). A transgenic Arabidopsis line harboring *AtENT6* promoter–GUS showed that AtENT6 is expressed in root, leaf, and flower vasculatures and in stomata, suggesting role of AtENT6 in the long-distance transport of nucleosides (Hirose *et al.*, 2008). In rice, the ENT members are expressed in the vasculature suggesting that they mediate uptake of transported cytokinins (Hirose *et al.*, 2005).

Recently, member of ATP-binding cassette (ABC) transporters AtABCG14 was identified as crucial for tZ root-to-shoot translocation (Ko *et al.*, 2014; Zhang *et al.*, 2014). Phenotype of knock-out mutant mirrors phenotype of plants overexpressing CKX or with loss of cytokinin signaling, and WT phenotype could be rescued by tZ application. The mutants had increased levels of tZ and DHZ in roots, while concentration in shoots was opposite (Ko *et al.*, 2014). Grafting experiments confirmed AtABCG14 significance in roots for long distance cytokinin transport and natural shoot development.

Cytokinin role in host-pathogen interaction

Besides cytokinin role in plant development, plant-associated microorganisms exploit cytokinins for their advantage. Formations of galls, green islands or local nutrient sinks are connected with cytokinin accumulation. Microorganisms may indirectly influence the cytokinin levels by modulating the host's cytokinin biosynthesis or manipulate them directly by *de novo* synthesis of cytokinins. These different approaches are well illustrated on two species of bacteria – *Agrobacterium tumefaciens* and *Rhodococcus fascians.* Whereas *A. tumefaciens* integrates *IPT* gene (located in T-DNA region on Ti plasmid) into host genome (Akiyoshi *et al*., 1984), *R. fascians* produces mixture of cytokinins directly with the use of genes in *fas* operon (Murphy *et al*., 1997; Pertry *et al*., 2009). In addition to common cytokinins, *R. fascians* also produces methylated derivates of iP (Radhika *et al.*, 2015). These compounds are active as canonical cytokinins and concurrently poor substrates for CKX. Methylation enhances their biological stability and helps them to persist longer in plant tissue. With both organisms, cytokinin accumulation entails deregulated cell division and malformation of plant tissue.

Another well studied example of bacterial plant pathogen is *Pseudomonas syringae.* Although it does not produce cytokinins during infection, *P. syringae* pv. *tomato* DC3000 activates Arabidopsis cytokinin signaling, which leads to suppression of defense signaling (Hann *et al.*, 2014).

Cytokinins are also important for establishment of arbuscular mycorrhiza (Barker and Tagu, 2000), as plants with fungal root symbionts have enhanced cytokinin accumulation in both shoots and roots (Allen *et al.*, 1980). Unfortunately, detailed research about role of cytokinins in fungal-root symbiosis is still missing.

Utilization of cytokinins as virulence factor in filamentous fungi is connected with (hemi)biotrophic plant pathogens. Cytokinins were identified in axenic cultures of various fungi, in which exclusive source of cytokinins is probably decay of prenylated tRNA, as *de novo* biosynthesis was not revealed (Murphy *et al.*, 1997; Behr *et al.*, 2012). Deletion of *tRNA-IPT* gene (*CKS1*) in rice pathogen *Magnaporthe oryzae* did not affect its *in vitro* growth and development, however mutant had impaired *in planta* growth and virulence (Figure 3), which was fully restored by an exogenous cytokinin application (Chanclud *et al.*, 2016). Authors hypothesized, that the impaired virulence of *cks1* mutant is the consequence of the absence of cytokinin production that would normally enfeeble host

defenses and modify nutrient fluxes for the pathogen's benefit. Fungal cytokinins can simultaneously prevent collapse of host photosynthesis during infection, for instance by limiting oxidative stress generated through photorespiration and, in consequence, allowing the establishment of the biotrophic phase. Rice host reacted to *cks1* mutant infection with elevated oxidative burst, and lower glucose, aspartate and glutamate content 48 hours after inoculation in infection site compared to complemented mutant strain. Similar results were obtained with maize pathogens *Ustilago maydis* (Bruce *et al.*, 2011; Morrison *et al.*, 2017) and *Colletotrichum graminicola* (Behr *et al.*, 2012).

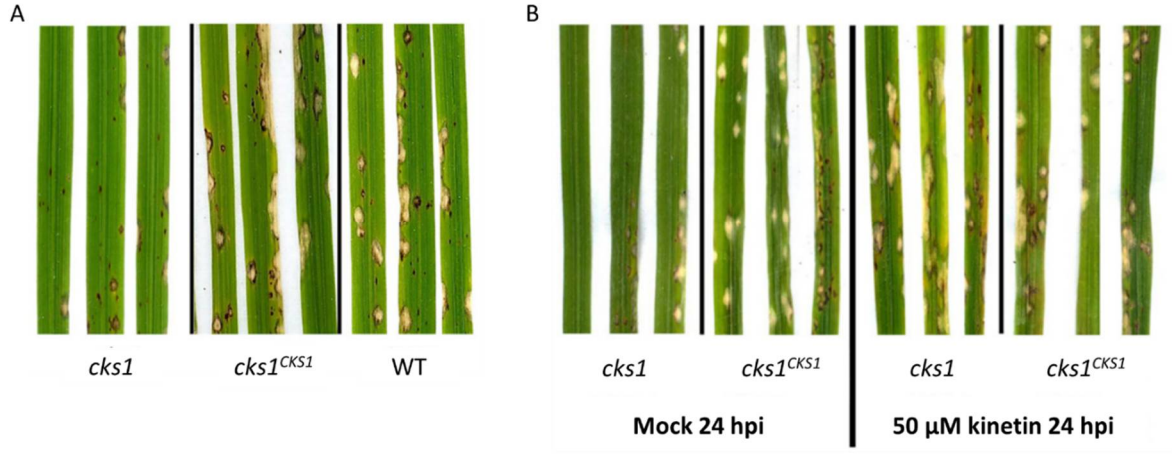

Figure 3 | Impact of *cks1* deletion on the virulence of *Magnaporthe oryzae*. (A) Disease symptoms are reduced with *cks1* mutant, while complemented control strain *cks1*^{CKS1} is comparable with WT strain as observed 6 days after inoculation. (B) Virulence of *cks1* strain is restored by application of 50 µM kinetin. Adapted from Chanclud *et al.*, 2016.

Crucial role of fungus-produced cytokinins in virulence was shown also in *Claviceps purpurea* (Figure 4), using mutants defective in cytokinin production (Hinsch *et al.*, 2015, 2016). Mutants with diminished cytokinin content had only reduced virulence (Δcpipt-log 88%, ΔcptRNA-ipt 56%), while double deletion ceased cytokinin production and mutant was not able to form honeydew or sclerotia. Microscopic analysis of dissected rye ears confirmed massive reduction of invasive hyphae, which cannot reach ovary.

Screening of secondary metabolites in *Fusarium pseudograminearum*, important pathogen of wheat and barley, identified novel class of cytokinin – pyrrole-substituted purine derivatives, termed Fusarium cytokinins (Sørensen *et al.*, 2018). These compounds

could activate plant cytokinin signaling and *in planta* RNAseq analysis after Fusarium cytokinin treatment showed extensive reprogramming of the host environment.

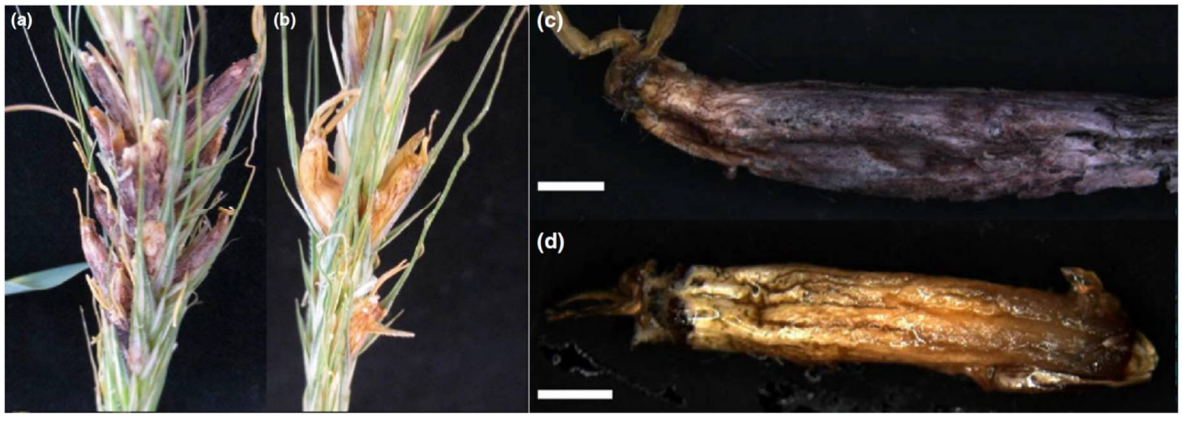

Figure 4 | Pathogenicity assay of *Claviceps purpurea* strains Cp20.1 and ΔcptRNA-ipt. (a, c) Sclerotia formed by Cp20.1; (b, d) sclerotia formed by ΔcptRNA-ipt after inoculation of intact rye plants with mycelial suspensions. Adapted from Hinsch *et al*., 2016.

Auxins

Plant growth and development is controlled by another group of hormones – auxins. They have been firstly described as diffusible factors affecting light oriented growth, and later first member of auxins– indole-3-acetic acid (IAA) was identified in *in vitro* bioassay (Bonner and Bandurski, 1952). IAA is the most abundant auxin in plants, therefore terms "auxin" and "IAA" are often interchangeable. Auxins are involved in cell elongation and stem proliferation, division and differentiation of cells in the cambium, or the initiation of root growth and the formation of lateral roots. An important role is in maintenance of apical dominance.

An overview of auxin biosynthesis, metabolism and degradation

Biosynthesis of auxins is complex, with many possible interconnected pathways (Figure 5). Amino acid L-tryptophan or indole compounds serve as precursors in Trp-dependent and Trp-independent pathway, respectively. As molecular and genetic basis of Trp-independent pathway remains mostly unknown, it will not be discussed.

Major biosynthetic pathway and the best studied in Arabidopsis is the two step conversion of Trp to IAA through indole-3-pyruvic acid (IPA) intermediate. First step is

catalyzed by tryptophan aminotransferase (EC 2.6.1.99), encoded by three gene homologues *TAA*, *TAR1* and *TAR2* (Stepanova *et al.*, 2008). IPA is converted directly to IAA by YUCCA (YUC) flavin-containing monooxygenase (EC 1.14.13.8), represented in Arabidopsis by 11 gene homologues (Cheng *et al.*, 2007). While these two enzymatic steps are essential for auxin biosynthesis, they were previously attributed to two different pathways. Connection between them was confirmed recently (Won *et al.*, 2011, Stepanova *et al.*, 2011). IPA pathway was not described in other organisms than plants, nevertheless IPA was detected in cultures of various fungi (Robinson *et al.*, 1998; Kulkarni *et al.*, 2013; this thesis). Current consensus is that IPA/YUC pathway is main auxin biosynthetic pathway in plants, conserved throughout the plant kingdom and that local auxin biosynthesis is necessary and sufficient for several developmental processes (Zhao, 2018). Additional pathway described involves decarboxylation of IPA by pyruvate decarboxylase into indole-3-acetaldehyde (IAAld), which is dehydrogenated into IAA by indole-3-acetaldehyde dehydrogenase (EC 1.2.3.7). Pathway was identified in maize smut fungus *Ustilago maydis* (Reineke *et al.*, 2008) and recently in fungal model *Neurospora crassa* (Sardar and Kempken, 2018). It is likely responsible for the auxins production by all *Fusarium* species as IPA and IAAld were detected in mycelium as well as in media of several FFC species (supplementary information in Niehaus *et al.*, 2016). However, IAAld could also be intermediate in tryptamine pathway and further research is inevitable for final description of Fusarium auxin biosynthesis. Tryptamine pathway named for tryptamine (TAM) intermediate was detected in Arabidopsis (Zhao *et al.*, 2001), rice (Ishihara *et al.*, 2008), and also in barley (Schneider *et al.*, 1972). In this pathway, Trp is decarboxylated by tryptophan decarboxylase (EC 4.1.1.28) to TAM, which was originally hypothesized to be converted to N-hydroxytryptamine (NHT) by flavin-containing monooxygenase YUCCA (Zhao *et al.*, 2001); YUCCA is now however confirmed to be part of IPA pathway, as described in previous text. Feeding experiments in pea (*Pisum sativum*) with deuterium-labeled intermediates confirmed that TAM is converted through IAAld to IAA, but the involvement of NHT could not be excluded (Quittenden *et al.*, 2009). TAM pathway was shown to be active in pea roots but not to operate in pea seeds (Tivendale *et al.*, 2010), implying that IAA biosynthesis is not uniform in every plant organ and more pathways cooperate to fulfill plant IAA demand. In transgenic tobacco plants overexpressing

tryptophan decarboxylase, high levels of TAM were not accompanied by increase of IAA (Songstad *et al.*, 1990).

Alternative IAA biosynthetic pathway is through indole-3-acetaldoxime (IAOx). Conversion of Trp to IAOx is catalyzed by cytochrome P450 enzymes CYP79B2 and CYP79B3 (EC 1.14.14.156) (Hull *et al.*, 2000). The physiological importance of IAOx-dependent IAA biosynthesis has been demonstrated by analysis of *cyp79b2 cyp79b3* double mutants, which have shorter hypocotyls and decreased IAA levels when grown at high temperatures (Zhao *et al.*, 2002). Arabidopsis plants overexpressing CYP79B2 accumulate indole-3-acetonitrile (IAN) (Zhao *et al.*, 2002), which is converted by nitrilase (EC 3.5.51) to IAA (Piotrowski *et al.*, 2001). IAOx was not detected in rice, maize, and tobacco, which do not have apparent CYP79B orthologues, and this pathway seems to be restricted to *Brassicaceae* (Sugawara *et al.*, 2009).

Another two-step biosynthetic pathway, with indole-3-acetamide (IAM) as intermediate, is widely utilized by microorganisms, especially by bacteria. IAA is formed via IAM in *Agrobacterium* (Camilleri and Jouanin, 1991) and also in some species of genus *Fusarium* (Tsavkelova *et al.*, 2012). Conversion is catalyzed by tryptophan-3-monooxygenase (iaaM, EC 1.13.12.13) and indole-3-acetamide hydrolase (iaaH). IAM was detected also in Arabidopsis (Pollmann et al., 2002); however further evidence of mutants affecting IAM pathway in plants is missing.

Overall, auxin production is present in broad range of organisms, from simple unicellular bacteria over filamentous fungi to complex green plants, and frequently more biosynthetic pathways cooperate in IAA biosynthesis.

Important aspect of auxin role in plant development is ability of cells/tissues to maintain concentration gradient, which is achieved by coordination of biosynthesis, degradation, conjugation and transport. Major route of IAA irreversible degradation in Arabidopsis is oxidation to 2-oxindole-3-acetic acid (oxIAA) (Östin *et al.*, 1998; Kowalczyk and Sandberg 2001; Pěnčík *et al.*, 2013). Reaction is catalyzed by dioxygenase AtDAO1 (Porco *et al.*, 2016). Disruption of *AtDAO1* did not affected IAA levels significantly, but loss of IAA degradation was compensated by strong increase of IAA conjugation. Formation of IAA conjugates represents another way of control of active IAA levels (reviewed in Ludwig-Müller 2011). Conjugation with amino acid leads to biologically inactive indole-3-acetic acid aspartic acid (IAA-Asp) and indole-3-acetic acid

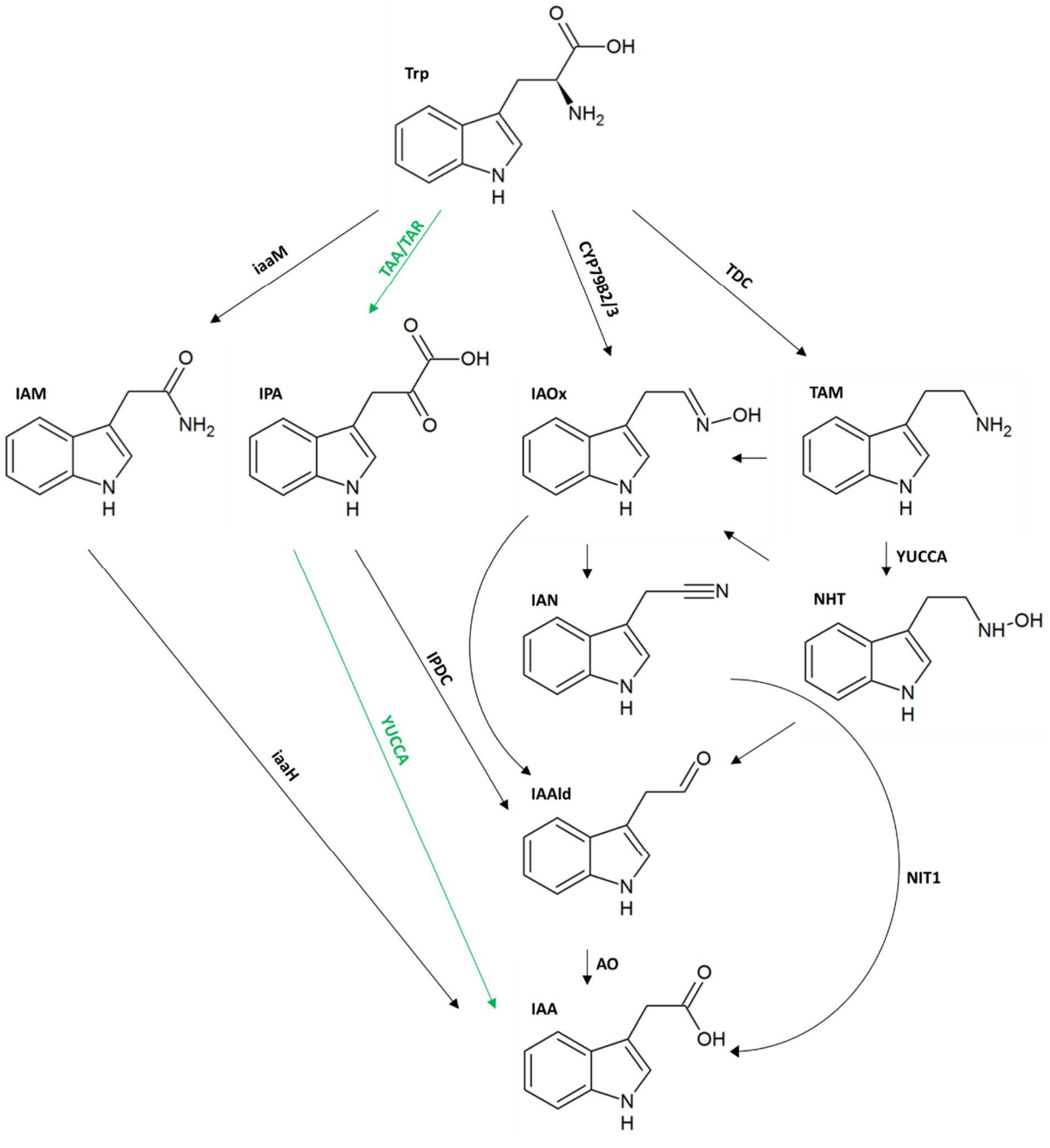

Figure 5 | Trp-dependent IAA biosynthesis pathways. Two-step pathway via IAM is catalyzed by tryptophan-3-monooxygenase (iaaM) and indole-3-acetamide hydrolase (iaaH). Alternatively, Trp can be deaminated into IPA by tryptophan aminotransferase (TAA, TAR), and then IPA is converted to IAA by flavin-containing monooxygenase YUCCA, identified only in plants (green arrows). Indole-3-pyruvic acid decarboxylase (IPDC) converts IPA to IAAld, which is converted to IAA by aldehyde oxidase. Conversion of Trp to IAOx is catalyzed by cytochrome P450 enzymes (CYP79B2/3). Nitrilase NIT1 converts indole-3-acetonitril IAN into IAA. Tryptophan is decarboxylated by tryptophan decarboxylase TDC to tryptamine (TAM); role of YUCCA in TAM conversion to N-hydroxytryptamine (NHT) is unlikely. When no enzyme is indicated, conversion is speculative and responsible enzyme is not known. Figure inspired by Tivendale *et al.*, 2014.

glutamic acid (IAA-Glu), which can also be further metabolized (Staswick *et al.*, 2005; Westfall *et al.*, 2010). The conversion of IAA to indole-3-acetic acid glucose (IAA-glc) is catalyzed by the UDP glucosyltransferase UGT84B1 (Jackson *et al.*, 2001). Conjugates constitute storage pool of inactive IAA, which can be released by hydrolysis.

Auxin transport and signaling

Early experiments on plant tropisms suggested that a mobile signal exists in the plant and it is transported through plant tissues in a highly controlled manner, for example, between the shaded and illuminated sides of a coleoptile (Went, 1974). The distribution of IAA in the plant body is realized over both short (cell to cell) and long distances (shoot to root). Auxin transport is carried over phloem fluid with photosynthetic assimilates by unique cell to cell mechanism of auxin gradient maintenance based on polar translocation across plasma membrane mediated by transporters. Polar auxin transport is explained by chemiosmotic hypothesis – pH of apoplast is slightly acidic and it enables part of IAA to stay in protonated form and enter cell. Cytosolic pH is almost neutral, which leaves IAA in deprotonated ionic form, which cannot passively leave cell and must be transported. Auxin translocation through plasma membrane against concentration gradient is mediated by PIN-forming (PIN) efflux carriers (Okada *et al.*, 1991; Petrášek *et al.*, 2006). PINs are necessary in early development of embryo, establishment of plant axis and correct growth of organs (Friml *et al.*, 2003; Benková *et al.*, 2003). Eight *PIN* genes were identified in Arabidopsis, differing in expression pattern and intracellular localization – PIN1-4 and PIN7 are localized on plasma membrane, while PIN5, PIN6 and PIN8 are localized on endoplasmic reticulum (ER; Mravec *et al.*, 2009; Bosco *et al.*, 2012; Bender *et al.*, 2013). The proposed role of ER localized PINs is the regulation of auxin homeostasis by subcellular compartmentalization, as auxin stored in ER lumen is presumably unavailable for polar transport and nuclear signaling. Furthermore, auxin in ER can serve as substrate for inactivation by ER-localized auxin conjugating enzymes (Mravec *et al.*, 2009). More recently PIN-likes (PILS) transporters have been functionally characterized as intracellular auxin translocators bound to endoplasmic reticulum essential for auxin availability for nuclear signalization (Barbez e*t al.*, 2012). Any Specific auxin transporter has not been functionally characterized in microbes so far, even though their orthologous genes are encoded in their genomes. Putative auxin efflux carrier (AEC) protein was detected in

Paenibacillus polymyxa and its sequence was used to determine various strains of *P. polymyxa* and *P. graminis* (Da Mota *et al.*, 2008), however evidence for auxin transport is missing.

Auxin signaling via auxin responsive transcription factors is subtly controlled by negative feed-back loop regulation of auxin receptor belonging to TRANSPORT INHIBITOR RESPONSE1/AUXIN SIGNALING F-BOX (TIR1/AFB) family and members of the Aux/IAA transcriptional repressor family (Tan *et al.*, 2007). Auxin acts as molecular glue bringing F-box proteins and interacting transcriptional repressor proteins together, leading to ubiquitination and subsequent degradation of repressor (for review see Leyser 2018). This signaling pathway was not identified in any organism outside plant kingdom so far.

Auxin role in host-pathogen interaction

Many different plant-associated bacteria are capable of IAA production, e.g. soil inhabiting genera such as *Pseudomonas, Rhizobium, Azotobacter, Klebsiella* (Apine and Jadhav, 2011). Roots exposed to optimal concentration of bacterial IAA have longer and more of lateral and primary roots. Auxin also participates in plant resistance against bacterial pathogens. When Arabidopsis plants were treated with fragment of flagellin (flg22), plants were more resistant to pathogen *Pseudomonas syringae* (Navarro *et al.*, 2006). Molecular basis of this resistance was described – plant exposure to flagellin induces expression of micro RNA that negatively regulates expression of nuclear auxin receptors by silencing. Repression of auxin signaling restricts *P. syringae* growth, which was proved also with mutant Arabidopsis plants overexpressing miR393 responsible for TIR1 silencing. On the other hand, overexpressing a TIR1 paralog that is partially resistant to miR393 enhances susceptibility to *Pseudomonas*. Bacterial IAA production and its role in host interaction is comprehensively discussed in recent review (Duca *et al.*, 2014).

Fungal IAA production is not associated only with plant-interacting fungal genera, suggesting innate auxin role for fungal development. Upon IAA treatment, yeast *Saccharomyces cerevisiae* develops into multicellular, pseudohyphal form (Prusty *et al.*, 2004; Rao *et al.*, 2010). Deletion of any amino acid/auxin:proton symport permeases with homology to plant AUX1 IAA transporters, makes yeast more resistant to IAA by

decreasing its uptake. This indicates that active auxin transport is important even in organism out of plant kingdom.

Auxin has often been suggested to play a role in the cross-talk between plant and fungal signaling during ectomycorrhizal establishment (Felten *et al.*, 2012). Beneficial endophyte *Piriformospora indica* is compromised in barley root colonization, when IAA biosynthesis gene is silenced (Hilbert *et al.*, 2012). The plant root colonizing and insect-pathogenic fungus *Metarhizium robertsii* has been shown to promote lateral root growth and root hair development of Arabidopsis (Liao *et al.*, 2017). When culture filtrate was applied to seedlings, IAA-regulated gene expression was activated, and application of culture filtrate to Arabidopsis mutant *rhd6* with root hair defective phenotype restored root hair growth (Figure 6). However, direct proof of the effect of fungus produced auxin on root hair development, using mutant of *M. robertsii* with complete loss of IAA production, is yet to be given.

Fusarium oxysporum is root-infecting pathogen with broad range of plant hosts, including model plant *Arabidopsis*. Disruption of auxin signaling genes led to resistance to *F. oxysporum* (Kidd *et al.*, 2011) and the same results were obtained with auxin transport mutants. Plants with mutated auxin efflux carrier PIN2/EIR1 had fewer root tips colonized (Diener, 2012). Auxin signaling is also required for resistance to necrotrophic pathogens such as *Botrytis cinerea* and *P. cucumerina* (Llorente *et al.*, 2008). Mechanisms by which auxin promotes colonization and symptom development are still enigmatic.

Some fungi induce tumors, for example corn smut causal agent *Ustilago maydis*. Fungal mutants affected in auxin production were still able to induce tumors in a similar manner to the wild-type strain, even though tumors contained a lower level of auxins (Reineke *et al.*, 2008). This suggests that auxin production by *U. maydis* is not required for the virulence of this pathogen. Likewise, auxins produced by phytopathogenic fungi *Aciculosporium take* (order Hypocreales) and *Magnaporthe oryzae* have been suspected of inducing morphological changes in the host plant called witches broom disease (Tanaka 2010; Tanaka *et al.*, 2011).

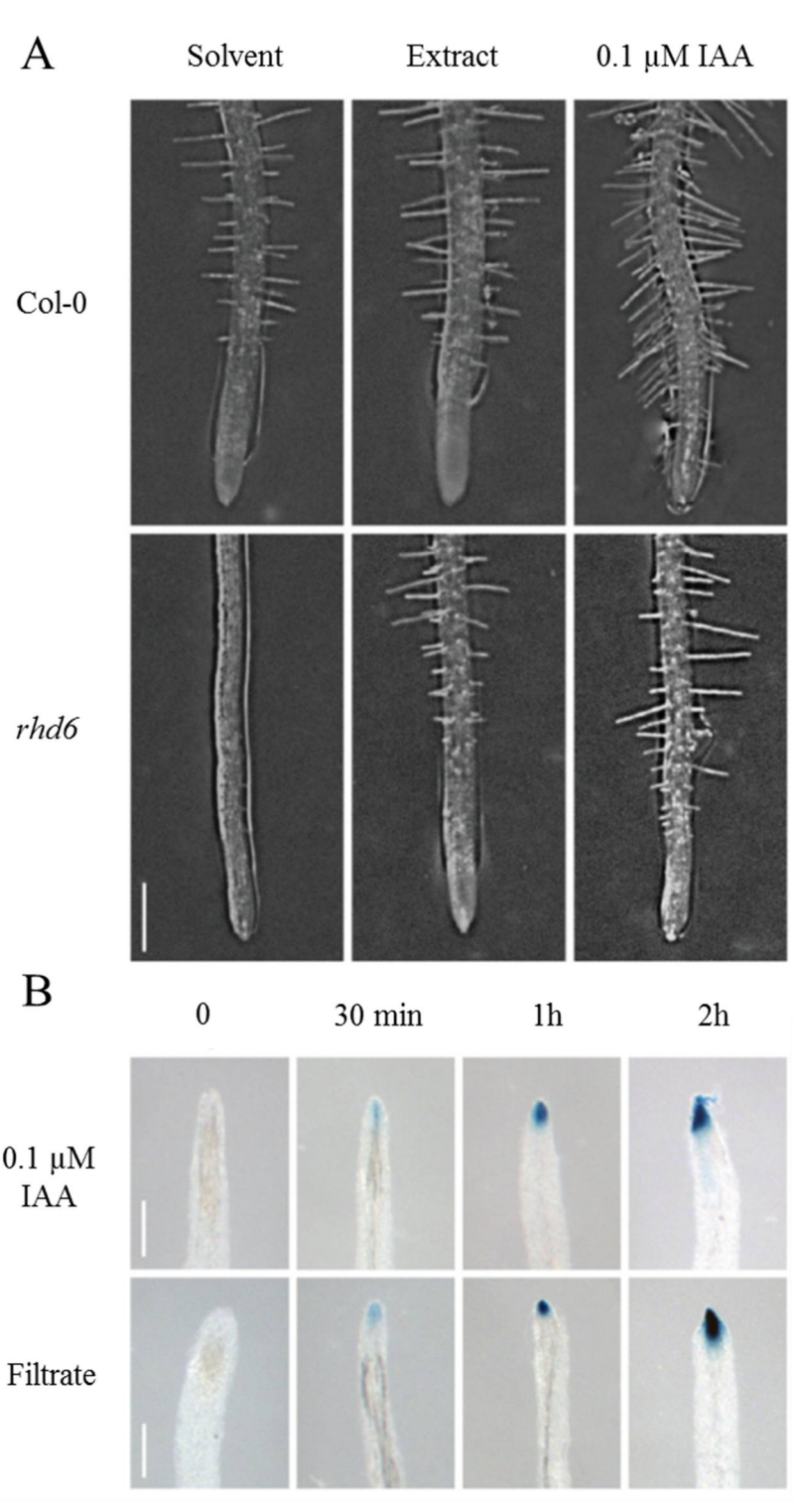

Figure 6 | Effects of *M. robertsii* in Arabidopsis. (A) Effect of methanol extract of culture filtrate on root hair in Arabidopsis WT Col-0 and mutant *rhd6*. (B) Induction of auxin-responsive genes expression by *M. robertsii* culture filtrate in Arabidopsis root tip. Adapted from Liao *et al*., 2017.

One of the most important and destructive fungal disease in cereal crops around the world – fusarium head blight – is caused by *Fusarium graminearum*. Yield loss is connected with grain contamination by mycotoxins (Bai and Shaner, 2004). *F. graminearum* can synthesize significant amounts of IAA, but exogenous IAA inhibited fungal biomass accumulation, increased hyphae branching (Figure 7), and delayed macroconidium germination (Luo *et al.*, 2016). Production of mycotoxin 15-acetyldeoxynivalenol was reduced after 1 mM IAN or IAA treatment, while slight increase of 15- acetyldeoxynivalenol was observed upon 0.1 mM IAA exposure.

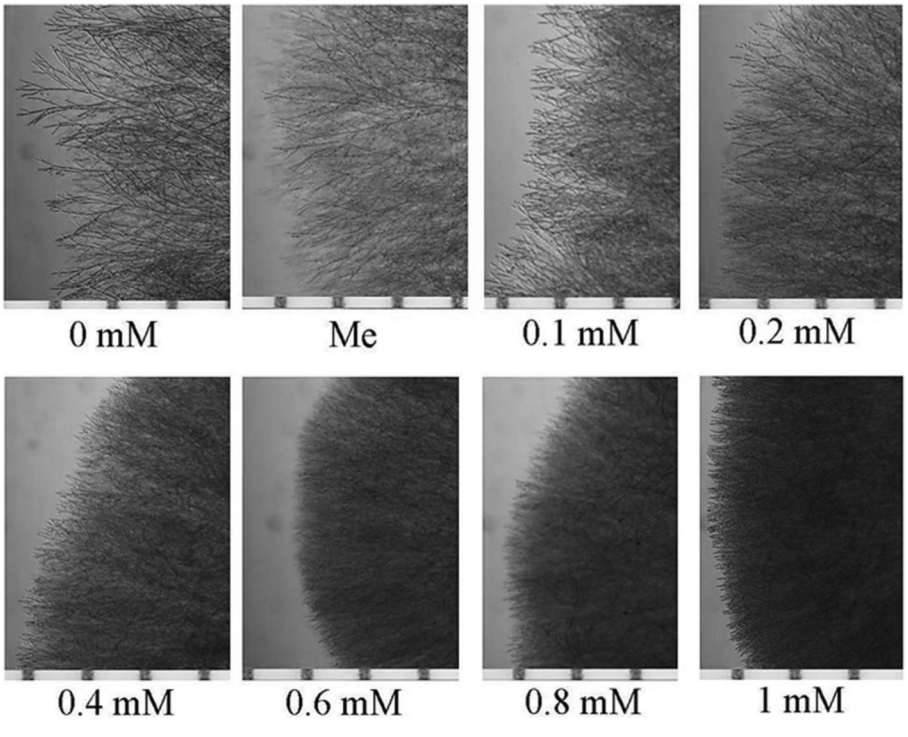

Figure 7 | Hyphal density of *F. graminearum* growing in the presence of increasing concentration of IAA. Plates were supplemented with different concentrations of IAA. 0 mM, untreated control; Me, control with methanol used to dissolve IAA (Luo *et al*., 2016).

Part III: Materials and methods

Fungal strains, media and growth conditions

The wild-type *C. purpurea* (Fr.) Tul. strain 20.1 (Hüsgen *et al*., 1999), a putatively haploid (benomyl-treated) derivative of the standard field isolate T5 (Fr.: Fr.) Tul. isolated from *Secale cereale* L. (Hohenheim, Germany), was used for the generation of mutants and as the wild type control in all experiments. Mycelia were grown on complete medium BII (Esser and Tudzynski, 1978) for cultivation and DNA isolation. Conidia were obtained from mycelia cultivated on Mantle medium (Mantle and Nisbet, 1976). For the cytokinin and auxin measurements, strains were grown in liquid BII or Mantle medium (without yeast extract, 30 g/l sucrose), in both cases on rotary shaker (250 rpm). All strains were cultivated in the dark at 26°C. Vector construction using the yeast recombinational method was performed in *Saccharomyces cerevisiae* strain FY834 (Winston *et al*., 1995).

F. fujikuroi (Ff) GA-producing strain IMI58289 was used (Commonwealth Mycological Institute, Kew, United Kingdom). The mango pathogen *F. mangiferae* MRC7560 (Fm), originating in Israel, is deposited in the culture collection of the Medical Research Council (MRC) (Tygerberg, South Africa). *F. verticillioides* M-3125 (Fv) (Fungal Genomics Stock Centre, Kansas State University, FGSC 7600) was provided by Robert Proctor and Daren W. Brown, United States Department of Agriculture, United States, respectively.

Plant material

Claviceps pathogenicity assays were performed using the cytoplasmic male sterile *S. cereale* Lo37-PxLo55-N (KWS Lochow GmbH) cultivar, which was cultivated in growth chambers under conditions of 15 h light (8000 Lux; 16–18°C)/9 h darkness (13–15°C). Before planting, seeds were stratified for 5–6 weeks at 1–2°C and vernalization took place in soil/compost 3:2 at 14–15°C (day) and 9–10°C (night) with 9 h light (6000–10 000 Lux). For *in planta* pathogenicity assays, florets of blooming ears (30–40 per ear) were inoculated with 5 µl of a suspension containing about 10^6 per ml conidia collected from Mantle agar. To avoid cross-contamination, the ears were covered with paper bags directly after inoculation.

Hybrid white sweet maize seeds variety Silver Queen (Johnnyseeds, United States) were sterilized by first soaking in 4% sodium hypochlorite for 10 min, rinsed twice with sterile water, and then soaking in 70% ethanol for 1 min and rinsed twice with sterile water. Seeds were inoculated by soaking in water containing 10^6 Fusarium spores per ml in a flask on a rotary shaker overnight (120 rpm). Inoculated seeds were dried for 2 h on air and placed in a Petri dish with moistened filter paper to germinate in the dark at 26°C. After 2 days, germinated seeds were moved into a hydroponic system consisting of plastic boxes with Hoagland solution. Seedlings were incubated in a growth chamber with a light/dark cycle (16 h/8 h) at the constant temperature of 25°C for 1-10 days. Roots and shoots of infected maize seedlings were separated and lyophilized before gene expression analysis.

Nucleic acid extraction and analysis

Standard recombinant DNA methods were used as described in Sambrook *et al.* (1989) and Ausubel *et al.* (1987). Genomic DNA from *C. purpurea* was prepared from lyophilized mycelia according to Cenis (1992). All PCR methods were performed according to user manual, diagnostic PCR using GoTAQ polymerase (Promega), and PCR amplifications of fusion proteins or complementation fragments were performed using the proof reading Phusion polymerase (Finnzymes). All primers used are listed in Table S1 and were synthesized by Sigma-Aldrich. Southern blotting was performed using Hybond-N + nylon filters (Amersham) according to the manufacturer's protocol. Filters were hybridized using RNA DIG-UTP labelled probes (Roche). DNA sequencing was carried out by commercial sequencing services. Protein and DNA sequence alignment, editing and organization were done with BioEdit (Hall, 1999). Further sequence analyses were performed using BLAST at the National Center for Biotechnology Information, Bethesda, MD, USA (Altschul *et al.*, 1997).

Replacement and complementation vector construction

All Claviceps transformation vectors were generated using the yeast recombinational cloning method (Colot *et al.*, 2006). Complementation and fusion protein vectors were constructed based on the described vector system (Christianson *et al.*, 1992; Schumacher, 2012).

The flanking regions of *CpAEC* were amplified with the following primers containing overlapping sequences towards the yeast shuttle-vector pRS426 or the phleomycin resistance cassette: (XbaI) 5F_Aec/5R_Aec for the 5′- spanning region (1212 bp); 3F_Aec/3R_Aec (EcoRI) for the 3′- spanning region (1221 bp). The PCR products, the linearized yeast shuttle vector pRS426 (Colot *et al*., 2006) and the phleomycin resistance cassette (amplified with primers CpBleF1/CpBleR1 from pRS426CpBle; 1847 bp) were transformed into yeast strain FY834 for homologous recombination. DNA was isolated from yeast cells using the SpeedPrep yeast plasmid isolation kit (DualSystems) and transformed into *E. coli* TOP10. After DNA isolation, restriction with XbaI/EcoRI resulted in a 3871 bp fragment that was used to transform the 20.1 strain of *C. purpurea*. For construction of the complementation vector pComp_nat_AEC, a 2777 bp fragment containing the coding region of *cpaec* as well as the sequences 949 bp upstream of it were amplified using the primers AEC_Compl_natP_fw/AEC_Compl_tgluc_rev, which contain overlapping sequences to the vector sequence of pNDH-OGG (linearized by SpeI/NotI) for homologous recombination. For construction of the complementation vector pComp_Olic_AEC, where AEC expression is driven by constitutive promotor OliC (Bailey *et al.*, 1989), a 1828 bp fragment of *CpAEC* was amplified with primers AEC_oliC_fw/AEC_Compl_tgluc_rev, which contain overlapping sequences to the vector sequence of pNDH_OGG (linearized by NcoI/NotI). The obtained plasmids were used to transform the *C. purpurea* Δcpaec mutant strain.

Fusion protein constructs

For protein localization, the C-terminal GFP fusion vector pLoc_AEC_GFP was prepared. A 1828 bp *CpAEC* genomic ORF sequence was amplified using primers AEC_Compl_oliC_fw/AEC_Compl_tgluc_rev, containing overhangs for vector pNDH-OGG (linearized by NcoI), where expression is driven by constitutive promotor OliC (Bailey *et al.*, 1989).

Fungal transformation

Protoplasts were prepared from *C. purpurea* strains as described previously (Jungehülsing *et al*., 1994). Integration events were confirmed by diagnostic PCR using specific primers as indicated (Table S1, Figure S2). Single spore isolation was carried out to obtain

homokaryons of putative transformants. Additionally, Southern blot analyses were performed with each deletion mutant to confirm single integration events. For complementation of Δcpaec, the mutants were transformed with 10 µg of pComp_nat_AEC or pComp_OliC_AEC. For localization of fusion protein AEC-GFP, *C. purpurea* 20.1 was transformed with 10 µg of pLoc_AEC_GFP.

Expression studies and quantitative RT-PCR

For detection of rye gene expression, cDNA of *Claviceps purpurea* 20.1 infected and uninfected plant material was analyzed. For detection of maize and Fusarium gene expression, roots and shoots of maize seedlings grown in a hydroponic system and infected by wild-type strains of *F. mangiferae*, *F. verticillioides* and *F. fujikuroi* were used. Total RNA was isolated using the RNAqueous kit and Plant RNA Isolation Aid solutions (Life Technology). The isolated RNA was treated twice with Ambion's TURBO DNase-free kit (Life Technology), and first-strand cDNA was synthesized using the RevertAid First Strand cDNA Synthesis Kit with an oligo(dT) primer (Thermo Scientific). qPCR reactions were performed with TaqMan Gene Expression Master Mix on a ViiA7™ Real-Time PCR System (Thermo Fisher Scientific) using a default program. Primers and Taqman probes for all rye, maize and fungal genes are listed in Table S1, primers were designed using PRIMER EXPRESS 3.0 (Life Technology).

Each rye sample was processed in four biological replicates, and at least two technical replicates were run for each biological replicate. Cytokinin-related gene sequences with detectable expression in developing rye ears were identified in RNA-seq data generated from a library prepared from infected rye ears (Oeser *et al.*, 2017), as at the time of experimental work public reference genome of rye was not available. Genes for *RR*, *HK* and *LOG* were numbered based on the closest rice orthologues (Ito and Kurata, 2006; Kurakawa *et al*., 2007) while those for *CKX*, *IPT*, β-actin and elongation factor 1 were based on barley orthologues (Mrízová *et al*., 2013). Predicted sequences were deposited in the NCBI database. Expression values were determined and statistically evaluated using DATAASSIST v3.0 (Life Technologies).

The maize target genes used were identified in a previous study (Vyroubalová *et al.*, 2009). For each condition, the three independent biological replicates were analyzed in three technical replicates. Expression of fungal genes was measured by absolute

quantification, whereas maize gene expression was obtained by relative quantification according to ΔΔCt method (Schmittgen and Livak, 2008). To ensure that primers amplified the desired gene target, amplicons for every primer pair were cloned into the pDRIVE vector (Qiagen) and sequenced. The cloned PCR products were also used as template to determine PCR efficiency and absolute levels of gene transcript in isolated RNA. The relative expression of the maize genes was normalized with respect to β-actin (BT086225) and elongation factor 1 (AF136829.1) gene expression.

Production of recombinant proteins

The coding regions of *CpIPT-LOG* and *CpLOG* as well as the IPT domain of *CpIPT-LOG* (from the start codon to the beginning of the intron at position 880) and the LOG domain of *CpIPT-LOG* (from ATG at position 1055 to the stop codon) were synthesized with codon optimization for *E. coli* expression by GeneArt service (Invitrogen) and subcloned with *Nde*I and *Hind*III overhangs into the pET28b(+) vector to generate N-terminal His-tagged recombinant proteins. *E. coli* BL21 Star (DE3) transformed with these constructs was grown in Luria-Bertani medium supplemented with kanamycin (50 μg ml^{-1}) at 37°C until the OD_{600} reached 0.6. Expression was induced by 0.4 mM isopropyl β-D-1-thiogalactopyranoside, after which the cells were incubated for 17 h with vigorous shaking at 18°C. Cells harvested by centrifugation (3000 *g*, 10 min) were suspended in lysis buffer (50 mM phosphate buffer, pH 8.0, supplemented with 0.3 M NaCl, 20% glycerol and 1 mM phenylmethylsulfonyl fluoride) and then disrupted using a French press at 25 000 psi. The cell lysate was clarified by centrifugation at 20 000 *g*, after which the supernatant was repeatedly loaded onto an equilibrated HisPur Cobalt column (Thermo Scientific) overnight. The column was subsequently washed with lysis buffer supplemented with 20 mM and 60 mM imidazole. The protein was then eluted with 120 mM imidazole, dialyzed against lysis buffer and concentrated using an ultrafiltration cell with a 10 kDa cutoff membrane.

IPT and LOG activity assay

Purified protein (25–70 μg) was added to the reaction mixture consisting of buffer (IPT or IPT-LOG coupled reaction: 30 mM Tris/acetate, pH 8.0; supplemented with 1 M betaine, 20 mM $MgCl_2$ and 5 mM β-mercaptoethanol; LOG reaction: 100 mM potassium phosphate

buffer, pH 7.0) and corresponding substrate. Kinetic parameters were determined using a reaction mixture containing 100 μM DMAPP or HMBDP (Echelon Biosciences, Salt Lake City, UT, USA) as the donor substrate and 0.5–25 μM AMP, ADP or ATP as the acceptor, or 100 μM AMP as acceptor and 0.5–25 μM DMAPP or HMBDP as donor respectively. In the case of LOG reaction, isopentenyladenosine 5'-monophosphate (iPRMP), *trans*-zeatin riboside 5'-monophosphate (tZRMP), *cis*-zeatin riboside 5'-monophosphate (cZRMP) (OlChemIm, Olomouc, Czech Rebublic) and the corresponding diphosphates and triphosphates (BIOLOG Life Science Institute, Bremen, Germany) were used as substrates at concentrations of 1–50 μM. After incubation for 10 min (or 30 min with weak substrates) at 30°C, the reactions were stopped by adding an equal volume of ethanol and heated for 5 min at 90°C. The samples were then purified by passage through 0.22 μm nylon filters and injected onto a C18 reverse-phase column (ZORBAX RRHD Eclipse Plus 1.8 μm, 2.1 × 50 mm; Agilent) coupled to an ultra-performance liquid chromatograph (Shimadzu Nexera). The column was eluted with a linear gradient of 15 mM ammonium formate, pH 4.0 (A) and methanol (B): 0 min, 5% B; 2–8 min, 70% B; flow rate of 0.40 ml min^{-1}; column temperature of 40°C. Peak areas were compared with those of injected standards (OlChemIm), and activity was calculated using LABSOLUTIONS software (Shimadzu). Kinetic parameters were calculated using GRAFIT Version 4.0.12. To determine the kinetic parameters of CpIPT-LOG for reactions involving DMAPP or HMBDP and AMP, excess (1 μg) CpLOG was added to the reaction mixture and a reaction rate was calculated in terms of newly formed iP.

Preparation of transgenic Arabidopsis plants

The cDNA sequences of *CpIPT-LOG*, *CpLOG* and the IPT domain of *CpIPT-LOG* were subcloned with *Asp718* and *Xba*I overhangs into a binary pBINHygTx vector downstream of the *CaMV 35S* promoter (Gatz *et al.*, 1992). The cDNA sequence of *CpAEC* was cloned with *AscI* and *SpeI* overhangs into pER8 vector, under control of estrogen inducible promotor (Zuo *et al.*, 2001). *Agrobacterium tumefaciens* strain GUS3101 harboring the binary vector with different transgenes was used to transform the *A. thaliana* ecotype Col-0 via the flower-dip procedure with vacuum infiltration (Clough and Bent, 1998). Transformed *Arabidopsis* plants were grown in a greenhouse until seed production. T1 progeny seeds of *Arabidopsis* transformants were surface sterilized and germinated on

Murashige–Skoog phytagel (pH 5.7) supplemented with hygromycin (30 mg l^{-1}) in a controlled environment chamber (12 h light, 5000 Lux, 21°C/12 h darkness, 18°C). Resistant seedlings were transferred to soil and placed in the greenhouse. Several homozygous lines for each construct with a single integration were selected from T2 progeny. For estradiol induction of *CpAEC* expression in transgenic plants, seeds were transferred on plates containing 17-β-estradiol (2 µM). Root lengths were calculated with EZ RHIZO software (Armengaud *et al.*, 2009).

Cytokinin measurements

Levels of cytokinin metabolites were determined in mycelium or cultivation medium. Freeze-dried mycelium was homogenized in mortar with pestle and liquid nitrogen. Stable isotope-labelled cytokinin internal standards (OlChemIm) were added, each at 1 pmol per sample, to check the recovery during the purification and to validate the determination. The samples were extracted with methanol/H_2O/formic acid (15:4:1, v/v/v), and clarified supernatants were subjected to solid phase extraction. First, non-polar compounds were removed on Speed SPE Octadecyl C18 cartridges (Applied Separation). Subsequently, basic compounds together with cytokinins were retained on Oasis MCX cartridges (Waters). The eluates were evaporated to dryness and the obtained solids dissolved in 20 µl of the mobile phase used for quantitative analysis. The samples were analyzed by ultra-high-performance liquid chromatography (Acquity UPLC; Waters) coupled to a Xevo TQ-S (Waters) triple quadrupole mass spectrometer equipped with an electro-spray interface. The purified samples were injected onto a C18 reversed-phase column (BEH C18; 1.7 µm; 2.1 × 50 mm; Waters). The column was eluted with a linear gradient (0 min, 10% B; 0–8 min, 50% B; flow-rate of 0.25 ml min^{-1}; column temperature of 40°C) of 15 mM ammonium formate (pH 4.0, A) and methanol (B). Quantification was achieved by multiple reaction monitoring of $[M + H]^+$ and the appropriate product ion. Quantification was performed with the MASSLYNX program (Waters) using a standard isotope dilution method. The ratio of endogenous cytokinin to the appropriate labelled standard was determined and further used to quantify the level of endogenous compounds in the original extract, according to the known quantity of the added internal standard.

Auxin measurements

Levels of the auxin IAA and IAA metabolites were determined in mycelium or cultivation medium using the method described by Novák *et al.* (2012). Freeze-dried mycelium was homogenized in mortar with pestle and liquid nitrogen. Briefly, approx. 1 mg of freeze-dried mycelia or 100 µl of media was extracted with 1 ml cold phosphate buffer (50 mM; pH 7.0) containing 0.1% sodium diethyldithiocarbamate, supplemented with internal standards. After centrifugation at 20 000 rpm for 10 min, one half of each sample was acidified with 1 M HCl to pH 2.7 and purified by solid phase extraction (SPE) using Oasis^{TM} HLB columns (30 mg, 1 ml; Waters, USA). For quantification of IPA, the second half of the sample was derivatized by cysteamine (0.25 M, pH 8.0) for 1 hour, acidified with 3 M HCl to pH 2.7 and purified by SPE. After evaporation under reduced pressure, samples were analyzed for auxin content using Acquity UHPLC (Waters, USA) linked to a triple quadrupole mass detector (Xevo TQ MSTM; Waters, USA).

Microscopic analyses

For microscopy of fusion proteins, mycelial plugs of the strains were cultivated in Gamborg B-5 basal salt mixture (Sigma-Aldrich), supplemented with 10 mM glucose and solidified with 1% agarose, on glass slides overnight. Fluorescence and light microscopies were performed with a Zeiss AxioScope A1 microscope. Green fluorescent protein (GFP) fluorescence was examined with filter set: excitation BP 455-483, beam splitter FT 493 and emission BP 199-529). Hoechst 33258 fluorescence was investigated using filter set: excitation BP 375-395, beam splitter FT 405 and emission BP 410-440).

Part IV: Biosynthesis of cytokinins in the biotrophic fungus *Claviceps purpurea*

Results

Cytokinin profile of rye ears is altered after ergot infection

Disease symptoms of some phytopathogenic fungi are associated with changes in cytokinin levels (Behr *et al.*, 2012; Jiang *et al.*, 2013). To analyze the cytokinin profile of *C. purpurea*-infected rye (*Secale cereale*) ears, samples of infected plant tissue were taken 5 and 10 days post inoculation (dpi), corresponding to the host tissue colonization phase and the sphacelial stage respectively. In control plants (unpollinated rye ears), zeatin-type cytokinins were significantly more abundant than iP, with cZ and DHZ riboside O-glucosides being the dominant forms (Table 1). Shortly after fungal inoculation (5 dpi), the levels of iP increased significantly, as did those of its riboside and 9-glucoside, but the levels of zeatin derivatives remained unchanged. Later, when the sphacelial tissue started to form (10 dpi), the levels of both iP- and tZ-type cytokinins decreased; this trend was especially pronounced for the nucleotides (Table 1). The overall levels of cZ derivatives did not change greatly, but the abundance of the free base and nucleotide forms increased dramatically at the expense of the O-glucoside storage forms (Table 1). The cytokinin content was also measured in infected ears at a later time point (approximately 25 dpi), when sclerotia accounted for the bulk of the mass of the analyzed material, and compared with that of noninfected sterile ears (Table 2). The total content of tZ and iP derivatives in the sclerotia was between 2 and 10 times greater than in the uninfected tissue; the tZ derivative profile was dominated by the free base, riboside and storage O- and N-glucosides. Increased levels of cytokinins, particularly iP derivatives, were observed in infected plants at 5 dpi and during the sclerotial phase (25 dpi), but the CK levels of the infected plants were lower than those of untreated controls at around 10 dpi (Table 1; Table 2). These results show that the hormonal levels of infected and uninfected rye tissues differ significantly.

Table 1 | Cytokinin contents of infected and mock-treated rye ears 5 and 10 dpi.

	5 dpi			10 dpi		
CK metabolite	Mock	20.1 infected	%	Mock	20.1 infected	%
iP	3.91 ± 0.83	8.76 ± 1.15*	224	7.58 ± 1.81	8.73 ± 1.74	115
iPR	12.17 ± 2.97	24.88 ± 5.89*	205	13.16 ± 3.24	5.09 ± 1.25*	39
iPRMP	16.05 ± 2.82	12.56 ± 2.06	78	25.75 ± 6.24	4.79 ± 1.13*	19
iP9G	3.61 ± 1.01	6.16 ± 1.46	171	12.00 ± 2.60	4.85 ± 0.88*	40
Total iP type	35.74	52.36	147	58.49	23.46	40
tZ	55.32 ± 4.46	58.06 ± 8.00	105	95.11 ± 19.22	62.16 ± 5.73*	65
tZR	8.89 ± 2.25	8.70 ± 2.28	98	18.49 ± 3.63	13.65 ± 2.72	74
tZRMP	158.18 ± 35.74	152.01 ± 33.49	96	325.88 ± 35.55	118.58 ± 35.80*	36
tZOG	37.71 ± 11.09	32.26 ± 9.67	86	47.72 ± 15.17	53.71 ± 12.38	113
tZROG	14.02 ± 1.25	14.45 ± 2.38	103	21.60 ± 1.28	19.37 ± 1.81	90
tZ9G	83.34 ± 14.46	80.17 ± 15.11	96	265.69 ± 70.78	139.16 ± 23.98*	52
Total tZ type	357.46	345.67	97	774.49	406.63	53
cZ	11.07 ± 2.37	7.21 ± 1.34	65	8.50 ± 0.27	51.81 ± 4.00*	610
cZR	9.84 ± 2.77	8.70 ± 1.68	88	11.27 ± 0.68	14.66 ± 2.08*	130
cZRMP	LOD	LOD		LOD	55.75 ± 22.73*	
cZOG	330.15 ± 36.42	370.27 ± 34.83	112	380.89 ± 79.53	365.76 ± 45.17	96
cZROG	395.07 ± 45.06	375.71 ± 13.17	95	462.66 ± 41.50	299.32 ± 21.35*	65
Total cZ type	746.13	761.89	102	863.32	787.30	91
DHZ	7.47 ± 0.58	3.03 ± 0.63*	41	9.19 ± 1.17	33.37 ± 7.44*	363
DHZR	16.99 ± 1.92	6.63 ± 1.27*	39	19.44 ± 5.04	35.40 ± 4.28*	182
DHZRMP	3.69 ± 0.62	1.96 ± 0.40*	53	4.55 ± 0.98	4.52 ± 0.88	99
DHZOG	47.13 ± 14.48	57.14 ± 17.40*	121	131.07 ± 28.25	188.58 ± 37.48*	144
DHZROG	269.59 ± 42.93	288.75 ± 48.46	107	561.58 ± 157.7	198.14 ± 24.25*	35
Total DHZ type	344.87	357.51	104	725.83	460.01	63

Percentages indicate the concentration of the relevant cytokinin in the infected plants relative to that in the mock-treated controls. Four biological replicates of infected and mock ears in both time-points were analyzed, each replicate in two technical replicates. Concentrations are in pmol per g of fresh weight. The asterisk indicates significant difference between mock and infected tissue according to Student's unpaired t-test at $P \leq 0.05$.
cZOG, cZ O-glucoside; cZR, cZ riboside; cZROG, cZR O-glucoside; DHZOG, DHZ O-glucoside; DHZR, DHZ riboside; DHZRMP, DHZR 5′-monophosphate; DHZROG, DHZR O-glucoside; iP9G, iP 9-glucoside; LOD, limit of detection; tZ9G, tZ 9-glucoside; tZOG, tZ O-glucoside; tZR, tZ riboside; tZROG, tZR O-glucoside.

Table 2 | Cytokinin content in infected rye ears with fully developed sclerotia and non-infected sterile rye ears (25 dpi).

CK metabolite	Mock	CpGal404 infected	%
iP	4.63 ± 2.52	7.59 ± 3.04	164
iPR	5.07 ± 3.22	3.32 ± 1.47	66
iPRMP	4.53 ± 1.04	5.79 ± 1.93	128
iP9G	4.17 ± 2.63	24.28 ± 9.08*	582
Total iP-type	**18.40**	**40.98**	**223**
tZ	42.51 ± 25.98	261.50 ± 93.94*	615
tZR	10.43 ± 2.65	90.19 ± 43.35*	865
tZRMP	18.54 ± 11.70	24.64 ± 11.97	133
tZOG	51.74 ± 33.12	1107.25 ± 78.60*	2140
tZROG	13.42 ± 9.04	229.82 ± 37.59*	1713
tZ9G	91.83 ± 50.43	620.81 ± 202.14*	676
Total tZ-type	**228.47**	**2334.21**	**1022**
cZ	7.02 ± 1.45	112.06 ± 15.59*	1597
cZR	7.07 ± 1.45	29.90 ± 7.92*	423
cZRMP	1.93 ± 0.81	33.08 ± 5.39*	1715
cZOG	360.60 ± 34.63	295.85 ± 57.20*	82
cZROG	1543.84 ± 660.51	277.67 ± 80.36*	18
Total cZ-type	**1920.48**	**748.56**	**39**
DHZ	1.65 ± 1.09	28. 31 ± 15.09*	1717
DHZR	6.51 ± 4.50	20.39 ± 11.12*	313
DHZRMP	0.19 ± 0.14	1.49 ± 0.72*	777
DHZOG	15.02 ± 10.33	45.28 ± 7.95*	302
DHZROG	338.88 ± 258.70	45.63 ± 5.48*	13
Total DHZ-type	**362.25**	**141.10**	**39**

Three biological replicates of infected and mock ears were analyzed, each replicate in two technical replicates. Spores of *Claviceps purpurea* strain Gal404 (Teva Czech Industries, Opava, Czech Republic) was used to infect sterile *Secale cereale* hybrid Lo115-PxLo114-N plants (KWS Lochow GmbH) in a small field experiment in the 2012 season in Olomouc, Czech Republic. Concentrations are in pmol g fresh weight-1. iP, isopentenyladenine; iPR, isopentenyladenosine; iPRMP, iPR 5'-monophosphate; iP9G, iP 9-glucoside; tZ, *trans*-zeatin; tZR, tZ riboside; tZRMP, tZR 5'-monophosphate; tZOG, tZ O-glucoside; tZROG, tZR O-glucoside; tZ9G, tZ 9-glucoside; cZ, *cis*-zeatin; cZR, cZ riboside; cZRMP, cZR 5'-monophosphate; cZOG, cZ O-glucoside; cZROG, cZR O-glucoside; DHZ, dihydrozeatin; DHZR, DHZ riboside; DHZRMP, DHZR 5'-monophosphate; DHZOG, DHZ O-glucoside; DHZROG, DHZR O-glucoside; *indicates significant difference between mock and infected tissue according to Student's unpaired t-tests at $P \leq 0.05$.

Rye perceives a cytokinin signal in early infection stages

To analyze the host's cytokinin metabolism during the infection process, quantitative real-time polymerase chain reaction (qPCR) of cytokinin-related rye genes was performed. Infected plant tissue was sampled shortly after infection and during the colonizing and the sphacelial stages, using mock-treated plants as controls. The expression of 10 cytokinin biosynthesis genes, including three *IPT* and seven *LOG* genes, and eight genes encoding cytokinin-degrading enzymes were analyzed. In addition, because cytokinin signal

transduction in plants is mediated by a His-Asp phosphorelay, the expression of the putative histidine kinase and six type A response regulator genes was also investigated (Figure 8). Clear differences were detected in the early infection stage: the infected rye plants exhibited strongly enhanced expression of five *CKX* genes (*ScCKX2.1*, *ScCKX2.2*, *ScCKX4*, *ScCKX8*, *ScCKX9*) as well as the sensory *HK* gene (*ScHK2*). The expression of three *RR* genes (*ScRR4*, *ScRR9*, *ScRR11*) was also induced in infected plants; together these results indicate the perception of a new cytokinin signal during this phase. However, only one *IPT* gene (*ScIPT10*) and one *LOG* gene (*ScLOG7*) were upregulated within the plant tissue, while two *LOG* genes (*ScLOG1*, *ScLOG5*) appeared to be downregulated relative to the uninfected control. In the colonizing phase, two *CKX* genes (*ScCKX4*, *ScCKX8*) and one *RR* gene (*ScRR9*) remained upregulated, but the expression of the plant's *IPT* genes did not differ significantly from that in the controls. In the sphacelial stage, *ScRR9* remained upregulated, but three other *RR* genes were downregulated. The expression of the host plants´ cytokinin biosynthesis and cytokinin-degrading genes was virtually identical to that in the uninfected controls during this phase (Figure 8). Overall, these data indicate that infected plants perceive a cytokinin signal, especially in the early stages of infection, but there is no pronounced change in the expression of the host plant's cytokinin biosynthesis genes.

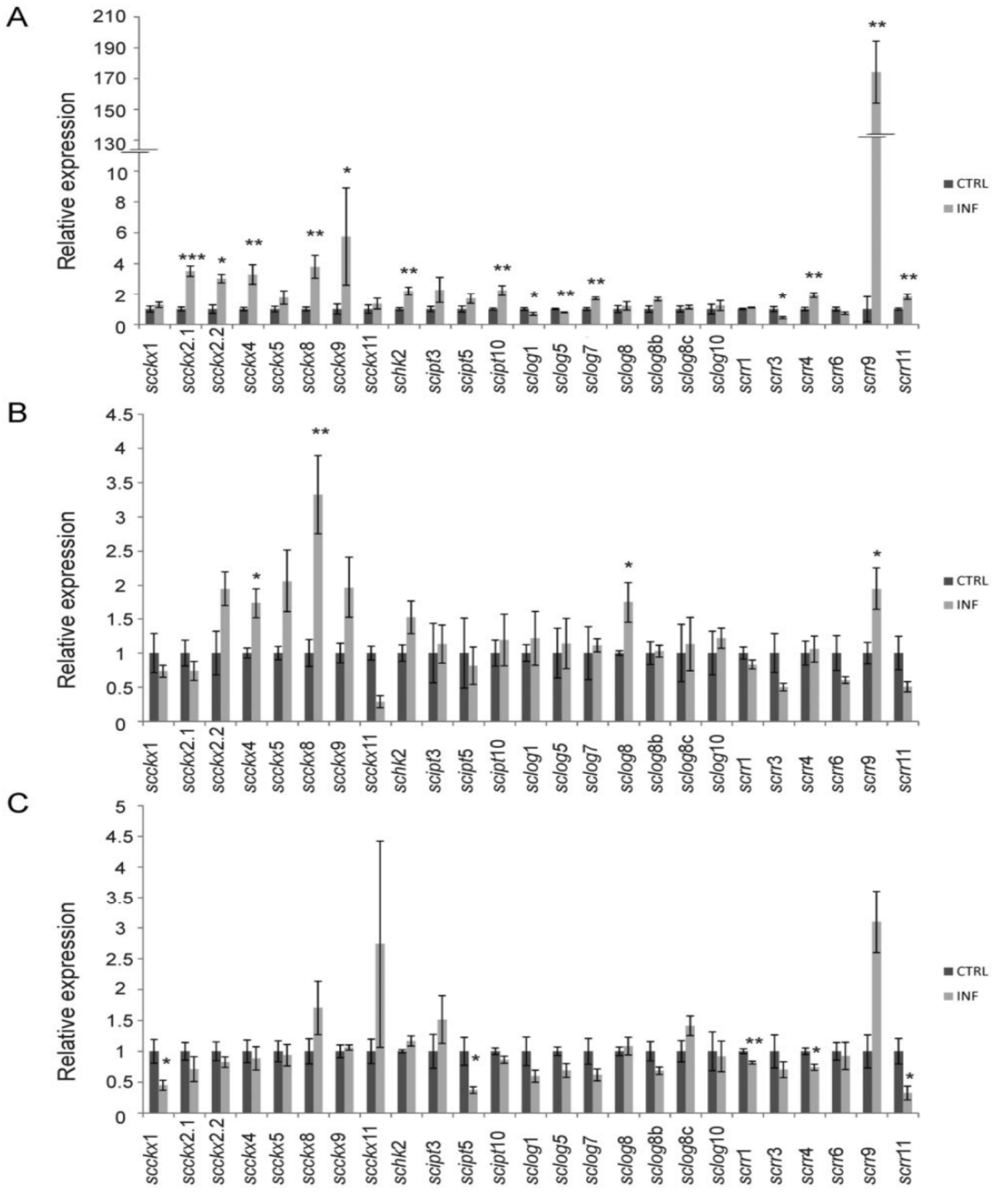

Figure 8 | Cytokinin metabolite gene expression of host plants during infection. The expression levels of cytokinin metabolite genes (cytokinin dehydrogenases, *scckx*; His-protein kinase, *ScHK*; adenylate isopentenyltransferase, *ScIPT*; cytokinin-specific phosphoribohydrolase 'lonely guy', *ScLOG*; response regulators, *ScRR*) were determined in ovaries infected with *Cp*20.1 (INF) and mock-treated ovaries (CTRL) (A) 3, (B) 6 and (C) 9 dpi. Expression levels were normalized against those of the rye housekeeping genes *ScEF1* (elongation factor 1) and *ScACT* (β-actin). Measurements were done in two technical and four biological replicates in each group. The single, double and triple asterisks (*, ** and ***) indicate significant differences between INF and CTRL according to Student's unpaired *t*-tests at $P \leq 0.05$ (n = 4); 0.01 and 0.001 respectively.

Identification of cytokinin biosynthetic genes in *C. purpurea*

To identify fungal proteins homologous to those that catalyze cytokinin biosynthesis in plants, BLASTp searches were performed against the Cp20.1 database (Schardl *et al.*, 2013). Using the sequence of LOG5 from *Arabidopsis thaliana* as a query, two annotated open reading frames were detected: *CPUR2269*; (E= 1.8×10^{-36}) and *CPUR4177* (E= 1.5×10^{-23}). The putative gene *CPUR2269* (794 bp, one 70 bp intron) encodes a protein of 240 amino acids (aa). Like plant *LOG*s, the gene product was annotated as a lysine decarboxylase and contains a cytokinin riboside 5' monophosphate phosphoribohydrolase domain (IPR5269); it was therefore termed *CpLOG*. The second putative gene *CPUR4177* (1585 bp, one 97 bp intron) encodes a protein of 495 aa containing the same IPR5269 domain at the C-terminus. In addition, an isopentenyltransferase domain (IPR2648) and a tRNA isopentenyltransferase domain (IPR2627) were identified in the N-terminal region of this protein. Because this gene apparently encodes a bi-functional enzyme, it was termed *CpIPT-LOG*. Remarkably, *CpIPT-LOG* is linked in a head-to-head orientation to the putative cytochrome P450 monooxygenase gene *CPUR4176* (2481 bp, 5 introns, 510aa). As secondary metabolite genes are often clustered in fungi, this gene was termed *CpP450*.

The fungal cytokinin biosynthetic genes encode functional enzymes

To determine whether the cytokinin biosynthetic genes from *C. purpurea* encode functional enzymes, CpIPT-LOG and CpLOG were heterologously expressed as His-tagged proteins and purified to homogeneity (Figure 9).

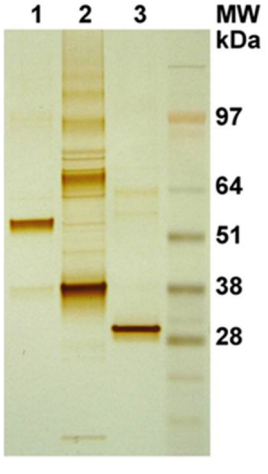

Figure 9 | Expression of recombinant *Claviceps* enzymes. Purified proteins were separated by NuPAGE SDS-PAGE (Thermo Scientific); lane 1, recombinant CpIPT-LOG (57 kDa); lane 2, recombinant IPT domain (36 kDa) from CpIPT-LOG; lane3, recombinant CpLOG (29 kDa). The size of the protein molecular mass marker is indicated to the right of the gel.

In addition, the IPT and LOG domains of *CpIPT-LOG* were expressed separately. The IPT domain showed strong transferase activity when DMAPP and AMP were used as donor and acceptor, respectively (Table 3), leading to the formation of iPRMP. CpLOG exhibited cytokinin-specific phosphoribohydrolase activity (Table 3), but the independently expressed LOG domain of CpIPT-LOG did not (data not shown). Surprisingly, the full-length CpIPT-LOG protein clearly exhibited both enzyme activities (Table 3). When the recombinant CpIPT-LOG protein was incubated with low concentrations of DMAPP and AMP, iP accumulated in the reaction mixture. However, when the substrate concentration was increased to > 20 μM and the enzyme concentration was increased proportionately, the intermediate iPRMP became detectable in the reaction mixture. Thus, *CpIPT-LOG* encodes a novel bifunctional enzyme that catalyzes the direct synthesis of active CKs. The enzymatic properties of the recombinant proteins are summarized in Table 3. CpLOG shows a slight preference for iPRMP relative to tZRMP and cZRMP: iPRMP is associated with the lowest K_m value and the highest k_{cat}/K_m ratio of these three compounds. In addition to cytokinin monophosphates, CpLOG can hydrolyze AMP and cytokinin diphosphates and triphosphates, although it has dramatically lower k_{cat} values for these substrates (Table 3). The CpIPT-LOG has a 180-fold higher ability to synthesize iP to tZ (Table 3). The limiting step in tZ production is the transfer of a hydroxymethylbutenyl group from (E)-4-hydroxy-3-methylbut-2-enyl diphosphate (HMBDP) to AMP. The kinetic parameters of the isolated IPT domain are comparable to those of the full-length protein (Table 3), indicating that the LOG domain does not influence transferase activity; it seems likely that the enzyme's two domains operate independently. The diphosphorylated and triphosphorylated species adenosine diphosphate (ADP) and adenosine triphosphate (ATP) cannot serve as acceptor substrates in the transferase reaction catalyzed by this enzyme; when either was added to the reaction mixture, the only products formed were iPRMP and iP. The formation of these products was independent of the incubation time and the amount formed was equimolar to the amount of recombinant protein in the reaction mixture (data not shown). The same production of iP and iPRMP was observed without the addition of any acceptor to the reaction mixture, indicating that the product was probably formed from AMP molecules that had bound to the active site of the IPT domain when it was expressed bacterially, and which could not subsequently be displaced by ADP or ATP.

Table 3 | Kinetic parameters of recombinant CpIPT-LOG and CpLOG proteins.

Enzyme	First substrate	Second substrate	K_m (µM)	V_{max} (nmol s^{-1} mg $protein^{-1}$	k_{cat} (min^{-1})	k_{cat}/K_m (s^{-1} M^{-1})
CpLOG	iPRMP	-	4.27 ± 1.71	37.4 ± 8.21	20.801	8.12×10^4
	tZRMP	-	57.63 ± 10.17	45.74 ± 10.32	25.345	7.33×10^3
	cZRMP	-	84.57 ± 20.15	188.06 ± 31.95	104.207	2.05×10^4
	tZRDP	-	23.37 ± 2.84	0.015 ± 0.003	0.008	5.89×10^1
	cZRDP	-	76.66 ± 15.69	0.093 ± 0.027	0.051	1.12×10^2
	tZRTP	-	66.58 ± 14.52	0.005 ± 0.001	0.003	7.21×10^{-1}
	cZRTP	-	64.56 ± 5.86	0.009 ± 0.001	0.005	1.24×10^1
	AMP	-	28.36 ± 3.20	2.045 ± 0.215	1.133	6.66×10^2
	ADP	-	43.23 ± 14.62	0.009 ± 0.003	0.005	2.01×10^1
	ATP	-	73.68 ± 15.12	0.005 ± 0.001	0.002	5.64×10^{-1}
CpIPT-LOG	iPRMP	-	9.01 ± 3.23	7.71 ± 1.34	8.397	1.55×10^4
	tZRMP	-	46.03 ± 13.24	31.62 ± 10.03	34.438	1.25×10^4
	cZRMP	-	61.40 ± 8.03	50.15 ± 15.88	54.620	1.48×10^4
	DMAPP	AMP	1.28 ± 0.27	14.74 ± 1.78	16.054	2.09×10^5
	HMBDP	AMP	12.21 ± 2.08	0.78 ± 0.22	0.849	1.16×10^3
	AMP	DMAPP	0.78 ± 0.31	5.26 ± 2.27	5.726	1.22×10^5
	AMP	HMBDP	0.86 ± 0.12	0.66 ± 0.17	0.721	1.40×10^4
IPT domain	DMAPP	AMP	1.75 ± 0.44	14.18 ± 5.08	9.755	9.29×10^4
	HMBDP	AMP	27.61 ± 6.36	0.46 ± 0.16	0.314	1.89×10^2
	AMP	DMAPP	0.52 ± 0.14	2.68 ± 0.59	1.844	5.91×10^4
	AMP	HMBDP	0.72 ± 0.23	0.23 ± 0.09	0.158	3.66×10^3

The kinetic parameters for all substrates were measured as described in the Material and Method section. All quoted values are means based on analyses of at least three independent reactions. Measurements were conducted at 30°C, pH 8.0, and the reactions were stopped at defined time points. Parameters were calculated using the GRAFIT Version 4.0.12 software package.; cZRDP, *cis*-zeatin riboside-5´-diphosphate; cZRTP, *cis*-zeatin riboside-5´-triphosphate; tZRDP, *trans*-zeatin riboside-5´-diphosphate; tZRTP, *trans*-zeatin riboside-5´-triphosphate.

CpIPT-LOG, *CpLOG* and the IPT domain of *CpIPT-LOG* were overexpressed under the control of the 35S promoter in *A. thaliana*. Homozygous 35S::CpLOG plants have longer primary roots and significantly darker rosette leaves than control plants (Figure 10). Conversely, 35S::CpIPT seedlings exhibited delayed growth because of retarded root development and also underwent premature senescence (Figure 10). *CpIPT-LOG* transformants were unable to form roots and died on selection plates, forming only bushy and stunted aerial parts (Figure 10). The observed phenotypes resemble typical response of plants towards cytokinin treatment (Smart *et al*., 1991; Faiss *et al*., 1997; Ioio *et al*., 2008). These data further support the hypothesis that the *Claviceps* genes encode functional cytokinin biosynthesis enzymes.

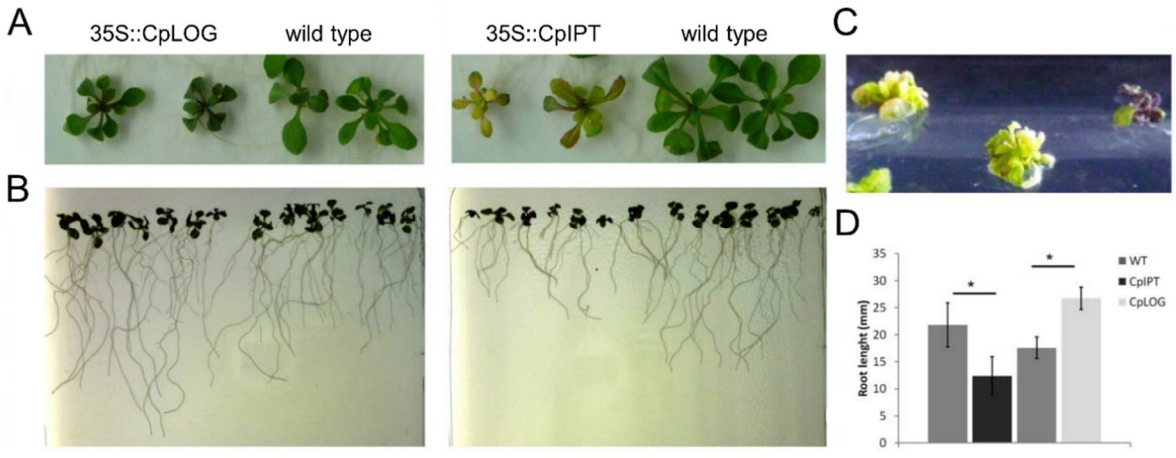

Figure 10 | Phenotypes of 35S::CpLOG, 35S::CpIPT and 35S::CpIPT-LOG transgenic *Arabidopsis* plants. (A) Twenty-one-day-old plants of 35S::CpLOG, 35S::CpIPT and the wild type grown on horizontal plates with MS phytagel. (B) Twelve-day-old seedlings of 35S::CpLOG, 35S::CpIPT and the wild type grown on vertical plates with MS phytagel. (C) Thirty-day-old plants of 35S::CpIPT-LOG regenerated on MS plates with hygromycin (30 mg l^{-1}). (D) Root length of 12-day-old 35S::CpLOG, 35S::CpIPT and the wild-type seedlings grown on vertical plates with MS phytagel; $*P \leq 0.05$, $n = 30$.

Discussion

Previous studies have demonstrated that interactions with phytopathogenic fungi can induce changes in plants' cytokinin levels (Behr *et al.*, 2012; Jiang *et al.*, 2013). However, neither the genes involved in their biosynthesis nor the relevant fungal biosynthetic pathways have previously been identified. This study presents the first evidence for a fungal gene cluster associated with *de novo* cytokinin biosynthesis. The cluster was identified in the biotrophic fungus *C. purpurea* and its functional characterization suggested the existence of the cytokinin production pathways depicted in Figure 11: the initial step, the formation of iP, is catalyzed by the bifunctional enzyme CpIPT-LOG. This enzyme exhibits both the IPT activity required for the isoprenylation of adenine and the LOG activity required for the activation of cytokinin nucleotides. Fungal genome analyses indicated that bifunctional enzymes of this sort are unique to species from the orders *Hypocreales* (including the genera *Fusarium*, *Epichloe*, *Aciculosporium*) and *Capnodiales* (e.g. *Zymoseptoria*; Figures S1, S2). A similar chimeric protein encoded by the bacterial *IPT* (*fasD*) and *LOG* (*fasF*) genes was recently identified in isolates of the bacterial plant pathogen *R. fascians* A21d2 but has yet to be functionally characterized (Creason *et al.*, 2014).

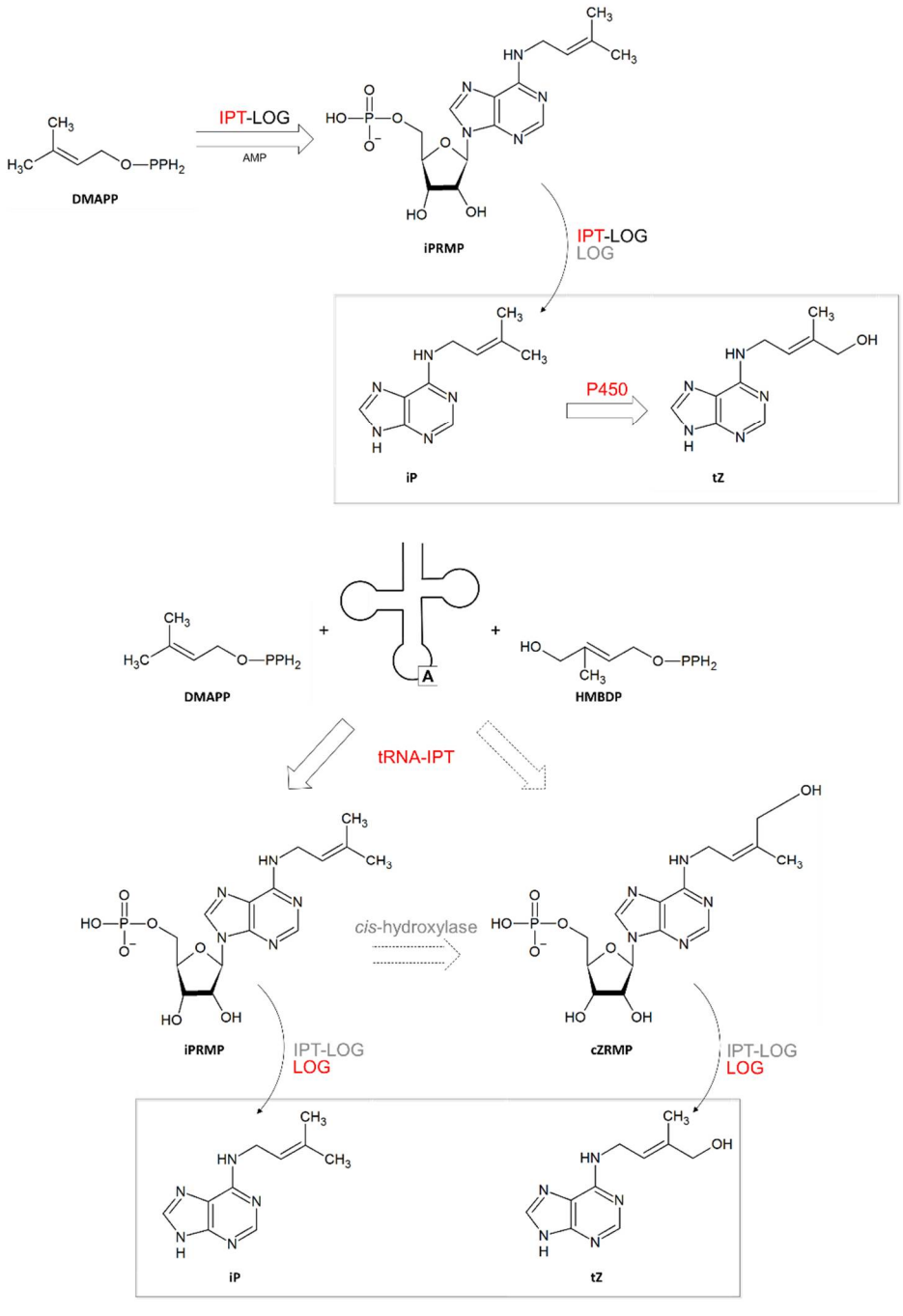

Figure 11 | Proposed *de novo* cytokinin biosynthesis and tRNA degradation pathways in *C. purpurea*. The bifunctional enzyme CpIPT-LOG catalyzes the prenylation of AMP using DMAPP as a side chain donor, producing iPRMP. The tRNA-IPT catalyzes the prenylation of tRNA either using DMAPP or (E)-4-hydroxy-3-methylbut-2-enyl diphosphate (HMBDP) as a side chain donor, leading to the formation of iPRMP or cZRMP respectively. These nucleosides are then converted into the corresponding active bases by the LOG domains of either CpLOG or CpIPT-LOG. Hydroxylation of iP derivatives to tZ derivatives is catalyzed by a cytochrome P450 monooxygenase (CpP450). Red labels indicate reactions known to be catalyzed by enzymes examined in this work; grey labels indicate reactions that may occur but are not expected to be important. Dashed lines indicate putative reactions for which the associated enzymes are yet to be identified.

Similarly, a fusion combining the activity of two plant enzymes, copalyl phosphate synthase and ent-kaurene synthase (*CPS/KS*), has been identified in the phytopathogenic fungus *F. fujikuroi*. CPS/KS catalyzes the conversion of geranylgeranyl diphosphate into ent-kaurene via entcopalyl diphosphate, a key step in gibberellic acid (GA) biosynthesis (Tudzynski *et al.*, 1998). The fusion of cytokinin-producing and cytokinin-activating functions in a single enzyme would give pathogenic fungi a potent tool for the *in situ* production of active cytokinins, as demonstrated by the fatal disruption of seedling morphology in Arabidopsis plants that constitutively overexpress *CpIPT-LOG* (Figure 10 C). Moreover, the CpIPT-LOG fusion is much more stable than plant IPTs when prepared in a heterologous prokaryotic system. The high potency of the novel bifunctional enzyme is further demonstrated by the measured kinetic constants (K_m and k_{cat}) of the IPT domain, which are much better than those estimated for plant enzymes (Kakimoto, 2001; Takei *et al.*, 2004). However, in contrast to the Agrobacterial IPT, which preferentially uses HMBDP to directly produce tZ-type cytokinins *in planta* (Sakakibara *et al.*, 2005; Ueda *et al.*, 2012), the transferase domain of the Claviceps enzyme preferentially uses DMAPP. The subsequent hydroxylation of iP to tZ is mediated via a cytokinin-specific cytochrome P450 monooxygenase encoded by a gene adjacent to *CpIPT-LOG* within the Cp20.1 genome. Because the levels of cZ derivatives in cultures of both Δcpp450 and Δcpipt-log mutants were comparable with those observed in wild-type cultures, it is unlikely that the *CpIPT-LOG*/*CpP450* gene cluster affects the formation of cZ-type cytokinins (Hinsch *et al.*, 2015). Because *C. purpurea* clearly has the ability to produce cytokinins, it also presumably has the ability to manipulate the cytokinin levels of infected rye plants, thus potentially changing the within-host environment in a pathogen advantageous way. Accordingly, the abundance of the most active cytokinin iP and its deactivated metabolites iPR and iP 9-glucoside in infected plants increased dramatically at 5 dpi (Table 1). During this colonization phase, none of the plant's known *IPT* genes were significantly upregulated (Figure 8). However, qPCR showed that the fungal *CpIPT-LOG* gene expression was upregulated at 3 and 5 dpi, indicating fungal cytokinin production at these time points. The low expression of *CpP450* at 5 and 10 dpi is consistent with the levels of tZ in the infected plants (Hinsch *et al.*, 2015). Content of tZ was identical to those of mock-treated control plants at 5 dpi. Subsequently (at 10 dpi), the tZ content of the infected plants fell below that of the uninfected controls (Table 1). Treatment of monocot plant tissues with exogenous

active cytokinins usually causes the upregulation of several *CKX* genes and the downregulation of *IPT* genes implicated in *de novo* cytokinin biosynthesis (Podlešáková *et al.*, 2012), so the high levels of iP (5 dpi) and the putative accumulation of tZ derivatives (3 dpi) caused by the fungal infection may induce the activity of cytokinin-degrading enzymes. In keeping with this hypothesis, the expression of several *CKX* genes was strongly induced during the early phase of infection (Figure 8), and the levels of preferred CKX substrates – iP and tZ derivatives except O-glucosides and the primary products of plant cytokinin biosynthesis (iPRMP and tZRMP) – fell at 10 dpi (Table 1).

The functions of fungus-borne cytokinins during host colonization were unclear because the Δcpipt-log and Δcpp450 deletion mutants still contained residual levels of cytokinins and exhibited similar levels of virulence as wild type (Hinsch *et al.*, 2015). However, as noted above, both Δcpipt-log and Δcpp450 were unaffected in cZ production. In *A. thaliana* and *P. patens*, it has been shown that tRNA-IPT cytokinin biosynthesis accounts for the majority of cZ production and also contributes to the formation of iP-type cytokinins (Miyawaki *et al.*, 2006; Lindner *et al.*, 2014). One copy of a *tRNA-IPT* gene is conserved in all of the sequenced genomes of the *Clavicipitaceae* family (Figure S1) and homologous proteins are present in all living organisms, except *Archaea* (Spíchal, 2012). Contribution of prenylated tRNA degradation to the total cytokinin pool in *C. purpurea* was shown with the deletion mutant of *CptRNA-IPT* (Hinsch *et al.*, 2016) which does not contain cZ type cytokinins and displays impaired virulence. The specific functions of cZ during the infection process are not clear. In theory, cZ could play a role in the preparation of the host tissue for infection as cZ-type cytokinins are overproduced during early-stage embryogenesis and are biologically active in *in vitro* support of embryo growth (Quesnelle and Emery, 2007). In addition, fungal cZ production might also mimic natural conditions during pollination. Cytokinins are involved in nutritional signaling (Cerutti and Delatorre, 2013), and could be thus required to nourish the fungus during infection; this putative role is partly confirmed by delayed sclerotia formation in ΔcptRNA-ipt mutant (Hinsch *et al.*, 2016). Double deletion mutant Δcpipt-log/ΔcptRNA-ipt does not produce any cytokinins and has strong virulence defects, as macroscopic disease symptoms are not visible and mutant rarely enters ovarian tissue (Hinsch *et al.*, 2016). This is powerful evidence for cytokinin role in interaction with plant host, nevertheless missing tRNA modification in ΔcptRNA-ipt mutant must be taken in account as it could influence protein translation (El

Yacoubi *et al.*, 2012). Indeed, mutant ΔcptRNA-ipt had reduced growth rate in axenic culture, which could influence fungal virulence (Hinsch *et al.*, 2016). To exclude possible negative effects of tRNA-IPT deletion on translation process, mutant strains of *C. purpurea* with heterologous maize *CKX1* expression were prepared (Kind *et al.*, 2018). The strains had great reduction of iP, iPR, tZ and tZR content, whereas cZ and cZR were less reduced or not affected, respectively. This approach enabled massive manipulation of cytokinin levels, comparable to Δcpipt-log/ΔcptRNA-ipt double deletion. Mutants with ZmCKX1 overexpression had reduced virulence to 41-67%, thus indicating that residual levels of zeatins are probably enough for successful infection. iP and tZ seem to be not essential for penetration and early invasion of the ovary, as was indicated by the WT-like growth on isolated ovaries (Kind *et al.*, 2018).

Impact of cytokinin-specific phosphoribohydrolase LOG activity on cytokinin composition and fungal virulence was studied with strains with deleted LOG genes (Kind *et al.*, 2018). Although the cytokinin composition was altered, both single and double deletion mutants still contained active cytokinin bases, confirming existence of LOG-independent cytokinin activation in fungi. Virulence of mutant strain remained unaffected as were conidia formation and growth in axenic culture. In contrast, the Δcpp450 mutant showed an altered sporulation phenotype in axenic cultures (Hinsch *et al.*, 2015). Sporulation occurred under non-inducing conditions and hyper-sporulation was observed under inducing conditions. These results suggest that hormonal balances influence fungal development. However, only the loss of tZ-type cytokinins in the Δcpp450 mutant cannot explain this phenomenon, because the Δcpipt-log mutant, with reduced tZ levels, does not have altered sporulation. It is possible that the sporulation changes in Δcpp450 are due to iP accumulation or interactions between the two cytokinin types. Nevertheless, transcriptomic analysis of *C. purpurea* treated with 1 µM iP for 24 h did not demonstrate any major change in expression (Kind *et al.*, 2018).

Part V: Expression of genes participating in cytokinin metabolism during interaction of Fusarium species with maize (*Zea mays L.*) seedlings

Results

Expression of fungal and plant genes involved in cytokinin metabolism during Fusarium – maize interaction

Infection of maize seedling by *F. mangiferae* led to a modest increase in cytokinin levels in shoots, while infection by *F. verticillioides* and *F. fujikuroi* led to a decrease (Vrabka *et al.*, 2019). To study the origin of cytokinin accumulation in *F. mangiferae*-infected maize tissues, the expression of fungal genes encoding enzymes involved in cytokinin synthesis (*IPT-LOG1* and *IPT-LOG2*), as well as maize genes encoding enzymes involved in cytokinin metabolism (*IPT* and *CKX*) were examined over 10 days post inoculation by qPCR (Table 4, 5). Total RNA was extracted from roots and shoots of seedlings infected by *F. mangiferae*, *F. verticillioides* and *F. fujikuroi*. The abundance of fungal transcripts coding for ubiquitin (*FmUBI*) and actin (*FvACT* and *FfACT*), two common housekeeping genes, served to follow the growth of the fungi (Table 4). The increase of transcripts in infected roots observed over time strongly indicates that all three fungi were able to colonize the plant roots and thrive. Fungal gene transcripts were detected in the shoots of maize only at 4 dpi and later. Of the fungal cytokinin synthesis genes, *IPT-LOG2* transcripts were much more readily and consistently present in roots infected with all three fungi (Table 4). While transcript for *FmIPT-LOG2* increased steadily with a maximum at 10 dpi, transcripts for *FvIPT-LOG2* peaked at 6 dpi, fourfold higher than *FmIPT-LOG2* at 10 dpi. In contrast, expression of *FfIPT-LOG2* was low at 3–4 dpi and decreased significantly out to 10 dpi. In shoots, fungal *IPT-LOG2* transcripts were detectable only after infection by *F. verticillioides* (Table 4).

Table 4 | Expression of fungal *IPT-LOG* genes in the roots and shoots of maize seedlings infected by *F. mangiferae*, *F. verticillioides*, and *F. fujikuroi.*

In roots of maize seedlings						
	Genes	**1 dpi**	**3 dpi**	**4 dpi**	**6 dpi**	**10 dpi**
F. mangiferae	*FmUBI*	19.1 ± 7.32	889 ± 492	2169 ± 823	2545 ± 285	7854 ± 3600
	FmIPTLOG1	n. d.	n. d.	n. d.	0.96 ± 0.57	0.35 ± 0.26
	FmIPTLOG2	n. d.	0.85 ± 0.74	17.4 ± 7.30	88.9 ± 58.6	716 ± 494
F. verticillioides	*FvACT*	7570 ± 1738	222859 ± 114805	450178 ± 157031	281578 ± 110834	232959 ± 13051
	FvIPTLOG1	n. d.	n. d.	2.86 ± 2.48	0.44 ± 0.16	n. d.
	FvIPTLOG2	n. d.	114 ± 61.3	1381 ± 599	2868 ± 1997	1121 ± 228
F. fujikuroi	*FfACT*	214 ± 108	18608 ± 100042	15222 ± 2830	57216 ± 18166	85585 ± 36355
	FfIPTLOG1	n. d.	0.47 ± 0.20	5.85 ± 2.34	n. d.	0.26 ± 0.22
	FfIPTLOG2	7.70 ± 5.25	106 ± 48.2	73.5 ± 31.6	n. d.	3.97 ± 2.09
In shoots of maize seedlings						
	Genes	**1 dpi**	**3 dpi**	**4 dpi**	**6 dpi**	**10 dpi**
F. mangiferae	*FmUBI*	-	-	121 ± 40.8	467 ± 214	183 ± 34.1
	FmIPTLOG1	-	-	n. d.	1.10 ± 1.55	n. d.
	FmIPTLOG2	-	-	1.83 ± 1.02	n. d.	n. d.
F. verticillioides	*FvACT*	-	-	16175 ± 8006	78167 ± 36366	106034 ± 52104
	FvIPTLOG1	-	-	n. d.	2.87 ± 2.41	n. d.
	FvIPTLOG2	-	-	344 ± 485	121 ± 143	n. d.
F. fujikuroi	*FfACT*	-	-	1872 ± 920	14695 ± 8425	18350 ± 3175
	FfIPTLOG1	-	-	0.03 ± 0.05	n. d.	n. d.
	FfIPTLOG2	-	-	n. d.	n. d.	n. d.

Quantity of *IPT-LOG1* and *IPT-LOG2* transcripts and transcripts for the house-keeping genes *UBI* (*F. mangiferae*) and *ACT* (*F. verticillioides* and *F. fujikuroi*) in 1 ng of total RNA extracted from the root and the shoot of infected plants. Each value is mean presented with standard deviation of six biological replicates (seedlings). ***** Significant difference between mock and Fusarium-infected tissue according to Student's unpaired t-tests at $p \leq 0.05$. n.d., not detected; –, not analyzed.

Analysis of expression of seven maize *IPTs* (*ZmIPT3b*, *ZmIPT4*, *ZmIPT5*, *ZmIPT6*, *ZmIPT7*, *ZmIPT8* and *ZmIPT9*) potentially involved in cytokinin metabolism in seedling roots or shoots was investigated (Table 5). In roots, transcripts for all seven *IPTs* were detected. At almost every time point after 1 dpi, transcripts for multiple *IPTs* accumulated significantly more in infected roots compared to uninfected roots (Table 5). By far, *ZmIPT7* transcripts accumulated the most at 10 dpi in roots infected by all three fungi. In the shoots, transcripts for five of the seven *ZmIPT* genes were detected (Table 5). The most significant accumulation was observed in seedlings infected by *F. mangiferae* at 6 dpi where transcripts of four *IPTs* (*ZmIPT3b*, *ZmIPT6*, *ZmIPT7* and *ZmIPT8*) were present 4.5- to 74-

fold greater than mock-treated seedlings or leaves of seedlings infected by the other two Fusarium species. At 10 dpi, *ZmIPT* levels had decreased to levels detectable in mock-treated leaves with the exception of *ZmIPT5*. The expression of two out of five cytokinin biosynthesis genes (*ZmIPT5* and *ZmIPT6*) were significantly elevated in shoots of seedlings infected for 10 dpi by *F. verticillioides* and to a lower extent *F. fujikuroi*. The increase of expression maize *IPT* genes appeared to be associated with the concomitant increase in *ZmCKX1* gene expression in the roots, as well as in the shoots of seedlings infected by Fusarium with a peak at 3–4 dpi and 6 dpi, respectively (Table 5). Seedlings infected by *F. mangiferae* showed the highest *ZmCKX1* expression followed by *F. fujikuroi* and then *F. verticillioides*.

Table 5 | Expression of maize *ZmCKX1* and *ZmIPT* genes in the roots and shoots of seedlings infected by *F. mangiferae*, *F. verticillioides* and *F. fujikuroi*.

		In the roots of maize seedlings				
	Gene	**1 dpi**	**3 dpi**	**4 dpi**	**6 dpi**	**10 dpi**
F. mangiferae	*ZmCKX1*	1.08 ± 0.13	14.1 ± 5.94*	118 ± 58.2*	6.11 ± 0.81*	145 ± 85.9*
	ZmIPT5	0.72 ± 0.23	3.34 ± 0.42*	0.97 ± 0.22	0.67 ± 0.13*	1.45 ± 0.37
	ZmIPT3b	0.88 ± 0.26	2.48 ± 0.94	1.82 ± 0.63	0.70 ± 0.13*	0.57 ± 0.04*
	ZmIPT6	1.10 ± 0.43	13.9 ± 4.43*	1.02 ± 0.05	0.56 ± 0.10*	1.66 ± 0.52
	ZmIPT8	0.84 ± 0.21	1.91 ± 0.50	0.68 ± 0.17	0.63 ± 0.15*	0.41 ± 0.13*
	ZmIPT9	1.05 ± 0.29	n.d.	0.58 ± 0.37	n.d.	0.47 ± 0.24*
	ZmIPT7	0.74 ± 0.34	0.55 ± 0.31*	0.68 ± 0.35	1.38 ± 0.41	6.24 ± 1.47*
	ZmIPT4	n.d.	3.28 ± 0.05*	0.55 ± 0.28	1.26 ± 0.45	1.21 ± 0.34
F. verticillioides	*ZmCKX1*	0.60 ± 0.02*	2.10 ± 0.64*	28.7 ± 12.5*	0.68 ± 0.12*	2.01 ± 0.90
	ZmIPT5	1.01 ± 0.34	1.78 ± 0.57	1.39 ± 0.31	0.31 ± 0.04*	2.33 ± 0.49*
	ZmIPT3b	0.72 ± 0.17	1.22 ± 0.33	1.25 ± 0.06	0.51 ± 0.10*	0.65 ± 0.10*
	ZmIPT6	1.01 ± 0.54	4.95 ± 2.36*	2.51 ± 0.51*	0.69 ± 0.23*	11.2 ± 6.87*
	ZmIPT8	1.24 ± 0.37	1.40 ± 0.40	0.95 ± 0.22	0.47 ± 0.06*	0.70 ± 0.07*
	ZmIPT9	0.92 ± 0.45	n.d.	0.43 ± 0.21*	n.d.	0.24 ± 0.16*
	ZmIPT7	1.10 ± 0.40	0.30 ± 0.22*	0.32 ± 0.18*	0.94 ± 0.10	6.51 ± 1.71*
	ZmIPT4	n.d.	0.95 ± 0.28	1.27 ± 0.58	1.56 ± 0.56	0.96 ± 0.32
F. fujikuroi	*ZmCKX1*	0.74 ± 0.10*	2.59 ± 0.41*	1.10 ± 0.27	3.59 ± 1.87	2.06 ± 0.62
	ZmIPT5	1.26 ± 0.21	2.16 ± 0.72	0.58 ± 0.34	2.03 ± 0.84	0.89 ± 0.41
	ZmIPT3b	0.87 ± 0.18	3.50 ± 1.49*	0.70 ± 0.29	1.77 ± 0.70	0.68 ± 0.36
	ZmIPT6	1.43 ± 0.44	5.01 ± 2.32*	0.61 ± 0.35	1.53 ± 0.69	1.68 ± 0.32
	ZmIPT8	0.89 ± 0.17	1.24 ± 0.31	0.94 ± 0.25	0.39 ± 0.29*	2.36 ± 1.09
	ZmIPT9	0.68 ± 0.39	n.d.	0.48 ± 0.24*	n.d.	n.d.
	ZmIPT7	1.13 ± 0.32	1.67 ± 0.38	0.28 ± 0.20*	1.93 ± 0.85	5.31 ± 2.41*
	ZmIPT4	n.d.	0.20 ± 0.13*	1.08 ± 0.47	n.d.	0.45 ± 0.25*

Table 5 | Expression of maize *ZmCKX1* and *ZmIPT* genes in the roots and shoots of seedlings infected by *F. mangiferae*, *F. verticillioides* and *F. fujikuroi* (continued).

In the shoots of maize seedlings				
	Gene	**4 dpi**	**6 dpi**	**10 dpi**
F. mangiferae	*ZmCKX1*	7.84 ± 2.68*	85.6 ± 12.9*	36.7 ± 10.2*
	ZmIPT5	0.79 ± 0.10	2.41 ± 1.05	9.98 ± 2.71*
	ZmIPT8	1.06 ± 0.32	9.81 ± 4.59*	0.65 ± 0.41
	ZmIPT3b	1.02 ± 0.57	4.53 ± 2.14*	0.64 ± 0.35
	ZmIPT6	3.20 ± 1.08*	74.1 ± 37.8*	2.63 ± 1.21
	ZmIPT7	0.22 ± 0.31	14.1 ± 6.91*	0.47 ± 0.27*
F. verticillioides	*ZmCKX1*	24.1 ± 8.21*	17.4 ± 10.7*	13.3 ± 2.89*
	ZmIPT5	0.88 ± 0.24	1.68 ± 0.63	26.8 ± 5.78*
	ZmIPT8	0.57 ± 0.14*	1.43 ± 0.85	1.46 ± 0.41
	ZmIPT3b	2.37 ± 1.04	1.06 ± 0.50	1.70 ± 0.37
	ZmIPT6	0.91 ± 0.45	12.9 ± 6.32*	18.6 ± 4.8*
	ZmIPT7	4.60 ± 2.22*	1.22 ± 0.57	0.38 ± 0.52
F. fujikuroi	*ZmCKX1*	1.28 ± 0.30	3.09 ± 1.08*	7.05 ± 3.58*
	ZmIPT5	1.70 ± 0.75	1.39 ± 0.65	12.5 ± 3.75*
	ZmIPT8	0.98 ± 0.31	0.38 ± 0.30*	0.74 ± 0.38
	ZmIPT3b	0.97 ± 0.35	0.97 ± 0.47	1.57 ± 0.68
	ZmIPT6	2.43 ± 1.18	0.80 ± 0.62	5.70 ± 3.43
	ZmIPT7	0.62 ± 0.42	0.67 ± 0.62	0.58 ± 0.29

Relative expression was compared to mock-treated seedlings. Mean values with standard deviations of six biological replicates are given. * indicates significant difference between mock and Fusarium-infected tissue according to Student's unpaired t-tests at $p \leq 0.05$ ($n = 6$).

Discussion

The study of expression of maize and fungal genes involved in cytokinin metabolism during infection with different Fusarium uncovered why fungal hormone synthesis minimally affected maize growth. Along with expression of cytokinin biosynthetic genes from both organisms, expression of a maize gene encoding a *CKX*, an enzyme involved in the irreversible degradation of cytokinins was detected. Thus, despite efforts by the fungus to alter cytokinin balance in maize tissue (either directly by producing cytokinins or indirectly by increasing plant cytokinin synthesis) overall levels were actively mitigated by the plant. This effort to restore hormone homeostasis was most clearly seen in *F. mangiferae* infected maize tissue where the highest levels of cytokinins paralleled the highest level of plant *CKX* expression observed (Vrabka *et al.*, 2019). As described earlier in Part IV, *Claviceps purpurea* possesses a unique biosynthetic pathway for cytokinin

production based on bifunctional IPT-LOG enzyme (Hinsch *et al.*, 2015). Two *IPT-LOG* gene homologs are present also in all of the Fusarium genomes examined. It was initially assumed that the activity of one or both might contribute to the massive cytokinin increase observed in maize tissue infected by *F. mangiferae* (Vrabka *et al*., 2019). Surprisingly, this appeared unlikely for multiple reasons. First, both *IPT-LOG1* and *IPT-LOG2* were either not expressed or minimally expressed during infection. Any potential impact of IPT-LOG in cytokinin levels seems even less likely for the other Fusarium as no significant cytokinin increase was detected, despite detecting an increase in expression of *F. verticillioides IPT-LOG2* in infected tissue. Second, *F. mangiferae IPT-LOG2* is likely not functional as its predicted open reading frame contains two stop codons 71 codons downstream from the start codon. Predicted 71 amino acid protein expressed in in *E. coli* exhibited no IPT and only weak LOG activity (Vrabka *et al*., 2019). And finally, an *IPT-LOG1* deletion mutant did not alter the amount of cytokinins that accumulated in inoculated seedlings while the overexpression mutant caused increase in cytokinin production (Vrabka *et al.*, 2019), similar to the *FfIPT-LOG1* overexpressing strain (Niehaus *et al.*, 2016). The second pathway for cytokinin production is based on tRNA decay which can contribute to the total amount of cytokinins produced by fungi and affect virulence as recently shown in several fungal species (Chanclud *et al.*, 2016; Hinsch *et al.*, 2016; Morrison *et al.*, 2017). An orthologue of tRNA-IPT was also identified in *F. mangiferae*. No significant differences were however observed among *F. mangiferae tRNA-IPT* mutants or *FmtRNA-IPT*/*IPT-LOG1* double deletion mutants in their ability to cause seedling disease symptoms or to lower plant CKX activity (Vrabka *et al.*, 2019). Taken together, the increase in plant endogenous cytokinin content is most likely not due to fungal synthesis but rather to activation by the fungus of maize cytokinin biosynthetic genes by a yet unknown mechanism. This response has already been observed for two biotrophic fungi, *Magnaporthe oryzae* (Jiang *et al.*, 2013) and *Colletotrichum graminicola* (Behr *et al.*, 2012), which lack *IPT-LOG* genes and induce a massive accumulation of cytokinins *in planta*. Up-regulation of maize *IPT* genes both in roots and shoots during infection by any of the fusaria strongly supports this hypothesis. The accumulation of *ZmIPT* transcripts was also accompanied by the up-regulation of the *ZmCKX1* gene, involved in cytokinin degradation. The accumulation of cytokinins in plant tissue may benefit fungi through increased sink activity and attraction of assimilates, providing essential energy for fungal

growth. Accordingly, fungi which primarily infect non-assimilating sink organs, flowers in the case of *F. mangiferae* and spikes in the case of *C. purpurea*, were found to induce strong accumulation of cytokinins. The practical consequence of the accumulation of cytokinins to the plant is host tissue malformation as observed in *F. mangiferae* infections which is likely due to a cytokinin-induced increase in cell division.

Part VI: Identification of putative auxin efflux carrier in *Claviceps purpurea*

Results

Identification of putative auxin transporters in *C. purpurea*

To identify fungal proteins homologous to those that transport auxin in plants, BLASTp search was performed against the Cp20.1 database (Schardl *et al.*, 2013). Using the sequence of PILS6 from *Arabidopsis thaliana* as a query, one annotated open reading frame was detected - *CPUR8219*; (E= 0.012). The putative gene *CPUR8219* has 1683 bp and 2 introns (85 and 60 bp), encodes a protein of 560 amino acids with predicted domains for membrane transporter proteins. Phylogenetic analysis using web tool on www.phylogeny.fr (Dereeper *et al.*, 2008) against auxin efflux carriers PINs and PILS showed, that this protein clusters with PILS2/6 (Figure 12). Homologous transporter is conserved in diverse fungal species from division *Ascomycetes* (Figure S3).

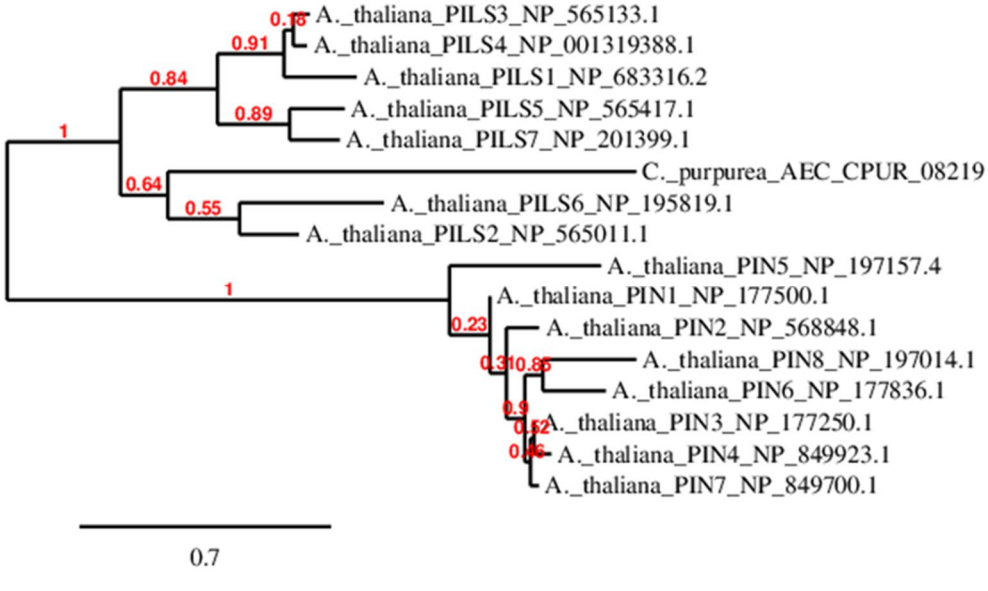

Figure 12 | Phylogenetic tree of auxin efflux carriers PILS and PINs in *A. thaliana* with C. *purpurea* AEC. The tree was constructed with MUSCLE, Gblocks, PhylML and TreeDyn over the webpage of www.phylogeny.fr.

The Δcpaec deletion mutants have unique IAA production profiles

To resolve the auxin transport in *C. purpurea*, deletion mutants of *CpAEC* were generated via a gene replacement strategy (Figure S4). Three independent deletion strains were obtained, confirmed by PCR and southern blotting (Figure S5). The deletion mutant does not show any morphological anomalies when grown on solid Mantle agar. Furthermore, the deletion mutant did not exhibit altered levels of virulence to the wild type when inoculated to flowering rye ears. Microscopic observation of dissected rye ovaries several days after inoculation showed same growth of hyphae through the pistil (data not shown). The IAA production profiles of Δcpaec and the wild-type strain Cp20.1 were determined after 7 days (or 4 hours) of cultivation in modified liquid Mantle media (Figure 13). Compared to the wild type after 7 days cultivation, the Δcpaec mutants contains 1.5 times higher concentrations of IAA in mycelium (Figure 13 A), and 20-30 times in medium (Figure 13 B). In the case of short-term cultivation for 4 hours, the Δcpaec deletion mutants had 10-20 times higher IAA content in mycelium (Figure 13 C) and 8-12 times higher IAA content in medium (Figure 13 D).

Total content of IAA in individual samples was calculated by multiplication of IAA concentration with obtained dry weight of mycelia or with volume of culture media (Figure 14). Early total IAA content in mycelia after 4 hours cultivation is greatly increased, yet this difference diminishes at 7 days; however increase in total IAA content in Δcpaec mutants compared to WT is still significant (Figure 14 A). Total content of IAA in medium of Δcpaec mutants increases over time, while that of Cp20.1 remains almost unchanged (Figure 14 B).

In addition to free IAA, content of its biosynthesis intermediate IPA was measured in fungal mycelia (Figure 15). Differences between Cp20.1 and Δcpaec mutants were significant only after 4 hours cultivation (Figure 15 A), when IPA levels were increased 2-3 times. After 7 days cultivation, IPA levels remained unchanged (Figure 15 B).

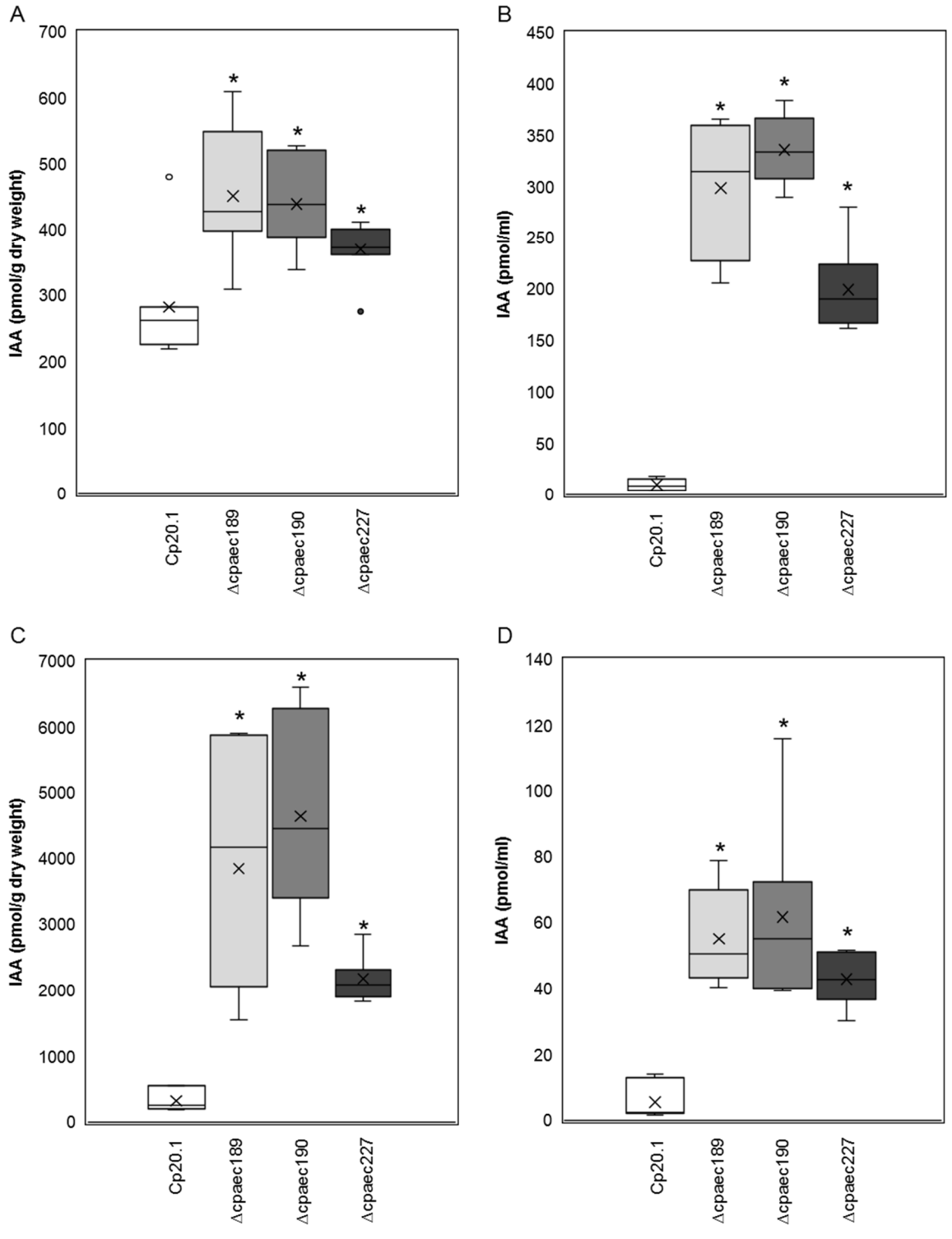

Figure 13 | Free active IAA levels of Δcpaec mutants. Content in freeze-dried mycelium (A, C) and modified Mantle medium (B, D) after 7 days (A, B) or 4 hours (C, D) cultivation. Graphs represent the values of six (A, B) or seven (C, D) independent biological replicates. Cp20.1 – WT *C. purpurea* 20.1, Δcpaec189, 190, 227 – independent deletion mutants of *CpAEC*. Asterisk indicates significant differences between mock and Δcpaec mutants according to Student's unpaired t-tests at $p \leq 0.05$ ($n = 6/7$).

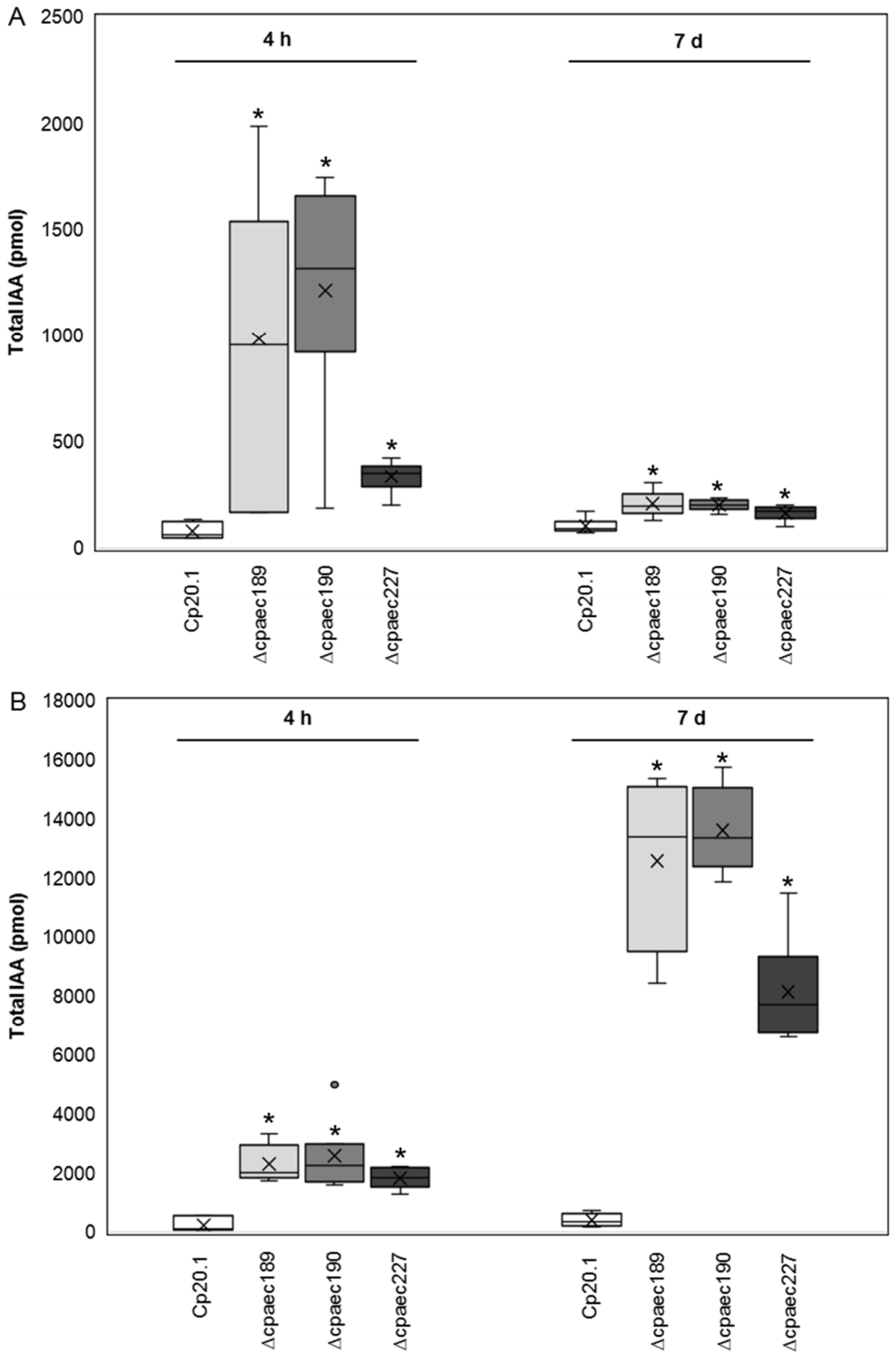

Figure 14 | Total active IAA levels of Δcpaec mutants. Total content in freeze-dried mycelium (A) and modified Mantle medium (B. Graphs represent the values of six (7 days) or seven (4 hours) independent biological replicates. Cp20.1 – WT *C. purpurea* 20.1, Δcpaec189, 190, 227 – independent deletion mutants of *CpAEC*. Asterisk indicates significant differences between mock and Δcpaec mutants according to Student's unpaired t-tests at $p \leq 0.05$ ($n = 6/7$).

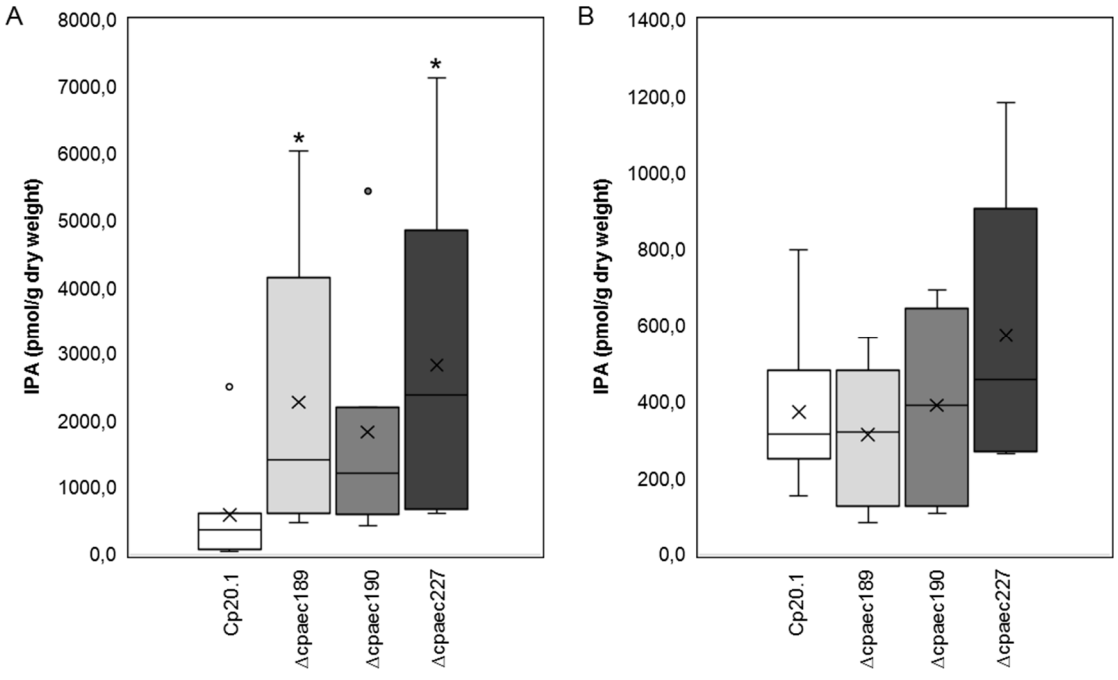

Figure 15 | Auxin biosynthesis intermediate IPA levels in Δcpaec mutants. Content in freeze-dried mycelium after 4 hours (A) or 7 days (B) cultivation. Graphs represent the values of six (B) or seven (A) independent biological replicates. Cp20.1 – WT *C. purpurea* 20.1, Δcpaec189, 190, 227 – independent deletion mutants of *CpAEC.* Asterisk indicates significant differences between mock and Δcpaec mutants according to Student's unpaired t-tests at $p \leq 0.05$ (n = 6/7).

Deletion mutants were complemented by reintroducing the original wild-type gene, and in addition, *CpAEC* was also introduced under constitutive promotor OliC. Complementation of Δcpaec did not restore WT IAA levels, although complemented mutants had altered IAA content (Figure S6). Transformation with *in situ* complementation vectors would be necessary for proper restoration of phenotype, as positional effect probably influences *CpAEC* expression.

Intracellular CpAEC-GFP localization

For subcellular localization, constitutively expressed *CpAEC* with C-terminal fusion with GFP (pLoc_AEC_GFP) was transformed into Cp20.1 strain (Figure 16). GFP signal seem to be localized intracellularly on membrane structures resembling endoplasmic reticulum.

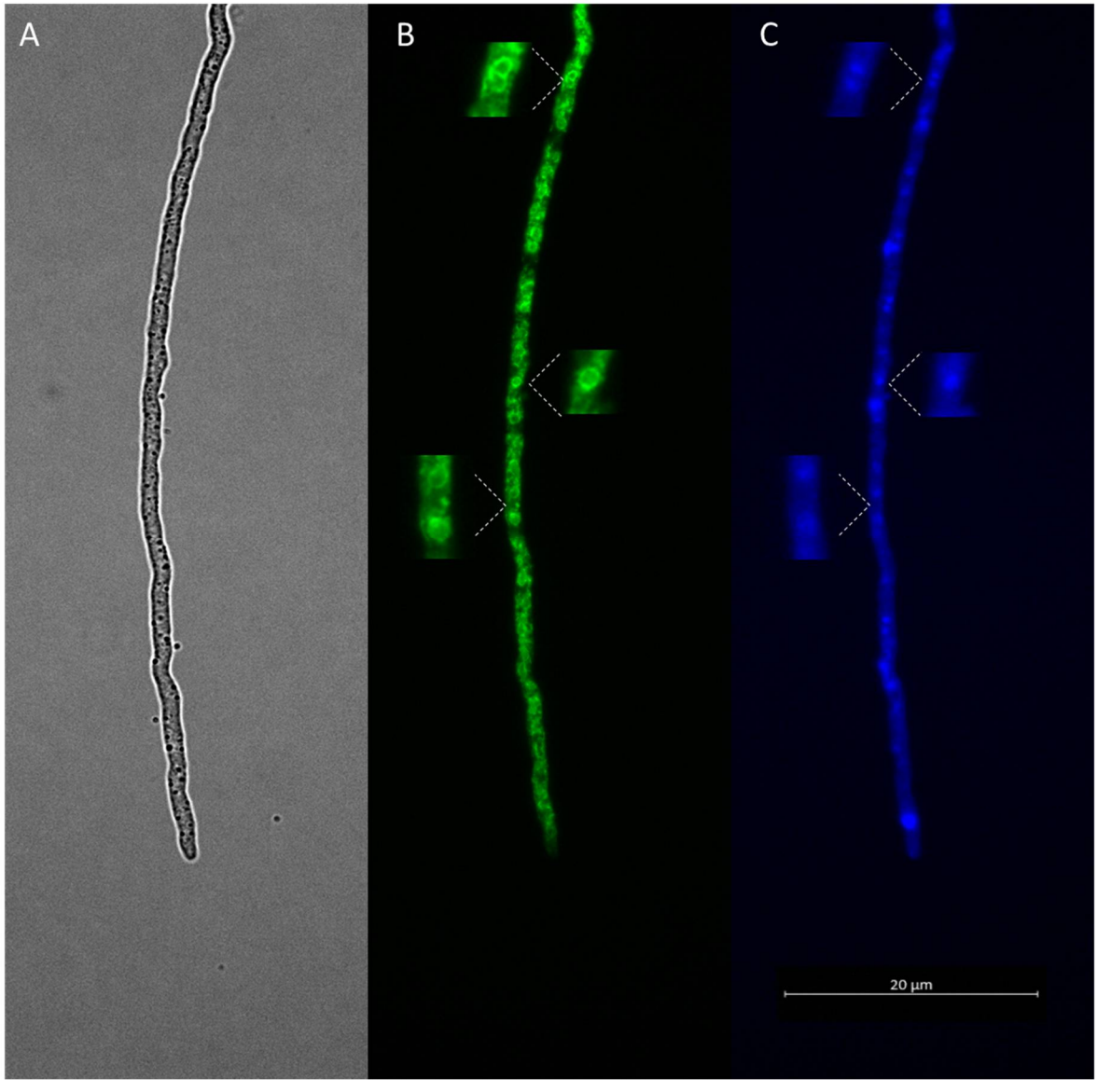

Figure 16 | *In vivo* localization of reporter gene fusion protein of CpAEC-GFP in Cp20.1. Microscopic analyses of hyphal tips of *C. purpurea* (Cp20.1) containing pLoc_AEC_GFP in bright-field (A). A GFP signal could be observed in subcellular plasmatic structures (B), surrounding nuclei stained by Hoechst 33258 (C).

Arabidopsis plants overexpressing *CpAEC* gene

To confirm function of CpAEC in IAA translocation, several independent lines of *Arabidopsis thaliana* overexpressing *CpAEC* gene under the control of estradiol inducible promoter (Zuo *et al.*, 2000) were prepared. Transgenic seedlings did not show any remarkable phenotypic alterations when grown on medium without estradiol (Figure 17). Upon estradiol induction, seedlings show significantly shortened primary roots and reduced number of lateral roots (Figure 17). Negative effect on aerial part growth was also apparent.

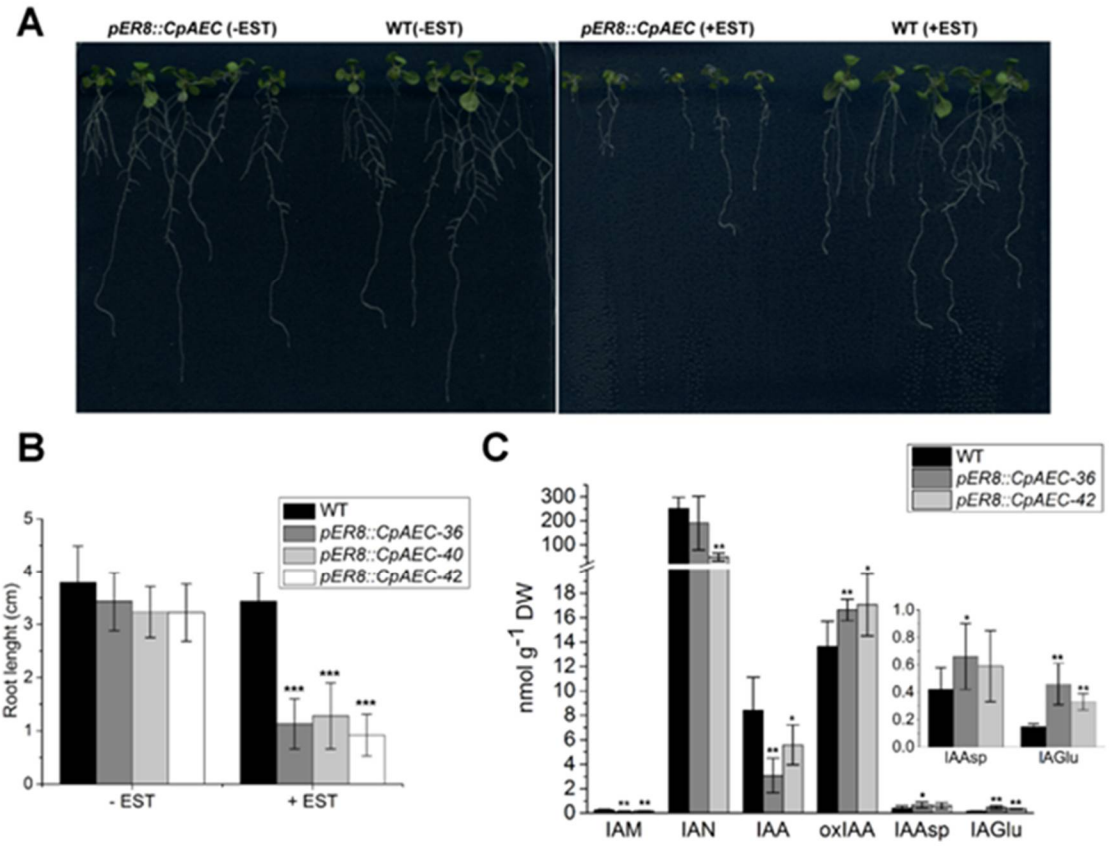

Figure 17 | Arabidopsis plants overexpressing *CpAEC* gene under the control of estradiol (EST) inducible promoter of pER8. (A) 14-day-old seedlings of WT and pER8::CpAEC-42 plants grown on MS medium in the absence (left) or presence (right) of estradiol (EST). (B) Root length of WT and three independent lines of pER8::CpAEC 14-day-old seedlings (n=15). (C) Auxin metabolite profile of 14-day-old pER8::CpAEC overexpressors and WT cultivated on MS media with EST. Mean values with standard deviations obtained from three biological replicates are presented. Concentrations of IAA and its metabolites and precursors are presented in nmol per gram of plant dry weight; IAM, indole-3-acetamide; IAN, indole-3-acetonitrile; IAA, indole-3-acetic acid; oxIAA, 2-oxindole-3-acetic acid; IAA-Asp, IAA-aspartate; IAA-Glu, IAA-glutamate. Asterisks (*, ** and ***) indicate significant differences between WT and pER8::CpAEC according to Student's unpaired t-test at P≤0.05, P≤0.01, P≤0.001, respectively.

Quantification of IAA, its precursors and deactivation products showed significantly less IAA and more aspartate and glutamate conjugates in transgenic seedlings than in WT (Figure 17 C). Except reduced amount of indole-3-acetonitrile and indole-3-acetamide and increased levels of IAA degradation product, 2-oxindole-3-acetic acid, concentration of all other metabolites was unchanged.

Discussion

Survey of *Claviceps purpurea* genome revealed one gene (*CPUR8219*) coding for a protein with high homology to PILS group of plant auxin efflux carriers. Evolutionary the oldest lineage of organisms where PILS but not PIN presence has been confirmed so far are green algae. Thus, intracellular auxin transport has preceded the evolution of PIN-dependent intercellular auxin transport (Feraru *et al.*, 2012). Similarly to plant PILS transporters, CpAEC seems to be localized intracellularly on structure resembling endoplasmic reticulum (Barbez *et al.*, 2012). Mycelium with knocked-out *CpAEC* gene does not show any morphological abnormalities. Phytopatogenic fungi produce IAA during interaction with host plant to induce defence genes (Kidd *et al*., 2011), or allow better penetration via cell expansion (Tanaka *et al.*, 2011). Spores of Δcpaec are able to fully invade ovary and host-pathogen interaction shows all usual symptoms of infection. Hence, CpAEC primary role is not to secrete auxin into plant tissue to endorse infection. Nevertheless, precise analysis of IAA revealed imbalanced concentration of IAA in Δcpaec mycelia grown in liquid culture as more IAA was retained in mycelium and more was detected also in culture filtrates. This is similar to Arabidopsis tissues with *pils2*/*pils5* mutation, which accumulate more free IAA and where it was hypothesized that PILS function in cellular auxin homeostasis by regulating auxin metabolism (Barbez *et al.*, 2012). Surprisingly, considerably more pronounced differences of IAA concentration in mycelium were observed after short-term cultivation than after 7 days. Comparison of short- and long-term cultivation reveals that while difference of IAA content between Cp20.1 and Δcpaec is higher in 4 hours mycelium, the main difference in IAA content after 7 days is in medium. Total content of IAA in mycelia of Δcpaec tends to levels of Cp20.1 over time, while total IAA content in media increases for Δcpaec mutants. These results suggest fungal effort to maintain intracellular balance of free IAA by secretion to media and CpAEC role in IAA metabolism. Similarly, experiments with Arabidopsis *pils2*/*pils5* double-mutant protoplasts showed significantly higher auxin export as demonstrated by increased extracellular IAA concentration, indicating reduced auxin retention capacity in *pils2*/*pils5* loss-of-function mutants (Barbez *et al.*, 2012). Hypothetical role of CpAEC could be in negative regulation of IAA biosynthesis, as indicated by increase of IAA biosynthesis intermediate IPA in mycelium of Δcpaec, primarily after 4 hours cultivation.

At the same time, increased IAA levels in Δcpaec could be a result of disturbed homeostasis of conjugated IAA forms, as was described in Arabidopsis *pils2*/*pils5* mutant, where ratio of conjugates IAA-Asp/IAA-Glu to free IAA decreased (Barbez *et al.*, 2012). Localization of PILS on ER membrane facilitates intracellular IAA accumulation; authors speculate that auxin conjugation might be localized to ER as well. Unfortunately, analysis of IAA conjugates content was not included in CpAEC experiment.

Based on measurements of auxin biosynthesis intermediates (P. Galuszka, unpublished results) and Cp20.1 genome mining, possible candidates for IAA biosynthesis were selected – *CPUR4616* (putative indole-3-acetamide hydrolase), *CPUR4612* (putative flavin monooxygenase YUCCA) and *CPUR5370/5371* (both tryptophan decarboxylase). Future monitoring of gene expression of these targets in Δcpaec could help to reveal main IAA biosynthesis pathway. However, only knock-out of multiple genes would bring definite answer, as IAA is frequently biosynthesized by more parallel pathways.

As CpAEC is the only member of auxin efflux carriers found in *C. purpurea* and seems to reside on ER membranes, other transporters might be present on plasma membrane of *C. purpurea.* Except PIN and PILS, plants contain two other groups of IAA specific membrane transporters - auxin influx carrier AUX/LAX (Kerr and Bennett, 2007) and ATP-binding cassette subfamily B (ABCB) transporter (Geisler and Murphy, 2008). Since not any AUX/LAX sequence is present in fungal genomes, some members of ABC transporter family, one of the largest and ubiquitous transporter families found in majority of organisms, might play role in IAA translocation in fungi. Exact role of PILS in planta is not known, but it presumably facilitates intracellular IAA accumulation or sequestration (Barbez *et al.*, 2012). Recently, the importance of PILS2, -3, and -5 for light-induced growth in apical hook development was shown (Béziat *et al.*, 2017). Negative regulation of organ growth was described for PILS6, with its abundance sensitive to high temperature (Feraru *et al.*, 2019). To verify that CpAEC really translocates auxin, the gene was overexpressed under the control of inducible promotor in Arabidopsis plants. Upon induction, CpAEC provoked same root phenotype as that observed for plant *PILS6* overexpressor (Feraru *et al.*, 2019). Plants also accumulate less free IAA and more amino acid conjugates similar to plants with constitutive expression of *PILS5* (Barbez *et al.*, 2012). The results suggest that fungal auxin efflux carrier is indeed specific for auxin

translocation; however its direct function is similarly to plant PILS largely unknown and probably redundant with other types of fungal transporters.

Part VII: Conclusions

Experiments showed that infection of rye by *C. purpurea* is accompanied by change of cytokinin levels. Gene expression study of selected rye genes participating in cytokinin metabolism and signaling confirmed response to cytokinin signal, however expression of cytokinin biosynthetic genes remained identical. *In silico* survey of *C. purpurea* genome revealed the presence of cytokinin-specific biosynthetic genes. Heterologous expression in bacteria and Arabidopsis confirmed that they encode functional *de novo* cytokinin biosynthetic enzymes, identified in a fungus for the first time. It was shown that cytokinin biosynthesis by *C. purpurea* occurs via a different mechanism to any that have previously been suggested to be involved in fungus–plant interactions. The results presented herein provided basis for follow-up *C. purpurea* research that has revealed importance of cytokinins in fungal pathogenicity.

Cytokinins play an important role in some *Fusarium*–host interactions. Expression study of maize and fungal genes involved in cytokinin metabolism during infection of maize with different *Fusarium* helped to reveal why the fungal hormone synthesis only minimally affected maize growth. Along with expression of cytokinin biosynthetic genes from both organisms, expression of a maize *CKX* encoding enzyme involved in the irreversible degradation of cytokinins was detected. Thus, despite efforts by the fungus to alter cytokinin balance in maize tissue (either directly by cytokinin production or indirectly by inducing plant cytokinin synthesis) overall levels were actively mitigated by the plant.

Genome of *Claviceps purpurea* contains one gene coding for putative auxin efflux carrier, whose disruption led to auxin intracellular imbalance. However, loss-of-function mutation did not result in any phenotypic alteration and mutant ability to infect rye was unchanged. Inducible heterologous expression of the gene in Arabidopsis led to change of root morphology, similar to that observed in Arabidopsis plants with constitutive expression of PILS auxin transporters.

Part VIII: Abbreviations

ABC	ATP-binding cassette transporters
ADP	adenosine diphosphate
AMP	adenosine monophosphate
ATP	adenosine triphosphate
CKX	cytokinin oxidase/dehydrogenase
CYP450	cytochrome P450
cZ	*cis*-zeatin
cZR	*cis*-zeatin riboside
cZRMP	*cis*-zeatin riboside 5'-monophosphate
DHZ	dihydrozeatin (N6-(4-hydroxy-3-methylbutyl)adenine)
DMAPP	dimethylallyl diphosphate
dpi	days post infection
EA	ergot alkaloids
ER	endoplasmic reticulum
ENT	equilibrative nucleoside transporter
FAD	flavin adenine dinucleotide
FFC	*Fusarium fujikuroi* complex
GA	gibberellins
GFP	green fluorescent protein
GUS	β-glucuronidase
HK	histidine kinase
HMBDP	(E)-4-hydroxy-3-methylbut-2-enyl diphosphate
HP	histidine-containing phosphotransfer protein
IAA	indole-3-acetic acid
IAA-Asp	indole-3-acetic acid aspartic acid
IAA-glc	indole-3-acetic acid glucose
IAA-Glu	indole-3-acetic acid glutamic acid
IAAld	indole-3-acetaldehyde
IAM	indole-3-acetamide
IAN	indole-3-acetonitrile

IAOx	indole-3-acetaldoxime
iP	N6-(Δ2-isopentenyl)adenine
IPA	indole-3-pyruvic acid
iPR	isopentenyladenosine
iPRMP	isopentenyladenosine 5'-monophosphate
IPT	isopentenyl transferase
LOG	Lonely Guy (cytokinin-specific phosphoribohydrolase)
MMD	mango malformation disease
NHT	N-hydroxytryptamine
oxIAA	2-oxindole-3-acetic acid
PUP	purine permease
qPCR	quantitative real-time polymerase chain reaction
RR	response regulators
TAM	tryptamine
T-DNA	transfer DNA of Ti plasmid
tZ	*trans*-zeatin
tZR	*trans*-zeatin riboside
tZRMP	*trans*-zeatin riboside 5'-monophosphate
WT	wild-type (organism; i.e. non-mutated)
YUC	YUCCA flavin-containing monooxygenase

Part IX: References

Abe, I., Tanaka, H., Abe, T., Noguchi, H. (2007). Enzymatic formation of unnatural cytokinin analogs by adenylate isopentenyltransferase from mulberry. *Biochemical and Biophysical Research Communications*, *355*, 795-800.

Akiyoshi, D. E., Klee, H., Amasino, R. M., Nester, E. W., Gordon, M. P. (1984). T-DNA of *Agrobacterium tumefaciens* encodes an enzyme of cytokinin biosynthesis. *Proceedings of the National Academy of Sciences*, *81*, 5994-5998.

Allen, M. F., Moore Jr, T. S., Christensen, M. (1980). Phytohormone changes in *Bouteloua gracilis* infected by vesicular–arbuscular mycorrhizae: I. Cytokinin increases in the host plant. *Canadian Journal of Botany*, *58*, 371-374.

Altschul, S. F., Madden, T. L., Schäffer, A. A., Zhang, J., Zhang, Z., Miller, W., Lipman, D. J. (1997). Gapped BLAST and PSI-BLAST: a new generation of protein database search programs. *Nucleic Acids Research*, *25*, 3389-3402.

Apine, O. A., Jadhav, J. P. (2011). Optimization of medium for indole-3-acetic acid production using *Pantoea agglomerans* strain PVM. *Journal of Applied Microbiology*, *110*, 1235-1244.

Argyros, R. D., Mathews, D. E., Chiang, Y. H., Palmer, C. M., Thibault, D. M., Etheridge, N., Argyros, D. A., Mason, M. G., Kieber, J. J., Schaller, G. E., (2008). Type B response regulators of Arabidopsis play key roles in cytokinin signaling and plant development. *The Plant Cell*, *20*, 2102-2116.

Armengaud, P., Zambaux, K., Hills, A., Sulpice, R., Pattison, R. J., Blatt, M. R., Amtmann, A. (2009). EZ-Rhizo: integrated software for the fast and accurate measurement of root system architecture. *The Plant Journal*, *57*, 945-956.

Ausubel, F. M., Brent, R., Kingston, R. E., Moore, D. D., Seidman, J. G., Smith, J. A., Struhl, K. (1987). Current Protocols in Molecular Biology. *John Wiley and Sons*, New York.

Bai, G., Shaner, G. (2004). Management and resistance in wheat and barley to Fusarium head blight. *Annual Review of Phytopathology*, *42*, 135-161.

Bailey, AM., Turner, G., Brown, J., Kerry-Williams, S., Wards, M., Plunt, PJ., & van den Hondel, CAMJJ. (1989). Analysis of the oliC promotor of *Aspergillus nidulans*. *Foundation for Biotechnical and Industrial Fermentation Research*, *6*, 101 – 109.

Barbez, E., Kubeš, M., Rolčík, J., Béziat, C., Pěnčík, A., Wang, B., Rosquette, M. R., Zhu, J., Dobrev, P. I., Lee, Y., Zažímalová, E., Petrášek, J., Geisler, M., Friml, J., Jürgen, K. V. (2012). A novel putative auxin carrier family regulates intracellular auxin homeostasis in plants. *Nature*, *485*, 119.

Barker, S. J., Tagu, D. (2000). The roles of auxins and cytokinins in mycorrhizal symbioses. *Journal of Plant Growth Regulation*, *19*, 144-154.

Behr, M., Motyka, V., Weihmann, F., Malbeck, J., Deising, H. B., Wirsel, S. G. (2012). Remodeling of cytokinin metabolism at infection sites of *Colletotrichum graminicola* on maize leaves. *Molecular Plant-Microbe Interactions*, *25*, 1073-1082.

Bender, R. L., Fekete, M. L., Klinkenberg, P. M., Hampton, M., Bauer, B., Malecha, M., Lindgren, K., Maki, J. A., Perera, M. A. D. N., Nikolau, B. J., Carter, C. J. (2013). PIN6 is required for nectary auxin response and short stamen development. *The Plant Journal*, *74*, 893-904.

Benková, E., Michniewicz, M., Sauer, M., Teichmann, T., Seifertová, D., Jürgens, G., Friml, J. (2003). Local, efflux-dependent auxin gradients as a common module for plant organ formation. *Cell*, *115*, 591-602.

Béziat, C., Barbez, E., Feraru, M. I., Lucyshyn, D., Kleine-Vehn, J. (2017). Light triggers PILS-dependent reduction in nuclear auxin signalling for growth transition. *Nature Plants*, *3*, 17105.

Bonner, J., Bandurski, R. S. (1952). Studies of the physiology, pharmacology, and biochemistry of the auxins. *Annual Review of Plant Physiology*, *3*, 59-86.

Bosco, C. D., Dovzhenko, A., Liu, X., Woerner, N., Rensch, T., Eismann, M., Eimer, S., Hegermann, J., Paponov, I. A., Ruperti, B., Heberle-Bors, E., Touraev, A., Cohen, J. D., Palme, K. (2012). The endoplasmic reticulum localized PIN8 is a pollen-specific auxin carrier involved in intracellular auxin homeostasis. *The Plant Journal*, *71*, 860-870.

Bruce, S. A., Saville, B. J., Emery, R. N. (2011). *Ustilago maydis* produces cytokinins and abscisic acid for potential regulation of tumor formation in maize. *Journal of Plant Growth Regulation*, *30*, 51-63.

Bürkle, L., Cedzich, A., Döpke, C., Stransky, H., Okumoto, S., Gillissen, B., Kühn, C., Frommer, W. B. (2003). Transport of cytokinins mediated by purine transporters of the PUP family expressed in phloem, hydathodes, and pollen of Arabidopsis. *The Plant Journal*, *34*, 13-26.

Caesar, K., Thamm, A. M., Witthöft, J., Elgass, K., Huppenberger, P., Grefen, C., Horak, J., Harter, K. (2011). Evidence for the localization of the Arabidopsis cytokinin receptors

AHK3 and AHK4 in the endoplasmic reticulum. *Journal of Experimental Botany*, *62*, 5571-5580.

Camilleri, C., Jouanin, L. (1991). The TR-DNA region carrying the auxin synthesis genes of the *Agrobacterium rhizogenes* agropine-type plasmid pRiA4: nucleotide sequence analysis and introduction into tobacco plants. *Molecular Plant-Microbe Interactions*, *4*, 155-162.

Cenis, J. L. (1992). Rapid extraction of fungal DNA for PCR amplification. *Nucleic Acids Research*, *20*, 2380.

Cerutti, T., Delatorre, C. A. (2013). Nitrogen and phosphorus interaction and cytokinin: responses of the primary root of *Arabidopsis thaliana* and the *pdr1* mutant. *Plant Science*, *198*, 91-97.

Chanclud, E., Kisiala, A., Emery, N. R., Chalvon, V., Ducasse, A., Romiti-Michel, C., Gravot, A., Kroj, T., Morel, J. B. (2016). Cytokinin production by the rice blast fungus is a pivotal requirement for full virulence. *PLoS Pathogens*, *12*, e1005457.

Cheng, Y., Dai, X., Zhao, Y. (2007). Auxin synthesized by the YUCCA flavin monooxygenases is essential for embryogenesis and leaf formation in Arabidopsis. *The Plant Cell*, *19*, 2430-2439.

Colot, H. V., Park, G., Turner, G. E., Ringelberg, C., Crew, C. M., Litvinkova, L., Weiss, R. L., Borkovich, K. A., Dunlap, J. C. (2006). A high-throughput gene knockout procedure for Neurospora reveals functions for multiple transcription factors. *Proceedings of the National Academy of Sciences*, *103*, 10352-10357.

Coufal-Majewski, S., Stanford, K., McAllister, T., Blakley, B., McKinnon, J., Chaves, A. V., Wang, Y. (2016). Impacts of cereal ergot in food animal production. *Frontiers in Veterinary Science*, *3*, 15.

Christianson, T. W., Sikorski, R. S., Dante, M., Shero, J. H., Hieter, P. (1992). Multifunctional yeast high-copy-number shuttle vectors. *Gene*, *110*, 119-122.

Clough, S. J., Bent, A. F. (1998). Floral dip: a simplified method for Agrobacterium-mediated transformation of *Arabidopsis thaliana*. *The Plant Journal*, *16*, 735-743.

Creason, A. L., Vandeputte, O. M., Savory, E. A., Davis II, E. W., Putnam, M. L., Hu, E., Swader-Hines, D., Mol, A., Baucher, M., Prinsen, E., Zdanowska, M., Givan, S.A., El Jaziri, M., Loper, J.E., Mahmud, T., Chang, J.H., (2014). Analysis of genome sequences from plant pathogenic *Rhodococcus* reveals genetic novelties in virulence loci. *PLoS One*, *9*, e101996.

Da Mota, F. F., Gomes, E. A., Seldin, L. (2008). Auxin production and detection of the gene coding for the Auxin Efflux Carrier (AEC) protein in *Paenibacillus polymyxa*. *The Journal of Microbiology*, *46*, 257-264.

Dereeper, A., Guignon, V., Blanc, G., Audic, S., Buffet, S., Chevenet, F., Dufayard, J.-F., Guindon, S., Lefort, V., Lescot, M., Claverie, J. M., Gascuel, O. (2008). Phylogeny.fr: robust phylogenetic analysis for the non-specialist. *Nucleic Acids Research*, *36*, 465-469.

Diener, A. (2012). Visualizing and quantifying *Fusarium oxysporum* in the plant host. *Molecular Plant-Microbe Interactions*, *25*, 1531-1541.

Dignani, M. C., Anaissie, E. (2004). Human fusariosis. *Clinical Microbiology and Infection*, *10*, 67-75.

Duca, D., Lorv, J., Patten, C. L., Rose, D., Glick, B. R. (2014). Indole-3-acetic acid in plant–microbe interactions. *Antonie Van Leeuwenhoek*, *106*, 85-125.

El-Showk, S., Ruonala, R., Helariutta, Y. (2013). Crossing paths: cytokinin signalling and crosstalk. *Development*, *140*, 1373-1383.

El Yacoubi, B., Bailly, M., de Crécy-Lagard, V. (2012). Biosynthesis and function of posttranscriptional modifications of transfer RNAs. *Annual Review of Genetics*, *46*, 69-95.

Esser, K., Tudzynski, P. (1978). Genetics of the ergot fungus *Claviceps purpurea*. *Theoretical and Applied Genetics*, *53*, 145-149.

Faiss, M., Zalubìlová, J., Strnad, M., Schmülling, T. (1997). Conditional transgenic expression of the ipt gene indicates a function for cytokinins in paracrine signaling in whole tobacco plants. *The Plant Journal*, *12*, 401-415.

Felten, J., Martin, F., Legué, V. (2012). Signalling in ectomycorrhizal symbiosis. *Signaling and Communication in Plant Symbiosis*, *45*, 123-142.

Feraru, E., Vosolsobě, S., Feraru, M. I., Petrášek, J., Kleine-Vehn, J. (2012). Evolution and structural diversification of PILS putative auxin carriers in plants. *Frontiers in Plant Science*, *3*, 227.

Feraru, E., Feraru, M. I., Barbez, E., Waidmann, S., Sun, L., Gaidora, A., Kleine-Vehn, J. (2019). PILS6 is a temperature-sensitive regulator of nuclear auxin input and organ growth in *Arabidopsis thaliana*. *Proceedings of the National Academy of Sciences*, *116*, 3893-3898.

Friml, J., Vieten, A., Sauer, M., Weijers, D., Schwarz, H., Hamann, T., Offringa, R., Jürgens, G. (2003). Efflux-dependent auxin gradients establish the apical–basal axis of Arabidopsis. *Nature*, *426*, 147.

Frébortová, J., Novák, O., Frébort, I., Jorda, R. (2010). Degradation of cytokinins by maize cytokinin dehydrogenase is mediated by free radicals generated by enzymatic oxidation of natural benzoxazinones. *The Plant Journal*, *61*, 467-481.

Freeman, S., Shtienberg, D., Maymon, M., Levin, A. G., Ploetz, R. C. (2014). New insights into mango malformation disease epidemiology lead to a new integrated management strategy for subtropical environments. *Plant Disease*, *98*, 1456-1466.

Galuszka, P., Frébort, I., Šebela, M., Sauer, P., Jacobsen, S., Peč, P. (2001). Cytokinin oxidase or dehydrogenase? Mechanism of cytokinin degradation in cereals. *European Journal of Biochemistry*, *268*, 450-461.

Galuszka, P., Popelková, H., Werner, T., Frébortová, J., Pospíšilová, H., Mik, V., Köllmer, I., Schmülling, T., Frébort, I. (2007). Biochemical characterization of cytokinin oxidases/dehydrogenases from *Arabidopsis thaliana* expressed in *Nicotiana tabacum* L. *Journal of Plant Growth Regulation*, *26*, 255-267.

Galuszka, P., Spíchal, L., Kopečný, D., Tarkowski, P., Frébortová, J., Šebela, M., Frébort, I. (2008). Metabolism of plant hormones cytokinins and their function in signaling, cell differentiation and plant development. *Studies in Natural Products Chemistry*, *34*, 203-264.

Gatz, C., Frohberg, C., Wendenburg, R. (1992). Stringent repression and homogeneous de-repression by tetracycline of a modified CaMV 35S promoter in intact transgenic tobacco plants. *The Plant Journal*, *2*, 397-404.

Geisler, M., Murphy, A. S. (2006). The ABC of auxin transport: the role of p-glycoproteins in plant development. *FEBS letters*, *580*, 1094-1102.

Giesbert, S., Schuerg, T., Scheele, S., Tudzynski, P. (2008). The NADPH oxidase Cpnox1 is required for full pathogenicity of the ergot fungus *Claviceps purpurea*. *Molecular Plant Pathology*, *9*, 317-327.

Gillissen, B., Bürkle, L., André, B., Kühn, C., Rentsch, D., Brandl, B., Frommer, W. B. (2000). A new family of high-affinity transporters for adenine, cytosine, and purine derivatives in Arabidopsis. *The Plant Cell*, *12*, 291-300.

Gordon, T. R. (2006). Pitch canker disease of pines. *Phytopathology*, *96*, 657-659.

Guarro, J., Gene, J. (1995). Opportunistic fusarial infections in humans. *European Journal of Clinical Microbiology and Infectious Diseases*, *14*, 741-754.

Haarmann, T., Rolke, Y., Giesbert, S., Tudzynski, P. (2009). Ergot: from witchcraft to biotechnology. *Molecular Plant Pathology*, *10*, 563-577.

Hall, T. A. (1999). BioEdit: a user-friendly biological sequence alignment editor and analysis program for Windows 95/98/NT. *Nucleic Acids Symposium Series, 41,* 1979-2000.

Hann, D. R., Domínguez-Ferreras, A., Motyka, V., Dobrev, P. I., Schornack, S., Jehle, A., Felix, G., Chinchilla, D., Rathjen, J.P., Boller, T. (2014). The Pseudomonas type III effector HopQ1 activates cytokinin signaling and interferes with plant innate immunity. *New Phytologist*, *201*, 585-598.

Hedden, P., Sponsel, V. (2015). A century of gibberellin research. *Journal of Plant Growth Regulation*, *34*, 740-760.

Hilbert, M., Voll, L. M., Ding, Y., Hofmann, J., Sharma, M., Zuccaro, A. (2012). Indole derivative production by the root endophyte *Piriformospora indica* is not required for growth promotion but for biotrophic colonization of barley roots. *New Phytologist*, *196*, 520-534.

Hinsch, J., Tudzynski, P. (2015). Claviceps: the Ergot fungus. *Molecular Biology of Food and Water Borne Mycotoxigenic and Mycotic Fungi,* 248-269.

Hinsch, J., Vrabka, J., Oeser, B., Novák, O., Galuszka, P., Tudzynski, P. (2015). *De novo* biosynthesis of cytokinins in the biotrophic fungus *Claviceps purpurea*. *Environmental Microbiology*, *17*, 2935-2951.

Hinsch, J., Galuszka, P., Tudzynski, P. (2016). Functional characterization of the first filamentous fungal tRNA-isopentenyltransferase and its role in the virulence of *Claviceps purpurea*. *New Phytologist*, *211*, 980-992.

Hirose, N., Makita, N., Yamaya, T., Sakakibara, H. (2005). Functional characterization and expression analysis of a gene, OsENT2, encoding an equilibrative nucleoside transporter in rice suggest a function in cytokinin transport. *Plant Physiology*, *138*, 196-206.

Hirose, N., Makita, N., Kojima, M., Kamada-Nobusada, T., Sakakibara, H. (2007). Overexpression of a type-A response regulator alters rice morphology and cytokinin metabolism. *Plant and Cell Physiology*, *48*, 523-539.

Hirose, N., Takei, K., Kuroha, T., Kamada-Nobusada, T., Hayashi, H., Sakakibara, H., (2008). Regulation of cytokinin biosynthesis, compartmentalization and translocation. *Journal of Experimental Botany*, *59*, 75–83.

Houba-Hérin, N., Pethe, C., d'Alayer, J., Laloue, M. (1999). Cytokinin oxidase from *Zea mays*: purification, cDNA cloning and expression in moss protoplasts. *The Plant Journal*, *17*, 615-626.

Hull, A. K., Vij, R., Celenza, J. L. (2000). Arabidopsis cytochrome P450s that catalyze the first step of tryptophan-dependent indole-3-acetic acid biosynthesis. *Proceedings of the National Academy of Sciences*, *97*, 2379-2384.

Hulvová, H., Galuszka, P., Frébortová, J., Frébort, I. (2013). Parasitic fungus Claviceps as a source for biotechnological production of ergot alkaloids. *Biotechnology Advances*, *31*, 79-89.

Hüsgen, U., Buttner, P., Muller, U., Tudzynski, P. (1999). Variation in karyotype and ploidy level among field isolates of *Claviceps purpurea*. *Journal of Phytopathology, 147,* 591-597.

Ioio, R. D., Linhares, F. S., Sabatini, S. (2008). Emerging role of cytokinin as a regulator of cellular differentiation. *Current Opinion in Plant Biology*, *11*, 23-27.

Ishihara, A., Hashimoto, Y., Tanaka, C., Dubouzet, J. G., Nakao, T., Matsuda, F., Nishioka, T., Miyagawa, H., Wakasa, K. (2008). The tryptophan pathway is involved in the defense responses of rice against pathogenic infection via serotonin production. *The Plant Journal*, *54*, 481-495.

Ito, Y., Kurata, N. (2006). Identification and characterization of cytokinin-signalling gene families in rice. *Gene*, *382*, 57-65.

Jackson, R. G., Lim, E. K., Li, Y., Kowalczyk, M., Sandberg, G., Hoggett, J., Ashford, D. A., Bowles, D. J. (2001). Identification and biochemical characterization of an Arabidopsis indole-3-acetic acid glucosyltransferase. *Journal of Biological Chemistry*, *276*, 4350-4356.

Jiang, C. J., Shimono, M., Sugano, S., Kojima, M., Liu, X., Inoue, H., Sakakibara, H., Takatsuji, H. (2013). Cytokinins act synergistically with salicylic acid to activate defense gene expression in rice. *Molecular Plant-Microbe Interactions*, *26*, 287-296.

Jungehülsing, U., Arntz, C., Smit, R., Tudzynski, P. (1994). The *Claviceps purpurea* glyceraldehyde-3-phosphate dehydrogenase gene: cloning, characterization, and use for the improvement of a dominant selection system. *Current Genetics*, *25*, 101-106.

Kabbara, S., Hérivaux, A., Dugé de Bernonville, T., Courdavault, V., Clastre, M., Gastebois, A., Osman, M., Hamze, M., Cock, J. M., Schaap, P., Papon, N. (2018). Diversity and evolution of sensor histidine kinases in eukaryotes. *Genome Biology and Evolution*, *11*, 86-108.

Kakimoto, T. (2001). Identification of plant cytokinin biosynthetic enzymes as dimethylallyl diphosphate: ATP/ADP isopentenyltransferases. *Plant and Cell Physiology*, *42*, 677-685.

Kakimoto, T. (2003). Perception and signal transduction of cytokinins. *Annual Review of Plant Biology*, *54*, 605-627.

Kerr, I. D., Bennett, M. J. (2007). New insight into the biochemical mechanisms regulating auxin transport in plants. *Biochemical Journal*, *401*, 613-622.

Kiba, T., Yamada, H., Sato, S., Kato, T., Tabata, S., Yamashino, T., Mizuno, T. (2003). The type-A response regulator, ARR15, acts as a negative regulator in the cytokinin-mediated signal transduction in *Arabidopsis thaliana*. *Plant and Cell Physiology*, *44*, 868-874.

Kidd, B. N., Kadoo, N. Y., Dombrecht, B., Tekeoglu, M., Gardiner, D. M., Thatcher, L. F., Aitken, E. A. B., Schenk, P. M., Manners, J. M., Kazan, K. (2011). Auxin signaling and transport promote susceptibility to the root-infecting fungal pathogen *Fusarium oxysporum* in Arabidopsis. *Molecular Plant-Microbe Interactions*, *24*, 733-748.

Kind, S., Hinsch, J., Vrabka, J., Hradilová, M., Majeská-Čudejková, M., Tudzynski, P., Galuszka, P. (2018). Manipulation of cytokinin level in the ergot fungus *Claviceps purpurea* emphasizes its contribution to virulence. *Current Genetics*, *64*, 1-17.

Ko, D., Kang, J., Kiba, T., Park, J., Kojima, M., Do, J., Kim, K.Y., Kwon, M., Endler, A., Song, W. Y., Martinoia, E., Sakakibara, H., Lee, Y. (2014). Arabidopsis ABCG14 is essential for the root-to-shoot translocation of cytokinin. *Proceedings of the National Academy of Sciences*, *111*, 7150-7155.

Konevega, A. L., Soboleva, N. G., Makhno, V. I., Peshekhonov, A. V., Katunin, V. I. (2006). Effect of modification of tRNA nucleotide 37 on the tRNA interaction with the A and P sites of the *Escherichia coli* 70S ribosome. *Molecular Biology*, *40*, 597-610.

Kowalczyk, M., Sandberg, G. (2001). Quantitative analysis of indole-3-acetic acid metabolites in Arabidopsis. *Plant Physiology*, *127*, 1845-1853.

Kudo, T., Kiba, T., Sakakibara, H. (2010). Metabolism and long-distance translocation of cytokinins. *Journal of Integrative Plant Biology*, *52*, 53-60.

Kulkarni, G. B., Sanjeevkumar, S., Kirankumar, B., Santoshkumar, M., & Karegoudar, T. B. (2013). Indole-3-acetic acid biosynthesis in Fusarium delphinoides strain GPK, a causal agent of Wilt in Chickpea. *Applied Biochemistry and Biotechnology*, *169*, 1292-1305.

Kurakawa, T., Ueda, N., Maekawa, M., Kobayashi, K., Kojima, M., Nagato, Y., Sakakibara, H., Kyozuka, J. (2007). Direct control of shoot meristem activity by a cytokinin-activating enzyme. *Nature*, *445*, 652.

Leyser, O. (2018). Auxin signaling. *Plant Physiology*, *176*, 465-479.

Leslie, J. F., Summerell, B. A. (2008). *The Fusarium Laboratory Manual*.

Liao, X., Lovett, B., Fang, W., St Leger, R. J. (2017). *Metarhizium robertsii* produces indole-3-acetic acid, which promotes root growth in Arabidopsis and enhances virulence to insects. *Microbiology*, *163*, 980-991.

Lindner, A. C., Lang, D., Seifert, M., Podlešáková, K., Novák, O., Strnad, M., Reski, R., von Schwartzenberg, K. (2014). Isopentenyltransferase-1 (IPT1) knockout in *Physcomitrella* together with phylogenetic analyses of IPTs provide insights into evolution of plant cytokinin biosynthesis. *Journal of Experimental Botany*, *65*, 2533-2543.

Llorente, F., Muskett, P., Sánchez-Vallet, A., López, G., Ramos, B., Sánchez-Rodríguez, C., Jordá, L., Parker, J., Molina, A. (2008). Repression of the auxin response pathway increases Arabidopsis susceptibility to necrotrophic fungi. *Molecular Plant*, *1*, 496-509.

Lo Presti, L., Lanver, D., Schweizer, G., Tanaka, S., Liang, L., Tollot, M., Zuccaro, A., Reissmann, S., Kahmann, R. (2015). Fungal effectors and plant susceptibility. *Annual Review of Plant Biology*, *66*, 513-545.

Ludwig-Müller, J. (2011). Auxin conjugates: their role for plant development and in the evolution of land plants. *Journal of Experimental Botany*, *62*, 1757-1773.

Luo, K., Rocheleau, H., Qi, P. F., Zheng, Y. L., Zhao, H. Y., Ouellet, T. (2016). Indole-3-acetic acid in *Fusarium graminearum*: identification of biosynthetic pathways and characterization of physiological effects. *Fungal Biology*, *120*, 1135-1145.

Mantle, P. G., Nisbet, L. J. (1976). Differentiation of *Claviceps purpurea* in axenic culture. *Microbiology*, *93*, 321-334.

Matic, S., Gullino, M. L., Spadaro, D. (2017). The puzzle of *bakanae* disease through interactions between *Fusarium fujikuroi* and rice. *Frontiers in Bioscience (Elite Edition)*, *9*, 333-344.

Miyawaki, K., Tarkowski, P., Matsumoto-Kitano, M., Kato, T., Sato, S., Tarkowska, D., Tabata, S., Sandberg, G., Kakimoto, T. (2006). Roles of Arabidopsis ATP/ADP isopentenyltransferases and tRNA isopentenyltransferases in cytokinin biosynthesis. *Proceedings of the National Academy of Sciences*, *103*, 16598-16603.

Mey, G., Oeser, B., Lebrun, M. H., Tudzynski, P. (2002). The biotrophic, non-appressorium-forming grass pathogen *Claviceps purpurea* needs a Fus3/Pmk1 homologous mitogen-activated protein kinase for colonization of rye ovarian tissue. *Molecular Plant-Microbe Interactions*, *15*, 303-312.

Morris, R. O., Bilyeu, K. D., Laskey, J. G., Cheikh, N. N. (1999). Isolation of a gene encoding a glycosylated cytokinin oxidase from maize. *Biochemical and Biophysical Research Communications*, *255*, 328-333.

Morrison, E. N., Emery, R. J. N., Saville, B. J. (2017). Fungal derived cytokinins are necessary for normal *Ustilago maydis* infection of maize. *Plant Pathology*, *66*, 726-742.

Murphy, A. M., Pryce-Jones, E., Johnstone, K., Ashby, A. M. (1997). Comparison of cytokinin production in vitro by *Pyrenopeziza brassicae* with other plant pathogens. *Physiological and Molecular Plant Pathology*, *50*, 53-65.

Mravec, J., Skůpa, P., Bailly, A., Hoyerová, K., Křeček, P., Bielach, A., Petrášek, J., Zhang, J., Gaykova, V., Stierhof, Y.-D., Dobrev, P. I., Schwarzerová, K., Rolčík, J., Seifertová, D., Luschnig, C., Benková, E., Zažímalová, E., Geisler, M., Friml, J. (2009). Subcellular homeostasis of phytohormone auxin is mediated by the ER-localized PIN5 transporter. *Nature*, *459*, 1136.

Mrízová, K., Jiskrová, E., Vyroubalová, Š., Novák, O., Ohnoutková, L., Pospíšilová, H., Frébort, I., Harwood, W. A., Galuszka, P. (2013). Overexpression of cytokinin dehydrogenase genes in barley (*Hordeum vulgare* cv. Golden Promise) fundamentally affects morphology and fertility. *PLoS One*, *8*, e79029.

Murphy, A. M., Pryce-Jones, E., Johnstone, K., Ashby, A. M. (1997). Comparison of cytokinin production *in vitro* by *Pyrenopeziza brassicae* with other plant pathogens. *Physiological and Molecular Plant Pathology*, *50*, 53-65.

Navarro, L., Dunoyer, P., Jay, F., Arnold, B., Dharmasiri, N., Estelle, M., Voinnet, O., Jones, J. D. (2006). A plant miRNA contributes to antibacterial resistance by repressing auxin signaling. *Science*, *312*, 436-439.

Niehaus, E. M., Münsterkötter, M., Proctor, R. H., Brown, D. W., Sharon, A., Idan, Y., Oren-Young, L., Sieber, C. M., Novák, O., Pěnčík, A., Tarkowská, D., Hromadová, K., Freeman, S., Maymon, M., Elazar, M., Youssef, S. A., El-Shabrawy, E. S. M., Shalaby, A. B. A., Houterman, P., Brock, N. L., Burkhardt, I., Tsavkelova, E., Dickschat, J. S., Galuszka P., Güldener, U., Tudzynski, B. (2016). Comparative "omics" of the *Fusarium fujikuroi* species complex highlights differences in genetic potential and metabolite synthesis. *Genome Biology and Evolution*, *8*, 3574-3599.

Novák, O., Hényková, E., Sairanen, I., Kowalczyk, M., Pospíšil, T., Ljung, K. (2012). Tissue-specific profiling of the *Arabidopsis thaliana* auxin metabolome. *The Plant Journal*, *72*, 523-536.

O'Donnell, K., Rooney, A. P., Proctor, R. H., Brown, D. W., McCormick, S. P., Ward, T. J., Frandsen, R. J. N., Lysøe, E., Rehner, S. A., Aoki, T., Robert, V. A., Crous, P. W., Groenewald, J. Z., Kang, S., Geiser, D. M. (2013). Phylogenetic analyses of RPB1 and RPB2 support a middle Cretaceous origin for a clade comprising all agriculturally and medically important fusaria. *Fungal Genetics and Biology*, *52*, 20-31.

Oeser, B., Heidrich, P. M., Müller, U., Tudzynski, P., Tenberge, K. B. (2002). Polygalacturonase is a pathogenicity factor in the *Claviceps purpurea*/rye interaction. *Fungal Genetics and Biology*, *36*, 176-186.

Oeser, B., Kind, S., Schurack, S., Schmutzer, T., Tudzynski, P., Hinsch, J. (2017). Cross-talk of the biotrophic pathogen *Claviceps purpurea* and its host *Secale cereale*. *BMC Genomics*, *18*, 273.

Okada, K., Ueda, J., Komaki, M. K., Bell, C. J., Shimura, Y. (1991). Requirement of the auxin polar transport system in early stages of Arabidopsis floral bud formation. *The Plant Cell*, *3*, 677-684.

Östin, A., Kowalyczk, M., Bhalerao, R. P., Sandberg, G. (1998). Metabolism of indole-3-acetic acid in Arabidopsis. *Plant Physiology*, *118*, 285-296.

Pačes, V., Werstiuk, E., Hall, R. H. (1971). Conversion of N6-(Δ2-isopentenyl) adenosine to adenosine by enzyme activity in tobacco tissue. *Plant Physiology*, *48*, 775-778.

Pertry, I., Václavíková, K., Depuydt, S., Galuszka, P., Spíchal, L., Temmerman, W., Stes, E., Schmülling, T., Kakimoto, T., Van Montagu, M. C. E., Strnad, M., Holsters, M., Tarkowski, P., Vereecke, D. (2009). Identification of *Rhodococcus fascians* cytokinins and their modus operandi to reshape the plant. *Proceedings of the National Academy of Sciences*, *106*, 929-934.

Pěnčík, A., Simonovik, B., Petersson, S. V., Henyková, E., Simon, S., Greenham, K., Zhang, Y., Kowalczyk, M., Estelle, M., Zažímalová, E., Novák, O., Sandberg, G., Ljung, K. (2013). Regulation of auxin homeostasis and gradients in Arabidopsis roots through the formation of the indole-3-acetic acid catabolite 2-oxindole-3-acetic acid. *The Plant Cell*, *25*, 3858-3870.

Petrášek, J., Mravec, J., Bouchard, R., Blakeslee, J. J., Abas, M., Seifertová, D., Wiśniewska, J., Tadele, Z., Kubeš, M., Čovanová, M., Dhonukshe, P., Skůpa, P., Benková, E., Perry, L., Křeček, P., Lee, O. R., Fink, G. R., Geisler, M., Murphy, A. S., Luschnig, C., Zažímalová, E., Friml, J. (2006). PIN proteins perform a rate-limiting function in cellular auxin efflux. *Science*, *312*, 914-918.

Píchová, K., Pažoutová, S., Kostovčík, M., Chudíčková, M., Stodůlková, E., Novák, P., Flieger, M., van der Linde, E., Kolařík, M. (2018). Evolutionary history of ergot with a new infrageneric classification (*Hypocreales: Clavicipitaceae: Claviceps*). *Molecular Phylogenetics and Evolution*, *123*, 73-87.

Piotrowski, M., Schönfelder, S., Weiler, E. W. (2001). The *Arabidopsis thaliana* isogene NIT4 and its orthologs in tobacco encode β-cyano-L-alanine hydratase/nitrilase. *Journal of Biological Chemistry*, *276*, 2616-2621.

Podlešáková, K., Zalabák, D., Čudejková, M., Plíhal, O., Szüčová, L., Doležal, K., Spíchal, L., Strnad, M., Galuszka, P. (2012). Novel cytokinin derivatives do not show negative effects on root growth and proliferation in submicromolar range. *PLoS One*, *7*, e39293.

Pollmann, S., Müller, A., Piotrowski, M., Weiler, E. W. (2002). Occurrence and formation of indole-3-acetamide in *Arabidopsis thaliana*. *Planta*, *216*, 155-161.

Porco, S., Pěnčík, A., Rashed, A., Voß, U., Casanova-Sáez, R., Bishopp, A., Golebiowska, A., Bhosale, R., Swarup, K., Peňáková, P., Novák, O., Staswick, P., Hedden, P., Phillips, A. L., Vissenberg, K., Bennett, M. J., Ljung, K. (2016). Dioxygenase-encoding AtDAO1 gene controls IAA oxidation and homeostasis in Arabidopsis. *Proceedings of the National Academy of Sciences*, *113*, 11016-11021.

Presello, D. A., Botta, G., Iglesias, J., Eyhérabide, G. H. (2008). Effect of disease severity on yield and grain fumonisin concentration of maize hybrids inoculated with *Fusarium verticillioides*. *Crop Protection*, *27*, 572-576.

Prusty, R., Grisafi, P., Fink, G. R. (2004). The plant hormone indoleacetic acid induces invasive growth in *Saccharomyces cerevisiae*. *Proceedings of the National Academy of Sciences*, *101*, 4153-4157.

Punwani, J. A., Hutchison, C. E., Schaller, G. E., Kieber, J. J. (2010). The subcellular distribution of the Arabidopsis histidine phosphotransfer proteins is independent of cytokinin signaling. *The Plant Journal*, *62*, 473-482.

Quittenden, L. J., Davies, N. W., Smith, J. A., Molesworth, P. P., Tivendale, N. D., Ross, J. J. (2009). Auxin biosynthesis in pea: characterization of the tryptamine pathway. *Plant Physiology*, *151*, 1130-1138.

Quesnelle, P. E., Emery, R. N. (2007). *cis*-Cytokinins that predominate in *Pisum sativum* during early embryogenesis will accelerate embryo growth in vitro. *Botany*, *85*, 91-103.

Rao, R. P., Hunter, A., Kashpur, O., Normanly, J. (2010). Aberrant synthesis of indole-3-acetic acid in *Saccharomyces cerevisiae* triggers morphogenic transition, a virulence trait of pathogenic fungi. *Genetics*, *185*, 211-220.

Radhika, V., Ueda, N., Tsuboi, Y., Kojima, M., Kikuchi, J., Kudo, T., Sakakibara, H. (2015). Methylated cytokinins from the phytopathogen *Rhodococcus fascians* mimic plant hormone activity. *Plant Physiology*, *169*, 1118-1126.

Reineke, G., Heinze, B., Schirawski, J., Buettner, H., Kahmann, R., Basse, C. W. (2008). Indole-3-acetic acid (IAA) biosynthesis in the smut fungus *Ustilago maydis* and its relevance for increased IAA levels in infected tissue and host tumour formation. *Molecular Plant Pathology*, *9*, 339-355.

Robinson, M., Riov, J., Sharon, A. (1998). Indole-3-acetic acid biosynthesis in *Colletotrichum gloeosporioides f. sp. aeschynomene*. *Applied and Environmental Microbiology*, *64*, 5030-5032.

Romanov, G. A., Lomin, S. N., Schmülling, T. (2018). Cytokinin signaling: from the ER or from the PM? That is the question! *New Phytologist*, *218*, 41-53.

Sakakibara, H., Kasahara, H., Ueda, N., Kojima, M., Takei, K., Hishiyama, S., Asami, T., Okada, K., Kamiya, Y., Yamaya, T., Yamaguchi, S. (2005). *Agrobacterium tumefaciens* increases cytokinin production in plastids by modifying the biosynthetic pathway in the host plant. *Proceedings of the National Academy of Sciences*, *102*, 9972-9977.

Sakakibara, H. (2006). Cytokinins: activity, biosynthesis, and translocation. *Annual Review of Plant Biology*, *57*, 431-449.

Sambrook, J., Fritsch, E. F., Maniatis, T. (1989). Molecular cloning: a laboratory manual (No. Ed. 2). *Cold spring harbor laboratory press*.

Sardar, P., Kempken, F. (2018). Characterization of indole-3-pyruvic acid pathway-mediated biosynthesis of auxin in *Neurospora crassa*. *PloS One*, *13*, e0192293.

Schardl, C. L., Young, C. A., Hesse, U., Amyotte, S. G., Andreeva, K., Calie, P. J., Fleetwood, D. J., Haws, D. C., Moore, N., Oeser, B., Panaccione, D. G. *et al*. (2013). Plant-symbiotic fungi as chemical engineers: multi-genome analysis of the *Clavicipitaceae* reveals dynamics of alkaloid loci. *PLoS Genetics*, *9*, e1003323.

Schmittgen, T. D., Livak, K. J. (2008). Analyzing real-time PCR data by the comparative CT method. *Nature Protocols*, *3*, 1101.

Schneider, E. A., Gibson, R. A., Wightman, F. (1972). Biosynthesis and metabolism of indol-3-yl-acetic acid: I. The native indoles of barley and tomato shoots. *Journal of Experimental Botany*, *23*, 152-170.

Schumacher, J. (2012). Tools for *Botrytis cinerea*: new expression vectors make the gray mold fungus more accessible to cell biology approaches. *Fungal Genetics and Biology*, *49*, 483-497.

Skoog, F., Armstrong, D. J. (1970). Cytokinins. *Annual Review of Plant Physiology*, *21*, 359-384.

Smart, C. M., Scofield, S. R., Bevan, M. W., Dyer, T. A. (1991). Delayed leaf senescence in tobacco plants transformed with tmr, a gene for cytokinin production in Agrobacterium. *The Plant Cell*, *3*, 647-656.

Songstad, D. D., De Luca, V., Brisson, N., Kurz, W. G., Nessler, C. L. (1990). High levels of tryptamine accumulation in transgenic tobacco expressing tryptophan decarboxylase. *Plant Physiology*, *94*, 1410-1413.

Sørensen, J. L., Benfield, A. H., Wollenberg, R. D., Westphal, K., Wimmer, R., Nielsen, M. R., Carere, J., Covarelli, L., Beccari, G., Powell, J., Yamashino, T., Kogler, H., Sondergaard, T. E., Gardiner, D. M. (2018). The cereal pathogen *Fusarium pseudograminearum* produces a new class of active cytokinins during infection. *Molecular Plant Pathology*, *19*, 1140-1154.

Spíchal, L., Rakova, N. Y., Riefler, M., Mizuno, T., Romanov, G. A., Strnad, M., Schmülling, T. (2004). Two cytokinin receptors of *Arabidopsis thaliana*, CRE1/AHK4 and AHK3, differ in their ligand specificity in a bacterial assay. *Plant and Cell Physiology*, *45*, 1299-1305.

Spíchal, L. (2012). Cytokinins–recent news and views of evolutionally old molecules. *Functional Plant Biology*, *39*, 267-284.

Staswick, P. E., Serban, B., Rowe, M., Tiryaki, I., Maldonado, M. T., Maldonado, M. C., Suza, W. (2005). Characterization of an Arabidopsis enzyme family that conjugates amino acids to indole-3-acetic acid. *The Plant Cell*, *17*, 616-627.

Steklov, M. Y., Lomin, S. N., Osolodkin, D. I., Romanov, G. A. (2013). Structural basis for cytokinin receptor signaling: an evolutionary approach. *Plant Cell Reports*, *32*, 781-793.

Stepanova, A. N., Robertson-Hoyt, J., Yun, J., Benavente, L. M., Xie, D. Y., Doležal, K., Schlereth, A., Jürgens, G., Alonso, J. M. (2008). TAA1-mediated auxin biosynthesis is essential for hormone crosstalk and plant development. *Cell*, *133*, 177-191.

Stepanova, A. N., Yun, J., Robles, L. M., Novak, O., He, W., Guo, H., Ljung, K., Alonso, J. M. (2011). The Arabidopsis YUCCA1 flavin monooxygenase functions in the indole-3-pyruvic acid branch of auxin biosynthesis. *The Plant Cell*, *23*, 3961-3973.

Sugawara, S., Hishiyama, S., Jikumaru, Y., Hanada, A., Nishimura, T., Koshiba, T., Zhano, Y., Kamiya, Y., Kasahara, H. (2009). Biochemical analyses of indole-3-acetaldoxime-dependent auxin biosynthesis in Arabidopsis. *Proceedings of the National Academy of Sciences*, *106*, 5430-5435.

Takei, K., Sakakibara, H., Sugiyama, T. (2001). Identification of genes encoding adenylate isopentenyltransferase, a cytokinin biosynthesis enzyme, in *Arabidopsis thaliana*. *Journal of Biological Chemistry*, *276*, 26405-26410.

Takei, K., Yamaya, T., Sakakibara, H. (2004). Arabidopsis CYP735A1 and CYP735A2 encode cytokinin hydroxylases that catalyze the biosynthesis of trans-zeatin. *Journal of Biological Chemistry*, *279*, 41866-41872.

Tan, X., Calderon-Villalobos, L. I. A., Sharon, M., Zheng, C., Robinson, C. V., Estelle, M., Zheng, N. (2007). Mechanism of auxin perception by the TIR1 ubiquitin ligase. *Nature*, *446*, 640.

Tanaka, E. (2010). Mechanisms of bamboo witches: Broom symptom development caused by endophytic/epiphytic fungi. *Plant Signaling & Behavior*, *5*, 415-418.

Tanaka, E., Koga, H., Mori, M., Mori, M. (2011). Auxin production by the rice blast fungus and its localization in host tissue. *Journal of Phytopathology*, *159*, 522-530.

Taya, Y., Tanaka, Y., Nishimura, S. (1978). 5′-AMP is a direct precursor of cytokinin in *Dictyostelium discoideum*. *Nature*, *271*, 545.

Tivendale, N. D., Davies, N. W., Molesworth, P. P., Davidson, S. E., Smith, J. A., Lowe, E. K., Reid, J. B., Ross, J. J. (2010). Reassessing the role of N-hydroxytryptamine in auxin biosynthesis. *Plant Physiology*, *154*, 1957-1965.

Tivendale, N. D., Ross, J. J., Cohen, J. D. (2014). The shifting paradigms of auxin biosynthesis. *Trends in Plant Science*, *19*, 44-51.

Tudzynski, B., Hölter, K. (1998). Gibberellin biosynthetic pathway in *Gibberella fujikuroi*: Evidence for a gene cluster. *Fungal Genetics and Biology*, *25*, 157-170.

Tsavkelova, E., Oeser, B., Oren-Young, L., Israeli, M., Sasson, Y., Tudzynski, B., Sharon, A. (2012). Identification and functional characterization of indole-3-acetamide-mediated IAA biosynthesis in plant-associated Fusarium species. *Fungal Genetics and Biology*, *49*, 48-57.

Ueda, N., Kojima, M., Suzuki, K., Sakakibara, H. (2012). *Agrobacterium tumefaciens* tumor morphology root plastid localization and preferential usage of hydroxylated prenyl donor is important for efficient gall formation. *Plant Physiology*, *159*, 1064-1072.

Vrabka, J., Niehaus, E. M., Münsterkötter, M., Proctor, R. H., Brown, D. W., Novák, O., Pěnčík, A., Tarkowská, D., Hromadová, K., Hradilová, M., Oklešťková, J., Oren-Young,

L., Idan, Y., Sharon, A., Maymon, M., Elazar, M., Freeman, S., Güldener, U., Tudzynski, B., Galuszka, P., Bergougnoux, V. (2019). Production and role of hormones during interaction of *Fusarium* species with maize (*Zea mays* L.) seedlings. *Frontiers in Plant Science*, *9*, 1936.

Vyroubalová, Š., Václavíková, K., Turečková, V., Novák, O., Šmehilová, M., Hluska, T., Ohnoutková, L., Frébort, I., Galuszka, P. (2009). Characterization of new maize genes putatively involved in cytokinin metabolism and their expression during osmotic stress in relation to cytokinin levels. *Plant Physiology*, *151*, 433-447.

Wang, F. F., Cheng, S. T., Wu, Y., Ren, B. Z., Qian, W. (2017). A bacterial receptor PcrK senses the plant hormone cytokinin to promote adaptation to oxidative stress. *Cell Reports*, *21*, 2940-2951.

Went, F. W. (1974). Reflections and speculations. *Annual Review of Plant Physiology*, *25*, 1-27.

Westfall, C. S., Herrmann, J., Chen, Q., Wang, S., Jez, J. M. (2010). Modulating plant hormones by enzyme action: the GH3 family of acyl acid amido synthetases. *Plant Signaling & Behavior*, *5*, 1607-1612.

Winston, F., Dollard, C., Ricupero-Hovasse, S. L. (1995). Construction of a set of convenient *Saccharomyces cerevisiae* strains that are isogenic to S288C. *Yeast*, *11*, 53-55.

Won, C., Shen, X., Mashiguchi, K., Zheng, Z., Dai, X., Cheng, Y., Kasahara, H., Kamiya, Y., Chory, J., Zhao, Y. (2011). Conversion of tryptophan to indole-3-acetic acid by TRYPTOPHAN AMINOTRANSFERASES OF ARABIDOPSIS and YUCCAs in Arabidopsis. *Proceedings of the National Academy of Sciences*, *108*, 18518-18523.

Wulfetange, K., Lomin, S. N., Romanov, G. A., Stolz, A., Heyl, A., Schmülling, T. (2011). The cytokinin receptors of Arabidopsis are located mainly to the endoplasmic reticulum. *Plant Physiology*, *156*, 1808-1818.

Zalabák, D., Galuszka, P., Mrízová, K., Podlešáková, K., Gu, R., Frébortová, J. (2014). Biochemical characterization of the maize cytokinin dehydrogenase family and cytokinin profiling in developing maize plantlets in relation to the expression of cytokinin dehydrogenase genes. *Plant Physiology and Biochemistry*, *74*, 283-293.

Zhang, K., Novak, O., Wei, Z., Gou, M., Zhang, X., Yu, Y., Yang, H., Cai, Y., Strnad, M., Liu, C. J. (2014). Arabidopsis ABCG14 protein controls the acropetal translocation of root-synthesized cytokinins. *Nature Communications*, *5*, 3274.

Zhao, Y., Christensen, S. K., Fankhauser, C., Cashman, J. R., Cohen, J. D., Weigel, D., Chory, J. (2001). A role for flavin monooxygenase-like enzymes in auxin biosynthesis. *Science*, *291*, 306-309.

Zhao, Y., Hull, A. K., Gupta, N. R., Goss, K. A., Alonso, J., Ecker, J. R., Normanly, J., Chory, C., Celenza, J. L. (2002). Trp-dependent auxin biosynthesis in Arabidopsis: involvement of cytochrome P450s CYP79B2 and CYP79B3. *Genes & Development*, *16*, 3100-3112.

Zhao, Y. (2018). Essential roles of local auxin biosynthesis in plant development and in adaptation to environmental changes. *Annual Review of Plant Biology*, *69*, 417-435.

Zuo, J., Niu, Q. W., Møller, S. G., Chua, N. H. (2001). Chemical-regulated, site-specific DNA excision in transgenic plants. *Nature Biotechnology*, *19*, 157.

Zürcher, E., Müller, B. (2016). Cytokinin synthesis, signaling, and function—advances and new insights. In *International Review of Cell and Molecular Biology*, 324, 1-38.

Zürcher, E., Liu, J., di Donato, M., Geisler, M., Müller, B. (2016). Plant development regulated by cytokinin sinks. *Science*, *353*, 1027-1030.

Part X: Resume

Mgr. Josef Vrabka

Address: Vodní 63/4
793 95 Město Albrechtice
Czech Republic

Phone: +420608434492

E-mail: pepa.vrabka@seznam.cz

Work Experience:

2019- Slezská nemocnice v Opavě
medical laboratory technician

2012-2018 Palacký University in Olomouc
Faculty of Science, Department of Biochemistry
Student research assistant, Ph.D. student
Research of *Claviceps purpurea*
Reference: prof. RNDr. Ivo Frébort, CSc., Ph.D.(ivo.frebort@upol.cz)

2013, 2014 3 months internship, University of Münster
Department of Molecular Biology and Biotechnology of Fungi
Reference: prof. Dr. Paul Tudzynski A.D. (tudzyns@uni-muenster.de)

Education:

2007-2012 Bsc, Msc. – Molecular and cellular biology, Faculty of Science, Palacký University in Olomouc, thesis with focus on *Claviceps purpurea*

Teaching Experience:

2012-2018 Laboratory Technique for Biochemists
Supervisor for 2 Bsc. and 2 Msc. students

Research Interests:

Molecular biology of filamentous fungi, host-pathogen interaction, secondary metabolism of fungi

Member of research teams:

2012-2015, GAČR project, GAP501/12/0597, Production of ergot alkaloid during the interaction of rye plant (*Secale cereale*) with fungus *Claviceps purpurea*.

2016-2018, GAČR project, GA16-10602S, Impact of phytohormones produced by fungi from order *Hypocreales* on pathogenicity.

Publications:

Hinsch, J., Vrabka, J., Oeser, B., Novák, O., Galuszka, P., Tudzynski, P. (2015). *De novo* biosynthesis of cytokinins in the biotrophic fungus *Claviceps purpurea*. *Environmental Microbiology, 17*, 2935-2951. IF - 5.932

Dzurová, L., Forneris, F., Savino, S., Galuszka, P., Vrabka, J., Frébort, I. (2015). The three-dimensional structure of "Lonely Guy" from *Claviceps purpurea* provides insights into the phosphoribohydrolase function of Rossmann fold-containing lysine decarboxylase-like proteins. *Proteins: Structure, Function, and Bioinformatics, 83,* 1539-1546. IF – 2.54

Kind, S., Hinsch, J., Vrabka, J., Hradilová, M., Majeská-Čudejková, M., Tudzynski, P., Galuszka, P. (2018). Manipulation of cytokinin level in the ergot fungus *Claviceps purpurea* emphasizes its contribution to virulence. *Current Genetics*, *64*, 1-17. IF – 3.574

Vrabka, J., Niehaus, E. M., Münsterkötter, M., Proctor, R. H., Brown, D. W., Novák, O., Pěnčík, A., Tarkowská, D., Hromadová, K., Hradilová, M., Oklešťková, J., Oren-Young, L., Idan, Y., Sharon, A., Maymon, M., Elazar, M., Freeman, S., Güldener, U., Tudzynski, B., Galuszka, P., Bergougnoux, V. (2019). Production and role of hormones during interaction of *Fusarium* species with maize (*Zea mays* L.) seedlings. *Frontiers in Plant Science*, *9*, 1936. IF – 3.677

Part XI: Supplemental information

Table S1 | Primers and Taqman probes used

Name	Sequence (5'-3')
	Replacement vector construction
CpBleF1	CGGAGACAGAAGATGATATTGAAGGAGCGATCGAGACCTAATACAGCCC
CpBleR1	GTTGGAGATTTCAGTAACGTTAAGTGGGCATTGCAGATGAGCTGTATCTG
5F_Aec	CCAGGGTTTTCCCAGTCACGACGGAATTCTCTTTGTTGTGCTCCGAGG
5R_Aec	CCACTTAACGTTACTGAAATCTCCAACGCAGAGTAATTCGTTGCCC
3F_Aec	CTCCTTCAATATCATCTTCTGTCTCCGACTGTGGTCAACGCCGAGAGTA
3R_Aec	ACAATTTCACACAGGAAACAGCGGATCCTGGAGAGTCTGGGCATCTAAC
	Diagnostic PCRs
dia_AEC_fw	ATGACGGCTTATGCATCTTGG
dia_AEC_WT_fw	GTCAAATCAAGCGGTGGCG
dia_AEC_rev	AACACCATGCACATCTCCG
phleooutHefe3	GAGCTCGGTATAAGCTCTCC
Phleohi3F2	GTGTTCAGGATCTCGATAAGATACG
	Complementation vector construction
AEC_Compl_natP_fw	TGCTCCTTCAATATCACTAGTTCATGACTGGGATGATCTTGGCATCG
AEC_Compl_tgluc_rev	CTAATCATACATCTTATCTACATACGTTAGCGCGCCCATTCAACGACCT
AEC_oliC_fw	CTCCATCACATCACAATCGATCCAACCATGGATATCGCTGGAGGC
	Fusion protein construct
AEC_oliC_fw	CTCCATCACATCACAATCGATCCAACCATGGATATCGCTGGAGGC
AEC_Cgfp_rev	CTTACCTCACCCTTGGAAACCATGCGCGCCCATTCAACGACCT
	Arabidopsis transformation
CpAUX_AscI_fw	AGGCGCGCCATGGATATCGCTGG
CpAUX_SpeI_rev	GACTAGTTTAGCGCGCCCATTC
	Rye expression studies
ScRR1_fw	CGAGCTCCTGCACAGATGGT
ScRR1_rev	GCAGAGCTGCAGCATGTCA
ScRR1_probe	CAACGGCTGCTTCCTCTCCTACCTGA
ScRR3_fw	GAGTTCTCCGACGACATGATCA
ScRR3_rev	CAGCTCATCATCACGGACTACTG
ScRR3_probe	ACCGGCTACGACCTGCTCAAGCG
ScRR4_fw	GGTGGACGACAGCGTCATC
ScRR4_rev	CACCGTGGTGACTTGGTAGGA
ScRR4_probe	CAAGCTCATCGAGATGCTGCTCAGGAC
ScRR6_fw	CCGCAGCTCCAAGTACAGAGT
ScRR6_rev	AGTAGTCGGTGATGATCATGTTCAC
ScRR6_probe	ACCACCGTGGACTCTGCGACCC
ScRR9_fw	GCGGCAGATGACGAAATTCTA
ScRR9_rev	GAACCAAGAAAGGAAAAAAGATTGA
ScRR9_probe	CCAAGACAAGCAGACCAAACCACAGTTG
ScRR11_fw	GATACGAGCTCCTAAAGAAGGTCAA
ScRR11_rev	TCCTTGTCGGCACGTTCTC
ScRR11_probe	AGTCATCCACGCTGAAGCAGATCCCC
ScACT_fw	TCAGTGGAGGAACGACCATGT
ScACT_rev	GCGGTGATCTCCTTGCTCAT

Table S1 | Primers and Taqman probes used (continued)

Name	Sequence (5'-3')
ScACT_probe	CCCTGGCATCGCCGACCG
ScEF1_fw	CGCAAGAGGAAGGGTCTCAA
ScEF1_rev	GCAAAACATGACCCCCAAAA
ScEF1_probe	AGCAGATGACCCCTCTATCCGATTTCGA
ScCKX1_fw	TCGTGCAGATGAAGGACAAGTAC
ScCKX1_rev	TTGTTATCTACTCAAAGGCGTTGGT
ScCKX1_probe	ACCCCAAGAGGCTGCTCTCCCCT
ScCKX2.1_fw	ACGAACAAAGCGCGAGAGAT
ScCKX2.1_rev	GGCTCGTCATCGTTGTCTTGA
ScCKX2.1_probe	ACCCTGATAGCCGCTCTCTTCGTGCT
ScCKX2.2_fw	ATCCCAAGGCGATCATGTCT
ScCKX2.2_rev	CCGATCGATTGGCTTTCG
ScCKX2.2_probe	AAAGAATTTTCACGTCCCCGCTGGC
ScCKX4_fw	CCCGGGACAGAGAATATTTCC
ScCKX4_rev	GGCGGATGCTGTTTGTCAA
ScCKX4_probe	AAGGCGTCGCTGCCCATGTCC
ScCKX5_fw	CCGGGCAGGGCATCTT
ScCKX5_rev	ATGGCAAGCAATCAGTCTTCTCA
ScCKX5_probe	CGCCGGCGCTCTTGTCCG
ScCKX8_fw	GGCAGACAGAGCTGCTTGTG
ScCKX8_rev	AAGGACGGCGGTGTACATGT
ScCKX8_probe	ACGCCATGGACCTCAAGGCGC
ScCKX9_fw	CCCATATTGCTCTATCCAGTGAAA
ScCKX9_rev	ATAGGAATCCCACCAGGTAGAAAA
ScCKX9_probe	TCCAGATGGGACAACCGAACATCAGC
ScCKX11_fw	CGTGCTCAAGGGCATGCT
ScCKX11_rev	GGTCCCACTTGCTCTTGATCA
ScCKX11_probe	CGACGGGCCCATGCTCATCTACC
ScHK2_fw	TGGCGAACTCCGATATTGG
ScHK2_rev	CGAATGGCTTGGAGACATAGC
ScHK2_probe	ACAGCAGACGTCATCCAGGCAACATATG
ScIPT3_fw	GAAGACCAAGCTGTCCATCGA
ScIPT3_rev	GCGAGGGGCACCTTGTTG
ScIPT3_probe	CGGCGAGGTCCTCAACGCCG
ScIPT5_fw	GAAACAATCCGCACGAAGAAC
ScIPT5_rev	ACCGTCAATGGCGATTGG
ScIPT5_probe	CCCCGAACTAGCTGCCACGCC
ScIPT10_fw	TGCCTGAATCACTTGAAATGAAA
ScIPT10_rev	GCCCAAGGAACACCCTGTT
ScIPT10_probe	TGCATACACACAAGCAAGGATCTCAAAACC
ScLOG1_fw	GGAGGCGTCGTGCTGATG
ScLOG1_rev	CAACCAAAATCTCAACACACTAGTATGA
ScLOG1_probe	CATCGCCGTCCCTTGTTGCTCAA
ScLOG5_fw	GCACCTAGGGTACTGACCATGAC
ScLOG5_rev	CAAATCCGCATCATCAGAGTTAGA
ScLOG5_probe	CCAGCCGGTTGCCATGCATGT
ScLOG7_fw	AGCAGAGATGGCTCGACGAT
ScLOG7_rev	CAGCTCCTCCATGGTTCCA
ScLOG7_probe	TGAAGCATTCATCGCTCTTCCAGGG
ScLOG8_fw	GAACCAGATGCCAAGCAACA
ScLOG8_rev	ACATCGATTAGGACGAGGTGATC
ScLOG8_probe	CCTGGTCCCGGAGCCGCTG
ScLOG8b_fw	GCGTCCGCCATCAAGCT
ScLOG8b_rev	GTTTGTCAACTAATCTTGGGTTGGT

Table S1 | Primers and Taqman probes used (continued)

Name	Sequence (5'-3')
ScLOG8b_probe	TCCGTGGACACCATGGCCTGC
ScLOG8c_fw	GGGAGACGGATCGCCTAGAC
ScLOG8c_rev	CATGCATCACGCTGACAGAAA
ScLOG8c_probe	CGCCGCATCATCGTCTCCGC
ScLOG10_fw	GTTGGACTGCTGAACGTGGAT
ScLOG10_rev	CGCGCTGACGAAGATGTG
ScLOG10_probe	CATCCGGCCGTCCCAGCG
	Fusarium expression studies
Fver IL1_F	ACGGAGGCGGCACAACT
Fver IL1_R	TCAGGCCCAGAAAGGTCAAC
Fver IL1_probe	ATGGGCGCAATCGCAAGCACTC
Fver IL2_F	GGGTCTATTTGGCGGATCTTC
Fver IL2_R	CCGCCGTAGACGAGTTTGTAG
Fver IL2_probe	TGCAGCCAAGAAGCTTGCATTTGCTC
Fman IL1_F	ACGGAGGCGGCACAACT
Fman IL1_R	TCAGGCCCAGAAAGCTCAAC
Fman IL1_probe	ATGGGCGCAATCGCAAGCACTC
Fman IL2_F	CGGGCTATTTGGCGGATCTTCGC
Fman IL2_R	CCGCCGTAGACGAGTTTGTAG
Fman IL2_probe	TGCAGCCAAGAAGCTTGCATTTGCTC
Ffuj IL1_F	GCATCTTTGGTGGTTCGTCAT
Ffuj IL1_R	ACAGACTCTGCCGAGTGACTTG
Ffuj IL1_probe	CGAGCCGGCCCATATAGAAGCCG
Ffuj IL2_F	GCTACAGTTTGCGAACGATCAA
Ffuj IL2_R	CCGCCAAATAGACCAACGA
Ffuj IL2_probe	TCCACCAATGGAACACTAAACTCTAGCCCC
Fman UBI_F	GATCCTCTTGTGCCCGAGATC
Fman UBI_R	CCGAGCTGTGGCCTCGTA
Fman UBI_probe	CCATGTCTACAAGACTGACCGACCCCG
Ffuj/Fver ACTIN_F	CATTGTCATGTCTGGTGGTACCA
Ffuj/Fver ACTIN_R	AGCAAGGGCAGTGATCTCCTT
Ffuj/Fver ACTIN_probe	CATGTACCCTGGTCTCTCCGACCGTATG
	Maize expression studies
ZmCKX1_F	CGGTGTCGCTGCTCTTCTC
ZmCKX1_R	ATCCAGTACAAGACCTACCTGGCG
ZmCKX1_probe	TGGCGAGGCTGCAGGAGCAGAACAGGAGG
ZmIPT3b_F	GATTGCGTGCAACAGAAACG
ZmIPT3b_R	GAAGGAAACAGAGATGCCTAGGTATT
ZmIPT3b_probe	CAAGCAGCTGCCCATTTTTGCCG
ZmIPT4_F	GGCGACGCGGAAAGC
ZmIPT4_R	CGGACGCCCCACATCTT
ZmIPT4_probe	CGCCGCCATCGAGGACATCAA
ZmIPT5_F	CCGCGCCGTGCATT
ZmIPT5_R	CCGTGGAGGCAAACATGGA
ZmIPT5_probe	AGTACAGCAGCAGCATGGTCACCGC
ZmIPT6_F	CCACGGAGGTGTTCCTGAAG
ZmIPT6_R	CCCATGCTGCTGTACTCTTGTT
ZmIPT6_probe	CGCCGCGCCCTGCATTG
ZmIPT7_F	AGGCTGGAGCGACATCCA
ZmIPT7_R	CGCGCTGTGCCTTTGG
ZmIPT7_probe	CTTCAGCTCAAGGTCGGGAACGCC
ZmIPT8_F	AGGGAGGAGACTGTGAATTCGA

Table S1 | Primers and Taqman probes used (continued)

Name	Sequence (5'-3')
ZmIPT8_R	AAAATTTGAACTGTCTAGTAGTGGTGGAT
ZmIPT8_probe	TTCTTCTTTTTGCTTTTGGTTCGTCCGTTC
ZmIPT9_F	CCACGCCGTGCATCGA
ZmIPT9_R	AGCAAACACGGGCACTACTTC
ZmIPT9_probe	CGTCGTCGCTGCGGCCAAT
ZmEF1_F	TGATACCCACCAAGCCTATGGT
ZmEF1_R	CATGTCGCGGACAGCAAAC
ZmEF1_probe	AGACATTCTCCGCGTTTCCTCCCCT
ZmACT_F	GAGCCACACCGTCCCTATCTAC
ZmACT_R	CACGACCAGCAAGGTCCAA
ZmACT_probe	AGGGTACACGCTTCCTCATGCTATTCTTCG

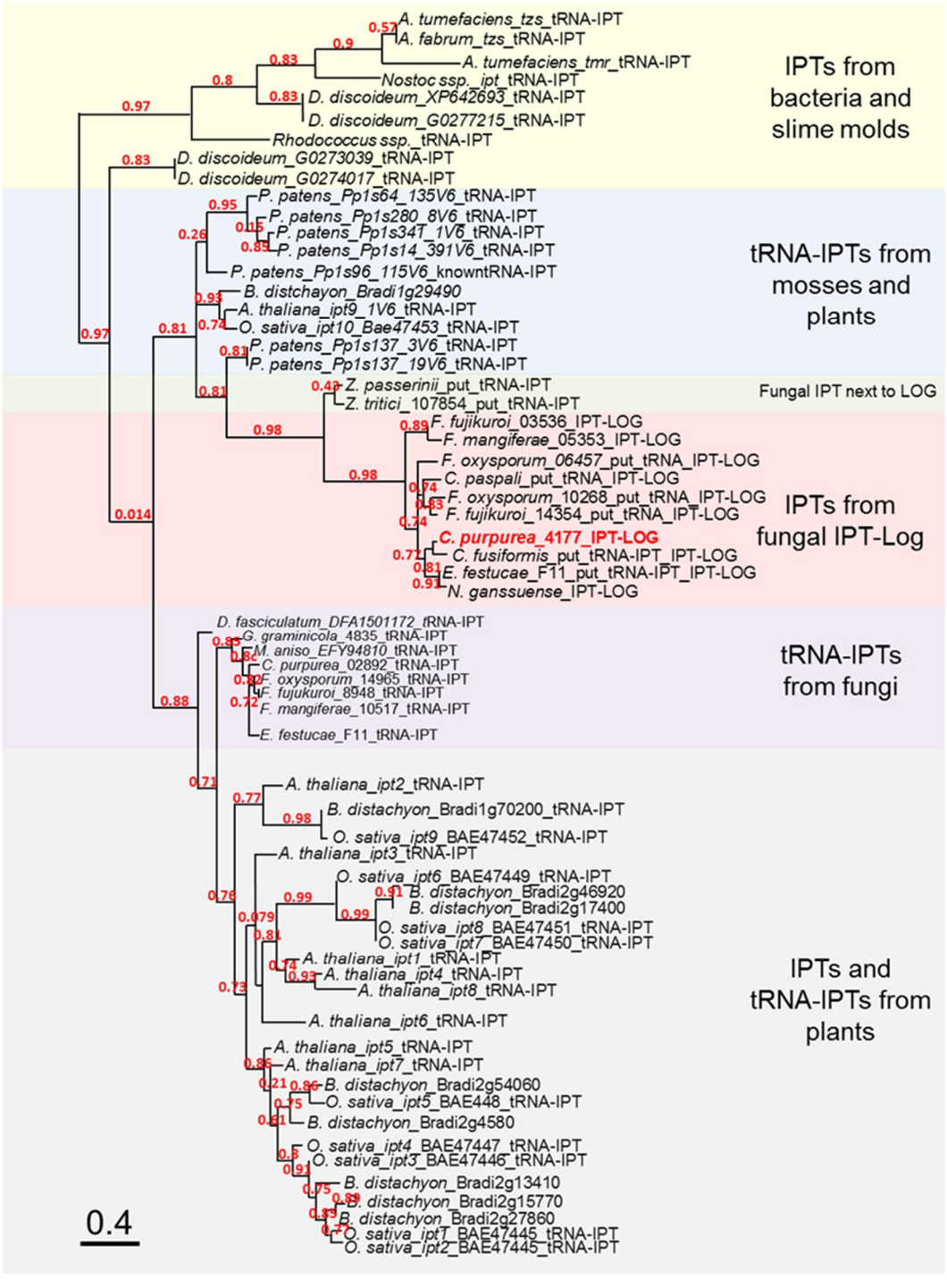

Figure S1 | Phylogenetic tree of IPT domains. The tree was constructed with MUSCLE, Gblocks, PhylML and TreeDyn over the webpage of www.phylogeny.fr. Descriptions used in the tree indicate the presence of certain InterProScan domains: tRNA-IPTs: IPR2627 (tRNA isopentenyltransferase); IPR18022 (tRNA Δ(2)-isopentenylpyrophosphate transferase); put_tRNA_IPT_LOGs: IPR2627 (tRNA isopentenyltransferase) + IPR5269 (cytokinin riboside 5'-monoP phosphoribohydrolase LOG); IPT-LOGs: IPR2648 (isopentenyltransferase) + IPR5269 (cytokinin riboside 5'-monoP phosphoribohydrolase LOG). Adopted from Hinsch *et al*. 2015.

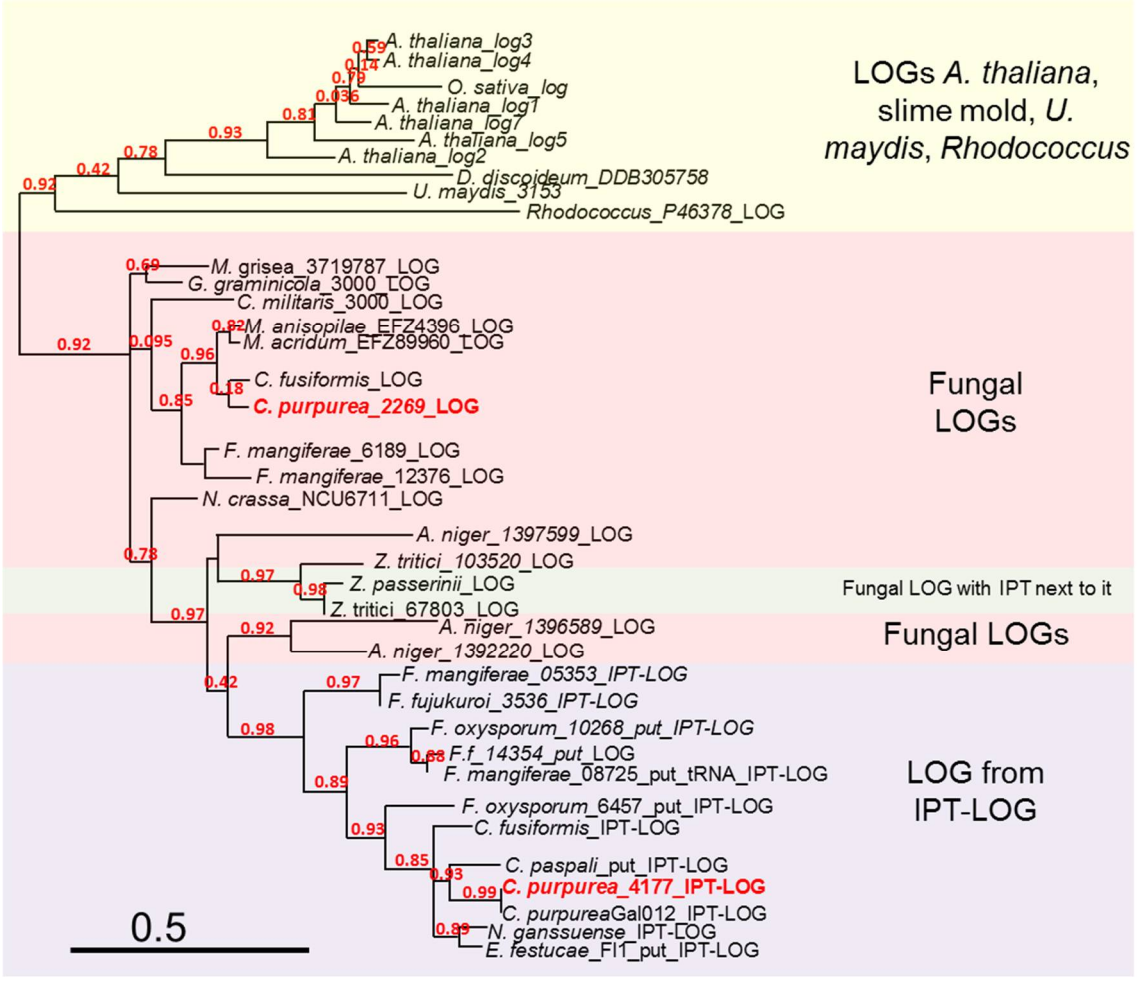

Figure S2 | Phylogenetic tree of LOG domains. The tree was constructed with MUSCLE, Gblocks, PhylML and TreeDyn over the webpage of www.phylogeny.fr. Descriptions used in the tree indicated the presence of certain InterProScan domains: LOGs: LOG: IPR0005269 (cytokinin riboside 5'-monoP phosphoribohydrolase LOG); put_tRNA_IPT_LOGs: IPR2627 (tRNA isopentenyltransferase) + IPR5269 (cytokinin riboside 5'-monoP phosphoribohydrolase LOG); IPT-LOGs: IPR2648 (isopentenyltransferase) + IPR5269 (cytokinin riboside 5'-monoP phosphoribohydrolase LOG). Adopted from Hinsch *et al*. 2015.

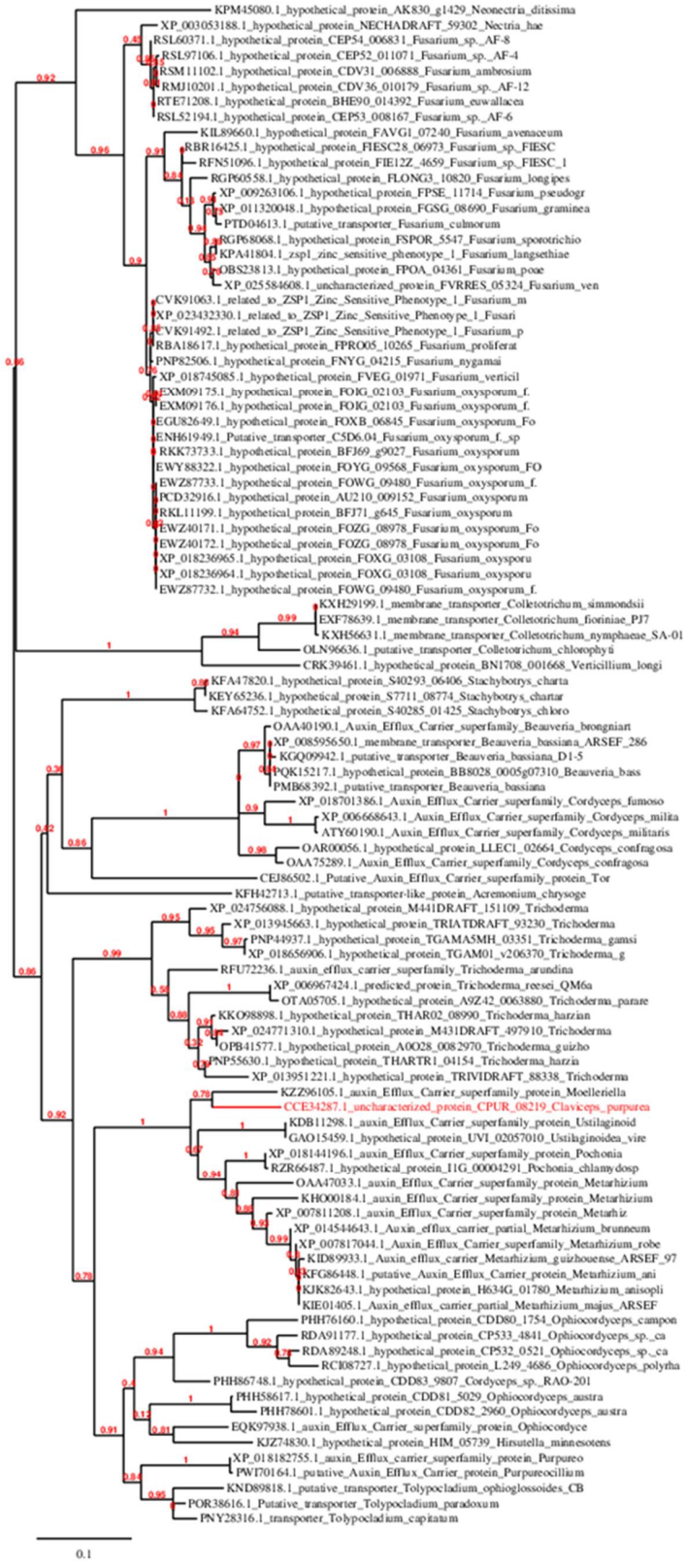

Figure S3 | Putative auxin effux carriers homologous to CpAEC in fungi from division *Ascomycetes*. Tree was generated by webtool www.phylogeny.fr.

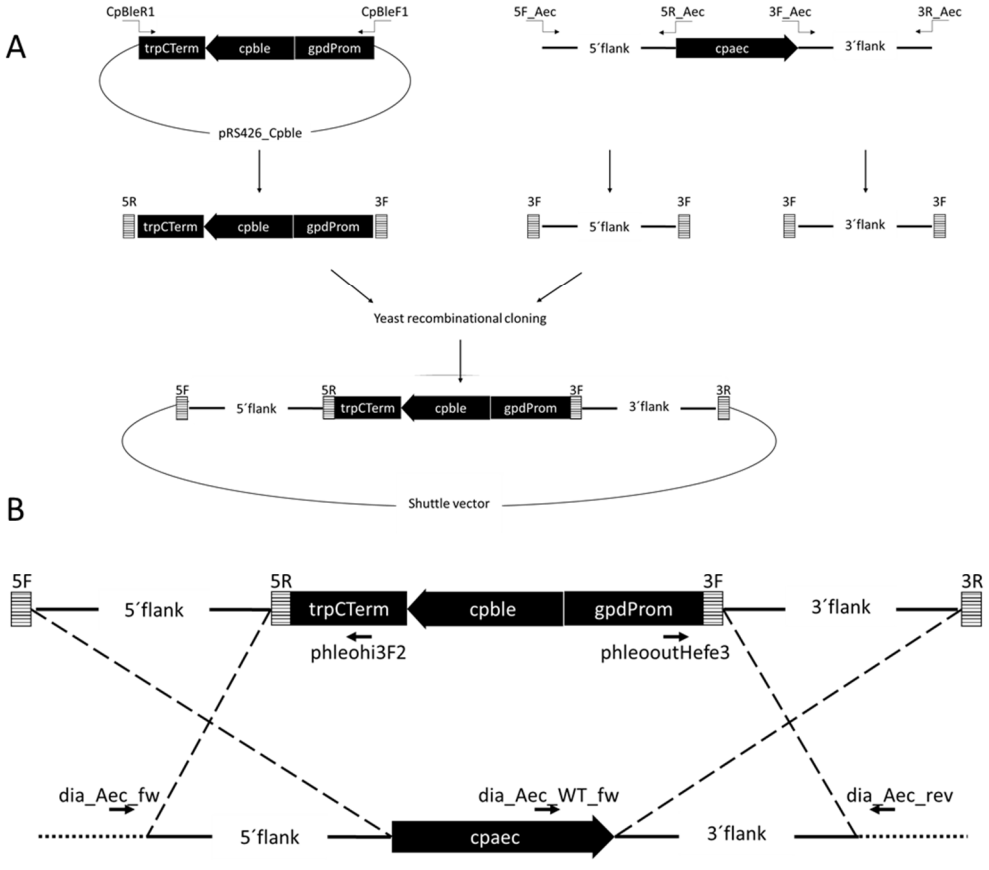

Figure S4 | Generation of the Δcpaec mutants. (A) The replacement vector was obtained by the yeast recombinational method. It was constructed by cloning the 3‘and 5‘flanking regions of *CpAEC* on each side of the phleomycin resistance cassette into the yeast shuttle plasmid vector pRS426 (see materials and methods for further details). The resulting replacement fragment was used to transform *C. purpurea* wild type strain Cp20.1. (B) The mutants were generated by homologous integration of the resistance cassette via a double crossover event between the homologous regions of the replacement fragment and the genomic region of *CpAEC*. Primers used for diagnostic PCRs are indicated. Primers and destination vectors are not drawn to scale.

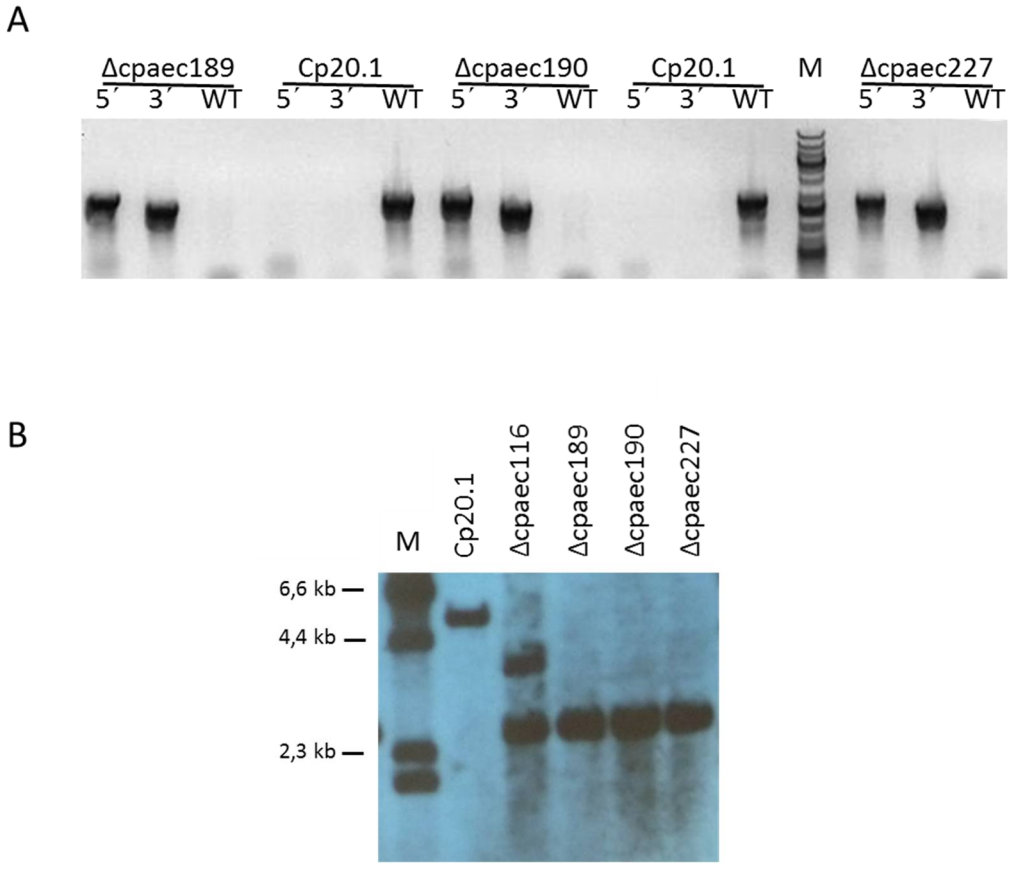

Figure S5 | Confirmation of *CpAEC* deletion. (A) Diagnostic PCRs of Δcpaec mutants and Cp20.1. For the deletion mutants a homologous integration event is documented by amplification of 5′and 3′ diagnostic fragments, resp., while lack of the wild type control fragments proves the absence of the wt gene in the mutants (M – GeneRuler 1 Kb plus DNA ladder, Thermo Scientific). (B) Southern Blot analyses of Δcpaec mutants. SalI digested genomic DNA of Cp20.1 and the Δcpaec mutants were probed with the 3'-flank of cpaec. Lack of wt fragment and single integration of the replacement fragment is evident for Δcpaec189/190/227, while Δcpaec116 has ectopic insertion.

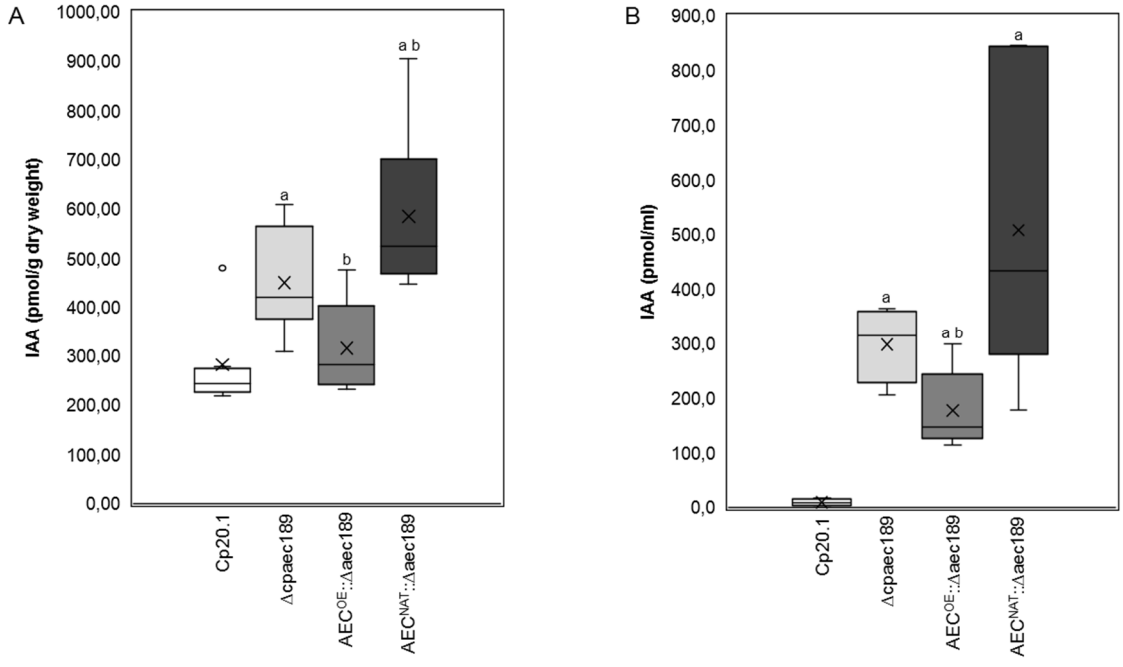

Figure S6 | Complementation of Δcpaec mutants. Free active IAA content in freeze-dried mycelium (A) and modified Mantle medium (B) after 7 days cultivation. Graphs represent the values of six independent biological replicates. Cp20.1 – WT Claviceps purpurea 20.1, Δcpaec189 - deletion mutant of *CpAEC*, AEC^{OE}::Δcpaec189 – complemented mutant with constitutive CpAEC expression, AEC^{NAT}::Δcpaec189 – complemented mutant with CpAEC expression controlled by native promotor. a, b represent significant differences according to Student's unpaired t-test at $P \leq 0.05$, when compared to Cp20.1 or Δcpaec189 respectively.

Part XII: Appendice I

Research article

***De novo* biosynthesis of cytokinins in the biotrophic fungus *Claviceps purpurea*.**

Hinsch, J., Vrabka, J., Oeser, B., Novák, O., Galuszka, P., Tudzynski, P.

Environmental Microbiology (2015), *17*, 2935-2951. doi:10.1111/1462-2920.12838

environmental microbiology

Environmental Microbiology (2015) **17**(8), 2935–2951 doi:10.1111/1462-2920.12838

De novo biosynthesis of cytokinins in the biotrophic fungus *Claviceps purpurea*

Janine Hinsch,[1†] Josef Vrabka,[2†] Birgitt Oeser,[1] Ondřej Novák,[2] Petr Galuszka[2] and Paul Tudzynski[1*]**

[1]*Institute of Plant Biology and Biotechnology, Westfälische Wilhelms-University Münster, Schlossplatz 8, 48143 Münster, Germany.*

[2]*Centre of the Region Haná for Biotechnological and Agricultural Research, Palacký University & Institute of Experimental Botany AS CR, Šlechtitelů 11, 78371 Olomouc, Czech Republic.*

Summary

Disease symptoms of some phytopathogenic fungi are associated with changes in cytokinin (CK) levels. Here, we show that the CK profile of ergot-infected rye plants is also altered, although no pronounced changes occur in the expression of the host plant's CK biosynthesis genes. Instead, we demonstrate a clearly different mechanism: we report on the first fungal *de novo* CK biosynthesis genes, prove their functions and constitute a biosynthetic pathway. The ergot fungus *Claviceps purpurea* produces substantial quantities of CKs in culture and, like plants, expresses enzymes containing the isopentenyltransferase and *lonely guy* domains necessary for *de novo* isopentenyladenine production. Uniquely, two of these domains are combined in one bifunctional enzyme, CpIPT-LOG, depicting a novel and potent mechanism for CK production. The fungus also forms *trans*-zeatin, a reaction catalysed by a CK-specific cytochrome P450 monooxygenase, which is encoded by *cpp450* forming a small cluster with *cpipt-log*. Deletion of *cpipt-log* and *cpp450* did not affect virulence of the fungus, but Δcpp450 mutants exhibit a hyper-sporulating phenotype, implying that CKs are environmental factors influencing fungal development.

Introduction

Phytohormones are not exclusively synthesized by plants, but are also produced by plant-interacting bacteria and fungi, which seemingly exploit the hormones' biological activities to reprogram the host plant's cells for their own benefit. It is possible that the biosynthesis of these compounds in microorganisms differs from that in plants. For example, higher plants and the fungus *Fusarium fujikuroi* produce structurally identical gibberellins. However, their biosynthetic pathways have fundamentally different reaction sequences, involve different enzymes and differ in their genetic organization (Hedden *et al.*, 2001). Two independent biosynthetic pathways for the main natural auxin, indole-3-acetic acid, have been identified in bacteria and plants; both of these pathways are also known in fungi (Tsavkelova *et al.*, 2012). The biosynthetic pathways of cytokinins (CKs) in plants and plant-associated bacteria have been investigated intensively (Frébort *et al.*, 2011). However, to date neither the CK biosynthetic pathway nor the corresponding genes have been identified in fungi.

CKs were originally defined as cell division-promoting compounds (Skoog and Armstrong, 1970). However, it has since been shown that they also play central roles in plant development and growth by regulating senescence, apical dominance, seed dormancy, root proliferation, nutritional signalling, and responses to biotic and abiotic stimuli (Galuszka *et al.*, 2008). Natural CKs consist of an adenine core with isoprenoid side-chain substituents at the N^6-terminus. CK sugar conjugates such as nucleosides, nucleotides and glucosides may also be formed. However, only the free base forms are considered to be biologically active in plant cells; the other conjugates are less active or inactive, and serve as translocation or storage forms (Sakakibara, 2006). The CK pool in plants is largely formed via two major biosynthetic pathways. The first involves a transfer RNA (tRNA) isopentenyltransferase (EC 2.5.1.75; tRNA-IPT), which isoprenylates specific adenosine moieties of certain tRNAs to increase the fidelity of translation by stabilization of codon–anticodon binding (Konevega *et al.*, 2006). These modified tRNAs are present in most kinds of organisms (Persson *et al.*, 1994), and their degradation contributes to the CK pool (Miyawaki *et al.*, 2006). The bulk of the plant CK pool is formed *de novo* via the second pathway. The first step of this pathway is catalysed by an adenylate IPT (EC 2.5.1.112), which transfers an isoprenoid moiety from dimethylallyl diphosphate (DMAPP) to the N^6-position of adenosine triphosphate or

Received 22 January, 2015; accepted 28 February, 2015. For correspondence. *E-mail tudzyns@uni-muenster.de; Tel. (+49) 251 83 24998; Fax (+49) 251 83 21601. **E-mail petr.galuszka@upol.cz; Tel. (+420) 58563 4923; Fax (+420) 58563 4933. †Both authors contributed equally to this work.

diphosphate, forming a nucleotide of isopentenyladenine (iP) (Kakimoto, 2001; Takei *et al*., 2001). This can be further hydroxylated to form *trans*-zeatin (*tZ*) riboside dihosphates or triphosphates by a P450 monooxygenase (Takei *et al*., 2004). The subsequent conversion of the resulting CK nucleotides into free bases is catalysed by a protein with CK-specific phosphoribohydrolase activity known as *lonely guy* (LOG) (Kurakawa *et al*., 2007).

Beyond their functions in plant development, CKs have been associated with plant–microorganism interactions that induce malformations of plant tissue such as flower deformation following *Fusarium moniliforme* infection (Van Staden and Nicholson, 1989; Jameson, 2000). In mycorrhizal symbiosis, the CK level is increased and the plant hormone can act as a signal, activating early nodulation genes (Van Rhijn *et al*., 1997; Miransari *et al*., 2014). Microorganisms may indirectly influence the CK level by modulating the host's CK biosynthesis or manipulate it directly by *de novo* synthesis of new CKs. One well-known example of the host modulation strategy is that used by the gall-forming bacterium *Agrobacterium tumefaciens*. An *ipt* gene (*tmr*) located on the T-DNA region of the Ti-plasmid is integrated into the host genome during infection. The pathogen-derived IPT is then activated inside the host cell, leading to the accumulation of high amounts of *tZ* and the induction of tumorigenesis (Akiyoshi *et al*., 1984). In contrast, the causal agent of leafy galls, *Rhodococcus fascians*, produces a mixture of CKs directly via the action of the *fas*-operon. The proposed biosynthetic pathway is similar to that seen in plants, involving an IPT as well as a cytochrome P450 monooxygenase and a LOG homologue (Murphy *et al*., 1997; Pertry *et al*., 2009).

Various apparent cases of fungal CK production have been reported. For example, early studies on mycorrhizal fungi revealed CK production by *Rhizopogon ochraceorubens* A. H. Smith and *Rhizopogon roseolus* (Miller, 1967; Crafts and Miller, 1974). Furthermore, axenic cultures of the hemi-biotrophic fungi *Pyrenopeziza brassicae* and *Magnaporthe oryzae* contain significant amounts of isoprenoid CKs (Murphy *et al*., 1997; Jiang *et al*., 2013), as do those of the biotrophs *Cladosporium fulvum* (Murphy *et al*., 1997) and *Ustilago maydis* (Stacey *et al*., 2011). In addition, the 'green islands' formed when *Colletotrichum graminicola* infects maize are CK rich (Behr *et al*., 2012).

The ergot fungus *Claviceps purpurea* is a biotrophic pathogen that infects the flowers of young unfertilized grasses. It enters the plant through the pistil and grows in a strictly polar manner through the transmitting tissue to the base of the ovary, where it taps the plant's vascular system to build up a persistent host–pathogen interface. The hyphae proliferate above this site, forming a sphacelial stroma. After 1 week, infected ears typically exude honeydew, a sugar-rich fluid containing the conidia of the fungus. Two weeks post-infection, honeydew formation ceases and a dark purple sclerotium is formed. During the infection process, *C. purpurea* keeps the plant cells alive for an extended period of time without inducing necrotic reactions (Tudzynski and Scheffer, 2004; Hinsch and Tudzynski, 2015).

In this study, we report on the altered CK profile and signalling of *C. purpurea*-infected rye ears. Differently than expected not only the host, but also the fungus is able to contribute to the CK pool during infection: *C. purpurea* contains a gene cluster involved in CK biosynthesis. To our knowledge, this is the first description of a *de novo* CK biosynthesis pathway in fungi. Like plants, the fungus contains functional IPT, LOG and P450 domains that catalyse the formation of iP and *tZ*. However, whereas the IPT and LOG domains are associated with separate enzymes in plants, they are fused in a single bifunctional enzyme in the fungus. The physiological significance of these findings and their evolutionary implications are discussed.

Results

CK profile of rye ears is altered after ergot infection

Disease symptoms of some phytopathogenic fungi are associated with changes in CK levels (Behr *et al*., 2012; Jiang *et al*., 2013). To analyse the CK profile of *C. purpurea*-infected rye (*Secale cereale*) ears, samples of infected plant tissue were taken 5 and 10 days post-inoculation (dpi), corresponding to the host tissue colonization phase and the sphacelial stage respectively. In control plants (unpollinated rye ears), zeatin-type CKs were significantly more abundant than iP, with *cis*-zeatin (*cZ*) and dihydrozeatin (DHZ) riboside O-glucosides being the dominant forms (Table 1). Shortly after fungal inoculation (5 dpi), the levels of iP increased significantly, as did those of its riboside and 9-glucoside, but the levels of zeatin derivatives remained unchanged. Later, when the sphacelial tissue started to form (10 dpi), the levels of both iP- and *tZ*-type CKs decreased; this trend was especially pronounced for the nucleotides (Table 1). The overall levels of *cZ* derivatives did not change greatly, but the abundance of the free base and nucleotide forms increased dramatically at the expense of the O-glucoside storage forms (Table 1). The CK content was also measured in infected ears at a later time point (approximately 25 dpi), when sclerotia accounted for the bulk of the mass of the analysed material, and compared with that of non-infected sterile ears (Table S1). The total content of *tZ* and iP derivatives in the sclerotia was between 2 and 10 times greater than in the uninfected tissue; the *tZ* derivative profile was dominated by the free base, riboside and storage O- and N-glucosides. Increased levels of CKs,

Table 1. CK contents of infected and mock-treated rye ears 5 and 10 dpi.

	5 dpi			10 dpi		
CK metabolite	Mock	20.1 infected	(%)	Mock	20.1 infected	%
iP	3.91 ± 0.83	8.76 ± 1.15*	224	7.58 ± 1.81	8.73 ± 1.74	115
iPR	12.17 ± 2.97	24.88 ± 5.89*	205	13.16 ± 3.24	5.09 ± 1.25*	39
iPRMP	16.05 ± 2.82	12.56 ± 2.06	78	25.75 ± 6.24	4.79 ± 1.13*	19
iP9G	3.61 ± 1.01	6.16 ± 1.46	171	12.00 ± 2.60	4.85 ± 0.88*	40
Total iP type	35.74	52.36	147	58.49	23.46	40
tZ	55.32 ± 4.46	58.06 ± 8.00	105	95.11 ± 19.22	62.16 ± 5.73*	65
*tZ*R	8.89 ± 2.25	8.70 ± 2.28	98	18.49 ± 3.63	13.65 ± 2.72	74
*tZ*RMP	158.18 ± 35.74	152.01 ± 33.49	96	325.88 ± 35.55	118.58 ± 35.80*	36
*tZ*OG	37.71 ± 11.09	32.26 ± 9.67	86	47.72 ± 15.17	53.71 ± 12.38	113
*tZ*ROG	14.02 ± 1.25	14.45 ± 2.38	103	21.60 ± 1.28	19.37 ± 1.81	90
*tZ*9G	83.34 ± 14.46	80.17 ± 15.11	96	265.69 ± 70.78	139.16 ± 23.98*	52
Total *tZ*-type	357.46	345.67	97	774.49	406.63	53
cZ	11.07 ± 2.37	7.21 ± 1.34	65	8.50 ± 0.27	51.81 ± 4.00*	610
*cZ*R	9.84 ± 2.77	8.70 ± 1.68	88	11.27 ± 0.68	14.66 ± 2.08*	130
*cZ*RMP	LOD	LOD		LOD	55.75 ± 22.73*	
*cZ*OG	330.15 ± 36.42	370.27 ± 34.83	112	380.89 ± 79.53	365.76 ± 45.17	96
*cZ*ROG	395.07 ± 45.06	375.71 ± 13.17	95	462.66 ± 41.50	299.32 ± 21.35*	65
Total cZ type	746.13	761.89	102	863.32	787.30	91
DHZ	7.47 ± 0.58	3.03 ± 0.63*	41	9.19 ± 1.17	33.37 ± 7.44*	363
DHZR	16.99 ± 1.92	6.63 ± 1.27*	39	19.44 ± 5.04	35.40 ± 4.28*	182
DHZRMP	3.69 ± 0.62	1.96 ± 0.40*	53	4.55 ± 0.98	4.52 ± 0.88	99
DHZOG	47.13 ± 14.48	57.14 ± 17.40*	121	131.07 ± 28.25	188.58 ± 37.48*	144
DHZROG	269.59 ± 42.93	288.75 ± 48.46	107	561.58 ± 157.7	198.14 ± 24.25*	35
Total DHZ type	344.87	357.51	104	725.83	460.01	63

Percentages indicate the concentration of the relevant CK in the infected plants relative to that in the mock-treated controls. Four biological replicates of infected and mock ears in both time-points were analysed, each replicate in two technical replicates. Concentrations are in pmol g fresh weight^{-1}. The asterisk indicates significant difference between mock and infected tissue according to Student's unpaired *t*-test at $P \leq 0.05$.

*c*ZOG, *c*Z O-glucoside; *c*ZR, *c*Z riboside; *c*ZROG, *c*ZR O-glucoside; DHZOG, DHZ O-glucoside; DHZR, DHZ riboside; DHZRMP, DHZR 5′-monophosphate; DHZROG, DHZR O-glucoside; iP9G, iP 9-glucoside; LOD, limit of detection; *tZ*9G, *tZ* 9-glucoside; *tZ*OG, *tZ* O-glucoside; *tZ*R, *tZ* riboside; *tZ*ROG, *tZ*R O-glucoside.

particularly iP derivatives, were observed in infected plants at 5 dpi and during the sclerotial phase (25 dpi), but the CK levels of the infected plants were lower than those of untreated controls at around 10 dpi (Table 1; Table S1). These results show that the hormonal levels of infected and uninfected rye tissues differ significantly.

Rye perceives a CK signal in early infection stages

To analyse the host's CK metabolism during the infection process, we performed quantitative real-time polymerase chain reaction (qPCR) of CK-related rye genes. Infected plant tissue was sampled shortly after infection and during the colonizing and the sphacelial stages, using mock-treated plants as controls. The expression of 10 CK biosynthesis genes, including three *ipt* and seven *log* genes, and eight genes encoding CK-degrading enzymes (CK dehydrogenases; CKX) were analysed. In addition, because CK signal transduction in plants is mediated by a His-Asp phosphorelay consisting of a sensory His-protein kinase (HK) and response regulators (RRs), the expression of the putative ScHK2 and six type A ScRR genes was also investigated (Fig. 1).

Clear differences were detected in the early infection stage: the infected rye plants exhibited strongly enhanced expression of five CKX genes (*scckx2.1*, *scckx2.2*, *scckx4*, *scckx8*, *scckx9*) as well as the sensory HK gene (*schk2*). The expression of three RR genes (*scrr4*, *scrr9*, *scrr11*) was also induced in infected plants; together, these results indicate the perception of a new CK signal during this phase. However, only one *ipt* gene (*scipt10*) and one *log* gene (*sclog7*) were upregulated within the plant tissue, while two *log* genes (*sclog1*, *sclog5*) appeared to be downregulated relative to the uninfected control. In the colonizing phase, two CKX genes (*scckx4*, *scckx8*) and one RR gene (*scrr9*) remained upregulated, but the expression of the plant's *ipt* genes did not differ significantly from that in the controls. In the sphacelial stage, *scrr9* remained upregulated, but three other RR genes were downregulated. The expression of the host plants' CK biosynthesis and CK-degrading genes was virtually identical to that in the uninfected controls during this phase (Fig. 1). Overall, these data indicate that infected plants perceive a CK signal, especially in the early stages of infection, but there is no pronounced change in the expression of the host plant's CK biosynthesis genes.

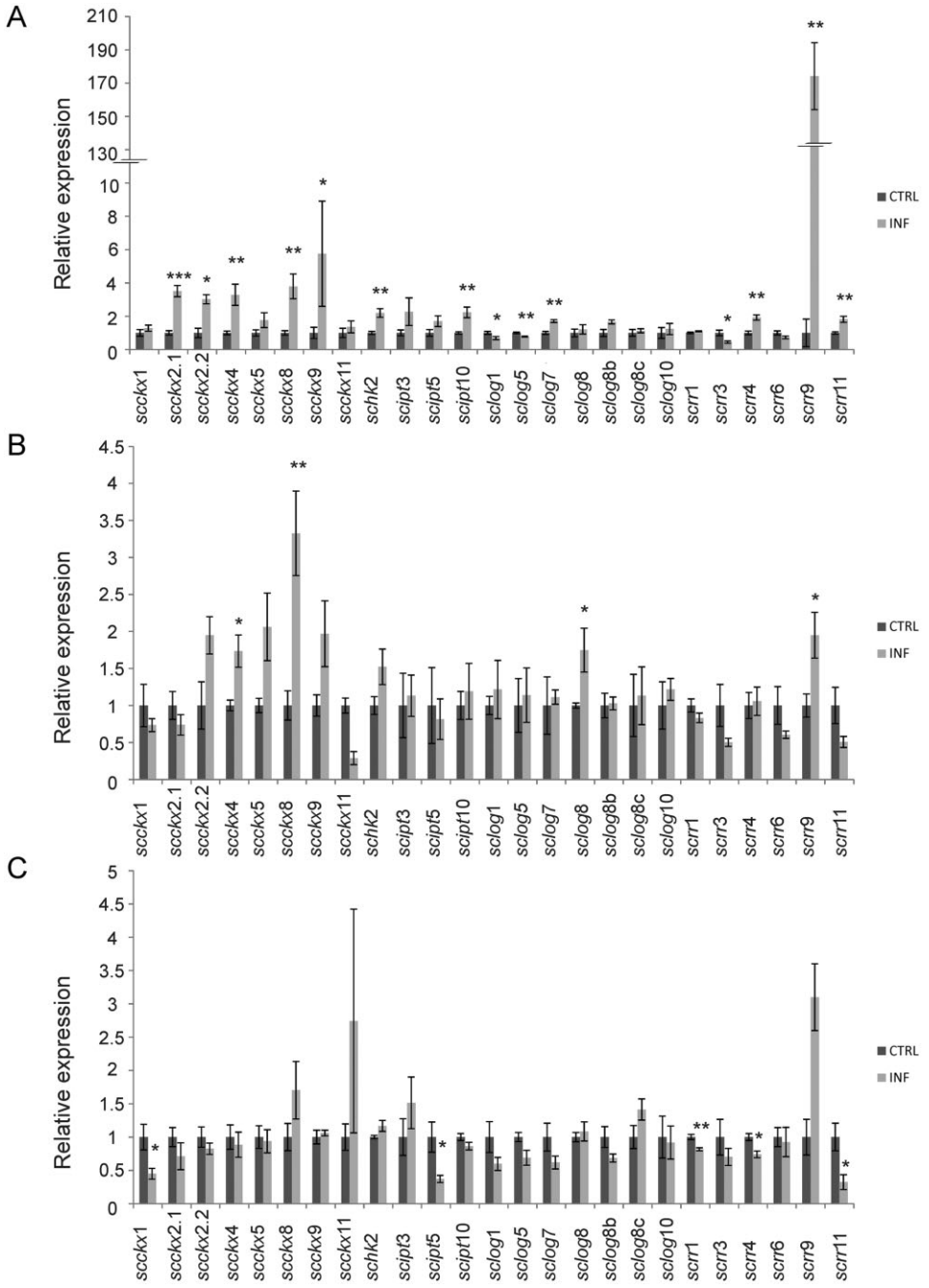

Fig. 1. CK metabolite gene expression of host plants during infection. The expression levels of CK metabolite genes (CK dehydrogenases, *sckx*; His-protein kinase, *schk*; adenylate isopentenyltransferase, *scipt*; CK-specific phosphoribohydrolase 'lonely guy', *sclog*; response regulators, *scrr*) were determined in ovaries infected with *Cp*20.1 (INF) and mock-treated ovaries (CTRL) (A) 3, (B) 6 and (C) 9 dpi. Expression levels were normalized against those of the rye housekeeping genes *scef1* (elongation factor 1) and *scact* (b-actin). Measurements were done in two technical and four biological replicates in each group. The single, double and triple asterisks (*, ** and ***) indicate significant differences between INF and CTRL according to Student's unpaired *t*-tests at $P < 0.05$; 0.01 and 0.001 respectively.

Claviceps purpurea produces a spectrum of CKs

To determine whether the CK signal perceived by the host plant might be induced by fungus-derived CKs, the ability of *C. purpurea* to synthesize the plant hormone was assessed. Samples from submerged cultures of wild-type *C. purpurea* (strain *Cp*20.1) were analysed for the presence of CKs. Significant amounts of iP, *t*Z and *c*Z derivatives were detected in lyophilized mycelia grown in two different media (Table 2). In the nutrient-rich BII medium,

Table 2. CK levels in the mycelia of the wild-type *C. purpurea* strain *Cp*20.1, the Δcpp450 knockout mutant and the Δcpipt-log knockout mutant.

Line CK metabolite	20.1 BII medium	20.1 Mantle medium	Δcpipt-log	%	Δcpp450	%
iP	93.83 ± 28.22	45.36 ± 8.71	33.34 ± 8.67	74	172.18 ± 17.95*	380
iPR	324.42 ± 54.16	6.81 ± 1.43	8.13 ± 0.61	119	11.75 ± 0.51*	173
iPRMP	135.84 ± 52.36	57.80 ± 10.18	50.66 ± 3.91	88	186.91 ± 32.34*	323
Total iP-type	554.09	109.97	92.13	84	370.84	337
tZ	83.20 ± 15.94	71.47 ± 14.94	13.64 ± 1.79*	19	1.85 ± 0.20*	3
*tZ*R	4.37 ± 0.78	4.52 ± 1.08	1.24 ± 0.17*	27	0.22 ± 0.03*	5
*tZ*RMP	19.05 ± 10.07	10.92 ± 1.81	6.51 ± 0.04	60	1.11 ± 0.27*	10
*tZ*OG	2.33 ± 1.44	7.07 ± 2.01	0.36 ± 0.11*	5	0.07 ± 0.00*	1
*tZ*ROG	58.93 ± 35.42	12.45 ± 3.00	0.51 ± 0.15*	4	0.43 ± 0.08*	3
Total *tZ*-type	167.88	106.43	22.26	21	3.68	3
cZ	28.09 ± 9.41	44.79 ± 2.30	40.86 ± 10.14	91	34.68 ± 5.07	77
*cZ*R	14.14 ± 8.09	22.39 ± 2.61	16.03 ± 4.95	72	11.20 ± 0.09*	50
*cZ*RMP	134.90 ± 16.35	211.64 ± 45.60	207.95 ± 17.48	98	194.30 ± 5.87	92
*cZ*OG	1.19 ± 1.08	4.74 ± 1.33	3.44 ± 0.31	73	4.18 ± 0.47	88
*cZ*ROG	LOD	6.92 ± 1.28	3.80 ± 0.88*	55	17.16 ± 1.68*	248
Total *cZ*-type	178.32	290.48	272.08	94	261.52	90

Percentages indicate the concentration of the corresponding CK in the deletion mutant relative to that in the wild-type *Cp*20.1 strain. Two biological replicates of 4-day-old cultures were analysed in two technical replicates each. The results presented are for one of the two mutants examined in each case (Δcpipt-log-2 and Δcpp450-1). Concentrations are in pmol g dry weight^{-1}. The asterisk indicates significant difference between mock and infected tissue according to Student's unpaired *t*-test at $P \leq 0.05$.
*c*ZOG, *c*Z O-glucoside; *c*ZR, *c*Z riboside; *c*ZROG, *c*ZR O-glucoside; LOD, limit of detection; *t*ZOG, *t*Z O-glucoside; *t*ZR, *t*Z riboside; *t*ZROG, *t*ZR O-glucoside.

C. purpurea produced higher amounts of iP derivatives (especially the riboside). Conversely, *c*Z derivatives were most abundant in the sporulation-inducing Mantle medium, and all three types of isoprenoid CKs were predominantly present as free bases or nucleotides. O-glucosides were detected in lower amounts, while N-glucosides were almost undetectable and only very small quantities of DHZ were observed. All of the detected CK derivatives other than the nucleotides were also present in the cultures' supernatants (Fig. S1).

Identification of CK biosynthetic genes in C. purpurea

The results presented above clearly demonstrate that *C. purpurea* can synthesize CKs. However, the biosynthetic pathway and proteins involved remain unknown. To identify fungal proteins homologous to those that catalyse CK biosynthesis in plants, BLASTp searches were performed against the *Cp*20.1 database (Schardl *et al.*, 2013). Using the sequence of LOG5 from *Arabidopsis thaliana* as a query, two annotated open reading frames were detected: *cpur2269*; (E = 1.8–36) and *cpur4177* (E = 1.5–23). The putative gene *cpur2269* (794 bp, one 70 bp intron) encodes a protein of 240 amino acids (aa). Like plant LOGs, the gene product was annotated as a lysine decarboxylase and contains a CK riboside 5′ monophosphate phosphoribohydrolase domain (IPR5269); it was therefore termed *cplog*. The second putative gene *cpur4177* (1585 bp, one 97 bp intron) encodes a protein of 495 aa containing the same IPR5269 domain at the C-terminus. In addition, an IPT domain (IPR2648) and a tRNA IPT domain (IPR2627) were identified in the N-terminal region of this protein. Because this gene apparently encodes a bifunctional enzyme, it was termed *cpipt-log*. BLASTp analyses showed that this gene is only conserved within the *Clavicipitaceae* and *Fusaria* spp. (Fig. S2). In contrast, LOG domain proteins are present in diverse fungal species (Fig. S3).

Remarkably, *cpipt-log* is linked in a head-to-head orientation to the putative cytochrome P450 monooxygenase gene *cp4176* (2481 bp, 5 introns, 510 aa). As secondary metabolite genes are often clustered in fungi, this gene was included in subsequent analyses and termed *cpp450*.

Expression of fungal CK biosynthetic genes

The expression patterns of the identified fungal genes in culture and *in planta* were investigated at various points in time using qPCR (Fig. 2). No clear trend was observed for *cplog*; its levels of expression were similar in all tested samples. Likewise, northern blot analyses indicated that its expression by cultures grown in BII and Mantle media did not differ significantly at any time point (Fig. S4). *Cpipt-log* was expressed weakly in axenic cultures. *In planta*, the level of *cpipt-log* expression at 5 dpi was half that observed at 3 dpi but greater than that at 10 dpi (Fig. 2B). *Cpp450* was expressed very weakly in axenic cultures and *in planta* at 5 and 10 dpi. However, its expression *in planta* during the early stage of infection (at 3 dpi) was eight times stronger than in subsequent stages in one replicate, and 30 times stronger in a second

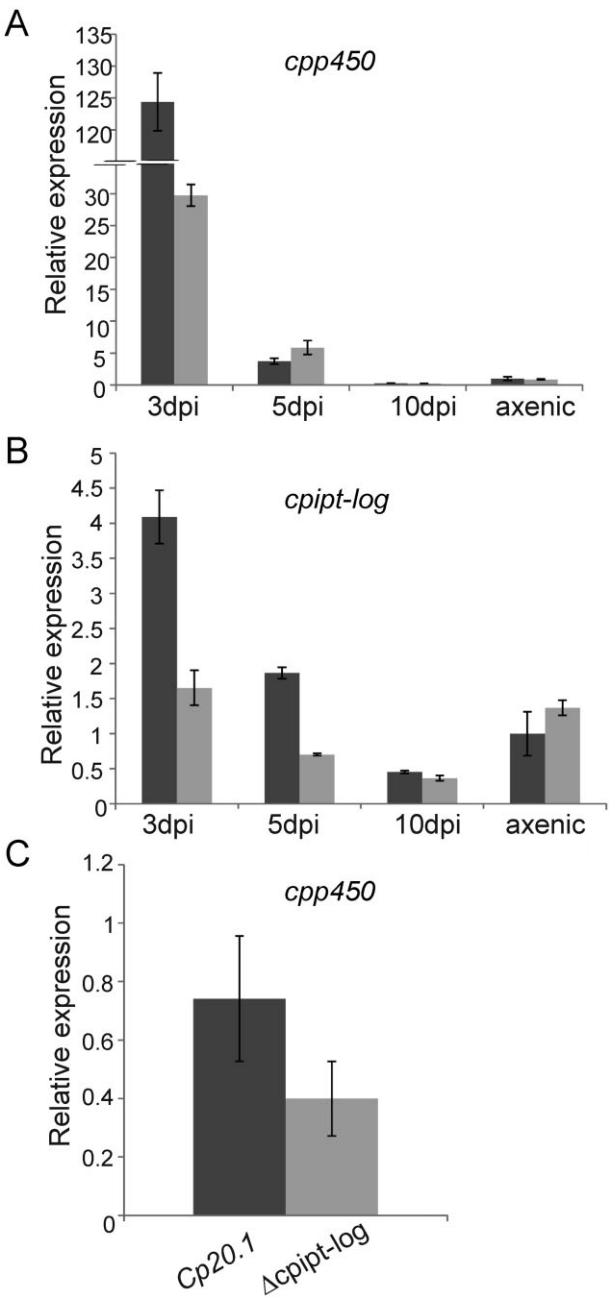

Fig. 2. Expression of *cpipt-log* and *cpp450* in axenic cultures and *in planta*. Expression levels were determined in the wild-type *Cp*20.1 strain 3, 5 and 10 dpi as well as in axenic cultures (cultivated in Mantle medium for 4 days) by qPCR. Expression levels were normalized against fungal housekeeping genes (β-tubulin, γ-actin and glyceraldehyde-3-phosphate dehydrogenase), error bars indicate technical replicates. (A) Expression of *cpp450* in two independent experiments. (B) Expression of *cpipt-log* in two independent experiments. (C) Expression of *cpp450* in the Δcpipt-log mutant and the wild-type *Cp*20.1 in axenic cultures.

(Fig. 2A). Thus, all three genes are expressed (albeit at different levels) in axenic cultures of *C. purpurea* and infected rye plants, with *cpipt-log* and *cpp450* being strongly induced during the early stages of infection.

The fungal CK biosynthetic genes encode functional enzymes

To determine whether the CK biosynthetic genes from *C. purpurea* encode functional enzymes, *cpipt-log* and *cplog* were heterologously expressed as His-tagged proteins and purified to homogeneity (Fig. S5). In addition, the IPT and LOG domains of *cpipt-log* were expressed separately. The IPT domain showed strong transferase activity when DMAPP and adenosine monophosphate (AMP) were used as donor and acceptor, respectively (Table 3), leading to the formation of isopentenyladenosine 5′-monophosphate (iPRMP). CpLOG exhibited CK-specific phosphoribohydrolase activity (Table 3), but the independently expressed LOG domain of CpIPT-LOG did not (data not shown). Surprisingly, the full-length CpIPT-LOG protein clearly exhibited both enzyme activities (Table 3). When the recombinant CpIPT-LOG protein was incubated with low concentrations of DMAPP and AMP, iP accumulated in the reaction mixture. However, when the substrate concentration was increased to > 20 μM and the enzyme concentration was increased proportionately, the intermediate iPRMP became detectable in the reaction mixture. Thus, *cpipt-log* encodes a novel bifunctional enzyme that catalyses the direct synthesis of active CKs.

The enzymatic properties of the recombinant proteins are summarized in Table 3. CpLOG shows a slight preference for iPRMP relative to *t*Z riboside 5′-monophosphate (*t*ZRMP) and *c*Z riboside 5′-monophosphate (*c*ZRMP) : iPRMP is associated with the lowest K_m value and the highest k_{cat}/K_m ratio of these three compounds. In addition to CK monophosphates, CpLOG can hydrolyse AMP and CK diphosphates and triphosphates, although it has dramatically lower k_{cat} values for these substrates (Table 3). The CpIPT-LOG has a 180-fold higher ability to synthesize iP to *t*Z (Table 3). The limiting step in *t*Z production is the transfer of a hydroxymethylbutenyl group from 1-hydroxy-2-methyl-2-(*E*)-butenyl 4-diphosphate (HMBDP) to AMP. The kinetic parameters of the isolated IPT domain are comparable to those of the full-length protein (Table 3), indicating that the LOG domain does not influence transferase activity; it seems likely that the enzyme's two domains operate independently. The diphosphorylated and triphosphorylated species adenosine diphosphate (ADP) and adenosine triphosphate (ATP) cannot serve as acceptor substrates in the transferase reaction catalysed by this enzyme; when either was added to the reaction mixture, the only products formed were the monophosphorylated iPRMP and iP. The formation of these products was independent of the incubation time and the amount formed was equimolar to the amount of recombinant protein in the reaction mixture (data not shown). The same production of iP and iPRMP was observed without the addition of any acceptor to the

Table 3. Kinetic parameters of recombinant CpIPT-LOG and CpLOG proteins.

Enzyme	First substrate	Second substrate	K_m (μM)	V_{max} (nmol s^{-1} mg protein^{-1})	k_{cat} (min^{-1})	k_{cat}/K_m (s^{-1}/M^{-1})
CpLOG	iPRMP	–	4.27 ± 1.71	37.54 ± 8.21	20.801	8.12×10^4
	*t*ZRMP	–	57.63 ± 10.17	45.74 ± 10.32	25.345	7.33×10^3
	*c*ZRMP	–	84.57 ± 20.15	188.06 ± 31.95	104.207	2.05×10^4
	*t*ZRDP	–	23.37 ± 2.84	0.015 ± 0.003	0.008	5.89×10^1
	*c*ZRDP	–	76.66 ± 15.69	0.093 ± 0.027	0.051	1.12×10^2
	*t*ZRTP	–	66.58 ± 14.52	0.005 ± 0.001	0.003	7.21×10^{-1}
	*c*ZRTP	–	64.56 ± 5.86	0.009 ± 0.001	0.005	1.24×10^1
	AMP	–	28.36 ± 3.20	2.045 ± 0.215	1.133	6.66×10^2
	ADP	–	43.23 ± 14.62	0.009 ± 0.003	0.005	2.01×10^1
	ATP	–	73.68 ± 15.12	0.005 ± 0.001	0.002	5.64×10^{-1}
CpIPT-LOG	iPRMP	–	9.01 ± 3.23	7.71 ± 1.34	8.397	1.55×10^4
	*t*ZRMP	–	46.03 ± 13.24	31.62 ± 10.03	34.438	1.25×10^4
	*c*ZRMP	–	61.40 ± 8.03	50.15 ± 15.88	54.620	1.48×10^4
	DMAPP	AMP	1.28 ± 0.27	14.74 ± 1.78	16.054	2.09×10^5
	HMBDP	AMP	12.21 ± 2.08	0.78 ± 0.22	0.849	1.16×10^3
	AMP	DMAPP	0.78 ± 0.31	5.26 ± 2.27	5.726	1.22×10^5
	AMP	HMBDP	0.86 ± 0.12	0.66 ± 0.17	0.721	1.40×10^4
IPT domain	DMAPP	AMP	1.75 ± 0.44	14.18 ± 5.08	9.755	9.29×10^4
	HMBDP	AMP	27.61 ± 6.36	0.46 ± 0.16	0.314	1.89×10^2
	AMP	DMAPP	0.52 ± 0.14	2.68 ± 0.59	1.844	5.91×10^4
	AMP	HMBDP	0.72 ± 0.23	0.23 ± 0.09	0.158	3.66×10^3

The kinetic parameters for all substrates were measured as described in the *Experimental procedures* section. All quoted values are means based on analyses of at least three independent reactions. Measurements were conducted at 30°C, pH 8.0, and the reactions were stopped at defined time points. Parameters were calculated using the GraFit Version 4.0.12 software package.
ADP, adenosine diphosphate; ATP, adenosine triphosphate; *c*ZRDP, *cis*-Zeatin riboside-5´-diphosphate; *c*ZRTP, *cis*-Zeatin riboside-5´-triphosphate; *t*ZRDP, *trans*-Zeatin riboside-5´-diphosphate; *t*ZRTP, *trans*-Zeatin riboside-5´-triphosphate.

reaction mixture, indicating that the product was probably formed from AMP molecules that had bound to the active site of the IPT domain when it was expressed bacterially, and which could not subsequently be displaced by ADP or ATP.

Cpipt-log, *cplog* and the IPT domain of *cpipt-log* were overexpressed under the control of the 35S promoter in *A. thaliana*. Homozygous 35S::CpLOG plants have longer primary roots and significantly darker rosette leaves than control plants (Fig. 3). Conversely, 35S::CpIPT seedlings exhibited delayed growth because of retarded root development and also underwent premature senescence (Fig. 3A,B,D). *Cpipt-log* transformants were unable to form roots and died on selection plates, forming only

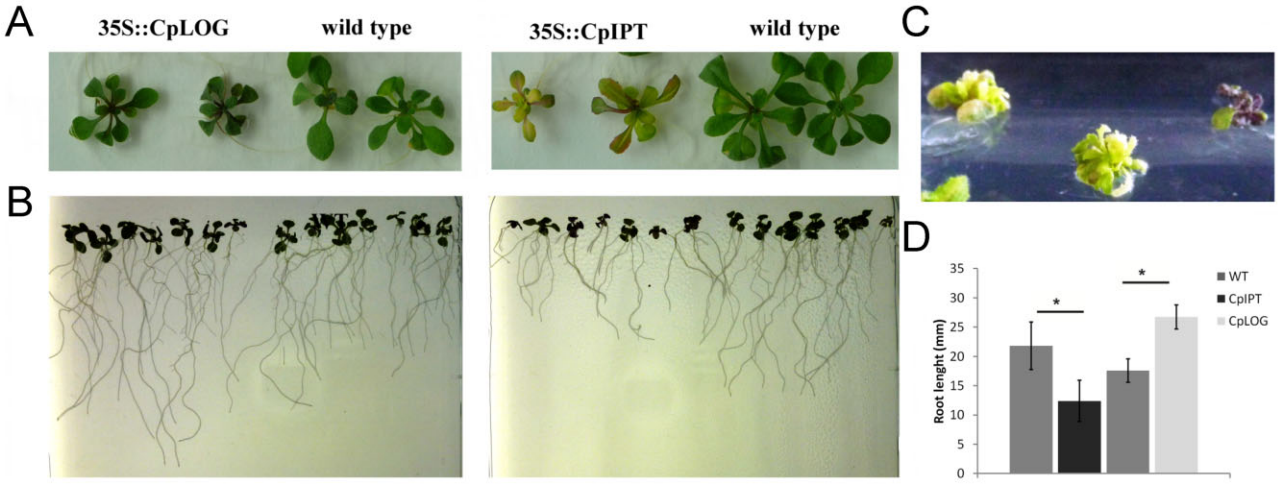

Fig. 3. Phenotypes of 35S::CpLOG, 35S::CpIPT and 35S::CpIPT-LOG transgenic *Arabidopsis* plants. (A) Twenty-one-day-old plants of 35S::CpLOG, 35S::CpIPT and the wild type grown on horizontal plates with MS phytagel. (B) Twelve-day-old seedlings of 35S::CpLOG, 35S::CpIPT and the wild type grown on vertical plates with MS phytagel. (C) Thirty-day-old plants of 35S::CpIPT-LOG regenerated on MS plates with hygromycin (30 mg l^{-1}). (D) Root length of 12-day-old 35S::CpLOG, 35S::CpIPT and the wild-type seedlings grown on vertical plates with MS phytagel; $^*P \leq 0.05$, $n = 30$.

bushy and stunted aerial parts (Fig. 3C). The observed phenotypes resemble typical reactions of plants towards CK treatment (Smart *et al*., 1991; Faiss *et al*., 1997; Ioio *et al*., 2008). These data further support the hypothesis that the *Claviceps* genes encode functional CK biosynthesis enzymes.

The Δcpipt-log and Δcpp450 deletion mutants have unique CK production profiles

In order to resolve the biosynthetic pathway of CKs in *C. purpurea*, deletion strains of *cpipt-log* and *cpp450* were generated via a gene replacement strategy (Figs S6 and S7). Deletion mutants were complemented by reintroducing the original wild-type genes. The CK production profiles of Δcpipt-log, Δcpp450 and the wild-type strain *Cp*20.1 were determined after 4 days of cultivation in liquid Mantle media (Table 1). Compared with the wild type, the Δcpp450 deletion mutant produces 3.3 times higher concentrations of iP derivatives but 97% lower concentrations of *t*Z derivatives. The formation of *t*Z was restored in complementation strains (Fig. S1). The depletion of *t*Z derivatives and corresponding increase in the abundance of iP forms of CKs in Δcpp450 confirms that *cpp450* encodes a CK-specific cytochrome P450 monooxygenase that catalyses the hydroxylation of iP to form *t*Z. Thus, *cpipt-log* and *cpp450* comprise a small CK biosynthetic gene cluster.

Surprisingly, neither of the Δcpipt-log mutants produced appreciably lower concentrations of iP derivatives than the *Cp*20.1 wild type. However, their production of all detectable *t*Z derivatives was five times lower than that of *Cp*20.1 (Table S1). To exclude the possibility that this effect was due to a decline in *cpp450* expression caused by the integration of the replacement fragment into the genomic region containing the closely linked *cpipt-log*, the mycelia of the Δcpipt-log mutants and *Cp*20.1 wild type were analysed by qPCR targeting the *cpp450* gene; there was no significant difference in *cpp450* expression between the two strains (Fig. 2C). The levels of *c*Z-derivatives produced by the two knockout strains were not significantly different to those produced by the wild type.

The Δcpipt-log and Δcpp450 deletions do not reduce virulence

To assess the impact of the *cpipt-log* and *cpp450* deletions on the virulence of *Cp*20.1, pathogenicity assays were performed on intact rye plants and dissected rye ovaries. Successful infection of intact rye plants can be monitored macroscopically by considering two parameters: the amount and time of appearance of honeydew and the formation of sclerotia. Of 33 rye ears inoculated with the Δcpp450 mutants, 32 showed wild-type like honeydew production and sclerotia formation (Fig. 4A). In total, 28 rye ears were inoculated with Δcpipt-log. Of these, 24 showed the typical signs of infection, resulting in an infection rate of 86%.

Microscopic analyses of dissected rye ovaries 5 days after inoculation with Δcpp450 and Δcpipt-log mutants revealed that the mutants' infection processes are indis-

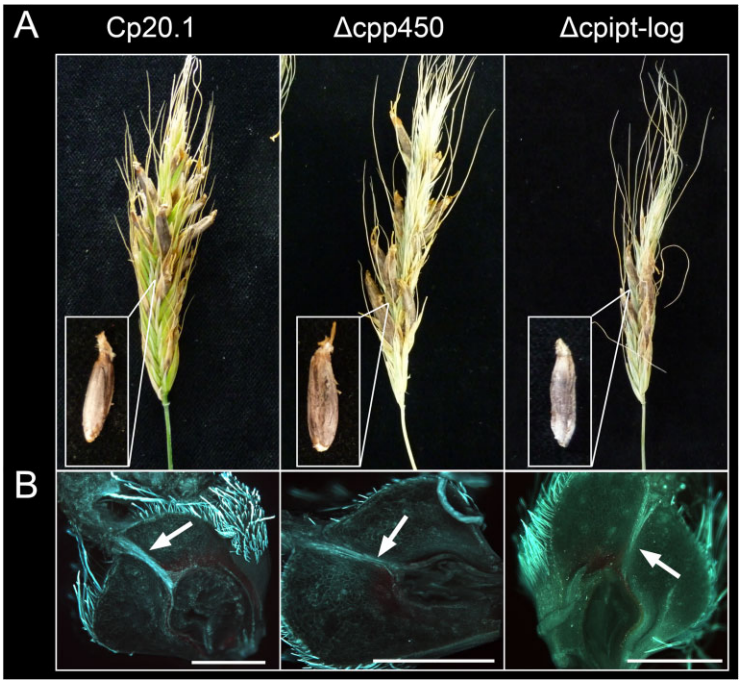

Fig. 4. Pathogenicity assays using the *C. purpurea* wild type *Cp*20.1 strain and the Δcpp450 and Δcpipt-log deletion mutants. (A) Rye ears were infected with conidia suspensions of the different strains. Honeydew formation and sclerotia formation were monitored for 3 weeks. (B) *In vitro* cultivated rye florets infected with the different strains. After 5 days, cross-sections of the ovaries were stained with aniline-blue (which emits green fluorescence), allowing the detection of fungal hyphae (indicated by arrows) within the plant tissue by fluorescence microscopy. The infection routes of Δcpp450 and Δcpipt-log are similar to those of the wild type (bars = 5 mm).

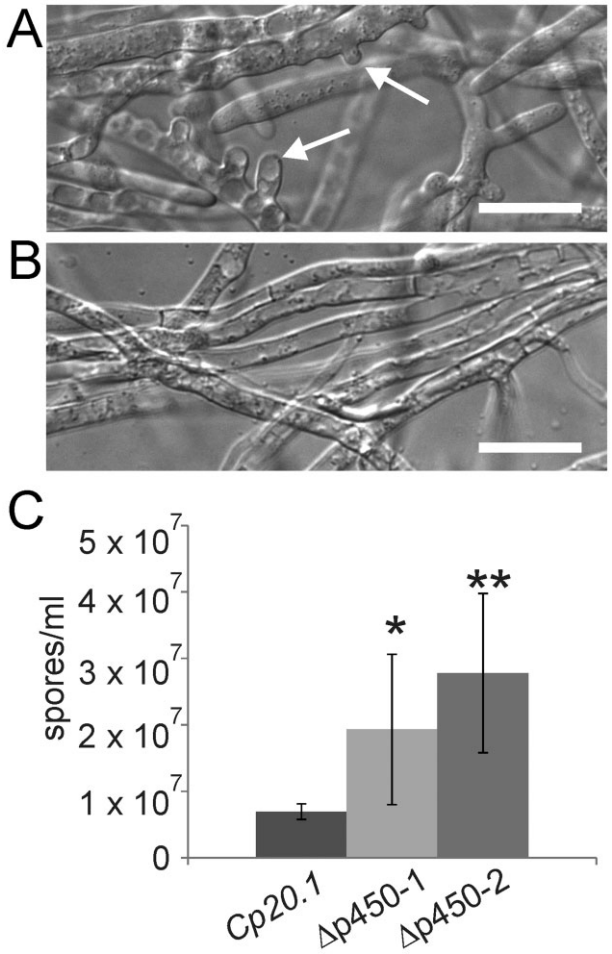

Fig. 5. Phenotype of the Δcpp450 deletion mutant and the wild-type strain *Cp*20.1. Strains were cultivated on the non-sporulation inducing BII medium for 10 days. (A) Microscopic analyses of Δcpp450 show frequent formation of conidiophores, which form the asexual spores of the fungus (indicated by arrows). (B) Under these conditions, the wild-type forms long unbranched hyphae. (C) Quantification of spore formation by the wild-type strain and the two deletion mutants on sporulation-inducing Mantle media after 10 days. The mutants show significantly higher sporulation rates than the wild type. Data shown represent one out of three biological replicates; the single and double asterisks (* and **) indicate significant differences between *Cp*20.1 and the mutants according to Student's unpaired *t*-test at $P < 0.05$ and 0.005 respectively.

tinguishable from those of the wild type (Fig. 5B) or the complemented strains (data not shown). This indicates that neither *cpp450* nor *cpipt–log* is essential for *C. purpurea* virulence.

CpP450 is involved in fungal differentiation

Microscopic analyses revealed that the morphological phenotype of Δcpp450 mutants on solid BII media differs from that of the wild type. Whereas the wild type forms long hyphae with relatively rare branches under these conditions (Fig. 5B), the mutant frequently forms conidiophores, which arise vertically from the hyphae to form the asexual spores of the fungus (conidia; Fig. 4A). The so formed conidia did not differ in shape and size from those formed by the wild type when grown on sporulation-inducing Mantle media (data not shown).

To quantify this formation of conidia, the Δcpp450 mutants as well as the corresponding complementants and the wild-type *Cp*20.1 were cultivated under sporulation inducing (Mantle media) and non-inducing (BII media) conditions. On BII media, as expected, the wild type and complementants showed no sporulation. In contrast, both Δcpp450 mutants sporulated frequently. This hyper-sporulating phenotype was also visible under sporulation-inducing conditions, which caused the Δcpp450 mutants to sporulate significantly more frequently than the wild type (Fig. 4C).

Discussion

Previous studies have demonstrated that interactions with phytopathogenic fungi can induce changes in plants' CK levels (Behr *et al*., 2012; Jiang *et al*., 2013). However, neither the genes involved in their biosynthesis nor the relevant fungal biosynthetic pathways have previously been identified. This study presents the first evidence for a fungal gene cluster associated with *de novo* CK biosynthesis. The cluster was identified in the biotrophic fungus *C. purpurea* and its functional characterization suggested the existence of the CK production pathways depicted in Fig. 6: the initial step, the formation of iP, is catalysed by the bifunctional enzyme CpIPT-LOG. This enzyme exhibits both the IPT activity required for the isoprenylation of adenine and the LOG activity required for the activation of CK nucleotides. Fungal genome analyses indicated that bifunctional enzymes of this sort are unique to species from the orders Hypocreales (including the genera *Fusarium*, *Epichloe*, *Aciculosporium*) and Capnodiales (e.g. *Zymoseptoria*; Figs S2, S3). A similar chimeric protein encoded by the bacterial *ipt* (*fasD*) and *log* (*fasF*) genes was recently identified in isolates of the bacterial plant pathogen *R. fascians* A21d2 but has yet to be functionally characterized (Creason *et al*., 2014). Similarly, a fusion combining the activity of two plant enzymes, copalyl phosphate synthase and *ent*-kaurene synthase (Cps/ks), has been identified in the phytopathogenic fungus *F. fujikuroi*. Cps/ks catalyses the conversion of geranylgeranyl diphosphate into *ent*-kaurene via ent-copalyl diphosphate, a key step in gibberellic acid (GA) biosynthesis (Tudzynski *et al*., 1998). The fusion of CK-producing and CK-activating functions in a single enzyme would give pathogenic fungi a potent tool for the *in situ* production of active CKs, as demonstrated by the

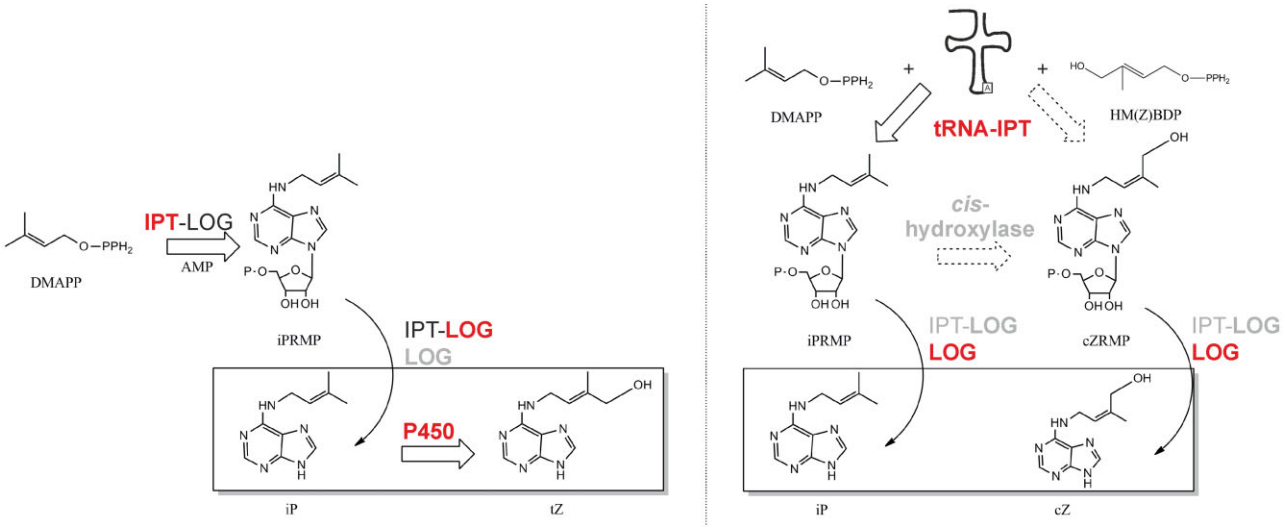

Fig. 6. Proposed *de novo* CK biosynthesis and tRNA degradation pathways in *C. purpurea*. The bifunctional enzyme CpIPT-LOG catalyses the prenylation of AMP using DMAPP as a side chain donor, producing iPRMP. The tRNA-IPT catalyses the prenylation of tRNA either using DMAPP or 4-hydroxy-3-methyl-2-(Z)-butenyl diphosphate [HM(Z)BDP] as a side chain donor, leading to the formation of iPRMP or *c*ZRMP respectively. These nucleosides are then converted into the corresponding active bases by the LOG domains of either CpLOG or CpIPT-LOG. Hydroxylation of iP derivatives to *tZ* derivatives is catalysed by a cytochrome P450 monooxygenase (CpP450). Red labels indicate reactions known to be catalysed by enzymes examined in this work; grey labels indicate reactions that may occur but are not expected to be important. Dashed lines indicate putative reactions for which the associated enzymes are yet to be identified.

fatal disruption of seedling morphology in *Arabidopsis* plants that constitutively overexpress *cpipt-log* (Fig. 3C). Moreover, the IPT-LOG fusion is much more stable than plant IPTs when prepared in a heterologous prokaryotic system. The high potency of the novel bifunctional enzyme is further demonstrated by the measured kinetic constants (K_m and k_{cat}) of the IPT domain, which are much better than those estimated for plant enzymes (Kakimoto, 2001; Takei *et al*., 2004). However, in contrast to the *Agrobacterial* IPT, which preferentially uses HMBDP to directly produce *tZ*-type CKs *in planta* (Sakakibara *et al*., 2005; Ueda *et al*., 2012), the transferase domain of the *Claviceps* enzyme preferentially uses DMAPP. The subsequent hydroxylation of iP to *tZ* is mediated via a CK-specific cytochrome P450 monooxygenase encoded by a gene adjacent to *cpipt-log* within the *Cp*20.1 genome. Because the levels of *cZ* derivatives in cultures of Δcpp450 and Δcpipt-log mutants were comparable with those observed in wild-type cultures, it is unlikely that the *cpipt-log/cpp450* gene cluster affects the formation of *cZ*-type CKs.

Because *C. purpurea* clearly has the ability to produce CKs, it also presumably has the ability to manipulate the CK levels of infected rye plants, thus potentially changing the within-host environment in a pathogen advantageous way. Accordingly, the abundance of the most active CK (iP) and its deactivated metabolites [isopentenyladenosine (iPR) and iP 9-glucoside] in infected plants increased dramatically at 5 dpi (Table 1). During this colonization phase, none of the plant's known *ipt* genes were significantly upregulated (Fig. 1). However, qPCR showed that the fungal *cpipt-log* gene was upregulated at 3 dpi and 5 dpi, indicating fungal CK production at these time points (Fig. 2). The low expression of *cpp450* at 5 and 10 dpi is consistent with the measured *tZ* contents of the infected plants, which were identical to those of mock-treated control plants at 5 dpi. Subsequently (at 10 dpi), the *tZ* content of the infected plants fell below that of the uninfected controls (Table 1). Treatment of monocot plant tissues with exogenous active CKs usually causes the upregulation of several CK oxidase/dehydrogenase (*ckx*) genes and the downregulation of *ipt* genes implicated in *de novo* CK biosynthesis (Podlešáková *et al*., 2012), so the high levels of iP (5 dpi) and the putative accumulation of *tZ* derivatives (3 dpi) caused by the fungal infection may induce the activity of CK-degrading enzymes. In keeping with this hypothesis, the expression of several *ckx* genes was strongly induced during the early phase of infection (Fig. 1), and the levels of preferred CKX substrates – iP and *tZ* derivatives except O-glucosides and the primary products of plant CK biosynthesis (iPRMP and *t*ZRMP) – fell at 10 dpi (Table 1).

The functions of fungus-borne CKs during host colonization remain unclear because the Δcpipt-log and Δcpp450 deletion mutants exhibit almost similar levels of virulence to the wild type. Assuming that the changes in CK production caused by these deletions in axenic culture are reproduced *in planta*, it appears that fungal *tZ* production is not required during the infection process.

Furthermore, the increased iP production induced by the Δcpp450 deletion also has no adverse effect on the infection process. However, the impact of low iP production on virulence could not be tested because surprisingly, the production of iP-type CKs by Δcpipt-log mutants was only slightly weaker than that by the wild type. This mild reduction may be due to the activity of a tRNA-IPT and an associated RNA degradation process. In *A. thaliana*, it has been shown that this ubiquitous CK pathway accounts for the majority of *c*Z production and also contributes to the formation of iP-type CKs (Miyawaki *et al*., 2006). To assess the contribution of prenylated RNA degradation to the total CK pool in fungi, the CK content was measured in the necrotrophic fungus *Botrytis cinerea*. This fungus lacks genes for *de novo* CK biosynthesis, and we could detect only low quantities of CKs in its cultures (data not shown), confirming previous findings (Murphy *et al*., 1997). The mycelium of *B. cinerea* contained similar amounts of iP, iPR and iPRMP to those found in *C. purpurea* Δcpipt-log, but no other CKs except for *c*ZRMP were detectable in significant quantities. Therefore, the remaining iP-derived CKs in the Δcpipt-log culture presumably originate from tRNA degradation. The drastically reduced *t*Z levels within the Δcpipt-log mutant could be explained by the rapid conversion of iP into *t*Z in the wild-type strain. However, it is not clear why the tRNA pathway-derived iPRMP molecules are not subsequently hydroxylated by CpP450. Interestingly, a deregulation of iP- and *t*Z-type levels was also observed in the moss *Physcomitrella patens* upon deletion of the tRNA-IPT gene, indicating that both CK production pathways are interconnected on the regulatory level (Lindner *et al*., 2014). One copy of a tRNA-IPT gene is conserved in all of the genomes of the *Clavicipitaceae* family that have been sequenced to date (Fig. S2). Recent studies on the nitrogen-fixing bacterium *Bradyrhizobium*, which colonizes the nodules of leguminous plants' roots, revealed a physiological role of RNA-derived CKs. Specifically, a strain with a defective copy of the tRNA-IPT gene exhibit delayed nodule formation and improper nodule development. The wild-type phenotype could be restored by reintroducing the *tRNA-ipt* gene or an *Agrobacterium ipt* gene from a *de novo* biosynthetic pathway into the genetic background of the tRNA-IPT knock-out strain (Podlešáková *et al*., 2013). It is therefore possible that the tRNA degradation pathway for CK synthesis may also be physiologically relevant in *C. purpurea*. Notably, nucleotides released by this pathway could be converted into active bases by the CpLOG protein.

In general, the *cis*-isomer of zeatin is considered to have much weaker biological activity than the *trans*-isomer. However, *c*Z has been shown to be the dominant CK in many monocot taxa such as the *Poaceae* (Gajdošová *et al*., 2011). It is speculated that *c*Z may be important for reproductive growth after pollination (Gajdošová *et al*., 2011). Interestingly, both LOG domains present within *C. purpurea* use *c*ZRMP as a substrate *in vitro.* As demonstrated for the IPT proteins of *A. tumefaciens*, the spatial distribution of substrate and enzyme *in vivo* can massively influence product formation (Ueda *et al*., 2012). It is therefore possible that the two different LOG-containing proteins expressed by *C. purpurea* function in different pathways. While *cpipt-log* only occurs in *Clavicipitaceae* and *Fusaria* ssp. and is closely linked to *cpp450*, which shows a similar expression pattern, *cplog*-like genes are present in many different species and this gene is not part of the small biosynthetic gene cluster described herein. Furthermore, it is constantly expressed and shows no induction *in planta* (Fig. S4). It may therefore be that CpLOG is involved in the activation of *c*ZRMP via the tRNA degradation pathway rather than *de novo* CK biosynthesis.

Surprisingly, the Δcpp450 mutants showed a distinct altered phenotype in axenic cultures. Sporulation was deregulated because (i) it occurred under non-inducing conditions and (ii) hyper-sporulation occurred under inducing conditions. This phenotype indicates that *cpp450* influences the fungus' asexual reproductive behaviour, which is governed by both genetic programming and environmental stimuli (Park and Yu, 2012). More generally, it suggests that hormonal balances influence fungal development. However, the mere absence of *t*Z-type CKs in the Δcpp450 mutant cannot explain this observation by itself because the Δcpipt-log mutant, which also has reduced *t*Z levels, does not exhibit abnormal sporulation. It is possible that the sporulation changes in Δcpp450 are due to iP accumulation or interactions between the two CK types. Various other cases in which microorganisms produce phytohormones that influence their own behaviour have been reported. For example, in the basidiomycete *Lentinus tigrinus*, CK levels vary during developmental stages. High quantities were especially associated to basidiospore formation within in the cap and to growth of vegetative hyphae (Rypacek and Sladky, 1972; 1973). In the slime mold *Dictyostelium discoideum*, iP and other CKs produced by *de novo* IPT activity are essential for the initiation of sporulation (Anjard and Loomis, 2008). The germination of the resulting spores could subsequently be inhibited by discadenine, an N^3-(3-amino-3-carboxypropyl) derivative of iP whose synthesis was proposed to be mediated by a hypothetical discadenine synthase (Ihara *et al*., 1980). Similarly, the filamentous saprophyte *Neurospora crassa* apparently responds to auxin treatment, which affects conidial germination and the elongation of young hyphae (Nakamura *et al*., 1978; Tomita *et al*., 1984). Interestingly, the ratio of CKs to auxins influences various developmental processes in plants (Su *et al*., 2011), and it was recently demonstrated that *C. purpurea* can produce substantial

quantities of auxins (P. Galuszka, unpubl. data). Therefore, similar CK–auxin interactions may be important in the hyphae of *C. purpurea*.

In conclusion, CK-specific biosynthetic genes and functional CK biosynthetic enzymes have been identified in a fungus for the first time. Our results show that CK biosynthesis by *C. purpurea* occurs via a different mechanism to any that have previously been suggested to be involved in fungus–plant interactions. While the increased iP content of leaf blades of rice seedlings infected by *M. oryzae* has been explained by post-transcriptional activation of plant IPTs (Jiang *et al*., 2013), the altered hormonal balance of maize plants infected by *C. graminicola* is probably caused by a fungal enzyme (Behr *et al*., 2012). However, there is no evidence of fungal CK biosynthesis in either case. In contrast, the results presented herein show that *C. purpurea* has evolved both mechanisms for prenylated tRNA degradation and a more effective and potent mechanism for *de novo* CK production. In addition, it was demonstrated that the differentiation of the fungus is partly regulated by changes in phytohormone levels.

Experimental procedures

Strains, media and growth conditions

The wild-type *C. purpurea* (Fr.) Tul. strain 20.1 (Hüsgen *et al*., 1999), a putatively haploid (benomyl-treated) derivative of the standard field isolate T5 (Fr. : Fr.) Tul. isolated from *S. cereale* L. (Hohenheim, Germany), was used for the generation of mutants and as the wild-type control in all experiments. Mycelia were grown on complete medium BII (Esser and Tudzynski, 1978) for cultivation and DNA isolation. Conidia were obtained from mycelia cultivated on Mantle medium (Mantle and Nisbet, 1976). For the CK measurements, strains were grown in liquid BII or Mantle medium (without yeast extract). All strains were cultivated in the dark at 26°C. Vector construction using the yeast recombinational method was performed in the yeast strain FY834 (Winston *et al*., 1995).

Nucleic acid extraction and analysis

Standard recombinational DNA methods were used as described in Sambrook and colleagues (1989) and Ausubel and colleagues (1987). Genomic DNA from *C. purpurea* was prepared from lyophilized mycelia according to Cenis (1992). PCR was performed as described in Sambrook and colleagues (1989) using BioTherm Polymerase (GeneCraft). PCR amplifications of fusion proteins or complementation fragments were performed using the proof reading Phusion polymerase (Finnzymes). All primers used are listed in Table S2 and were synthesized by Biolegio (Nijmegen). Southern blotting was performed using Hybond-N + nylon filters (Amersham) according to the manufacturer's protocol. Filters were hybridized using [α-^{32P}]-dCTP-labelled probes. DNA sequencing was carried out as described in Moore and colleagues (2002). Protein and DNA sequence alignment, editing and organization were done with DNA Star (Madison). Further sequence analyses were performed using BLAST at the National Center for Biotechnology Information, Bethesda, MD, USA (Altschul *et al*., 1997).

Replacement and complementation vector construction

All vectors were generated using the yeast recombinational cloning method (Colot *et al*., 2006). Complementation and fusion protein vectors were constructed based on the described vector system (Christianson *et al*., 1992; Schumacher, 2012).

CpIPT-LOG

The flanking regions of *cpipt-log* were amplified with the following primers containing overlapping sequences towards the yeast shuttle-vector pRS426 or the phleomycin resistance cassette: 5F_Ipt-Log/5R_Ipt-Log for the 5′-spanning region (1212 bp); 3F_Ipt-Log/3R_Ipt-Log (EcoRI) for the 3′-spanning region (1221 bp). The PCR products, the linearized yeast shuttle vector pRS426 (Colot *et al*., 2006) and the phleomycin resistance cassette (amplified with primers CpBleF1/CpBleR1 from pRS426CpBle; 1847 bp) were transformed into yeast strain FY834 for homologous recombination. DNA was isolated from yeast cells using the SpeedPrep yeast plasmid isolation kit (DualSystems) and transformed into *E scherichia coli*. After DNA isolation, restriction with EcoRI resulted in a 4316 bp fragment that was used to transform the 20.1 strain of *C. purpurea*. For construction of the complementation vector pComp_IPT-Log, a 3214 bp fragment containing the coding region of *cpipt-log* as well as the sequences 1330 bp upstream and 250 bp downstream of it were amplified using the primers IPT_Log_Compl_natP_fw/IPT_Log_Compl_rev, which contain overlapping sequences to the vector sequence of pNDH-OCT for homologous recombination. The obtained plasmid was used to transform the *C. purpurea* Δcpipt-log mutant strain.

CpP450

Replacement vector construction was performed in the same way as for the deletion of *cpipt-log*, using the primers 5F_P450 (BamHI)/5R_P450 for the 5′ flanking region (1154 bp) and 3F__P450/3R__P450 (HindIII) for the 3′ flanking region (1122 bp) of the *cpp450* gene. The 4208 bp replacement fragment was excised by restriction with BamHI and HindIII. The complementation vector pCompP450 contains a 3532 bp fragment including the coding region of *cpp450* as well as 949 bp upstream and 89 bp downstream. The fragment was cloned into the SpeI/NotI restricted vector pNDH-OCT, and the resulting plasmid was used to transform the *C. purpurea* Δcpp450 mutant strains.

Fungal transformation

Protoplasts were prepared from *C. purpurea* strains as described previously (Jungehülsing *et al*., 1994). Integration

events were confirmed by diagnostic PCR using specific primers as indicated (Table S2). Single spore isolation was carried out to obtain homokaryons of putative transformants. Additionally, Southern blot analyses were performed with each deletion mutant to confirm single integration events. For complementation of Δcpp450 and Δcpipt-log, the mutants were transformed with 10 μg of pComp:*cpp450* and pComp:*cpipt-log* respectively.

Expression studies and quantitative RT-PCR

For detection of fungal gene expression, cDNA of infected and uninfected *in planta* material was analysed. Total RNA was isolated using the RNeasy Midi Kit from Qiagen, and reverse transcription PCR was performed using the Superscript II (Invitrogen) and 2 μg of total RNA as a template, according to the manufacturer's instructions. qPCR reactions were performed with the Bio-Rad iQ SYBR Green Supermix and the iCycler Thermal Cycler (Bio-Rad). Programming, data collection and analyses were performed with the iCycler iQ Real-Time Detection System Software Version 3.0 (Bio-Rad). The expression of all tested fungal genes was normalized to the expression of genes encoding β-tubulin (CCE34429.1; Tub_uni/Tub_rev), γ-actin (AEI72275.1; Actin_uni/Actin_rev) and glyceraldehyde-3-phosphate dehydrogenase (X73282.1; Gpd_uni/Gpd_rev) as described in Giesbert and colleagues (2008). Expression was verified in at least two independent biological replicates.

For detection of rye gene expression, cDNA of infected and uninfected *in planta* material was analysed. Total RNA was isolated using the RNAqueous kit and Plant RNA Isolation Aid solutions (Life Technology). The isolated RNA was treated twice with Ambion's TURBO DNase-free kit (Life Technology), and first-strand cDNA was synthesized using the RevertAid H Minus Moloney murine leukemia virus reverse transcriptase with an oligo(dT) primer (Thermo Scientific). qPCR reactions were performed with TaqMan Gene Expression Master Mix on a ViiA7 Real-Time PCR System (Life Technology) using a default program. Primers and Taqman probes for all rye genes, listed in Table S2, were designed using Primer Express 3.0 (Life Technology). Each sample was processed in four biological replicates, and at least two technical replicates were run for each biological replicate. Expression values were determined and statistically evaluated using DataAssist v3.0 (Life Technologies). CK-related genes with detectable expression in developing rye ears were found in RNA-seq data generated from a library prepared from infected rye ears (B. Oeser, J. Hinsch and P. Tudzynski, unpubl. data). Genes for RR, HK and LOG were numbered based on the closest rice orthologues (Ito and Kurata, 2006; Kurakawa *et al.*, 2007) while those for CKX, IPT, b-actin and elongation factor 1 were based on barley orthologues (Mrízová *et al.*, 2013). Predicted sequences were deposited in the NCBI database (Table S2).

Production of recombinant proteins

The coding regions of *cpipt-log* and *cplog* as well as the IPT domain of *cpipt-log* (from the start codon to the beginning of the intron at position 880) and the LOG domain of *cpipt-log* (from ATG at position 1055 to the stop codon) were synthesized with codon optimization for *E. coli* expression by GeneArt service (Invitrogen) and subcloned with *Nde*I and *Hind*III overhangs into the pET28a(+) vector to generate N-terminal His-tagged recombinant proteins. *Escherichia coli* BL21 Star (DE3) transformed with these constructs was grown in Luria Broth medium supplemented with kanamycin at 37°C until the OD_{600} reached 0.6. Expression was induced by treatment with 0.4 mM isopropyl β-D-1-thiogalactopyranoside, after which the cells were incubated for 17 h with vigorous shaking at 18°C. Harvested cells were dissolved in lysis buffer (50 mM phosphate buffer, pH 8.0, supplemented with 0.3 M NaCl, 20% glycerol and 1 mM phenylmethylsulfonyl fluoride) and then disrupted using a French press at 25 000 psi. The cell lysate was clarified by centrifugation at 20 000 *g*, after which the supernatant was repeatedly loaded onto an equilibrated HisPur Cobalt column (Thermo Scientific) overnight. The column was subsequently washed with lysis buffer supplemented with 20 mM and 60 mM imidazole. The protein was then eluted with 120 mM imidazole, dialysed against lysis buffer without imidazole and concentrated using an ultrafiltration cell with a 10 kDa cutoff membrane.

IPT and LOG activity assay

Purified protein (25–70 μg) was added to the reaction mixture (IPT or IPT-LOG coupled reaction: 30 mM Tris/acetate, pH 8.0; supplemented with 1 M betaine, 20 mM $MgCl_2$ and 5 mM β-mercaptoethanol; LOG reaction: 100 mM K^+phosphate buffer, pH 7.0). Kinetic parameters were determined using a reaction mixture containing 100 μM DMAPP or HMBDP (Echelon Biosciences, Salt Lake City, UT, USA) as the donor substrate and 0.5–25 μM AMP, ADP or ATP as the acceptor, or 100 μM AMP as acceptor and 0.5–25 μM DMAPP or HMBDP as donor respectively. In the case of LOG reaction, iPRMP, *t*ZRMP, *c*ZRMP (OlChemIm) and the corresponding diphospahtes and triphosphates (BIOLOG Life Science Institute, Bremen, Germany) were used as substrates at concentrations of 1–50 μM. After incubation for 10 min (or 30 min with weak substrates) at 30°C, the reactions were stopped by adding an equal volume of ethanol and heated for 5 min at 90°C. The samples were then purified by passage through 0.22 μm nylon filters and injected onto a C18 reverse-phase column (ZORBAX RRHD Eclipse Plus 1.8 μm, 2.1 × 50 mm; Agilent) coupled to an Ultra performance liquid chromatograph (Shimadzu Nexera). The column was eluted with a linear gradient of 15 mM ammonium formate, pH 4.0 and methanol (B): 0 min, 5% B; 2–8 min, 70% B; flow rate of 0.40 ml min^{-1}; column temperature of 40°C. Peaks were compared with injected standards (OlChemIm), and activity was calculated from subtracted peak areas using LabSolutions software (Shimadzu). Kinetic parameters were calculated using GraFit Version 4.0.12. To determine the kinetic parameters of CpIPT-LOG for reactions involving DMAPP or HMBDP and AMP, excess (1 μg) CpLOG was added to the reaction mixture and a reaction rate was calculated in terms of newly formed iP.

Preparation of transgenic Arabidopsis plants

The cDNA sequences of *cpipt-log*, *cplog* and the IPT domain of *cpipt-log* were subcloned with *Asp718* and *Xba*I overhangs

into a binary pBINHygTx vector downstream of the *CaMV 35S* promoter (Gatz *et al*., 1992). *Agrobacterium tumefaciens* strain GUS3101 harbouring the binary vectors with different transgenes was used to transform the *A. thaliana* ecotype Col-0 via the flower-dip procedure with vacuum infiltration (Clough and Bent, 1998). Transformed *Arabidopsis* plants were grown in a greenhouse until seed production. T1 progeny seeds of *Arabidopsis* transformants were surface sterilized and germinated on Murashige–Skoog phytagel (pH 5.7) supplemented with hygromycin (30 mg l^{-1}) in a controlled environment chamber (12 h light, 5000 Lux, 21°C/12 h darkness, 18°C). Resistant seedlings were transferred to soil and placed in the greenhouse. Several homozygous lines for the *cplog* and *cpipt* constructs with a single integration were selected from T2 progeny because of Mendel's segregation laws on the phytagel plates with the selection. Root lengths were calculated with EZ RHIZO software (Armengaud *et al*., 2009).

Fungal CK measurements

Stable isotope-labelled CK internal standards (OlChemIm) were added, each at 1 pmol per sample, to check the recovery during the purification and to validate the determination. The samples were extracted with methanol/H_2O/formic acid (15:4:1, v/v/v), and clarified supernatants were subjected to solid phase extraction. First, non-polar compounds were removed on Speed SPE Octadecyl C18 cartridges (Applied Separation). Subsequently, basic compounds together with CKs were retained on Oasis MCX cartridges (Waters). The eluates were evaporated to dryness and the obtained solids dissolved in 20 μl of the mobile phase used for quantitative analysis. The samples were analysed by ultra-high performance liquid chromatography (Acquity UPLC; Waters) coupled to a Xevo TQ-S (Waters) triple quadrupole mass spectrometer equipped with an electro-spray interface. The purified samples were injected onto a C18 reversed-phase column (BEH C18; 1.7 μm; 2.1 × 50 mm; Waters). The column was eluted with a linear gradient (0 min, 10% B; 0–8 min, 50% B; flow-rate of 0.25 ml min^{-1}; column temperature of 40°C) of 15 mM ammonium formate (pH 4.0, A) and methanol (B). Quantification was achieved by multiple reaction monitoring of $[M + H]^+$ and the appropriate product ion. Quantification was performed with the MASSLYNX program (Waters) using a standard isotope dilution method. The ratio of endogenous CK to the appropriate labelled standard was determined and further used to quantify the level of endogenous compounds in the original extract, according to the known quantity of the added internal standard.

Samples, whose CK contents are presented in Fig. S1, were eluted from Oasis MCX cartridges and purified by loading onto immuno-affinity columns with specificity toward isoprenoid CKs (OlChemIm) and after the elution and evaporation applied onto a C18 reverse-phase column (ZORBAX RRHD Eclipse Plus 1.8 μm, 2.1 × 50 mm, Agilent) coupled to Ultra performance liquid chromatography (Shimadzu Nexera). The column was eluted with a linear gradient of 15 mM ammonium formate, pH 4.5 and methanol (B): 0 min, 5% B; 2–28 min, 50% B; flow rate of 0.40 ml min^{-1}; column temperature of 40°C. Peaks were compared with injected standards (OlChemIm), and activity was calculated from subtracted peak areas using LABSOLUTIONS software (Shimadzu). The unretained fraction from the immuno-affinity column was treated with alkaline phosphatase (Thermo Scientific) for 1 h at 37°C and purified again on the immuno-affinity column to estimate the samples' contents of CK riboside monophosphates.

Plant growth conditions, infection, and sampling

Pathogenicity assays were performed using the cytoplasmic male sterile *S. cereale* Lo37-PxLo55-N (KWS Lochow GmbH) cultivar, which was cultivated in growth chambers under conditions of 15 h light (8000 Lux; 16–18°C)/9 h darkness (13–15°C). Before planting, seeds were stratified for 5–6 weeks at 1–2°C and vernalization took place in soil/compost 3:2 at 14–15°C (day) and 9–10°C (night) with 9 h light (6000–10 000 Lux). For *in planta* pathogenicity assays, florets of blooming ears (30–40 ear^{-1}) were inoculated with 5 μl of a suspension containing about 10^6 ml^{-1} conidia collected from Mantle agar, as described in Tenberge and colleagues (1996). To avoid cross-contamination, the ears were covered with paper bags directly after inoculation. For *in planta* measurements of CK levels, three ears per sample were infected with conidia of *C. purpurea* or mock treated with water. Ears were harvested and directly frozen in liquid nitrogen before being pulverized to facilitate further analysis. The *in vitro* pathogenicity assay was performed as described in Scheffer and Tudzynski (2006).

Microscopic analyses

For microscopic studies *in planta*, rye ovaries were stained with KOH-aniline-blue as described previously (Scheffer and Tudzynski, 2006) and examined with a Zeiss DiscoveryV20 stereo microscope fitted with an AxioCam MRc camera (Zeiss). Image analysis was performed with AXIOVISION REL 4.8 software (Zeiss).

Acknowledgements

We thank A. Schmidt for technical support, and the Deutsche Forschungsgemeinschaft (Tu50/21-1) and the National Science Foundation, Czech Republic (grant number P501/12/0597) for financial support. P.G. was partly supported by the Operational Program Education for Competitiveness – European Social Fund (project CZ.1.07/2.3.00/20.0165).

References

Akiyoshi, D.E., Klee, H., Amasino, R.M., Nester, E.W., and Gordon, M.P. (1984) T-DNA of *Agrobacterium tumefaciens* encodes an enzyme of cytokinin biosynthesis. *PNAS* **81:** 5994–5998.

Altschul, S.F., Madden, T.L., Schaffer, A.A., Zhang, J.H., Zhang, Z., Miller, W., and Lipman, D.J. (1997) Gapped BLAST and PSI-BLAST: a new generation of protein database search programs. *Nucleic Acids Res* **25:** 3389–3402.

Anjard, C., and Loomis, W.F. (2008) Cytokinins induce sporulation in *Dicytystelium*. *Development* **135:** 819–827.

Armengaud, P., Zambaux, K., Hills, A., Sulpice, R., Pattison, R.J., Blatt, M.R., and Amtmann, A. (2009) EZ-Rhizo: integrated software for the fast and accurate measurement of root system architecture. *Plant J* **57:** 945–956.

Ausubel, F.M., Brent, R., Kingston, R.E., Moore, D.D., Seidmann, J.G., Smith, J.A., and Struhl, K. (1987) *Current Protocols in Molecular Biology*. New York, USA: John Wiley & Sons.

Behr, M., Motyka, V., Weihmann, F., Malbeck, J., Deising, H.B., and Wirsel, S.G.R. (2012) Remodeling of cytokinin metabolism at infection sites of *Colletotrichum graminicola* on maize leaves. *Mol Plant Microbe Interact* **25:** 1073–1082.

Cenis, J.L. (1992) Rapid extraction of fungal DNA for PCR amplification. *Nucleic Acids Res* **20:** 2380.

Christianson, T.W., Sikorski, R.S., Dante, M., Shero, J.H., and Hieter, P. (1992) Multifunctional yeast high-copy-number shuttle vectors. *Gene* **110:** 119–122.

Clough, S.J., and Bent, A.F. (1998) Floral dip: a simplified method for *Agrobacterium*-mediated transformation of *Arabidopsis thaliana*. *Plant J* **16:** 735–743.

Colot, H.V., Park, G., Turner, G.E., Ringelberg, C., Crew, C.M., Litvinkova, L., *et al*. (2006) A high-throughput gene knockout procedure for *Neurospora* reveals functions for multiple transcription factors. *PNAS* **103:** 10352–10357.

Crafts, C.B., and Miller, C.O. (1974) Detection and identification of cytokinins produced by mycorrhizal fungi. *Plant Physiol* **54:** 586–588.

Creason, A.L., Vandeputte, O.M., Savory, E.A., Davis, E.W., II, Putnam, M.L., Hu, E., *et al*. (2014) Analysis of genome sequences from plant pathogenic *Rhodococcus* reveals genetic novelties in virulence loci. *PLoS ONE* **9:** e101996. doi:10.1371/journal.pone.0101996.

Esser, K., and Tudzynski, P. (1978) Genetics of the ergot fungus *Claviceps purpurea*. *Theor Appl Genet* **53:** 145–149.

Faiss, M., Zalubilová, J., Strnad, M., and Schmülling, T. (1997) Conditional transgenic expression of the *ipt* gene indicates a function for cytokinins in paracrine signaling in whole tobacco plants. *Plant J* **12:** 401–415.

Frébort, I., Kowalska, M., Hluska, T., Frébortová, J., and Galuszka, P. (2011) Evolution of cytokinin biosynthesis and degradation. *J Exp Bot* **62:** 2431–2452.

Gajdošová, S., Spíchal, L., Kamínek, M., Hoyerová, K., Novák, O., Dobrev, P.I., *et al*. (2011) Distribution, biological activities, metabolism, and the conceivable function of *cis*-zeatin-type cytokinins in plants. *J Exp Bot* **62:** 2827–2840.

Galuszka, P., Spíchal, L., Kopečný, D., Tarkowski, P., Frébortová, J., Šebela, M., and Frébort, I. (2008) Metabolism of plant hormones cytokinins and their function in signaling, cell differentiation and plant development. *Stud Nat Prod Chem* **34:** 203–264.

Gatz, C., Frohberg, C., and Wendenburg, R. (1992) Stringent repression and homogeneous derepression by tetracycline of a modified CaMV 35S promoter in intact transgenic tobacco plants. *Plant J* **2:** 397–404.

Giesbert, S., Schürg, T., Scheele, S., and Tudzynski, P. (2008) The NADPH oxidase Cpnox1 is required for full pathogenicity of the ergot fungus *Claviceps purpurea*. *Mol Plant Pathol* **9:** 317–327.

Hedden, P., Phillips, A.L., Rojas, M.C., Carrera, E., and Tudzynski, B. (2001) Gibberellin biosynthesis in plants and fungi: a case of convergent evolution? *J Plant Growth Regul* **20:** 319–331.

Hinsch, J., and Tudzynski, P. (2015) *Claviceps*: the Ergot fungus. In *Molecular Biology of Food and Water Borne Mycotoxigenic and Mycotic Fungi of Humans*. Russell, R., and Paterson, M. (eds). Boca Raton, Florida, USA: CRC Press, pp. 229–250. in press.

Hüsgen, U., Büttner, P., Müller, U., and Tudzynski, P. (1999) Variation in karyotype and ploidy level among field isolates of *Claviceps purpurea*. *J Phytopathol* **147:** 591–597.

Ihara, M., Taya, Y., and Nishimura, S. (1980) Developmental regulation of cytokinin, spore germination inhibitor discadenine and related enzymes in *Dictyostelium discoideum*. *Exp Cell Res* **126:** 273–278.

Ioio, R.D., Linhares, F.S., and Sabatini, S. (2008) Emerging role of cytokinin as a regulator of cellular differentiation. *Curr Opin Plant Biol* **11:** 23–27. doi:org/10.1016/j.pbi.2007.10.006.

Ito, Y., and Kurata, N. (2006) Identification and characterization of cytokinin-signalling gene families in rice. *Gene* **382:** 57–65.

Jameson, P. (2000) Cytokinins and auxins in plant-pathogen interactions – an overview. *Plant Growth Regul* **32:** 369–380.

Jiang, C.J., Shimono, M., Sugano, S., Kojima, M., Liu, X., Inoue, H., *et al*. (2013) Cytokinins act synergistically with salicylic acid to activate defense gene expression in rice. *Mol Plant Microbe Interact* **26:** 287–296.

Jungehülsing, U., Arntz, C., Smit, R., and Tudzynski, P. (1994) The *Claviceps purpurea* glyceraldehyde-3-phosphate dehydrogenase gene: cloning, characterization, and use for the improvement of a dominant selection system. *Curr Genet* **25:** 101–106.

Kakimoto, T. (2001) Identification of plant cytokinin biosynthetic enzymes as dimethylallyl diphosphate: ATP/ADP isopentenyltransferases. *Plant Cell Physiol* **42:** 677–685.

Konevega, A.L., Soboleva, N.G., Makhno, V.I., Peshekhonov, A.V., and Katunin, V.I. (2006) The effect of modification of tRNA nucleotide-37 on the tRNA interaction with the P- and A-site of the 70S ribosome *Escherichia coli*. *Mol Biol* **40:** 669–683.

Kurakawa, T., Ueda, N., Maekawa, M., Kobayashi, K., Kojima, M., Nagato, Y., *et al*. (2007) Direct control of shoot meristem activity by a cytokinin-activating enzyme. *Nature* **445:** 652–655.

Lindner, A.C., Lang, D., Seifert, M., Podlešáková, K., Novák, O., Strnad, M., *et al*. (2014) Isopentenyltransferase-1 (IPT1) knockout in *Physcomitrella* together with phylogenetic analyses of IPTs provide insights into evolution of plant cytokinin biosynthesis. *J Exp Bot* **65:** eru142.

Mantle, P.G., and Nisbet, L.J. (1976) Differentiation of *Claviceps purpurea* in axenic culture. *J Gen Microbiol* **93:** 321–334.

Miller, C.O. (1967) Zeatin and zeatin riboside from a mycorrhizal fungus. *Science* **157:** 1055–1057.

Miransari, M., Abrishamchi, A., Khoshbakht, K., and Niknam, V. (2014) Plant hormones as signals in arbuscular

mycorrhizal symbiosis. *Crit Rev Biotechnol* **34:** 123–133. doi:10.3109/07388551.2012.731684.

Miyawaki, K., Tarkowski, P., Matsumoto-Kitano, M., Kato, T., Sato, S., Tarkowska, D., *et al*. (2006) Roles of *Arabidopsis* ATP/ADP isopentenyltransferases and tRNA isopentenyltransferases in cytokinin biosynthesis. *PNAS* **103:** 16598–16603.

Moore, S., de Vries, O.M., and Tudzynski, P. (2002) The major Cu, Zn SOD of the phytopathogen *Claviceps purpurea* is not essential for pathogenicity. *Mol Plant Pathol* **3:** 9–22.

Mrízová, K., Jiskrová, E., Vyroubalová, S., Novák, O., Ohnoutková, L., Pospíšilová, H., *et al*. (2013) Overexpression of cytokinin dehydrogenase genes in barley (*Hordeum vulgare* cv. Golden Promise) fundamentally affects morphology and fertility. *PLoS ONE* **8:** e79029.

Murphy, A.M., Pryce-Jones, E., Johnstone, K., and Ashby, A.M. (1997) Comparison of cytokinin production in vitro by *Pyrenopeziza brassicae* with other plant pathogens. *Physiol Mol Plant Pathol* **50:** 53–65.

Nakamura, T., Kawanabe, Y., Takiyama, E., Takahashi, N., and Murayama, T. (1978) Effects of auxin and gibberellin on conidial germination in *Neurospora crassa*. *Plant Cell Physiol* **19:** 705–709.

Park, H.S., and Yu, J.H. (2012) Genetic control of asexual sporulation in filamentous fungi. *Curr Opin Microbiol* **15:** 669–677.

Persson, B.C., Esberg, B., Ólafsson, Ó., and Björk, G.R. (1994) Synthesis and function of isopentenyl adenosine derivatives in tRNA. *Biochemie* **76:** 1152–1160.

Pertry, I., Václavíková, K., Depuydt, S., Galuszka, P., Spíchal, L., Temmerman, W., *et al*. (2009) Identification of *Rhodococcus fascians* cytokinins and their modus operandi to reshape the plant. *PNAS* **106:** 929–934.

Podlešáková, K., Zalabák, D., Čudejková, M., Plíhal, O., Szüčová, L., Doležal, K., *et al*. (2012) Novel cytokinin derivatives do not show negative effects on root growth and proliferation in submicromolar range. *PLoS ONE* **7:** e39293. doi:10.1371/journal.pone.0039293.

Podlešáková, K., Fardoux, J., Patrel, D., Bonaldi, K., Novák, O., Strnad, M., *et al*. (2013) Rhizobial synthesized cytokinins contribute to but are not essential for the symbiotic interaction between photosynthetic *Bradyrhizobia* and *Aeschynomene* legumes. *Mol Plant Microbe Interact* **26:** 1232–1238.

Rypacek, V., and Sladky, Z. (1972) The character of endogenous growth regulators in the course of development in the fungus *Lentinus tigrinus*. *Mycopathol Mycol Appl* **46:** 65–72.

Rypacek, V., and Sladky, Z. (1973) Relation between the level of endogenous growth regulators and the differentiation of the fungus *Lentinus tigrinus* studied in a synthetic medium. *Biol Plant* **15:** 20–26.

Sakakibara, H. (2006) Cytokinins: activity, biosynthesis, and translocation. *Annu Rev Plant Biol* **57:** 431–449.

Sakakibara, H., Kasahara, H., Ueda, N., Kojima, M., Takei, K., Hishiyama, S., *et al*. (2005) *Agrobacterium tumefaciens* increases cytokinin production in plastids by modifying the biosynthetic pathway in the host plant. *Proc Natl Acad Sci USA* **102:** 9972–9977.

Sambrook, J., Fritsch, E.F., and Maniatis, T. (1989) *Molecular Cloning: A Laboratory Manual*, 2nd edn. Cold Spring Harbor, NY, USA: Cold Spring Harbor Laboratory Press.

Schardl, C.L., Young, C.A., Hesse, U., Amyotte, S.G., Andreeva, K., Calie, P.J., *et al*. (2013) Plant-symbiotic fungi as chemical engineers: multi-genome analysis of the Clavicipitaceae reveals dynamics of alkaloid loci. *PLoS Genet* **9:** e1003323.

Scheffer, J., and Tudzynski, P. (2006) In vitro pathogenicity assay for the ergot fungus *Claviceps purpurea*. *Mycol Res* **110:** 465–470.

Schumacher, J. (2012) Tools for *Botrytis cinerea*: new expression vectors make the gray mold fungus more accessible to cell biology approaches. *Fungal Genet Biol* **49:** 483–497.

Skoog, F., and Armstrong, D.J. (1970) Cytokinins. *Annu Rev Plant Physiol* **21:** 359–384.

Smart, C.M., Scofield, S.R., Bevan, M.W., and Dyer, T.A. (1991) Delayed leaf senescence in tobacco plants transformed with *tmr*, a gene for cytokinin production in *Agrobacterium*. *Plant Cell* **3:** 647–656.

Stacey, B.A., Saville, B.J., and Emery, R.J.N. (2011) *Ustilago maydis* produces cytokinins and abscisic acid for potential regulation of tumor formation in maize. *J Plant Growth Regul* **30:** 51–63.

Su, Y., Liu, Y., and Zhang, X. (2011) Auxin–cytokinin interaction regulates meristem development. *Mol Plant* **4:** 616–625.

Takei, K., Sakakibara, H., and Sugiyama, T. (2001) Identification of genes encoding adenylate isopentenyltransferase, a cytokinin biosynthesis enzyme, in *Arabidopsis thaliana*. *J Biol Chem* **276:** 26405–26410.

Takei, K., Yamaya, T., and Sakakibara, H. (2004) *Arabidopsis* CYP735A1 and CYP735A2 encode cytokinin hydroxylases that catalyze the biosynthesis of *trans*-zeatin. *J Biol Chem* **279:** 41866–41872.

Tenberge, K.B., Homann, V., Oeser, B., and Tudzynski, P. (1996) Structure and expression of two polygalacturonase genes of *Claviceps purpurea* oriented in tandem and cytological evidence for pectinolytic enzyme activity during infection of rye. *Phytopathology* **86:** 1084–1097.

Tomita, K., Murayama, T., and Nakamura, T. (1984) Effects of auxin and gibberellin on elongation of young hyphae in *Neurospora crassa*. *Plant Cell Physiol* **25:** 355–358.

Tsavkelova, E., Oeser, B., Oren-Young, L., Israeli, M., Sasson, Y., Tudzynski, B., and Sharon, A. (2012) Identification and functional characterization of indole-3-acetamide-mediated IAA biosynthesis in plant-associated *Fusarium* species. *Fungal Genet Biol* **49:** 48–57.

Tudzynski, B., Kawaide, H., and Kamiya, Y. (1998) Gibberellin biosynthesis in *Gibberella fujikuroi*: cloning and characterization of the copalyl diphosphate synthase gene. *Curr Genet* **34:** 234–240.

Tudzynski, P., and Scheffer, J. (2004) *Claviceps purpurea*: molecular aspects of a unique pathogenic lifestyle. *Mol Plant Pathol* **5:** 377–388.

Ueda, N., Kojima, M., Suzuki, K., and Sakakibara, H. (2012) *Agrobacterium tumefaciens* tumor morphology root plastid localization and preferential usage of hydroxylated prenyl donor is important for efficient gall formation. *Plant Physiol* **159:** 1064–1072.

Van Rhijn, P., Fang, Y., Galili, S., Shaul, O., Atzmon, N., Wininger, S., *et al*. (1997) Expression of early nodulin genes in alfalfa mycorrhizae indicates that signal transduction pathways used in forming arbuscular mycorrhizae and Rhizobium-induced nodules may be conserved. *Proc Natl Acad Sci USA* **94:** 5467–5472.

Van Staden, J., and Nicholson, R.I.D. (1989) Cytokinins and mango flower malformation II. The cytokinin complement produced by *Fusarium moniliforme* and the ability of the fungus to incorporate [$^{8\text{-}14}$C]adenine into cytokinins. *Physiol. Mol Plant Pathol* **35:** 423–431.

Winston, F., Dollard, C., and Ricupero-Hovasse, S.L. (1995) Construction of a set of convenient *Saccharomyces cerevisiae* strains that are isogenic to S288C. *Yeast* **11:** 53–55.

Supporting information

Additional Supporting Information may be found in the online version of this article at the publisher's web-site:

Fig. S1. Cytokinin content in mycelia (A) and media (B) of *C. purpurea* wild-type strain *Cp*20.1, knock-out strains and respective complementants. Sum of all iP, *t*Z and cZ types of cytokinin is presented. Mycelia were cultivated for 4 days in Mantle media in two biological replicates before purification via immunoaffinity columns and high-performance liquid chromatography analysis.

Fig. S2. Phylogenetic tree of IPT domains. The tree was done with MUSCLE, GBLOCKS, PHYLML and TREEDYN over the webpage of http://www.phylogeny.fr. Descriptions used in the tree indicated the presence of certain InterProScan domains: tRNA-IPTs: IPR2627 (tRNA isopentenyltransferase); IPR18022 [tRNA Δ(2)-isopentenylpyrophosphate transferase]; put_tRNA_IPT_LOGs: IPR2627 (tRNA isopentenyltransferase) + IPR5269 (cytokinin riboside 5′-monoP phosphoribohydrolase LOG); IPT-LOGs: IPR2648 (isopentenyltransferase) + IPR5269 (cytokinin riboside 5′-monoP phosphoribohydrolase LOG).

Fig. S3. Phylogenetic tree of LOG domains. The tree was done with MUSCLE, GBLOCKS, PHYLML and TREEDYN over the webpage of http://www.phylogeny.fr. Descriptions used in the tree indicated the presence of certain InterProScan domains: LOGs: LOG: IPR0005269 (cytokinin riboside 5′-monoP phosphoribohydrolase LOG); put_tRNA_IPT_LOGs: IPR2627 (tRNA isopentenyltransferase) + IPR5269 (cytokinin riboside 5′-monoP phosphoribohydrolase LOG); IPT-LOGs: IPR2648 (isopentenyltransferase) + IPR5269 (cytokinin riboside 5′-monoP phosphoribohydrolase LOG).

Fig. S4. Expression of *cplog* in axenic culture and in planta. (A) Expression levels were determined in the wild-type *Cp*20.1 during infection 3, 5 and 10 as well as in axenic cultures (cultivated in Mantle medium for 4 days) by qPCR. Expression levels were normalized to fungal housekeeping genes (β-tubulin, γ-actin, and glyceraldehyde-3-phosphate dehydrogenase). One experiment is exemplarily shown. (B) Northern blot analyses were performed with RNA isolated from *Cp*20.1 cultivated in BII and Mantle media for 3 and 4 days. The coding sequence of *cplog* was used as a probe.

Fig. S5. Expression of recombinant *Claviceps* enzymes. Purified proteins were separated by NuPAGE SDS-PAGE (Thermo Scientific); lane 1, recombinant CpIPT-LOG (57 kDa); lane 2, recombinant IPT domain (36 kDa) from CpIPT-LOG; lane3, recombinant CpLOG (29 kDa). The size of the protein molecular mass marker is indicated to the right of the gel.

Fig. S6. Generation of the Δcpp450 mutants. (A) The replacement vector was obtained by the yeast recombinational method. It was constructed by cloning the 3′ and 5′ flanking regions of *cpp450* on each side of the phleomycin resistance cassette into the yeast shuttle vector pRS426 plasmid (see *Experimental procedures* for further details). The resulting replacement fragment was used to transform *C. purpurea* wild type strain *Cp*20.1. (B) The mutants were generated by homologous integration of the resistance cassette via a double cross over event between the homologous regions of the replacement fragment and the genomic region of *cpp450*. Primers used for diagnostic PCRs are indicated. Primers and destination vectors are not drawn to scale. (C) Diagnostic PCRs of Δcpp450 mutants and *Cp*20.1. For the deletion mutants, a homologous integration event is documented by amplification of 5′and 3′ diagnostic fragments, resp., while lack of the wild-type control fragments proves the absence of the wt gene in the mutants (λ restricted with *Hind*III, fragment sizes are indicated on the left). (D) Southern blot analyses of Δcpp450 mutants. *Xho*I digested genomic DNA of *Cp*20.1 and the Δcpp450 mutants were probed with the 3′-flank of *cpp450*. Lack of wt fragment and single integration of the replacement fragment is evident.

Fig. S7. Generation of the Δcpipt-log mutant. (A) The replacement vector was obtained by the yeast recombinational method. It was constructed by cloning the 3′ and 5′ flanking regions of *cpipt-log* on each side of the phleomycin resistance cassette into the yeast shuttle vector pRS426 plasmid (see materials and methods for further details). The resulting replacement fragment was used to transform *C. purpurea* wild type strain *Cp*20.1. (B) The mutant was generated by homologous integration of the resistance cassette via a double cross over event between the homologous regions of the replacement fragment and the genomic region of *cpipt-log*. Primers used for diagnostic PCRs are indicated. Primers and destination vectors are not drawn to scale. (C) Diagnostic PCRs of Δcpipt-log and *Cp*20.1. For the deletion mutant, a homologous integration event is documented by amplification of 5′and 3′ diagnostic fragments, resp., while lack of the wild-type control fragments proves the absence of the wt gene in the mutant (λ restricted with *Hind*III, fragment sizes are indicated on the left). (D) Southern blot analyses of Δcpipt-log. *Kpn*I digested genomic DNA of *Cp*20.1 and Δcpipt-log was probed with the 5′-flank of *cpipt-log*. Lack of wt fragment and single integration of the replacement fragment is evident.

Table S1. Cytokinin content in infected ears with fully developed sclerotia and non-infected sterile rye ears (25 dpi).

Table S2. Oligonucleotide primers used in this study.

Part XIII: Appendice II

Research article

Production and role of hormones during interaction of *Fusarium* species with maize (*Zea mays* L.) seedlings.

Vrabka, J., Niehaus, E. M., Münsterkötter, M., Proctor, R. H., Brown, D. W., Novák, O., Pěnčík, A., Tarkowská, D., Hromadová, K., Hradilová, M., Oklešťková, J., Oren-Young, L., Idan, Y., Sharon, A., Maymon, M., Elazar, M., Freeman, S., Güldener, U., Tudzynski, B., Galuszka, P., Bergougnoux, V.

Frontiers in Plant Science (2019), *9*, 1936. doi: 10.3389/fpls.2018.01936

frontiers in Plant Science

ORIGINAL RESEARCH
published: 11 January 2019
doi: 10.3389/fpls.2018.01936

Production and Role of Hormones During Interaction of *Fusarium* Species With Maize (*Zea mays* L.) Seedlings

*Josef Vrabka[1], Eva-Maria Niehaus[2], Martin Münsterkötter[3], Robert H. Proctor[4], Daren W. Brown[4], Ondřej Novák[5,6], Aleš Pěnčik[5,6], Danuše Tarkowská[5,6], Kristýna Hromadová[1], Michaela Hradilová[1], Jana Oklešťková[5,6], Liat Oren-Young[7], Yifat Idan[7], Amir Sharon[7], Marcel Maymon[8], Meirav Elazar[8], Stanley Freeman[8], Ulrich Güldener[9], Bettina Tudzynski[2], Petr Galuszka[1†] and Veronique Bergougnoux[1]**

[1] Department of Molecular Biology, Centre of the Region Haná for Biotechnological and Agricultural Research, Faculty of Science, Palacký University, Olomouc, Czechia, [2] Institut für Biologie und Biotechnologie der Pflanzen, Molecular Biology and Biotechnology of Fungi, Westfälische Wilhelms-Universität Münster, Münster, Germany, [3] Functional Genomics and Bioinformatics, Sopron University, Sopron, Hungary, [4] National Center for Agricultural Utilization Research, United States Department of Agriculture, Peoria, IL, United States, [5] Institute of Experimental Botany, Czech Academy of Sciences, Olomouc, Czechia, [6] Department of Metabolomics, Centre of the Region Haná for Biotechnological and Agricultural Research, Faculty of Science, Palacký University, Olomouc, Czechia, [7] Department of Molecular Biology and Ecology of Plants, Tel Aviv University, Tel Aviv, Israel, [8] Department of Plant Pathology and Weed Research, Agricultural Research Organization (ARO), The Volcani Center, Rishon LeZion, Israel, [9] Department of Bioinformatics, TUM School of Life Sciences Weihenstephan, Technical University of Munich, Munich, Germany

It has long been known that hormones affect the interaction of a phytopathogen with its host plant. The pathogen can cause changes in plant hormone homeostasis directly by affecting biosynthesis or metabolism in the plant or by synthesizing and secreting the hormone itself. We previously demonstrated that pathogenic fungi of the *Fusarium* species complex are able to produce three major types of hormones: auxins, cytokinins, and gibberellins. In this work, we explore changes in the levels of these hormones in maize and mango plant tissues infected with *Fusarium*. The ability to produce individual phytohormones varies significantly across *Fusarium* species and such differences likely impact host specificity inducing the unique responses noted *in planta* during infection. For example, the production of gibberellins by *F. fujikuroi* leads to elongated rice stalks and the suppression of gibberellin biosynthesis in plant tissue. Although all *Fusarium* species are able to synthesize auxin, sometimes by multiple pathways, the ratio of its free form and conjugates in infected tissue is affected more than the total amount produced. The recently characterized unique pathway for cytokinin *de novo* synthesis in *Fusarium* appears silenced or non-functional in all studied species during plant infection. Despite this, a large increase in cytokinin levels was detected in *F. mangiferae* infected plants, caused likely by the up-regulation of plant genes responsible for their biosynthesis. Thus, the accumulation of active cytokinins may contribute to mango malformation of the reproductive organs upon infection of mango trees. Together, our findings provide insight into the complex role fungal and plant derived hormones play in the fungal–plant interactions.

Keywords: auxin, cytokinin, *Fusarium*, host–pathogen interaction, gibberellin, mango malformation disease (MMD)

OPEN ACCESS

Edited by:
Pierre Fobert, National Research Council Canada (NRC-CNRC), Canada

Reviewed by:
Nora A. Foroud, Agriculture and Agri-Food Canada, Canada
Aiping Zheng, Sichuan Agricultural University, China
Rajesh N. Patkar, Maharaja Sayajirao University of Baroda, India

***Correspondence:**
Veronique Bergougnoux
veronique.bergougnoux@upol.cz

† Deceased

Specialty section:
This article was submitted to Plant Microbe Interactions, a section of the journal Frontiers in Plant Science

Received: *29 March 2018*
Accepted: *12 December 2018*
Published: *11 January 2019*

Citation:
Vrabka J, Niehaus E-M, Münsterkötter M, Proctor RH, Brown DW, Novák O, Pěnčik A, Tarkowská D, Hromadová K, Hradilová M, Oklešťková J, Oren-Young L, Idan Y, Sharon A, Maymon M, Elazar M, Freeman S, Güldener U, Tudzynski B, Galuszka P and Bergougnoux V (2019) Production and Role of Hormones During Interaction of Fusarium Species With Maize (Zea mays L.) Seedlings. Front. Plant Sci. 9:1936. doi: 10.3389/fpls.2018.01936

INTRODUCTION

The genus *Fusarium* is a filamentous fungus found readily in soil around the world and associated with multiple crop species. Although it can interact with plants as an endophyte, its growth as a biotroph, hemibiotroph, or necrotroph cause significant agronomic losses worldwide. Currently, the genus *Fusarium* is divided into 20 species complexes and nine monotypic lineages (O'Donnell et al., 2013). Species from the *Fusarium fujikuroi* complex (FFC) are best known for their ability to induce diseases such as "bakanae" in rice (Matic et al., 2017), ear and stalk rot in maize (Presello et al., 2008), pitch canker in pine (Gordon, 2006) and mango malformation disease (MMD) in mango (Freeman et al., 2014). Some disease symptoms can be clearly linked to hormone production by the fungi. In fact, culture filtrate of *Fusarium fujikuroi* (*Gibberella fujikuroi*) was the first source from which gibberellins (GAs) were isolated and identified several decades ago (Hedden and Sponsel, 2015). It was only later discovered that GAs are ubiquitous plant hormones that promote normal stem elongation. The contribution of additional GAs to infected rice plants by *F. fujikuroi* leads to abnormally long stems which is the typical "bakanae" symptom observed. The gene cluster responsible for GA synthesis in *F. fujikuroi* has been extensively characterized (Tudzynski and Hölter, 1998).

The production of other hormones such as cytokinins (CKs), auxins and ethylene by fusaria was first suggested over 35 years ago based on their detection in culture filtrates (Mańka, 1980; Van Staden and Nicholson, 1989; Thakur and Vyas, 1983). CKs can be produced by the tRNA decay pathway, which is conserved in almost all living organisms, or by *de novo* synthesis. The tRNA pathway was shown to contribute to CK content in some fungi including *Claviceps purpurea* (Chanclud et al., 2016; Hinsch et al., 2016; Morrison et al., 2017). Recently, we found evidence for possible *de novo* CK synthesis by members of the FFC based on whole genome sequence analysis (Niehaus et al., 2016). We identified two homologous gene clusters, designated CK1 and CK2 located near the GA gene cluster. Each cluster contains two genes: *IPTLOG* and *P450*. *IPTLOG* codes for an enzyme with dual activity: the isopentenyl transferase domain (IPT) is responsible for the conjugation of dimethylallyl pyrophosphate with ATP to form a CK precursor, which is then hydrolyzed by the phosphoribohydrolase domain (*LOG*) to form the CK isopentenyladenine (iP). *P450* codes for a putative cytochrome P450 monooxygenase which catalyzes the hydroxylation of iP to form the CK *trans*-zeatin (*tZ*; Hinsch et al., 2015).

The major auxin indole-3-acetic acid (IAA) can be produced by at least three pathways. The indole-3-acetamide (IAM) pathway, present in all FFC species, converts tryptophan into IAA via an IAM intermediate (Tsavkelova et al., 2012). The orchid endophytic *F. proliferatum* ET1 synthesizes the most IAA among the *Fusarium* examined via the IAM pathway (Tsavkelova et al., 2012). The second pathway involves indole-3-acetaldehyde and is likely responsible for the low level of auxins produced by all other *Fusarium* as this intermediate was detected in mycelium as well as in media of several FFC species (Niehaus et al., 2016). In the smut fungus *Ustilago maydis*, two genes encoding an indole-3-acetaldehyde dehydrogenase and a tryptophan aminotransferase were characterized as responsible for IAA production (Reineke et al., 2008). A possible third pathway for auxins could be mediated by a *Fusarium* gene with homology to the plant gene *YUCCA*, which codes for a key enzyme in plant auxin biosynthesis (Kasahara, 2015) located between the GA and CK clusters. A contribution of the possible YUCCA pathway to auxin production in fungi has not been yet functionally proved.

The phytohormones jasmonates, salicylic acid (SA), ethylene and abscisic acid play a vital role defending plants against fungal pathogens such as *Fusarium oxysporum* (Dempsey and Klessig, 2012; Di et al., 2016). In contrast, the role of CKs and auxins is poorly understood. In some fungus–host interactions, CKs are essential for full virulence of the pathogen (Chanclud et al., 2016; Hinsch et al., 2016). In *Ustilago maydis*, the loss of CK production leads to fewer and smaller tumors in maize (Morrison et al., 2017). The CKs detected in *Magnaporthe oryzae* infected rice leaves have been proposed to serve as a signal to mobilize nutrients, to increase levels of photosynthesis in host leaves or to activate SA-mediated defense responses (Jiang et al., 2013). In *F. mangiferae* infected mango trees, changes in CK and GA levels are associated with the inflorescence and vegetative malformations and reduction in fruit yield (Bist and Ram, 1986; Nicholson and van Staden, 1988).

In addition to changes in GA content in rice seedlings infected by *F. proliferatum*, IAA content was twofold higher in leaves and 1.5-fold lower in roots of a susceptible cultivar. In contrast, changes in a resistant cultivar of the same magnitude were reversed (Quazi et al., 2015). IAA contributes to host vulnerability to a pathogen by inducing acidification and loosening of the cell wall. Resistance to pathogens has been attributed to IAA-amino acid conjugating enzymes which lead to IAA deactivation (Fu et al., 2011). Some bacterial and fungal pathogens can "hijack" auxin metabolism in plant hosts leading to more IAA-aspartic acid (IAA-Asp) conjugate, known to have a role in disease promotion (González-Lamothe et al., 2012). Arabidopsis roots and leaves infected with *F. oxysporum*, and causing wilt disease, show alterations in auxin homeostasis and an up-regulation of plant genes implicated in auxin biosynthesis. However, plant mutants in genes related to auxin synthesis or application of exogenous auxin did not show changes in susceptibility or resistance to this pathogen while mutants defective in auxin signaling and transport conferred pathogen resistance, suggesting a role for auxin in modulating defense responses (Kidd et al., 2011).

In the present study, we examined the relative differences in three major groups of hormones, GAs, auxins and CKs, in plant tissues infected by wild-type (WT) and mutant species of the *F. fujikuroi* complex (FFC). We also examined how FFC species impact expression of maize CK genes during an infection. Finally, the hormonal role in pathogenicity and symptom development (e.g., MMD in mango) is discussed.

MATERIALS AND METHODS

Fungal Strains

F. fujikuroi (Ff) IMI58289 (Commonwealth Mycological Institute, Kew, United Kingdom) served as wild type (WT), GA-producing strain. The mango pathogen *F. mangiferae* MRC7560 (Fm), originating in Israel, is deposited in the culture collection of the Medical Research Council (MRC) (Tygerberg, South Africa). *F. proliferatum* NRRL 62905 (*Fp_N*), *F. proliferatum* ET1 (*Fp_E*) and *F. verticillioides* M-3125 (*Fv*) (Fungal Genomics Stock Centre, Kansas State University, FGSC 7600) were provided by Elena Tsavkelova, Moscow State University, Russia, Robert Proctor and Daren W. Brown, United States Department of Agriculture, United States, respectively. The following strains were previously described and were derived from the strains listed above: Ff_IAA, *Fp*_E_IAA, Fm_IAA, Fv_IAA overexpressing both *IAAM*, coding for a tryptophan monooxygenase and *IAAH*, coding for an indole-3 acetamide hydrolase; *Fp_E_IL1*, *Fm_IL1*, *Ff_IL1* and *Fv_IL1* overexpressing *IPTLOG1*; *Fp_E_IL2*, *Fm_IL2*, *Ff_IL2* and *Fv_IL2* overexpressing *IPTLOG2*; *Fp_E_IL1P1*, *Fm_IL1P1*, *Ff_IL1P1* and *Fv_IL1P1* overexpressing both *IPTLOG1* and *P450-1*; and *Fp_E_IL2P2*, *Fm_IL2P2*, *Ff_IL2P2* and *Fv_IL2P2* overexpressing both *IPTLOG2* and *P450-2*. *IPTLOG1/2* and *P450-1/2* originated from *F. fujikuroi* IMI58289 (**Table 1**) (Niehaus et al., 2016).

Generation of New Fungal Strains

Creation of deletion and overexpression vectors was accomplished via a yeast recombinational cloning system using *Saccharomyces cerevisiae* strain FGSC 9721 (FY834) obtained from the Fungal Genetics Stock Center, Kansas State University (Schumacher, 2012). The deletion vectors contained about 1 kb of the 5′ flank and 3′ flank of the respective target gene that were amplified with 5F/5R and 3F/3R primers, respectively (**Supplementary Table S1**). The hygromycin resistance cassette was amplified from pSCN44 as template with the primer pair Hph-F/Hph-R. The cassette consists of the hygromycin B phosphotransferase gene (*hph*) and the *trpC* promoter from *Aspergillus nidulans* (Staben et al., 1989). The resistance cassette, the shuttle vector pRS426 (Christianson et al., 1992) and the 5′ and 3′ flanks were cloned into FY834 creating vectors pΔ*Fm_IL1* and pΔ*Fm_tI*. For deletion of *IPTLOG1* in the Δ*Fm_tI* background, a nourseothricin resistance gene driven by the *oliC* promoter from *A. nidulans* was used. To overexpress (OE) *IPTLOG1* and *IPTLOG2* in *F. mangiferae*, the respective genes were amplified by PCR from *F. mangiferae*

TABLE 1 | Strains of *Fusarium* species used to infect maize seedlings in the current study and their ability to produce phytohormones in axenic culture.

Strain	Overexpressed genes	Abbreviation	Phytohormone production		
			GA	IAA	CK
F. proliferatum ET1	–	*Fp_E*	+	+	+
F. proliferatum NRRL62905	–	*Fp_N*	LOD	+	+
F. verticillioides M-3125	–	*Fv*	LOD	+	+
F. fujikuroi IMI58289	–	*Ff*	+++	+	+
F. mangiferae MRC7560	–	*Fm*	LOD	+	+
F. proliferatum ET1	*FpIAAH*, *FpIAAM*	*Fp_E_IAA*	ND	+++	+
F. verticillioides M-3125	*FpIAAH*, *FpIAAM*	*Fv_IAA*	ND	+++	+
F. fujikuroi IMI58289	*FpIAAH*, *FpIAAM*	*Ff_IAA*	ND	+++	++
F. mangiferae MRC7560	*FpIAAH*, *FpIAAM*	*Fm_IAA*	ND	+++	+
F. proliferatum ET1	*FfIPTLOG1*	*Fp_E_IL1*	ND	ND	+++
F. proliferatum ET1	*FfIPTLOG2*	*Fp_E_IL2*	ND	ND	+++
F. proliferatum ET1	*FfIPTLOG1*, *FfP450-1*	*Fp_E_IL1P1*	ND	ND	+++
F. proliferatum ET1	*FfIPTLOG2*, *FfP450-2*	*Fp_E_IL2P2*	ND	ND	+++
F. verticillioides M-3125	*FfIPTLOG1*	*Fv_IL1*	ND	+	+++
F. verticillioides M-3125	*FfIPTLOG2*	*Fv_IL2*	ND	ND	+++
F. verticillioides M-3125	*FfIPTLOG1*, *FfP450-1*	*Fv_IL1P1*	ND	ND	+++
F. verticillioides M-3125	*FfIPTLOG2*, *FfP450-2*	*Fv_IL2P2*	ND	+	+++
F. fujikuroi IMI58289	*FfIPTLOG1*	*Ff_IL1*	ND	ND	+++
F. fujikuroi IMI58289	*FfIPTLOG2*	*Ff_IL2*	ND	ND	+++
F. fujikuroi IMI58289	*FfIPTLOG1*, *FfP450-1*	*Ff_IL1P1*	ND	ND	+++
F. fujikuroi IMI58289	*FfIPTLOG2*, *FfP450-2*	*Ff_IL2P2*	ND	ND	+++
F. mangiferae MRC7560	*FfIPTLOG1*	*Fm_IL1*	ND	ND	+
F. mangiferae MRC7560	*FfIPTLOG2*	*Fm_IL2*	ND	ND	+
F. mangiferae MRC7560	*FfIPTLOG1*, *FfP450-1*	*Fm_IL1P1*	ND	ND	+++
F. mangiferae MRC7560	*FfIPTLOG2*, *FfP450-2*	*Fm_IL2P2*	ND	ND	++

The number of + characters indicate the levels of hormone detected compared to the respective parent or WT strain; LOD, below the limit of detection; ND, not determined.

genomic DNA. The amplified genes together with a *Not*I and *Nco*I restricted plasmid pNAN-OGG (Schumacher, 2012), containing a hygromycin resistance cassette, were transformed into FY834 creating vectors pOE:*FmIL1* and pOE:*FmIL2*. The PCR derived fragments were verified by sequence analysis using the BigDye® Terminator v3.1 cycle sequencing kit and the ABI Prism® 3730 Genetic Analyzed (Applied Biosystems, Foster City, CA, United States).

Transformation of *Fusarium* spp. was carried out according to Wiemann et al. (2013). Regeneration of transformed protoplasts was performed over 4–5 days at 28°C in regeneration medium (0.7M sucrose, 0.05% yeast extract) containing either 100 $\mu g.mL^{-1}$ nourseothricin (Werner-Bioagents, Germany) or 100 $\mu g.mL^{-1}$ hygromycin (Calbiochem, Germany). Transformants were purified by single spore isolation to homokaryons. Vector integration events were confirmed by diagnostic PCR using appropriate primers (**Supplementary Table S1**). For this work, the following *F. mangiferae* mutants were generated: Δ*Fm_IL1* (deletion of *IPTLOG1*), Δ*Fm_tl* (deletion of *tRNA-IPT*), ΔΔ*Fm_IL1/tl* (deletion of both *IPTLOG1* and *tRNA-IPT*), *Fm_FmIL1* (over-expression of Fm*IPTLOG1*), *Fm_FmIL2* (over-expression of Fm*IPTLOG2*) and *Fm_FjIL1* (over-expression of Ff*IPTLOG1*).

Fungal Cultivation Methods

Conidial inoculum of each *Fusarium* strain, used for maize seedling infections in the hydroponic system, were prepared from 7-day-old potato dextrose agar plates, cultivated at 28°C. Spores were mechanically dislodged with a loop in 10 mL of sterile water, filtered and the spore concentration was determined using a Bürker counting chamber. Conidial inoculum for the maize seedling assay in soil were prepared by growing *Fusarium* strains for 3 days in mung bean medium at 28°C (Bai and Shaner, 1996).

For CK quantification, *F. mangiferae* strains were first cultivated for 3 days in 300-mL Erlenmeyer flasks with 100 mL Darken medium (Darken et al., 1959) on a rotary shaker at 180 rpm at 28°C; 500 μL of this culture was then used to inoculate 100 mL of ICI (Imperial Chemical Industries, United Kingdom) media (Geissman et al., 1966) containing 60 mM glutamine as a nitrogen source and 40 g per L of glucose. Growth proceeded for 7 days on a rotary shaker at 28°C in the dark. The culture filtrates were harvested and lyophilized prior to analysis.

Plant Material

Hybrid white sweet maize variety Silver Queen (Johnnyseeds, United States) was used for all maize related experiments. Roots and shoots of infected maize seedlings were separated and lyophilized before hormone profiling and gene expression analysis. Infected mango material was obtained from a 25-year-old heavily infected mango malformation diseased orchard (cv. Keitt) located in northern Israel, close to Kibbutz Ma'agan (320 42' 23" N; 36' 31" E). Healthy mango material was obtained from 3-year-old trees (cv. Keitt) cultivated in a nursery located in the Volcani Center, Bet Dagan, Israel. The various sampled tissues were as follows: diseased malformed and healthy inflorescence tissue (young panicles, 1-month after development), diseased malformed and healthy inflorescence tissue (mature panicles, 2- to 3-month after development), swollen and healthy buds (1-month before bud break). Immediately after sampling, floral and bud material was frozen in liquid nitrogen and lyophilized.

Virulence Assays

Maize Seedling Assay in Soil

Maize seeds were sterilized by soaking in 0.82% sodium hypochlorite for 1 min and then rinsed twice in sterile water for 1 min. The seeds were inoculated by soaking for 2 days in 30 mL of mung bean medium cultures of individual *Fusarium* strains. Ten seeds were sown in a water-saturated soil mixture, consisting of sphagnum peat moss, vermiculite and dolomite lime (Sunshine Redi-Earth Professional Growing Mix), in a 10-cm^2 plastic pot to a depth of 1 cm. The pots were incubated in a growth chamber with a light dark cycle consisting of 14 h light at 30°C and 10 h dark at 20°C.

Disease severity was assessed as follows: (i) at 7 days after sowing, percent germination was determined by counting the number of seedlings per 10 seeds sown in each pot; (ii) at 20 days after sowing, seedling height was determined by measuring the height of each seedling from the soil line to the top of the longest leaf; and (iii) seedling weight was determined as fresh weight by cutting a seedling at the soil line. The resulting data were subjected to analysis of variance (ANOVA), and statistically significant differences between means were determined by a least squares means test using a Bonferroni adjustment. These analyses were done using SAS Statistical Software (SAS Institute Inc.).

Maize Seedling Assay in Hydroponic System

Maize seeds were sterilized by first soaking in 4% sodium hypochlorite for 10 min, rinsed twice with sterile water, and then soaking in 70% ethanol for 1 min and rinsed twice with sterile water. Seeds were inoculated by soaking in water containing 10^6 *Fusarium* spores per mL in a flask on a rotary shaker overnight (120 rpm). Inoculated seeds were dried for 2 h and placed in a petri dish with moistened filter paper to germinate in the dark at 26°C. After 2 days, germinated seeds were moved into a hydroponic system consisting of plastic boxes with Hoagland solution. Seedlings were incubated in a growth chamber with a light/dark cycle (16 h/8 h) at the constant temperature of 25°C.

Plant Hormone Extraction and Quantification

Control and infected maize seedling shoots and roots were analyzed for GAs using the method described by Urbanová et al. (2013) with minor modifications. Briefly, approximately 10 mg of lyophilized tissue were ground to a powder using 3-mm zirconium oxide beads and extracted overnight at 4°C with 1 mL of ice-cold 80% acetonitrile containing 5% formic acid. Seventeen internal GAs standards ($[^2H_2]GA_1$, $[^2H_2]GA_3$, $[^2H_2]GA_4$, $[^2H_2]GA_5$, $[^2H_2]GA_6$, $[^2H_2]GA_7$, $[^2H_2]GA_8$, $[^2H_2]GA_9$, $[^2H_2]GA_{15}$, $[^2H_2]GA_{19}$, $[^2H_2]GA_{20}$, $[^2H_2]GA_{24}$,

$[^2H_2]GA_{29}$, $[^2H_2]GA_{34}$, $[^2H_2]GA_{44}$, $[^2H_2]GA_{51}$ and $[^2H_2]GA_{53}$; purchased from professor Lewis Mander, Australia) were added to each sample. The homogenates were centrifuged at 19,000 rpm at 4°C for 10 min, and the resulting supernatants were passed through an ion exchange SPE cartridges (Waters) prior to analysis by high pressure-liquid chromatography-tandem mass spectrometry (Micromass). GAs were detected using multiple-reaction monitoring mode of the transition of the ion $[M–H]^-$ to the appropriate product ion. The Masslynx 4.1 software (Waters) was used to quantify the GAs levels by the standard isotope dilution method (Rittenberg and Foster, 1940).

Levels of the auxin IAA and IAA metabolites were determined in the maize seedling shoots and roots using the method described by Novák et al. (2012). Briefly, approximately 5 mg of lyophilized tissue was extracted with 1 mL cold phosphate buffer (50 mM; pH 7.0) containing 0.1% sodium diethyldithiocarbamate, supplemented with internal standards. After centrifugation at 20,000 rpm for 10 min, one half of each sample was acidified with 1 M HCl to pH 2.7 and subjected to solid phase extraction using an Oasis^{TM} HLB column (Waters). For quantification of indole-3-pyruvic acid, the second half of the sample was derivatized with cysteamine (0.25 M, pH 8.0) for 1 h, acidified with 3 M HCl to pH 2.7 and purified by solid phase extraction. After evaporation under reduced pressure, samples were analyzed for auxin content by Acquity UPLC^{TM} linked to Xevo TQ MSTM (Waters).

Levels of CKs were determined in the maize seedling shoots and roots essentially as described by Hinsch et al. (2015) using a high-pressure liquid chromatography (Acquity UPLC^{TM}; Waters) coupled to a triple quadrupole mass detector (Xevo TQ MSTM; Waters) equipped with an electro-spray interface. To check CK recovery and to validate peak identity, isotope-labeled CK internal standards (OlChemIm, Czechia) were added, each at 1 pmol, to samples prior to extraction. Levels of CKs were determined in lyophilized culture filtrates of *F. mangiferae* without addition of internal standards. Filtrates were purified on immuno-affinity columns (OlchemIm) after pre-purification on Speed SPE Octadecyl C18 cartridges (Applied Separation) and Oasis MCX cartridges (Waters) as described by Hinsch et al. (2016). CKs were quantified after separation on a C18 reverse-phase column (ZORBAX RRHD Eclipse Plus 1.8 μm, 2.1 × 150 mm, Agilent) coupled to the Ultra performance liquid chromatography (Shimadzu Nexera).

Cytokinin dehydrogenase (CKX) activity was measured in extracts of lyophilized and powdered maize seedling shoots and roots extracted with 20-fold excess (w/v) of 0.2M Tris/HCl, pH 8.0, 0.3% Triton-X. The CKX activity was determined spectrophotometrically with 0.5 mM dichlorophenolindophenol as an electron acceptor and 0.25 mM isopentenyladenine as a substrate (Frébort et al., 2002). All measurements were performed in four biological replicates. The protein content was estimated by the method of Bradford (1976) with bovine serum albumin as a standard.

All results are presented as mean value ± standard deviation from at least three independent biological replicates; statistical significance of results was revealed by Student's unpaired *t*-tests or ANOVA at $p \leq 0.05$ (Statistica 13.3, TIBCO Software Inc.).

Gene Expression Profiling by Quantitative Real-Time PCR (qPCR)

Total RNA was isolated from roots and shoots of maize seedlings grown in a hydroponic system and infected by wild-type strains of *F. mangiferae, F. verticillioides* and *F. fujikuroi*. Each treatment was analyzed in three independent biological replicates; each biological replicate was represented by the shoots or roots of five maize seedlings. Approximately 100 mg of tissue for each independent biological replica ($n = 3$) was ground in liquid nitrogen and RNA was extracted and purified with the RNAqueous kit (Thermo Fisher Scientific). The RNA was treated with DNAse (TURBO DNA-free kit; Thermo Fisher Scientific) and cDNA was obtained using a RevertAid First Strand cDNA Synthesis Kit (Thermo Fisher Scientific) from 2 μg of total RNA as the template, according to the manufacturer's instructions. qPCR was performed using TaqMan Gene Expression Master Mix (Thermo Fisher Scientific) in a Viia7^{TM} Real-Time PCR System (Thermo Fisher Scientific). For both fungal and maize genes, primers and TaqMan probes were designed with Primer Express 3.0 software (Thermo Fisher Scientific, **Supplementary Table S1**). The maize target genes used here were identified in a previous study (Vyroubalová et al., 2009). For each condition, the three independent biological replicates were analyzed in three technical replicates. Expression of fungal genes was measured by absolute quantification, whereas maize gene expression was obtained by relative quantification according to ΔΔCt method (Schmittgen and Livak, 2008). To ensure that primers amplified the desired gene target, amplicons for every primer pair were cloned into the pDRIVE vector (Qiagen) and sequenced. The cloned PCR products were also used as template to determine PCR efficiency and absolute levels of gene transcript in isolated RNA. The relative expression of the maize genes were normalized with respect to β-actin (BT086225) and elongation factor 1 (AF136829.1) gene expression. Expression values were determined and statistically evaluated with DataAssist v3.0 Software (Thermo Fisher Scientific).

RESULTS

We previously demonstrated that *F. proliferatum* strain ET1 (isolated from the roots of an epiphytic orchid), *F. fujikuroi* (a pathogen of rice) and *F. mangiferae* (a pathogen of mango) are able to penetrate and invade maize seedlings and to cause blight disease symptoms similar to *F. verticillioides* and *F. proliferatum* strain NRRL 62905, two pathogens of maize (Niehaus et al., 2016). Here, we found that *F. mangiferae* also can cause seedling disease by affecting the growth of maize primary roots and overall root system development (**Figure 1**). In the current study, we examined the hormonal status in maize plant tissues infected by the following *Fusarium*: *F. verticillioides*, *F. proliferatum* strain NRRL 62905, *F. proliferatum* strain ET1, *F. fujikuroi* and *F. mangiferae*, as well as auxin/CK accumulating or deficient mutant strains derived thereof. All of the strains were able to synthesize CK in axenic culture while mutants overexpression *IPTLOG1* and *P450-1* accumulated more (**Table 1**). *F. proliferatum* ET1, *F. verticillioides*, *F. fujikuroi*

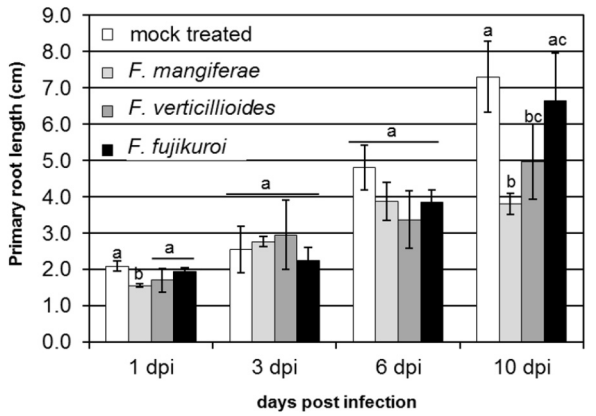

FIGURE 1 | Effect of infection by *F. verticillioides*, *F. mangiferae* and *F. fujikuroi* on the length of primary root of maize seedlings. Hydroponic growth of seedlings for 10 days. Average value of 20 infected seedlings with standard deviations is presented. Bars indicated by the same letter are not statistically significantly different (ANOVA; $p \leq 0.1$).

and *F. mangiferae* strains expressing *IAAH* and *IAAM* from *F. proliferatum* synthesized more IAA than wild-type (**Table 1**). Some GAs were detected in *F. proliferatum* while significantly more was detected in *F. fujikuroi* axenic cultures (**Table 1**).

Infection by *Fusarium* Induced Changes in Gibberellins (GAs) Status in Maize Seedlings

Gibberellin content was measured in infected roots and shoots 10 days post inoculation (dpi) as active forms (GA_1, GA_3, GA_4, GA_5, GA_7, GA_{13}), precursors (GA_9, GA_{12}, GA_{15}, GA_{19}, GA_{20}, GA_{24}, GA_{44}, and GA_{53}) and deactivation products (GA_8, GA_{29}, GA_{34}, and GA_{51}) (referred to as GA turnover) (**Table 2**). 13-Hydroxylated (GA_1, GA_3, GA_5) and 13-non-hydroxylated (GA_4, GA_7, GA_{13}) active forms, precursors, and deactivation products were also measured (**Supplementary Table S2**).

In the roots of maize seedlings infected by *F. verticillioides* and *F. proliferatum* NRRL62905, a slight decrease or no change in active GAs was observed. This, coupled with an increase in GA precursor and deactivated product, suggest a tight regulation of GA status in the roots upon infection. In contrast, a marginal to significant increase in active GAs was observed in the root of maize infected by *F. mangiferae* (3-fold), *F. proliferatum* ET1 (1.9-fold) and *F. fujikuroi* (52-fold) (**Table 2**). The accumulation of active GAs was consistent with the accumulation of GA precursors, notably the 13-non-hydroxylated GA_9 and GA_{12}, observed in the maize roots infected by all of the *Fusarium* species (**Supplementary Table S2**). Because these three species also produce significant GAs in axenic culture, the increased GAs we detected in infected plants might reflect a failure in the ability of the plant to maintain root GA homeostasis upon infection.

The amount of GAs detected in shoots of mock-treated maize seedlings was similar to the amount detected in roots. Active GAs accumulated significantly more in the shoots of maize seedlings whose roots were infected only by *F. proliferatum* NRRL 62905 (native maize pathogen) and *F. fujikuroi*. In contrast to roots, active GA accumulation in the shoots appeared related to an accumulation of GA_{12} (13-non-hydroxylated) and GA_{53} (13-hydroxylated). Also GA_9 levels in infected shoots were twofold to fourfold lower than those found in the non-infected shoots. Taken together, these results suggest that the root-to-shoot translocation of maize-generated GAs was reduced during the infection process, or that the biosynthesis or origin of shoot GAs is via a different mechanism (**Supplementary Table S2**). Interestingly the infection by *F. verticillioides*, the other native maize pathogen, led to a decrease in active GAs in both roots and shoots of infected seedlings, suggesting that success of infection of maize by *F. verticillioides* might be independent of GAs, at least 10 days post inoculation.

Infection by *Fusarium* Induced Changes in Auxin (IAA) Status in Maize Seedlings

The levels of auxin IAA, its precursors and deactivation products were analyzed in the roots of maize seedlings 10 days

TABLE 2 | Quantification of gibberellins (GAs) in maize seedlings grown in soil and infected by different *Fusarium* strains (10 dpi).

	Mock-treated	*Fp_N*	*Fp_E*	*Fm*	*Ff*	*Fv*
			Roots of infected plants			
Active GAs	26.8 ± 1.1	25.5 ± 3.4	75.3 ± 22.2*	36.2 ± 1.9*	11776 ± 665.6*	20.5 ± 1.3*
Precursors	367.0 ± 81.1	619.7 ± 72.4*	843.2 ± 100.5*	928.2 ± 59.7*	1159.6 ± 59.2*	492.5 ± 35.2*
Turnover	233.4 ± 40.2	373.1 ± 14.6*	437.4 ± 28.0*	726.8 ± 81.2*	12134.0 ± 649.7*	209.8 ± 9.8
			Shoots of infected plants			
Active GAs	27.4 ± 0.4	71.4 ± 7.7*	35.2 ± 9.5*	30.1 ± 2.4	325.2 ± 33.2*	15.7 ± 1.5*
Precursors	636.1 ± 61.4	625.7 ± 75.9	484.9 ± 56.1*	530.8 ± 45.2	634.7 ± 86.7	339.9 ± 27.0*
Turnover	180.0 ± 21.5	304.4 ± 20.5*	143.5 ± 26.6*	108.9 ± 7.4*	552.2 ± 67.6*	194.0 ± 2.0

*Mean values with standard deviations obtained from four to six biological replicates (independent seedlings) are presented; * indicates significant differences between mock and Fusarium-infected tissue according to Student's unpaired t-tests at $p \leq 0.05$ ($n = 4$–6). Concentrations of phytohormones are in pmol per g dry weight plant material. Active GAs: sum of active GAs (GA_1, GA_3, GA_4, GA_5, GA_7, GA_{13}); precursors: sum of GA precursors (GA_9, GA_{12}, GA_{15}, GA_{19}, GA_{20}, GA_{24}, GA_{44}, and GA_{53}); turnover: sum of deactivated GAs (GA8, GA29, GA34, and GA51); Fp_N, F. proliferatum NRRL62905; Fp_E, F. proliferatum ET1; Fm, F. mangiferae; Ff, F. fujikuroi; Fv, F. verticillioides.*

TABLE 3 | Quantification of auxin (IAA) in the roots of maize seedlings grown in soil and infected by different *Fusarium* strains (10 dpi).

	Mock-treated	*Fv*	*Fp*_N	*Fp*_E	*Fm*	*Ff*	*Fp*_E_IAA	*Ff*_IAA
Active IAA	590 ± 106	1501 ± 958	1004 ± 421	1520 ± 618	3723 ± 848*	473 ± 88	21234 ± 19574	57402 ± 24206*
Total precursors	6782 ± 2041	7435 ± 707	6188 ± 2595	10820 ± 3955	13158 ± 4700*	4784 ± 3508	35152 ± 16119*	77237 ± 34802*
Storage (IAA-Glc)	4833 ± 1603	261 ± 33*	593 ± 0	574 ± 37*	239 ± 68*	888 ± 126*	n.d.	n.d.
Total turnover	11267 ± 2582	9136 ± 2220	6799 ± 1304*	7047 ± 766*	9734 ± 1526*	5093 ± 876*	32401 ± 25657	75963 ± 20478*

*Mean values with standard deviations obtained from three biological replicates (independent seedlings) are presented; * indicates significant differences between mock-treated and Fusarium-infected tissue according to Student's unpaired t-tests at $p \leq 0.05$ ($n = 3$). Concentrations of phytohormones are in pmol per g dry weight plant material. Fv, F. verticillioides; Fp_N, F. proliferatum NRRL62905; Fp_E, F. proliferatum ET1; Fm, F. mangiferae; Ff, F. fujikuroi; Fp_E_IAA, Fp_E strain overexpressing IAAM and IAAH genes; Ff_IAA, F.f strain overexpressing IAAM and IAAH genes; IAA, indole-3-acetic acid; IAA-Glc, IAA-glucose; n.d., not determined.*

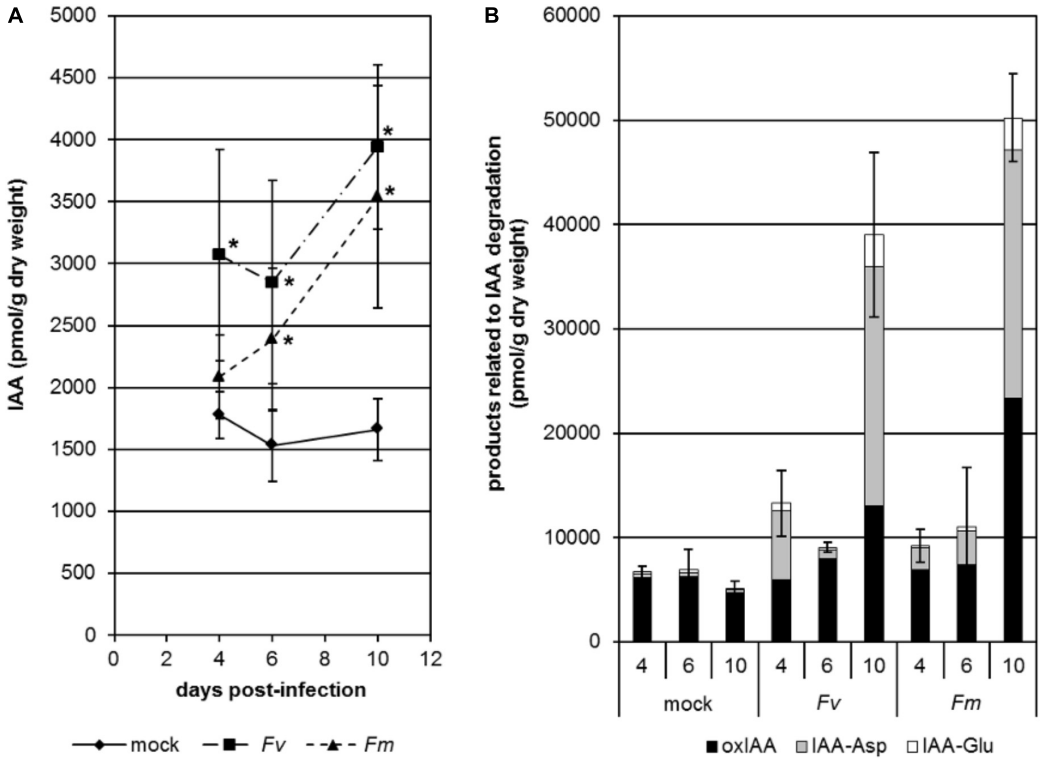

FIGURE 2 | Changes in free active IAA **(A)** and products related to IAA degradation **(B)** in the roots of maize seedlings infected by *F. verticillioides* (*Fv*) and *F. mangiferae* (*Fm*). The analysis was performed after 4, 6, and 10 days of hydroponic growth post inoculation (dpi). Graphs represent the mean value of three independent biological replicates; bars represent the standard error. * indicates significant differences between mock and *Fusarium*-infected tissue according to Student's unpaired *t*-tests at $p \leq 0.05$ ($n = 3$). IAA, indole-3-acetic acid; oxIAA, 2-oxindole-3-acetic acid; IAA-Asp, IAA-aspartate; IAA-Glu, IAA-glutamate.

after infection with different *Fusarium* species (**Table 3** and **Supplementary Table S3**). Infection by any of the fusaria (except *F. fujikuroi*) seemingly induced the accumulation of free IAA although only significant for *F. mangiferae* (**Table 3**). The amount of IAA-glucose, a storage form of IAA, was significantly reduced in the infected roots of maize seedlings in four of the five fusaria. It is possible that the accumulation of free IAA resulted from the release of IAA from the glucose-conjugate. No significant difference in IAA precursor content could be observed between mock-treated roots and infected roots. Overall, infection led to an accumulation of compounds related to IAA degradation, especially IAA-Asp which may be indicative of IAA turnover needed to maintain basal endogenous IAA levels (**Supplementary Table S3**). Albeit not significant, we did note an increase in the indole-3-pyruvic acid (IPyA), an IAA precursor of the YUCCA pathway, in tissue infected with *F. mangiferae*, suggesting the activation of this pathway in either the plant or fungus. No significant difference in the pool of auxin and auxin derivatives between the mock-treated and infected seedlings was noted, except for *F. mangiferae* (**Supplementary Table S3**) which suggests that most *Fusarium* strains did not secrete substantial amounts of auxins into the plant tissue and that the auxins that were detected were likely of plant origin.

In order to study the dynamics of IAA changes during infection by *Fusarium*, we analyzed the content of free IAA and products related to IAA degradation in the roots of maize seedlings infected with *F. verticillioides* or *F. mangiferae* grown hydroponically (**Figure 2**). In both cases, we saw an accumulation

TABLE 4 | Quantification of maize cytokinins and CKX activity in seedlings grown in soil and infected by different *Fusarium* strains (10 dpi).

	Mock-treated	*Fv*	*Fp_N*	*Fp_E*	*Fm*	*Ff*	*Ff_IL2P2*
				Roots of infected plants			
Total iP	319.6 ± 36.1	414.2 ± 27.3*	328.7 ± 72.6	239.4 ± 68.8	655.0 ± 160.8*	317.4 ± 55.6	1038.7 ± 318.5*
Total *t*Z	215.1 ± 28.2	303.3 ± 55.8	189.0 ± 46.3	171.4 ± 52.8	1017.7 ± 275.7*	209.6 ± 62.7	4276.9 ± 196.7*
Total *c*Z	5276.2 ± 783.5	6241.8 ± 1188.6	5976.7 ± 1215.2	5424.1 ± 765.6	7730.9 ± 1555.8	5425.0 ± 332.4	6738.4 ± 934.7
Total DHZ	35.8 ± 2.5	58.0 ± 4.4*	35.4 ± 9.5	41.5 ± 11.2	571.6 ± 89.1*	32.9 ± 9.1	1527.0 ± 340.6*
Total CKs	5846.7 ± 735.7	7017.3 ± 1120.4	6288.0 ± 1177.6	5876.4 ± 887.2	9975.2 ± 1658.9*	5984.8 ± 438.8	13581.1 ± 711.3*
CKX activity	0.54 ± 0.32	1.37 ± 0.57	1.60 ± 0.65	0.99 ± 0.42	147 ± 50*	1.39 ± 0.55	16.3 ± 8.32*
				Shoots of infected plants			
Total iP	31.8 ± 7.7	56.7 ± 15.9	167.0 ± 50.1*	112.0 ± 28.4*	176.8 ± 30.9*	151.6 ± 41.7*	n.d.
Total *t*Z	17.2 ± 1.6	29.7 ± 5.1*	16.2 ± 0.2	20.6 ± 0.2	555.6 ± 105.7*	21.4 ± 5.6	n.d.
Total *c*Z	5031.0 ± 980.8	3482.1 ± 103.4*	4303.4 ± 227.3	4214.4 ± 578.8	9110.9 ± 1034.7*	2327.1 ± 293.0*	n.d.
Total DHZ	39.3 ± 10.2	17.4 ± 1.7*	32.3 ± 7.7	49.1 ± 5.8	2721.5 ± 630.1*	45.3 ± 9.0	n.d.
Total CKs	5119.2 ± 972.6	3559.6 ± 95.3*	4518.9 ± 199.3	4396.2 ± 555.7	12564.7 ± 486.7*	2545.5 ± 339.0*	n.d.
CKX activity	0.21 ± 0.10	4.11 ± 2.34*	0.52 ± 0.33	0.93 ± 0.45	12.3 ± 7.86*	0.87 ± 0.36	n.d.

*Mean values with standard deviations obtained from three biological replicates (independent seedlings) are presented; * indicates significant differences between mock and Fusarium-infected tissue according to Student's unpaired t-tests at $p \leq 0.05$ ($n = 3$). Concentrations of phytohormones are in pmol per g dry weight plant material. The cytokinin oxidase/dehydrogenase (CKX) activity is expressed as pkat per mg of extracted proteins; iP, isopentenyladenine; tZ, trans-zeatin; cZ, cis-zeatin; DHZ, dihydro-zeatin; Fp_N, F. proliferatum NRRL62905; Fp_E, F. proliferatum ET1; Fm, F. mangiferae; Ff, F. fujikuroi; Fv, F. verticillioides; Ff_IAA, F. fujikuroi overexpressing IAAM and IAAH genes; Ff_IL2P2, F. fujikuroi overexpressing IPTLOG2 and P450-2 genes; ND, not determined.*

of free IAA in the roots as soon as 4 dpi (**Figure 2A**). At the end of the experiment, i.e., at 10 dpi, free IAA was significantly increased more than twofold in fungal infected seedlings. Accumulation of compounds related to IAA turnover was also observed during infection. This was particularly significant at 10 dpi with IAA-Asp contributing to the greatest extent (**Figure 2B**).

Infection by *Fusarium* Affects CK Status in Maize Seedlings

The four plant CKs were extracted and quantified from roots and shoots of maize seedlings infected with different *Fusarium* species grown in soil for 10 days (**Table 4** and **Supplementary Table S4**). Infection by both *F. proliferatum* species did not significantly modify the overall CK levels while infection by *F. verticillioides* and *F. fujikuroi* led to a modest decrease in CK levels (1.4- and 2.2-fold, respectively) in shoots only. In contrast, infection by *F. mangiferae* led to a modest increase in CK levels (1.4-fold) in shoots only. We did note that the predominant CK present in the seedlings was *c*Z which accounted for most of the overall change in total CKs observed (**Table 4** and **Supplementary Table S4**). The overall increase in free active CK correlated with a concomitant increase in CK precursors and glucoside derivatives suggesting that mechanisms exist to adjust levels of endogenous CKs within the plant due to changing growth conditions (**Supplementary Table S4**). The most significant increases observed were for tissues infected with *F. mangiferae* which contained significantly more CKs of all types, except for *c*Z derivatives. In roots, the amount of the two major active CKs, iP and *t*Z, were 4- and 53-fold higher, respectively; in the shoots, iP and *t*Z was 5- and 11-fold higher than observed in mock-treated plants, respectively (**Supplementary Table S4**). Infection by *F. fujikuroi* did not affect CK status in the roots. Our observation that maize seedlings infected with *F. fujikuroi* overexpressing CK biosynthetic genes *FfIPTLOG2* and *FfP450-2* (*Ff_IL2P2*) accumulated even more iP, *t*Z and DHZ suggest that the fungi were able to produce CKs *in planta* (**Table 4** and **Supplementary Table S4**).

Cytokinin levels *in planta* are regulated *inter alia* by irreversible degradation by cytokinin oxidase/dehydrogenase (CKX). Therefore, we measured CKX activity in the roots and shoots of maize seedlings infected by the different *Fusarium*. CKX activity was most strongly stimulated in the roots and shoots infected with *F. mangiferae* and the CK-overproducing strain *Fj_IL2P2*. A small but significant increase in CKX activity was also observed in the shoots, but not roots, infected by *F. verticillioides* which was consistent with an overall decrease in CK content compared to shoots of mock-treated seedlings (**Table 4**). Taken together, these data suggest that the regulation of CK levels upon infection by *Fusarium* involves production and glucosylation as well as degradation by CKX.

We also determined CK levels in maize seedlings grown hydroponically during infection by *F. verticillioides* and *F. mangiferae* at 4, 6, and 10 dpi (**Figure 3**). An increase in total CK content was observed in the roots of mock-treated seedlings over the time course indicating that CKs naturally accumulate during development (**Figure 3A**). The same trend was observed for roots of seedlings infected by both *Fusarium*. The observation that roots infected by *F. mangiferae* accumulated significantly more CKs than the non-infected roots suggest that this fungus either induced additional plant CK synthesis, or produced CKs itself which then accumulated in the roots. The same observation was noted during the interaction between *F. mangiferae* and mango, its natural host (**Supplementary Table S5**). In contrast, the overall CK content was lower in shoots of maize seedlings infected by fusaria than in the roots. No significant change in

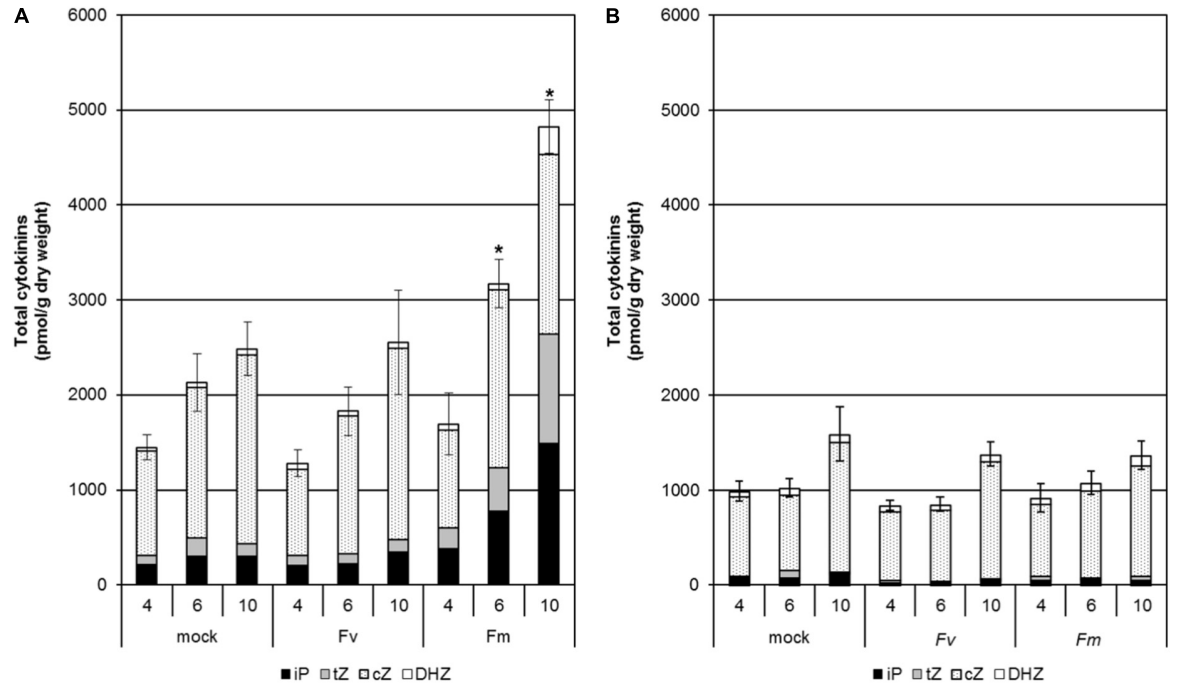

FIGURE 3 | Changes in content of the different active CKs in the roots **(A)** and shoots **(B)** of maize seedlings infected with *F. verticillioides* and *F. mangiferae*. The analysis was performed at 4, 6, and 10 days of hydroponic growth post inoculation (dpi). Graphs represent the mean value of three independent biological replicates, each containing a pool of five seedlings; bars represent the standard error. * indicates significant differences between mock and *Fusarium*-infected tissue according to Student's unpaired *t*-tests at $p \leq 0.05$ ($n = 3$). Concentrations of hormones are in pmol per g dry weight. The sums of all isopentenyladenine (iP), *trans*-zeatin (*tZ*), *cis*-zeatin (*cZ*) and dihydrozeatin (DHZ) type cytokinins are presented.

CK content was observed during the time-course, either upon infection by *F. verticillioides* or *F. mangiferae* (**Figure 3B**).

Expression of Fungal and Plant Genes Involved in CK Metabolism During *Fusarium*–Maize Interaction

To study the origin of CK accumulation in *F. mangiferae*-infected maize *tissues*, the expression of fungal genes encoding enzymes involved in CK synthesis (*IPTLOG1* and *IPTLOG2*), as well as maize genes encoding enzymes involved in CK metabolism (*IPT* and *CKX*) were examined over 10 days post inoculation by qPCR (**Tables 5**, **6**). Total RNA was extracted from roots and shoots of seedlings infected by *F. mangiferae*, *F. verticillioides* and *F. fujikuroi*. The abundance of fungal transcripts coding for ubiquitin (*FmUBI*) and actin (*FvACT* and *FfACT*), two common housekeeping genes, served to follow the growth of the fungi (**Table 5**). The increase in transcripts in infected roots observed over time strongly indicate that all three fungi were able to colonize the plant roots and thrive. Fungal gene transcripts were detected in the shoots of maize only at 4 dpi and later. Of the fungal CK synthesis genes, *IPTLOG2* transcripts were much more readily and consistently present in roots infected with all three fungi (**Table 5**). While transcript for *FmIPTLOG2* increased steadily with a maximum at 10 dpi, transcripts for *FvIPTLOG2* peaked at 6 dpi, fourfold higher than *FmIPTLOG2* at 10 dpi. In contrast, expression of *FfIPTLOG2* was low at 3–4 dpi and decreased significantly out to 10 dpi. In shoots, fungal *IPTLOG2* transcripts were detectable only after infection by *F. verticillioides* (**Table 5**).

Analysis of expression of seven maize *IPTs* (*ZmIPT3b*, *ZmIPT4*, *ZmIPT5*, *ZmIPT6*, *ZmIPT7*, *ZmIPT8* and *ZmIPT9*) potentially involved in CK metabolism in seedling roots or shoots was investigated (**Table 6**). In roots, transcripts for all seven *IPT*s were detected. At almost every time point after 1 dpi, transcripts for multiple IPTs accumulated significantly more in infected roots compared to uninfected roots (**Table 6**). By far, *ZmIPT7* transcripts accumulated the most at 10 dpi in roots infected by all three fungi. In the shoots, transcripts for five of the seven *ZmIPT* genes were detected (**Table 6**). The most significant accumulation was observed in seedlings infected by *F. mangiferae* at 6 dpi where transcripts of four *IPTs* (*ZmIPT3b*, *ZmIPT6*, *ZmIPT7* and *ZmIPT8*) were present 4.5- to 74-fold greater than mock-treated seedlings or leaves of seedlings infected by the other two *Fusarium* species. At 10 dpi, *ZmIPT* levels had decreased to levels detectable in mock-treated leaves with the exception of *ZmIPT5*. The expression of two out of five CK biosynthesis genes (*ZmIPT5* and *ZmIPT6*) were significantly elevated in leaves of seedlings infected for 10 dpi by *F. verticillioides* and to a lower extent *F. fujikuroi*.

The increase of expression maize *IPT* genes appeared to be associated with the concomitant increase in *ZmCKX1* gene expression in the roots, as well as in the shoots of seedlings infected by *Fusarium* with a peak at 3–4 dpi and 6 dpi,

TABLE 5 | Expression of fungal *IPTLOG* genes in the roots and shoots of maize seedlings infected by *F. mangiferae*, *F. verticillioides,* and *F. fujikuroi.*

In the roots of maize seedlings						
	Genes	**1 dpi**	**3 dpi**	**4 dpi**	**6 dpi**	**10 dpi**
F. mangiferae	*FmUBI*	19.1 ± 7.32	889 ± 492	2169 ± 823	2545 ± 285	7854 ± 3600
	FmIPTLOG1	n.d.	n.d.	n.d.	0.96 ± 0.57	0.35 ± 0.26
	FmIPTLOG2	n.d.	0.85 ± 0.74	17.4 ± 7.30	88.9 ± 58.6	716 ± 494
F. verticillioides	*FvACT*	7570 ± 1738	222859 ± 114805	450178 ± 157031	281578 ± 110834	232959 ± 13051
	FvIPTLOG1	n.d.	n.d.	2.86 ± 2.48	0.44 ± 0.16	n.d.
	FvIPTLOG2	n.d.	114 ± 61.3	1381 ± 599	2868 ± 1997	1121 ± 228
F. fujikuroi	*FfACT*	214 ± 108	18608 ± 10042	15222 ± 2830	57216 ± 18166	85585 ± 36355
	FfIPTLOG1	n.d.	0.47 ± 0.20	5.85 ± 2.34	n.d.	0.26 ± 0.22
	FfIPTLOG2	7.70 ± 5.25	106 ± 48.2	73.5 ± 31.6	n.d.	3.97 ± 2.09
In the shoots of maize seedlings						
	Genes	**1 dpi**	**3 dpi**	**4 dpi**	**6 dpi**	**10 dpi**
F. mangiferae	*FmUBI*	–	–	121 ± 40.8	467 ± 214	183 ± 34.1
	FmIPTLOG1	–	–	n.d.	1.10 ± 1.55	n.d.
	FmIPTLOG2	–	–	1.83 ± 1.02	n.d.	n.d.
F. verticillioides	*FvACT*	–	–	16175 ± 8006	78167 ± 36366	106034 ± 52104
	FvIPTLOG1	–	–	n.d.	2.87 ± 2.41	n.d.
	FvIPTLOG2	–	–	344 ± 485	121 ± 143	n.d.
F. fujikuroi	*FfACT*	–	–	1872 ± 920	14695 ± 8425	18350 ± 3175
	FfIPTLOG1	–	–	0.03 ± 0.05	n.d.	n.d.
	FfIPTLOG2	–	–	n.d.	n.d.	n.d.

*Quantity of IPTLOG1 and IPTLOG2 transcripts and transcripts for the house-keeping genes UBI (F. mangiferae) and ACT (F. verticillioides and F. fujikuroi) in 1ng of total RNA extracted from the root and the shoot of infected plants. Each value is mean presented with standard deviation of six biological replicates (seedlings). *Significant difference between mock and Fusarium-infected tissue according to Student's unpaired t-tests at $p \leq 0.05$. n.d., not detected; –, not analyzed.*

respectively (**Table 6**). Seedlings infected by *F. mangiferae* showed the highest *ZmCKX1* expression followed by *F. fujikuroi* and then *F. verticillioides*.

Effect of Fungal Auxin/Cytokinin Modification on the Pathogenicity of *Fusarium* in Maize Seedlings

In order to better understand the role of fungal auxin IAA and CKs in pathogenicity, we examined strains of *Fusarium* with altered IAA and CK metabolism. *F. verticillioides*, *F. proliferatum* ET1, *F. mangiferae* and *F. fujikuroi* strains over-expressing genes encoding enzymes for IAA synthesis (*IAAH* and *IAAM*) and for CK synthesis (*IPTLOG1* and *IPTLOG2*, and P450-1 and P450-2) were generated previously (Niehaus et al., 2016). For this study, we created *F. mangiferae* single and double deletion mutants of *IPTLOG1* and *tRNA-IPT*, encoding a putative tRNA-IPT critical for a tRNA-decay-based CK biosynthetic pathway (FMAN_10018). We also created *F. mangiferae IPTLOG1* and *IPTLOG2* overexpression mutants as well as a *F. mangiferae* mutant overexpressing *IPTLOG1* from *F. fujikuroi* (**Table 7**).

Initial analysis of 7-day-old cultures of the new strains indicated significant differences between the mutants and wild-type (**Table 7**). The *FmIPTLOG1* mutant presented a slight, but not significant, decrease in *t*Z-type CKs. The lack of *c*Z derivatives in the *FmtRNA-IPT* mutant indicate that the transferase encoded by this gene is responsible for most *c*Z production in *F. mangiferae*. Trace production of iP and *t*Z in this deletion mutant excluded a unique role of *FmtRNA-IPT* in CK synthesis, suggesting *de novo* CKs production is mediated by *FmIPTLOG1*, *FmIPTLOG2* or both genes. No CKs were detected in the *FmtRNA-IPT/FmIPTLOG1* double mutant indicating that *FmIPTLOG1* but not *FmIPTLOG2* was critical for CK production in *F. mangiferae*. This was supported by a significantly higher level of CK content in the *IPTLOG1* as compared to the *IPTLOG2* overexpression strain. Indeed, while the *FmIPTLOG2* overexpression strain did not differ from the WT strain, up-regulation of *FmIPTLOG1* led to significant accumulation of iP and DHZ. A similar increase in CK types was observed in the *F. mangiferae* strain overexpressing the *IPTLOG1* gene from *F. fujikuroi* indicating that *IPTLOG1* gene function was conserved in both species (**Supplementary Table S6**).

To explore whether the modification of fungal CK or IAA content can impact virulence, we examined the ability of the different IAA and CK accumulating strains to cause maize seedling blight (**Supplementary Figure S1**). Seed germination rate, seedling height and seedling weight were usually lower than uninoculated plants, after 20 days growth (**Supplementary Table S6**), except for *F. fujikuroi* infected seedlings. In almost all cases, however, such differences were not statistically significant, due likely to variability between biological replicas. Nevertheless, the results indicate that both WT and IAA/CK-gene-overexpression strains of *F. mangiferae, F. proliferatum* and *F. verticillioides* could inhibit maize seed germination

TABLE 6 | Expression of maize Zm*CKX1* and Zm*IPT* genes in the roots and shoots of seedlings infected by *F. mangiferae*, *F. verticillioides* and *F. fujikuroi.*

In the roots of maize seedlings						
	Genes	**1 dpi**	**3 dpi**	**4 dpi**	**6 dpi**	**10 dpi**
F. mangiferae	*ZmIPT5*	0.72 ± 0.23	3.34 ± 0.42*	0.97 ± 0.22	0.67 ± 0.13*	1.45 ± 0.37
	ZmIPT3b	0.88 ± 0.26	2.48 ± 0.94	1.82 ± 0.63	0.70 ± 0.13*	0.57 ± 0.04*
	ZmIPT6	1.10 ± 0.43	13.9 ± 4.43*	1.02 ± 0.05	0.56 ± 0.10*	1.66 ± 0.52
	ZmIPT8	0.84 ± 0.21	1.91 ± 0.50	0.68 ± 0.17	0.63 ± 0.15*	0.41 ± 0.13*
	ZmIPT9	1.05 ± 0.29	n.d.	0.58 ± 0.37	n.d.	0.47 ± 0.24*
	ZmIPT7	0.74 ± 0.34	0.55 ± 0.31*	0.68 ± 0.35	1.38 ± 0.41	6.24 ± 1.47*
	ZmIPT4	n.d.	3.28 ± 0.05*	0.55 ± 0.28	1.26 ± 0.45	1.21 ± 0.34
	ZmCKX1	1.08 ± 0.13	14.1 ± 5.94*	118 ± 58.2*	6.11 ± 0.81*	145 ± 85.9*
F. verticillioides	*ZmIPT5*	1.01 ± 0.34	1.78 ± 0.57	1.39 ± 0.31	0.31 ± 0.04*	2.33 ± 0.49*
	ZmIPT3b	0.72 ± 0.17	1.22 ± 0.33	1.25 ± 0.06	0.51 ± 0.10*	0.65 ± 0.10*
	ZmIPT6	1.01 ± 0.54	4.95 ± 2.36*	2.51 ± 0.51*	0.69 ± 0.23*	11.2 ± 6.87*
	ZmIPT8	1.24 ± 0.37	1.40 ± 0.40	0.95 ± 0.22	0.47 ± 0.06*	0.70 ± 0.07*
	ZmIPT9	0.92 ± 0.45	n.d.	0.43 ± 0.21*	n.d.	0.24 ± 0.16*
	ZmIPT7	1.10 ± 0.40	0.30 ± 0.22*	0.32 ± 0.18*	0.94 ± 0.10	6.51 ± 1.71*
	ZmIPT4	n.d.	0.95 ± 0.28	1.27 ± 0.58	1.56 ± 0.56	0.96 ± 0.32
	ZmCKX1	0.60 ± 0.02*	2.10 ± 0.64*	28.7 ± 12.5*	0.68 ± 0.12*	2.01 ± 0.90
F. fujikuroi	*ZmIPT5*	1.26 ± 0.21	2.16 ± 0.72	0.58 ± 0.34	2.03 ± 0.84	0.89 ± 0.41
	ZmIPT3b	0.87 ± 0.18	3.50 ± 1.49*	0.70 ± 0.29	1.77 ± 0.70	0.68 ± 0.36
	ZmIPT6	1.43 ± 0.44	5.01 ± 2.32*	0.61 ± 0.35	1.53 ± 0.69	1.68 ± 0.32
	ZmIPT8	0.89 ± 0.17	1.24 ± 0.31	0.94 ± 0.25	0.39 ± 0.29*	2.36 ± 1.09
	ZmIPT9	0.68 ± 0.39	n.d.	0.48 ± 0.24*	n.d.	n.d.
	ZmIPT7	1.13 ± 0.32	1.67 ± 0.38	0.28 ± 0.20*	1.93 ± 0.85	5.31 ± 2.41*
	ZmIPT4	n.d.	0.20 ± 0.13*	1.08 ± 0.47	n.d.	0.45 ± 0.25*
	ZmCKX1	0.74 ± 0.10*	2.59 ± 0.41*	1.10 ± 0.27	3.59 ± 1.87	2.06 ± 0.62
In the shoots of maize seedlings						
	Genes	**1 dpi**	**3 dpi**	**4 dpi**	**6 dpi**	**10 dpi**
F. mangiferae	*ZmIPT5*	–	–	0.79 ± 0.10	2.41 ± 1.05	9.98 ± 2.71*
	ZmIPT8	–	–	1.06 ± 0.32	9.81 ± 4.59*	0.65 ± 0.41
	ZmIPT3b	–	–	1.02 ± 0.57	4.53 ± 2.14*	0.64 ± 0.35
	ZmIPT6	–	–	3.20 ± 1.08*	74.1 ± 37.8*	2.63 ± 1.21
	ZmIPT7	–	–	0.22 ± 0.31	14.1 ± 6.91*	0.47 ± 0.27*
	ZmCKX1	–	–	7.84 ± 2.68*	85.6 ± 12.9*	36.7 ± 10.2*
F. verticillioides	*ZmIPT5*	–	–	0.88 ± 0.24	1.68 ± 0.63	26.8 ± 5.78*
	ZmIPT8	–	–	0.57 ± 0.14*	1.43 ± 0.85	1.46 ± 0.41
	ZmIPT3b	–	–	2.37 ± 1.04	1.06 ± 0.50	1.70 ± 0.37
	ZmIPT6	–	–	0.91 ± 0.45	12.9 ± 6.32*	18.6 ± 4.8*
	ZmIPT7	–	–	4.60 ± 2.22*	1.22 ± 0.57	0.38 ± 0.52
	ZmCKX1	–	–	24.1 ± 8.21*	17.4 ± 10.7*	13.3 ± 2.89*
F. fujikuroi	*ZmIPT5*	–	–	1.70 ± 0.75	1.39 ± 0.65	12.5 ± 3.75*
	ZmIPT8	–	–	0.98 ± 0.31	0.38 ± 0.30*	0.74 ± 0.38
	ZmIPT3b	–	–	0.97 ± 0.35	0.97 ± 0.47	1.57 ± 0.68
	ZmIPT6	–	–	2.43 ± 1.18	0.80 ± 0.62	5.70 ± 3.43
	ZmIPT7	–	–	0.62 ± 0.42	0.67 ± 0.62	0.58 ± 0.29
	ZmCKX1	–	–	1.28 ± 0.30	3.09 ± 1.08*	7.05 ± 3.58*

*Relative expression was compared to mock-treated seedlings. Mean values with standard deviations of six biological replicates are given. * indicates significant difference between mock and Fusarium-infected tissue according to Student's unpaired t-tests at $p \leq 0.05$ (n = 6).*

and reduce the height and weight of seedlings resulting from germinated seeds. The variability between biological replicas suggest that the strains were inconsistent in their ability to cause seedling-blight symptoms. The *F. verticillioides* overexpression strains were the exception in that they caused statistically significant reductions in seedling weight compared to the control treatment (**Supplementary Table S6**). The most reduced height and weight (albeit not statistically significant) was observed on

TABLE 7 | Different *F. mangiferae* mutant strains derived from MRC7560 with altered CK metabolisms and their ability to produce CKs in axenic culture.

Strain	Deletion (Δ)/overexpressed (OE) gene	Abbreviation	CK content (pmol.L^{-1} of culture filtrate)			
			iP-types	*t*Z-types	*c*Z-types	DHZ-types
F. mangiferae MRC7560	–	*Fm*	7.4 ± 6.9	17.2 ± 13.7	78.4 ± 45.0	2.45 ± 2.18
F. mangiferae MRC7560	Δ*IPTLOG1*	Δ*Fm_IL1*	5.5 ± 2.8	4.7 ± 3.3	47.8 ± 19.4	<LOD
F. mangiferae MRC7560	Δ*tRNA-IPT*	Δ*Fm_tI*	3.9 ± 2.4	10.2 ± 6.5	<LOD	<LOD
F. mangiferae MRC7560	Δ*IPTLOG1*/Δ*tRNA-IPT*	Δ Δ*Fm_IL1/tI*	<LOD	<LOD	<LOD	<LOD
F. mangiferae MRC7560	*IPTLOG1* (OE)	*Fm_FmIL1*	89.4 ± 55.3*	49.0 ± 17.2	91.6 ± 38.4	398.0 ± 32.8*
F. mangiferae MRC7560	*IPTLOG2* (OE)	*Fm_FmIL2*	11.5 ± 4.9	23.4 ± 13.8	65.7 ± 35.2	5.65 ± 2.6
F. mangiferae MRC7560	*FfIPTLOG1* (OE)	*Fm_FfIL1*	261.0 ± 12.0*	115 ± 64.9*	51.9 ± 10.9	2595.0 ± 1642.0*

*Mean values of two independent cultures are given. * indicates significant differences between WT and mutant strain according to Student's unpaired t-tests at $p \leq 0.05$ ($n = 2$). Concentrations are in pmol per 1 l of culture filtrate. iP-types, isopentenyladenine derivatives; tZ-types, trans-zeatin derivatives; cZ-types, cis-zeatin derivatives; DHZ-types, dihydrozeatin derivatives; <LOD, below the limit of detection.*

TABLE 8 | Pathogenicity test of *F. mangiferae* (MRC7560) wild type and mutants on maize seedlings grown in a hydroponic system and their ability to induce CKX activity.

Strain	Germination (%)	Shoots		Root		
		Height (cm)	Weight (g)	Length (cm)	Weight (g)	CKX activity (pkat mg^{-1})
Not infected	85 ± 22^{a}	21.8 ± 2.5^{a}	0.78 ± 0.06^{a}	7.4 ± 0.9^{a}	0.23 ± 0.01^{a}	0.82 ± 0.43^{a}
WT	69 ± 19^{ab}	18.3 ± 2.1^{b}	0.58 ± 0.04^{b}	4.8 ± 0.8^{b}	0.15 ± 0.05^{b}	47.4 ± 16.2^{b}
Δ*Fm_IL1*	65 ± 14^{ab}	19.2 ± 2.2^{b}	0.62 ± 0.03^{b}	5.4 ± 1.2^{b}	0.18 ± 0.05^{ab}	68.4 ± 12.1^{bc}
Δ*Fm_tI*	61 ± 14^{b}	19.2 ± 1.4^{b}	0.63 ± 0.02^{b}	5.3 ± 0.5^{b}	0.17 ± 0.03^{b}	53.6 ± 14.1^{b}
Δ Δ*Fm_IL1/tI*	65 ± 26^{ab}	18.3 ± 1.7^{b}	0.50 ± 0.07^{c}	4.2 ± 0.6^{b}	0.14 ± 0.03^{bc}	82.7 ± 15.3^{c}
Fm_FmIL1	63 ± 18^{ab}	14.7 ± 1.8^{c}	0.47 ± 0.08^{c}	1.9 ± 0.9^{c}	0.10 ± 0.04^{c}	159.2 ± 9.5^{d}
Fm_FmIL2	68 ± 18^{ab}	16.9 ± 1.5^{b}	0.56 ± 0.04^{b}	3.6 ± 1.0^{b}	0.14 ± 0.01^{b}	80.1 ± 7.1^{c}

Effect of deletion and overexpression of cytokinin biosynthetic genes (FmIPTLOG1, FmIPTLOG2, FmtRNA-IPT) on the ability of Fusarium mangiferae to alter seed germination, growth of the seedlings and induce CKX activity evaluated 10 days post inoculation. Values for all measurement are means with standard deviation from 40 seeds/plants grown in four independent containers. The CKX activity is expressed as pkat per mg of extracted proteins. Values within a column that are followed by the same letter are not statistically significantly different (ANOVA; $P \leq 0.1$). See ***Table 7*** *for strain gene designation.*

seedlings infected by WT strain of *F. mangiferae*, similarly to previous work (Niehaus et al., 2016). In contrast, a reduction in growth was not observed for seedlings infected with the *F. mangiferae* overexpression strains. Another difference noted was that the *F. fujikuroi* strain overexpressing the CK1 cluster gene *FfIPTLOG1* significantly impacted seedling weight (but not height) as compared to all other *F. fujikuroi* strains and the control treatment.

Because we found that infection by *F. mangiferae* induced significant changes in CK content in both roots and shoots of maize seedlings, we examined the ability of CK-over accumulating and CK-deficient strains of *F. mangiferae* to affect maize seedling growth (**Table 8**). Mean height of seedlings infected by all strains including WT was significantly lower and the length of the primary root was significantly shorter 10 dpi in contrast to non-infected seedlings (**Table 8**). The most significant change was observed in seedlings infected with the strain overexpressing *FmIPTLOG1*. Seedlings dry weight or primary root length was significantly correlated with their reduced growth (**Table 8**). Besides CK content, the ability of the strains to activate plant CKX activity was monitored. All strains were able to induce a significant increase of CKX activity in infected root tissue compared to uninoculated plants. Three strains, the *IPTLOG1*/*tRNA-IPT* (Δ Δ Fm_IL1/tI) double mutant and the two strains overexpressing the *F. mangiferae IPTLOG1* and *IPTLOG2* accumulated significantly more CKX activity than plants infected with WT (**Table 8**). Deletion of *IPTLOG1* or *tRNA-IPT* did not statistically significantly change CKX levels.

DISCUSSION

Hormone signaling networks are believed to play a significant role in regulating plant–microbe interactions. The stress hormones SA, jasmonic acid and ethylene are well known to induce plant defense responses against various pathogens including *Fusarium oxysporum* (Dempsey and Klessig, 2012; Di et al., 2016). Far less is known about the involvement of the morphogenetic hormones CKs and auxins in fungal–plant interactions. In a previous comparative "omics" analysis of species of the *Fusarium fujikuroi* species complex (FFC), we found evidence that FFC species can synthesize CKs and auxins in addition to the previously described production of the morphogenetic hormone GAs (Niehaus et al., 2016). Here, we examined the accumulation of these hormones *in planta* during a *Fusarium*–host plant interaction, their

metabolism and their possible contribution to disease symptoms.

Plants Tend to Restore Hormone Homeostasis Disturbed by the Pathogen

Although fungal infections in general can alter endogenous plant hormone levels, we found that pathogen produced hormones rarely affect plant growth and development. Recently, we confirmed that only two out of five studied FFC species were able to produce GAs, despite the fact that four of the *Fusarium* genomes contain the biosynthetic ability (Niehaus et al., 2016). *F. fujikuroi's* unique ability to produce significant quantities of GAs leads to the elongation of rice seedling stems, the classic symptom of "bakanae" disease, and supports the efficient invasion of rice tissue and penetration of plant cells by hyphae (Wiemann et al., 2013). In this study, the expression of maize and fungal genes involved in CK metabolism during infection with different *Fusarium* helped reveal why fungal hormone synthesis minimally affected maize growth. Along with expression of CK biosynthetic genes from both organisms, we detected expression of a maize gene encoding a CKX, an enzyme involved in the irreversible degradation of CKs. Thus, despite efforts by the fungus to alter CK balance in maize tissue (either directly by producing CKs or indirectly by increasing plant CK synthesis) overall levels were actively mitigated by the plant. This effort to restore hormone homeostasis was most clearly seen in *F. mangiferae* infected maize tissue where the highest levels of CKs paralleled the highest level of plant CKX expression observed.

Cytokinins Present in *F. mangiferae* Infected Tissue Are of Plant Origin

The quantification of hormones in infected tissue revealed a significant accumulation of CKs upon *F. mangiferae* infection. The accumulation of CKs correlates with the observed retarded proliferation and elongation of maize seedlings roots infected with *F. mangiferae*, compared to roots of mock- or other *Fusarium*-treated plants. In contrast, roots infected with the four other *Fusarium* contained a slight increase in CKs suggesting that CKs contributed minimally to the disease symptoms noted.

A recent study in *Claviceps purpurea* revealed a unique biosynthetic pathway for CK production based on the IPTLOG enzyme (Hinsch et al., 2015). Here, we describe two *IPTLOG* gene homologs present in all of the *Fusarium* genomes examined. We assumed initially that the activity of one or both might contribute to the massive CK increase observed in maize tissue infected by *F. mangiferae*. To our surprise, this appeared unlikely for multiple reasons. First both *IPTLOG1* and *IPTLOG2* were either not expressed or minimally expressed during infection. Any potential impact of *IPTLOG* in CK levels seems even less likely for the other *Fusarium* as we did not detect a significant CK increase, despite detecting an increase in expression of *F. verticillioides IPTLOG2* in infected tissue. Second, *F. mangiferae IPTLOG2* is likely not functional as its predicted open reading frame contains two stop codons 71 codons downstream from the start codon. We expressed the predicted 71 amino acid protein in *E. coli* and found that it exhibited no IPT and only weak LOG activity (data not shown). We also overexpressed *IPTLOG2* in the wild-type and found that it did not lead to more CKs than the WT *in planta*. And finally, an *IPTLOG1* deletion mutant did not alter the amount of CKs that accumulated in inoculated seedlings while the overexpression mutant did lead to an increase in CK production, similarly to the *FfIPTLOG1* overexpressing strain (Niehaus et al., 2016).

The second pathway for CK production is based on tRNA decay. This pathway can contribute to the total amount of CKs produced by fungi and effect virulence as recently shown in several fungal species (Chanclud et al., 2016; Hinsch et al., 2016; Morrison et al., 2017). Here, we identified an ortholog of *tRNA-IPT* responsible for CK synthesis in *F. mangiferae*. No significant differences were observed among *F. mangiferae tRNA-IPT* mutants nor *FmtRNA-IPT/IPTLOG1* double deletion mutants in their ability to cause seedling disease symptoms or to lower plant CKX activity. Taken together, the increase in plant endogenous CK content is most likely not due to fungal synthesis but rather to activation by the fungus of maize CK biosynthetic genes by a yet unknown mechanism. This response has already been observed for two biotrophic fungi, *Magnaporthe oryzae* (Jiang et al., 2013) and *Colletotrichum graminicola* (Behr et al., 2012), which lack *IPTLOG* genes and induce a massive accumulation of CKs *in planta*. In our study, up-regulation of maize *IPT* genes both in roots and shoots during infection by any of the fusaria strongly supports this hypothesis. The accumulation of Zm*IPT* transcripts was also accompanied by the up-regulation of the *ZmCKX1* gene, involved in CK degradation.

The accumulation of CKs in plant tissue may benefit fungi through increased sink activity and attraction of assimilates, providing essential energy for fungal growth. Accordingly, fungi which primarily infect non-assimilating sink organs, flowers in the case of *F. mangiferae* and spikes in the case of *C. purpurea*, were found to induce strong accumulation of CKs. The practical consequence of the accumulation of CKs to the plant is host tissue malformation as observed in *F. mangiferae* infections which is likely due to a CK-induced increase in cell division.

Accumulation of Active Cytokinins Might Be the Cause of Mango Flower Malformation

It has been previously suggested that the presence of CKs in infected mango tissues may be related to pathogenicity (Nicholson and van Staden, 1988; Van Staden and Nicholson, 1989). Because we revealed in the present study that infection especially by *F. mangiferae* induced accumulation of endogenous CK in maize seedling tissue, we wondered whether a same response could be observed in mango, the natural host of *F. mangiferae*. Malformed tissue of mango buds and panicles contained up to fourfold higher iP and *t*Z free bases, the two CK forms shown to efficiently activate known CK receptors (Lomin et al., 2015). Since the association of *F. mangiferae* with mango tissue is long-term, in contrast to the short-term association we studied in maize, the CK homeostasis in mango tissues seems to be balanced as the concentration of some other CK forms were

lowered to make the total CK pool in infected and healthy organs equal. The elevated levels of CK free bases we observed could be crucial to maintain levels of CK signal transduction required or responsible for development of the malformed mango tissue. Recently, a whole transcriptome analysis conducted on mango tissue during a long-term interaction with *F. mangiferae* revealed a significant deregulation of 12 plant genes likely associated with *zeatin* biosynthesis. The genes were described as coding for IPTs, tRNA-IPT, CKXs and CK-specific hydroxylases (Liu et al., 2016). Similarly, crown galls induced by *Agrobacterium tumefaciens* or induced by *Rhodococcus fascians* infections require elevated levels of active CKs for the development of the malformed plant tissues (Frébort et al., 2011).

Taken together, the elevated CK in plant tissue infected by *F. mangiferae* is likely due to the induction of plant CK synthesis by the fungus by an unknown mechanism. One possibility is through the action of other phytohormones or volatiles. Intriguingly, the largest up-regulation in maize *IPT* genes was observed in the shoots 6 dpi when fungal hyphae were sparse. The plant pathogen *Alternaria alternata* has already been shown to produce volatile compounds which dramatically increase CK content in the rosette leaves of *Arabidopsis* (Sánchez-López et al., 2016). Although *F. mangiferae* can produce the volatile phytohormone ethylene, for which a role in mango tissue malformation has been hypothesized (Ansari et al., 2013, 2015), based on our transcriptomic data, ethylene-response gene expression in maize tissue infected by *F. mangiferae* was attenuated suggesting that ethylene is likely not responsible for CK elevation upon *Fusarium* infection.

Possible Role of IAA-Aspartate in Responses to *Fusarium* Infection

Besides over-accumulating CKs, roots infected with *F. mangiferae* also contain a high level of auxin (IAA), similar to roots infected with *F. proliferatum* ET1. In *F. proliferatum* ET1, IAA accumulation was related to the activation of the IAM pathway. As *F. mangiferae* does not have a functional IAM pathway, the higher amount of free IAA might be attributed to the IPyA pathway possible via a *YUCCA* gene homolog located between the GA and CK clusters. Except for *F. proliferatum* ET1, *F. mangiferae* is the only species that up-regulated this gene upon infection (Niehaus et al., 2016). Recently, it has been shown that elevated CK levels promote auxin biosynthesis in young roots (Jones et al., 2010); while exogenously applied auxin activates CK degradation (Werner et al., 2006). These trends in mutual regulation of metabolism can be overruled by local, developmentally context-specific cues (Bielach et al., 2012). We observed a twofold increase in total auxin turnover in tissue infected by *Fusarium* strains overexpressing either of the CK clusters. Auxin–CK interactions determine several processes *in planta* and have an essential impact on root and shoot morphology (Werner et al., 2001).

Infection by fungi greatly affect the auxin status in the plant host, marked by differential regulation of genes involved in IAA synthesis and conjugation (Niehaus et al., 2016). In the present study, the ratio between free and conjugated IAA revealed large differences between root tissues infected by different species and indicated that the process of IAA conjugation or conjugate hydrolysis may be part of the maize response to *Fusarium*. Surprisingly, higher accumulation of the aspartate-conjugate (IAA-Asp) was detected in *F. mangiferae* infected roots in contrast to roots infected by other *Fusarium* or mock-treated roots. IAA-Asp is an irreversible, non-active conjugate and a precursor of IAA degradation in plants (Ludwig-Müller, 2011). Prior to degradation, IAA-Asp can promote disease development induced by several pathogens in different plant species (González-Lamothe et al., 2012). For instance, *Arabidopsis* inoculated with the fungal necrotroph *Botrytis cinerea* accumulates huge amount of IAA-Asp that seemed to promote plant susceptibility to pathogens via the transcription of virulence genes (González-Lamothe et al., 2012).

Quantification of IAA-conjugates in axenic cultures revealed that *F. mangiferae* is the only *Fusarium* tested that is not able to form IAA-Asp (Niehaus et al., 2016). This lack of endogenous IAA-Asp suggests a potentially unique role of this molecule in plant–pathogen interaction. The ability of *F. mangiferae* to induce IAA-Asp production or its retention *in planta* earlier or more efficiently than the other *Fusarium* may be related to how *F. mangiferae* interacts with its host mango. Tissue infected by *F. verticillioides,* an endophyte and pathogen of maize, also accumulated more IAA-Asp than tissue infected by the other three fusaria but to a lower extent than *F. mangiferae*. Alongside IAA-Asp accumulation, *F. verticillioides* was also the second *Fusarium* isolate beside *F. mangiferae*, which was able to extensively accumulate CKs upon infection, especially in the upper part of the plant. Hence, the observed overproduction of plant CKs can be a consequence of the accumulation of IAA-Asp in infected tissue. How *Fusarium* spp. or the plant itself perceives and responds to IAA-Asp changes, whether IAA-Asp affects other fungal virulence factors and how the plant responds to IAA-Asp changes, will require further studies.

CONCLUSION

Hormones, including GAs, auxins and CKs, play an important role in some *Fusarium*–host interactions. *Fusarium* species, particularly of the FFC, evolved multiple biosynthetic pathways for their *de novo* synthesis. Over time, due likely to changing evolutionary pressures, these biosynthetic genes have been lost or gained on multiple independent occasions. The characterization of CKs in Sordariomycetes provides an example how CK production may have been selected for during fungal evolution and their interaction with a plant host. CK production by the bi-functional enzyme IPTLOG appears to be an evolutionary relic, persisting only in some species such as *Claviceps purpurea* (Hinsch et al., 2015), which was replaced by a biosynthetic pathway based on the degradation of the isoprenylated tRNA (Chanclud et al., 2016). Here, we present evidence that although *Fusarium* can synthesize CKs, increases in CK levels *in planta* during an infection is likely through fungal induced changes in plant CK biosynthesis, by a yet unknown mechanism. We also revealed the existence of an alternative biosynthetic pathway for

auxin production, in addition to the IAM pathway which was originally identified in bacteria. However, despite the potential functionality of this alternative pathway, the IAM pathway is the only one substantially induced during infection of the host plant. Overall, *Fusarium* species appear much more likely to manipulate plant auxin homeostasis by hydrolysis of IAA-amino acid and sugar conjugates or perhaps, regulating enzymes participating in synthesis, than *de novo* synthesis.

AUTHOR CONTRIBUTIONS

PG, BT, RP, E-MN, and JV designed the research. JV, ON, AP, DT, KH, MH, VB, JO, AS, SF, LO-Y, YI, MM, and ME performed the experiments and data collection. Analysis of data was ensured by PG, UG, MtM, E-MN, JV, and VB. PG, BT, DB, and VB wrote and revised the manuscript. All authors approved the final version of the manuscript.

FUNDING

This study was funded by two grants of the Czech Science Foundation (16-10602S and 18-10349S) and by the Hungarian Széchenyi 2020 Program (GINOP-2.3.2-15-2016-00052).

SUPPLEMENTARY MATERIAL

The Supplementary Material for this article can be found online at: https://www.frontiersin.org/articles/10.3389/fpls.2018.01936/full#supplementary-material

REFERENCES

Ansari, M. W., Rani, V., Shukla, A., Bains, G., Pant, R. C., and Tuteja, N. (2015). Mango (*Mangifera indica* L.) malformation: a malady of stress ethylene origin. *Physiol. Mol. Biol. Plants* 21, 1–8. doi: 10.1007/s12298-014-0258-y

Ansari, M. W., Shukla, A., Pant, R. C., and Tuteja, N. (2013). First evidence of ethylene production by *Fusarium mangiferae* associated with mango malformation. *Plant Signal. Behav.* 8:e22673. doi: 10.4161/psb.22673

Bai, G. H., and Shaner, G. (1996). Variation in *Fusarium graminearum* and cultivar resistance to wheat scab. *Plant Dis.* 80, 975–979. doi: 10.1094/PD-80-0975

Behr, M., Motyka, V., Weihmann, F., Malbeck, J., Deising, H. B., and Wirsel, S. G. R. (2012). Remodeling of cytokinin metabolism at infection sites of *Colletotrichum graminicola* on maize leaves. *Mol. Plant Microbe. Interact.* 25, 1073–1082. doi: 10.1094/MPMI-01-12-0012-R

Bielach, A., Duclercq, J., Marhavý, P., and Benková, E. (2012). Genetic approach towards the identification of auxin-cytokinin crosstalk components involved in root development. *Philos. Trans. R. Soc. Lond. B Biol. Sci.* 367, 1469–1478. doi: 10.1098/rstb.2011.0233

Bist, L. D., and Ram, S. (1986). Effect of malformation on changes in endogenous gibberellins and cytokinins during floral development of mango. *Sci. Hortic.* 28, 235–241. doi: 10.1016/0304-4238(86)90005-1

Bradford, M. M. (1976). A rapid and sensitive method for the quantitation of microgram quantities of protein utilizing the principle of protein-dye binding. *Anal. Biochem.* 72, 248–254. doi: 10.1016/0003-2697(76)90527-3

Chanclud, E., Kisiala, A., Emery, N. R. J., Chalvon, V., Ducasse, A., Romiti-Michel, C., et al. (2016). Cytokinin production by the rice blast fungus is a pivotal requirement for full virulence. *PLoS Pathog.* 12:e1005457. doi: 10.1371/journal.ppat.1005457

Christianson, T. W., Sikorski, R. S., Dante, M., Shero, J. H., and Hieter, P. (1992). Multifunctional yeast high-copy-number shuttle vectors. *Gene*, 110, 119–122. doi: 10.1016/0378-1119(92)90454-W

Darken, M. A., Jensen, A. L., and Shu, P. (1959). Production of gibberellic acid by fermentation. *Appl. Microbiol.* 7, 301–303.

Dempsey, D. A., and Klessig, D. F. (2012). SOS - too many signals for systemic acquired resistance? *Trends Plant Sci.* 17, 538–545. doi: 10.1016/j.tplants.2012.05.011

Di, X., Takken, F. L. W., and Tintor, N. (2016). How phytohormones shape interactions between plants and the soil-borne fungus *Fusarium oxysporum*. *Front. Plant Sci.* 7:170. doi: 10.3389/fpls.2016.00170

Frébort, I., Kowalska, M., Hluska, T., Frébortová, J., and Galuszka, P. (2011). Evolution of cytokinin biosynthesis and degradation. *J. Exp. Bot.* 62, 2431–2452. doi: 10.1093/jxb/err004

Frébort, I., Šebela, M., Galuszka, P., Werner, T., Schmülling, T., and Peè, P. (2002). Cytokinin oxidase/cytokinin dehydrogenase assay: optimized procedures and applications. *Anal. Biochem.* 306, 1–7. doi: 10.1006/abio.2002.5670

Freeman, S., Shtienberg, D., Maymon, M., Levin, A. G., and Ploetz, R. C. (2014). New insights into mango malformation disease epidemiology lead to a new integrated management strategy for subtropical environments. *Plant Dis.* 98, 1456–1466. doi: 10.1094/PDIS-07-14-0679-FE

Fu, J., Liu, H., Li, Y., Yu, H., Li, X., Xiao, J., et al. (2011). Manipulating broad-spectrum disease resistance by suppressing pathogen-induced auxin accumulation in rice. *Plant Physiol.* 155, 589–602. doi: 10.1104/pp.110.163774

Geissman, T. A., Verbiscar, A. J., Phinney, B. O., and Cragg, G. (1966). Studies on the biosynthesis of gibberellins from (-)-kaurenoic acid in cultures of *Gibberella fujikuroi*. *Phytochemistry* 5, 933–947. doi: 10.1016/S0031-9422(00)82790-9

González-Lamothe, R., El Oirdi, M., Brisson, N., and Bouarab, K. (2012). The conjugated auxin indole-3-acetic acid-aspartic acid promotes plant disease development. *Plant Cell* 24, 762–777. doi: 10.1105/tpc.111.095190

Gordon, T. R. (2006). Pitch canker disease of pines. *Phytopathology* 96, 657–659. doi: 10.1094/PHYTO-96-0657

Hedden, P., and Sponsel, V. (2015). A century of gibberellin research. *J. Plant Growth Regul.* 34, 740–760. doi: 10.1007/s00344-015-9546-1

Hinsch, J., Galuszka, P., and Tudzynski, P. (2016). Functional characterization of the first filamentous fungal tRNA-isopentenyltransferase and its role in the virulence of *Claviceps purpurea*. *New Phytol.* 211, 980–992. doi: 10.1111/nph.13960

Hinsch, J., Vrabka, J., Oeser, B., Novák, O., Galuszka, P., and Tudzynski, P. (2015). De novo biosynthesis of cytokinins in the biotrophic fungus *Claviceps purpurea*. *Environ. Microbiol.* 17, 2935–2951. doi: 10.1111/1462-2920.12838

Jiang, C.-J., Shimono, M., Sugano, S., Kojima, M., Liu, X., Inoue, H., et al. (2013). Cytokinins act synergistically with salicylic acid to activate defense gene expression in rice. *Mol. Plant. Microbe. Interact.* 26, 287–296. doi: 10.1094/MPMI-06-12-0152-R

Jones, B., Gunnerås, S. A., Petersson, S. V., Tarkowski, P., Graham, N., May, S., et al. (2010). Cytokinin regulation of auxin synthesis in Arabidopsis involves a homeostatic feedback loop regulated via auxin and cytokinin signal transduction. *Plant Cell* 22, 2956–2969. doi: 10.1105/tpc.110.074856

Kasahara, H. (2015). Current aspects of auxin biosynthesis in plants. *Biosci. Biotechnol. Biochem.* 80, 1–9. doi: 10.1080/09168451.2015.1086259

Kidd, B. N., Kadoo, N. Y., Dombrecht, B., Tekeoglu, M., Gardiner, D. M., Thatcher, L. F., et al. (2011). Auxin signaling and transport promote susceptibility to the root-infecting fungal pathogen *Fusarium oxysporum* in Arabidopsis. *Mol. Plant. Microbe. Interact.* 24, 733–748. doi: 10.1094/MPMI-08-10-0194

Liu, F., Wu, J.-B., Zhan, R.-L., and Ou, X.-C. (2016). Transcription profiling analysis of mango-fusarium mangiferae interaction. *Front. Microbiol.* 7:1443. doi: 10.3389/fmicb.2016.01443

Lomin, S. N., Krivosheev, D. M., Steklov, M. Y., Arkhipov, D. V., Osolodkin, D. I., Schmülling, T., et al. (2015). Plant membrane assays with cytokinin receptors underpin the unique role of free cytokinin bases as biologically active ligands. *J. Exp. Bot.* 66, 1851–1863. doi: 10.1093/jxb/eru522

Ludwig-Müller, J. (2011). Auxin conjugates: their role for plant development and in the evolution of land plants. *J. Exp. Bot.* 62, 1757–1773. doi: 10.1093/jxb/erq412

Mańka, M. (1980). Auxin and gibberellin-like substances synthesis by *Fusarium* isolates pathogenic to corn seedlings. *Acta Microbiol. Pol.* 29, 365–374.

Matic, S., Gullino, M. L., and Spadaro, D. (2017). The puzzle of bakanae disease through interactions between *Fusarium fujikuroi* and rice. *Front. Biosci.* 9:333–344. doi: 10.2741/e806

Morrison, E. N., Emery, R. J. N., and Saville, B. J. (2017). Fungal derived cytokinins are necessary for normal *Ustilago maydis* infection of maize. *Plant Pathol.* 66, 726–742. doi: 10.1111/ppa.12629

Nicholson, R. I. D., and van Staden, J. (1988). Cytokinins and mango flower malformation. i. tentative identification of the complement in healthy and malformed inflorescences. *J. Plant Physiol.* 132, 720–724. doi: 10.1016/S0176-1617(88)80235-9

Niehaus, E.-M., Münsterkötter, M., Proctor, R. H., Brown, D. W., Sharon, A., Idan, Y., et al. (2016). Comparative "Omics" of the *Fusarium fujikuroi* species complex highlights differences in genetic potential and metabolite synthesis. *Genome Biol. Evol.* 8, 3574–3599. doi: 10.1093/gbe/evw259

Novák, O., Hényková, E., Sairanen, I., Kowalczyk, M., Pospíšil, T., and Ljung, K., (2012). Tissue-specific profiling of the *Arabidopsis thaliana* auxin metabolome. *Plant J.* 72, 523–536. doi: 10.1111/j.1365-313X.2012.05085.x

O'Donnell, K., Rooney, A. P., Proctor, R. H., Brown, D. W., McCormick, S. P., Ward, T. J., et al. (2013). Phylogenetic analyses of RPB1 and RPB2 support a middle Cretaceous origin for a clade comprising all agriculturally and medically important fusaria. *Fungal Genet. Biol.* 52, 20–31. doi: 10.1016/j.fgb.2012.12.004

Presello, D. A., Botta, G., Iglesias, J., and Eyhérabide, G. H. (2008). Effect of disease severity on yield and grain fumonisin concentration of maize hybrids inoculated with *Fusarium verticillioides*. *Crop Prot.* 27, 572–576. doi: 10.1016/j.cropro.2007.08.015

Quazi, S. A. J., Meon, S., Jaafar, H., and Ahmad, Z. A. B. M. (2015). The role of phytohormones in relation to bakanae disease development and symptoms expression. *Physiol. Mol. Plant Pathol.* 90, 27–38. doi: 10.1016/j.pmpp.2015.02.001

Reineke, G., Heinze, B., Schirawski, J., Buettner, H., Kahmann, R., and Basse, C. W. (2008). Indole-3-acetic acid (IAA) biosynthesis in the smut fungus *Ustilago maydis* and its relevance for increased IAA levels in infected tissue and host tumour formation. *Mol. Plant Pathol.* 9, 339–355. doi: 10.1111/j.1364-3703.2008.00470.x

Rittenberg, D., and Foster, G. L. (1940). A new procedure for quantitative analysis by isotope dilution, with application to the determination of amino acids and fatty acids. *J. Biol. Chem.* 133:737.

Sánchez-López, Á. M., Baslam, M., De Diego, N., Muñoz, F. J., Bahaji, A., Almagro, G., et al. (2016). Volatile compounds emitted by diverse phytopathogenic microorganisms promote plant growth and flowering through cytokinin action. *Plant. Cell Environ.* 39, 2592–2608. doi: 10.1111/pce.12759

Schmittgen, T. D., and Livak, K. J. (2008). Analyzing real-time PCR data by the comparative C_T method. *Nat. Protoc.* 3, 1101–1108. doi: 10.1038/nprot.2008.73

Schumacher, J. (2012). Tools for *Botrytis cinerea*: new expression vectors make the gray mold fungus more accessible to cell biology approaches. *Fungal Genet. Biol.* 49, 483–497. doi: 10.1016/j.fgb.2012.03.005

Staben, C., Jensen, B., Singer, M., Pollock, J., Schechtman, M., Kinsey, J., et al. (1989). Use of a bacterial Hygromycin B resistance gene as a dominant selectable marker in Neurospora crassa transformation. *Fungal Gen. Rep.* 36, 79–81. doi: 10.4148/1941-4765.1519

Thakur, M. S., and Vyas, K. M. (1983). Production of plant growth regulators by some *Fusarium* species. *Folia Microbiol.* 28, 124–129. doi: 10.1007/BF02877368

Tsavkelova, E., Oeser, B., Oren-Young, L., Israeli, M., Sasson, Y., Tudzynski, B., et al. (2012). Identification and functional characterization of indole-3-acetamide-mediated IAA biosynthesis in plant-associated *Fusarium* species. *Fungal Genet. Biol.* 49, 48–57. doi: 10.1016/j.fgb.2011.10.005

Tudzynski, B., and Hölter, K. (1998). Gibberellin biosynthetic pathway in *Gibberella fujikuroi*: evidence for a gene cluster. *Fungal Genet. Biol.* 25, 157–170. doi: 10.1006/fgbi.1998.1095

Urbanová, T., Tarkowská, D., Novák, O., Hedden, P., and Strnad, M. (2013). Analysis of gibberellins as free acids by ultra performance liquid chromatography–tandem mass spectrometry. *Talanta* 112, 85–94. doi: 10.1016/j.talanta.2013.03.068

Van Staden, J., and Nicholson, R. I. D. (1989). Cytokinins and mango flower malformation II. the cytokinin complement produced by *Fusarium moniliforme* and the ability of the fungus to incorporate [8-14C] adenine into cytokinins. *Physiol. Mol. Plant Pathol.* 35, 423–431. doi: 10.1016/0885-5765(89)90061-1

Vyroubalová, Š., Václavíková, K., Turečková, V., Novák, O., Šmehilová, M., Hluska, T., et al. (2009). Characterization of new maize genes putatively involved in cytokinin metabolism and their expression during osmotic stress in relation to cytokinin levels. *Plant Physiol.* 151, 433–447. doi: 10.1104/pp.109.142489

Werner, T., Köllmer, I., Bartrina, I., Holst, K., and Schmülling, T. (2006). New insights into the biology of cytokinin degradation. *Plant Biol.* 8, 371–381. doi: 10.1055/s-2006-923928

Werner, T., Motyka, V., Strnad, M., and Schmülling, T. (2001). Regulation of plant growth by cytokinin. *Proc. Natl. Acad. Sci. U.S.A.* 98, 10487–10492. doi: 10.1073/pnas.171304098

Wiemann, P., Sieber, C. M. K., von Bargen, K. W., Studt, L., Niehaus, E.-M., Espino, J. J., et al. (2013). Deciphering the cryptic genome: genome-wide analyses of the rice pathogen *Fusarium fujikuroi* reveal complex regulation of secondary metabolism and novel metabolites. *PLoS Pathog.* 9:e1003475. doi: 10.1371/journal.ppat.1003475

Conflict of Interest Statement: The authors declare that the research was conducted in the absence of any commercial or financial relationships that could be construed as a potential conflict of interest.